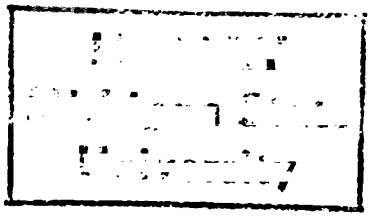

This is to certify that the

dissertation entitled

An Approach Toward Minimizing Chemical Interference in FAB Mass Spectra: The Development and Application of Thermally-Assisted FAB

presented by

Bradley Lynn Ackermann

has been accepted towards fulfillment of the requirements for

Ph.D. degree in Chemistry

Major professor

Date 22 January 1987

AN APPROACH TOWARD MINIMIZING CHEMICAL INTERFERENCE
IN FAB MASS SPECTRA.
THE DEVELOPMENT AND APPLICATION OF [illegible]

By

Bradley Lynn Ackermann

A DISSERTATION

Submitted to
Michigan State University
in partial fulfillment of the requirements
for the degree of

DOCTOR OF PHILOSOPHY

Department of Chemistry

1986

AN APPROACH TOWARD MINIMIZING CHEMICAL INTERFERENCE IN FAB MASS SPECTRA: THE DEVELOPMENT AND APPLICATION OF THERMALLY-ASSISTED FAB

By

Bradley Lynn Ackermann

A DISSERTATION

Submitted to
Michigan State University
in partial fulfillment of the requirements
for the degree of

DOCTOR OF PHILOSOPHY

Department of Chemistry

1986

ABSTRACT

AN APPROACH TOWARD MINIMIZING CHEMICAL INTERFERENCE IN FAB MASS SPECTRA: THE DEVELOPMENT AND APPLICATION OF THERMALLY-ASSISTED FAB

BY

Bradley Lynn Ackermann

In 1981, a new method of ionization for nonvolatile molecules known as fast atom bombardment (FAB) was introduced. FAB uses an energetic atom beam (6-10keV) to effect desorption-ionization (DI) of nonvolatile solutes directly from the condensed state, thus obviating the requirement of sample volatility which limits conventional ionization methods for mass spectrometry. In this process, viscous liquids such as glycerol, are used as matrices to improve DI efficiency and to increase the longevity of analyte signals. Unfortunately, FAB mass spectra are often repleat with peaks from chemical interference which restrict the information that may be obtained for the analyte. Interferences can be classified into two major categories. The first includes impurities which remain after analyte isolation/purification, and is especially problematic in samples of biological origin. The second type of chemical interference originates from the matrix used for FAB.

An example of the first type, also known as sample-related interference, is presented in the context of the analysis of the

urinary metabolites of the analgesic acetaminophen by means of the off-line combination of reverse phase HPLC and FAB. Recommendations are made for efficient use of these two methods with specific regard to minimizing chemical interferences. In addition, a method for calculating analyte signal to background (S/B) values is introduced as a means of evaluating the quality of the FAB mass spectrum.

A method known as thermally-assisted FAB (TA-FAB) is introduced as a means of minimizing matrix-related background. TA-FAB is essentially a method for preparing new matrices for FAB from substances inherently too immobile to act as FAB matrices, by heating them within the source of the mass spectrometer during FAB. Success to date has been achieved using aqueous saccharide solutions as TA-FAB matrices. Several important improvements to FAB result from thermal control of the matrix including a selection against matrix background, and the possibility of valid background subtraction. The development of TA-FAB is described in the context of applications of the technique to the analysis of several representative nonvolatile biomolecules including a series of cyclic tetrapeptide mycotoxins. In the final section, the hypothesis of ternary perculation (TP) is submitted to account for behavior observed during TA-FAB.

Dedicated to the memory of

RALPH CURTIS ACKERMANN

ACKNOWLEDGEMENTS

This dissertation is dedicated to the memory of my father, Ralph Curtis Ackermann, whose guidance and direction enabled me to reach this goal in my life. His constant love and encouragement has had an influence on my life which cannot be understated or forgotten. It is gratifying to know at least one person who would be delighted to read this work.

Acknowledgements are essentially a time to reflect and give thanks to those people who made an accomplishment possible and who deserve a share of the triumph (please, only 1 page per person).

First, a heartfelt thanks to all the teachers who collectively abetted my desire to pursue chemistry: Dick Welsh (Dearborn High), Dave Klein and Jack Schubert (Hope College), and especially Jack Watson and Jack Holland (Michigan State).

Next, thanks to all the people associated with the Mass Spec Facility at MSU who made the burden of graduate school bearable and often entertaining. Specific thanks are due to Brian Musselman for training, Mike Davenport for technical assistance, and Vicki McPharlin for secretarial services and of course for persevering through the onerous task of typing this dissertation. I am also indebted to Curt Heine for his participation in the latter stages of this project.

A special thanks goes to my family, especially to my mother who provided encouragement every step of the way. This accomplishment would not have been possible without her help.

No acknowledgement would be complete without recognizing the 1984 World Champion Detroit Tigers for their great accomplishment and the inspiration they provided. In addition, the Dow Chemical Company deserves thanks for the fellowships I received that made it possible to attend as many Tiger games as possible.

A special recognition must be given to Andrea in appreciation for her work involved in the preparation of this dissertation; it certainly would have been difficult without her help. The constant love she gave to me throughout this period shall always be remembered.

Finally, much gratitude goes to the members of the Chem House who threw a Halloween party which enabled me to experience the best part about MSU, Andrea.

TABLE OF CONTENTS

LIST OF TABLES

LIST OF FIGURES

Chapter 1

LITERATURE REVIEW

I. Introduction

Research in the life sciences has always relied upon concomitant advancements in analytical methods to provide data which are both reliable and informative. Although by comparison the application of mass spectrometry to problems of biological origin is relatively recent, its participation has expanded into several areas including: biochemistry, medicine, pharmacology, agriculture, toxicology, and the environment. Reasons for this are numerous. First, mass spectrometry (MS) has traditionally been known for its capability as a method for trace analysis. Secondly, the on-line combination with gas chromatography (GC) and more recently liquid chromatography (HPLC) have made mass spectrometry the method of choice for the analysis of complex mixtures such as urine, plasma, and biological extracts. Furthermore, mass spectrometry is a tool frequently used for structural analysis. This particular area has been significantly advanced by the introduction of instrumental methods known collectively as mass spectrometry/mass spectrometry (MS/MS) (1). Finally, recent advances in ionization methods have enabled mass spectra to be directly acquired from several nonvolatile biomolecules which were either too large, polar, or thermally laible to be successfully analyzed using conventional methods of ionization (2).

Conventional methods, as defined here, refer to those in which the analyte must be present in the gas phase, under the conditions of

the mass spectrometer prior to ionization. This category, which includes electron impact (EI) and chemical ionization (CI), still accounts for the vast majority of analyses performed by mass spectrometry. Under EI gas phase analyte molecules are ionized as a result of collisions with electrons (70 eV) produced from a tungsten filament. The distribution of internal energy acquired by the analyte leads to two possible events: (1) formation of a molecular ion ($M^{\ddagger}$) produced by removal of an electron from the analyte and (2) fragmentation by unimolecular dissociation of the molecular ion to yield a series of fragment ions indicative of molecular structure. Often under the conditions of EI little or no molecular ions are observed making molecular weight assignments difficult or impossible. In 1966 Munson and Field reported a method for attaining larger abundances of molecular ions known as chemical ionization (3). Under CI, the ionizing species are ions formed from electron impact of a reagent gas, usually methane, present at a high pressure (1 torr) relative to the analyte. Reagent ions, such as CH_5^+, ionize the sample by exothermic proton transfer to form $(M+H)^+$ ions. Fragmentation can accompany chemical ionization, but occurs to a much lesser extent than in electron impact.

Unfortunately, both EI and CI are limited to samples which may be placed into the gas phase prior to ionization. Hence, they found little use for the analysis of polar biomolecules such as peptides and oligosaccharides which simply degrade upon heating. A viable and routine method to make nonvolatile molecules more amenable to analysis by conventional mass spectrometry is to prepare a chemical derivative of the analyte to make it more volatile. While this

approach can be used for several classes of biomolecules (4), derivatization frequently reduces the amount of structural information gained through fragmentation and also increases the molecular weight of the molecule. Since boiling points increase with molecular weight, there appears to be a practical limit to this approach. Consequently, prior to the advent of techniques for the ionization of nonvolatile molecules, there was little need for the development of mass analyzing devices (e.g., magnets, quadrupoles) capable of exceeding 1000u, and the application of mass spectrometry to several classes of biomolecules was considered either not feasible or impractical.

Beginning with the emergence of field desorption (FD) by Beckey in 1969 (5) and plasma desorption (PD) by Macfarlane in 1974 (6) there has been a proliferation of methods for the ionization of nonvolatile molecules (7). Not surprisingly, there has been a corresponding increase in the application of mass spectrometry to the life sciences. These techniques, known collectively as desorption-ionization (DI) methods (7), differ from conventional methods in that the sample is analyzed directly from the condensed state, thereby obviating the requirement for sample volatility. Although DI methods may differ greatly in their approach to desorption-ionization, each involves the input of energy (in a variety of forms) to the sample to effect the transformation of analyte molecules (or pre-formed ions), present in the condensed state, into gas phase ions which may then undergo mass analysis and detection.

The focus of this dissertation is on a relatively new member to the DI family, known as fast atom bombardment (FAB). Fast atom bombardment was introduced by Barber and coworkers at the University of Manchester Institute of Science and Technology (UMIST), in England in 1981 (8). As shown in Figure 1.1, FAB effects desorption-ionization by having the sample, which is dissolved in a viscous liquid such as glycerol, undergo particle impact by an energetic atom beam (6-10 keV) usually composed of either argon or xenon neutrals. FAB has its origin in another ionization technique known as secondary ion mass spectrometry (SIMS). SIMS, like FAB uses a keV primary beam to effect desorption-ionization except that the incident particles are ions instead of neutrals. Originally, SIMS was designed as a technqiue for surface analysis of elemental or inorganic materials; the "dynamic" or high flux approach to this technique is capable of microscopic resolution and depth profiling (9). However, in 1976, Benninghoven demonstrated that if the incident flux of the ion beam was reduced (10^{-9} A cm^{-2}) to minimize surface damage, nonvolatile organic materials could be analyzed using the so-called "static" method (also known as molecular SIMS) (10). In the nomenclature of SIMS, the "sputtered" ions from the sample that undergo mass analysis, are known collectively as the secondary ion beam, from which the name SIMS arises. For historical reasons the same term is applied to ions detected by FAB as indicated in Figure 1.1. The use of a primary atom beam to effect sputtering was by no means original as Devienne years earlier had bombarded a variety of materials with a kilovolt atom beam as part of a technique called molecular beam surface analysis (MBSA) (11).

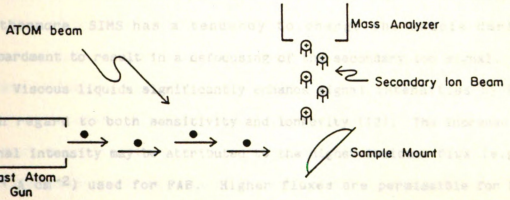

Figure 1.1 Schematic diagram showing arrangement of atom gun and sample probe at focal point of the mass spectrometer during FAB. Reprinted from "Introduction to Mass Spectrometry", by J. T. Watson with permission from Raven Press.

The real discovery by Barber et al. was the enhancement to desorption-ionization by FAB conferred by the use of a viscous liquid matrix. This discovery was probably an act of serendipity because these workers originally chose to use an atom beam for instrumental reasons; charged particles are difficult to direct into the source of a double focusing mass spectrometer because of the high source potential. An atom beam, on the other hand, requires no focusing. Furthermore, SIMS has a tendency to charge the sample during bombardment to result in a defocusing of the secondary ion signal.

Viscous liquids significantly enhance signal intensities by FAB with regard to both sensitivity and longevity (12). The increase in signal intensity may be attributed to the higher incident flux (e.g., 10^{-4} A cm^{-2}) used for FAB. Higher fluxes are permissible for FAB because glycerol resists surface damage which is known to limit the beam intensity that may be used for molecular SIMS. The longevity of FAB is ostensibly related to the ability of viscous liquids to renew their surface and replenish the analyte during bombardment. In this manner, FAB spectra may be acquired for periods on the order of 30 minutes (12), a phenomenon which makes FAB amenable to several ancillary experiments including exact mass determination and MS/MS. Since evidence suggests that the desorbed species reside predominantly in the upper few monolayers of the sample/matrix solution (13), a diffusion controlled mechanism was originally proposed by Barber et al. to account for the surface replenishment of the analyte and hence the observed sample lifetimes (12).

These advantages, coupled to the relatively low cost and instrumental simplicity, have made FAB the most widely practiced DI

method at present. Viscous liquids have now been applied to molecular SIMS to form a technique referred to as liquid SIMS or LSMIS (14). In addition to the benefits mentioned previously, viscous liquids such as glycerol resist the deleterious effect of sample charging by the primary ion beam. (14).

Although the introduction of liquid matrices has brought considerable attention to particle impact methods, FAB is certainly not free of problems. Perhaps foremost are problems associated with chemical interference in FAB mass spectra. Chemical interference refers to the presence of unwanted peaks in a FAB mass spectrum which are either sample-related or matrix-related. Background peaks present a limitation to FAB in that their superposition upon an analyte mass spectrum reduces the certainty of proposed structural and molecular weight assignments. The problems and approaches to confronting chemical interference in FAB are outlined in Chapter 2.

The primary goal of this research was to devise ways to contend with chemical interference in FAB. An initial project, which is the topic of Chapter 4, dealt specifically with sample-related chemical interference in the context of the FAB analysis of the urinary metabolites of the analgesic acetaminophen isolated by reverse phase HPLC (15). Sample-related interference refers to contaminants which remain after analyte purification and is especially prevalent in samples from biological origin. In this study suggestions were made toward the efficient, off-line combination of these two analytical methods with the emphasis being to reduce background in the resultant FAB mass spectra. The quality of the data obtained were judged using an empirical method developed for calculation of signal to

background (S/B) ratios for candidate peaks in FAB mass spectra using relative intensity data.

The remainder of the research was primarily devoted to the development and application of a new approach to FAB called thermally-assisted FAB or TA-FAB (16), the details of which are introduced at the conclusion of Chapter 2. Basically, TA-FAB involves the formation of new matrices for FAB by resistive heating of materials too immobile to act as matrices, in situ during FAB. The additional variable of temperature (e.g., thermal control) leads to several new advantages for FAB including a selection against background and the potential for a valid subtraction of background.

Prior to addressing these topics, background information about the FAB process shall be given to put the reader in a better position to understand and judge the merit of the results and discussion presented subsequently. In the sections on FAB which follow, no attempt shall be made to judge or discuss the results. Rather, the sections are intended to supply basic information and references to anyone who wishes to learn more about FAB. Hence, the informed reader may wish to begin reading Chapter 2 at this point.

II. Survey of Desorption-Ionization (DI) Methods

A brief discussion of the evolution of desorption-ionization is presented to serve as a point of reference for subsequent discussion of FAB. Only the major DI methods are discussed with the emphasis being primarily historical. More detailed information can be obtained from several review articles on DI (2,7,17).

A. Field Desorption (FD)

Desorption-ionization essentially began when Hans Beckey of the University of Bonn published the mass spectrum of glucose, a compound of low volatility, which was desorbed/ionized by a new method requiring no derivatization called field desorption (5). By field desorption (FD), samples deposited onto a special "activated" emitter undergo thermal desorption in the presence of large electric fields (c.a. 10^8V/cm). The yielded product ions are predominantly molecular entities ($M^{\ddagger}$, $(M+H)^+$, M_2^+, $(M+Na)^+$) whose relative abundances are a function of the applied temperature (18). The emitters most frequently used are tungsten wires to which fine, hair-like dendrites of carbon have been grown. FD was the commercially available method of choice for DI during the 1970s and is still used today. Unfortunately, several experimental difficulties experienced with FD limit its use currently such as: transiently-produced ion signals, a paucity of fragmentation, and a relatively high level of required operator expertise (19).

B. Plasma Desorption

The ability to produce desorption-ionization by high energy (MeV) particle bombardment was discovered in 1974 by Macfarlane at Texas A & M who noticed that intact molecules could be desorbed from organic films present during the fission fragmentation of ^{252}Cf (6). Since that time, ^{252}Cf plasma desorption (PD) has produced several

amazing achievements including the mass spectrum of one synthetically blocked deoxyoligonucleotide (MW 6957) and the intact dimer of another (MW 12,637) (20). During the fission of ^{252}Cf, cesium and technicium ions are emitted. The high energy technicium ions are used to bombard the backside of a foil coated with an organic sample with approximately 100 MeV. Simultaneous to these events, the cesium ions initiate a gating pulse in the time-of-flight (TOF) mass spectrometer used for ion detection. TOF offers the advantage of a theoretically unlimited mass range but suffers severely in attainable mass resolution.

Another form of PD known as heavy ion induced desorption has received considerable attention. Using the Tandem Accelerator in Uppsala, Sweden, Bo Sundqvist and coworkers used 90 MeV ^{127}I ions to obtain the first mass spectrum of human insulin (MW 5803) (21). Results obtained by plasma desorption indicate that it is the best method for observing high mass molecules by DI, and also can achieve the greatest sensitivity (17). It has been shown that keV particle impact techniques (SIMS, FAB) dissipate energy via a collisional cascade which depends on both the momentum and angle of the incident particles (22). In contrast, during MeV particle impact (PD) energy transfer occurs primarily through electronic excitation of the sample molecules. The increased sensitivity and mass range has been explained by an increase in the rate of energy dissipation (dE/dx) into the sample when using MeV as opposed to KeV particles (20). Unfortunately, due to the instrumentation necessary for PD, it has remained a very esoteric technique. In fact, it was related in a recent review by Macfarlane, there are only 8 such facilities in the

world (23). However, a ^{252}Cf PD instrument is now being offered commercially by a Swedish company, BIO-ION Nordic AB, Uppsala, Sweden, which is expected to proliferate the use of this technique (23).

C. Secondary Ion Mass Spectrometry (SIMS)

In 1976 Alfred Benninghoven, of the University of Munster, demonstrated the ability to perform desorption-ionization using a defocused keV ion beam to analyze a series of 15 amino acids (10). In contrast to PD, static SIMS was readily available to almost any laboratory that did surface analysis and consequently became more widely adopted. However, because most SIMS instruments were equipped with quadrupole mass analyzers (upper limit 1000 u) the high mass capabilities of this method were not initially exploited. Also unlike FD, samples analyzed by SIMS could give spectra for an hour if the flux was kept low enough to avoid the accumulation of a "critical dose" (c.a. 10^{13} particles/cm^2) which is the point where surface damage becomes significant and molecular ions cease to be observed (24). Since the yield of secondary ions depends on the incident flux, increases in sensitivity comes at the expense of sample longevity.

Static SIMS is usually performed off of metal surfaces such as silver which produce efficient yields of molecular adduct ions (e.g., $(M+Ag)^+$). However, the sensitivity of a static SIMS analysis can be further increased by producing pre-formed analyte ions. For example, Cooks reported the use of p-toluene sulfonic acid to increase the

yield of $(M+H)^+$ ions in the SIMS spectra of several biomolecules (25). More recently, he demonstrated that increased yields are possible at high primary fluxes when solids, such as ammonium chloride, are used as a matrices (26). The results were explained by the desorption of analyte-matrix clusters which desolvate in the gas phase to give intact molecular adducts, as opposed to the pyrolysis products normally seen at high fluxes due to surface damage. As mentioned previously, even greater fluxes, and hence sensitivity, may be obtained using viscous liquid matrices such as glycerol (LSIMS). Not only do liquid matrices allow for surface renewal, they also provide an excellent environment for pre-formed ion generation.

LSIMS has demonstrated results comparable to FAB (14); this finding is not unexpected as both techniques are keV particle impact methods which rely on a collisional cascade to effect desorption-ionization. In fact, the general consensus among investigators is that no fundamental difference results from changing the sign of an incident keV particle (27).

D. Laser Desorption (LD)

The applications of lasers to mass spectrometry date back to the late 1960s and are certainly too numerous to cite here. However, information regarding the fundamental applications and instrumental configurations may be found in a review by Hillenkamp (28). Although most instruments are designed in-house, a commercially available instrument now exists (29). The instrument, known as the LAMMA (Laser Microprobe Mass Analysis), is capable of performing both

surface analysis and desorption-ionizaiton. An example of the latter is the use of laser desorption to study the glycoside digitonin (MW1228). The performance and application of the LAMMA were the subjects of a series of review articles (30,31).

The operational parameters in LD vary as much as the analytes studied. For example, the range of wavelengths used varies from 250 nm to 10.6μm, while the variation in irradiation times and power densities are 30 ps to greater than a minute and 10 to 10^{10} W/cm^2, respectively (17). Laser desorption experiments generally belong to two classes: (1) long irradiation time, low power density and (2) short irradiation time, high power density. The second set of experimental conditions are the predominant choice for the analysis of nonvolatile biomolecules because the results obtained are similar to particle impact methods. The second class usually refers to the case where the laser pulse is <100 ns and the power density > 10^7 W/cm^2. To meet these requirements the LAMMA uses a Q-switched (pulse = 15 ns) neodymium - YAG laser whose output is quadrupled in frequency to give a power density of 10^{10}-10^{11} W/cm^2 for a 0.5μm diameter spot. Proposed mechanisms for laser desorption are based upon the rapid transfer of thermal energy into the sample (32-34). Hence, power density is a far more important variable than wavelength to DI by this method. Unfortunately, several factors affecting power dissipation as well as sample/matrix effects combine to give poorer reproducibility than other DI methods (30). Also, the sample preparation and instrumentation involved with LD require more operator expertise than other DI methods such as FAB.

E. In-Beam Methods

The term "in-beam" has been loosely applied to a series of thermal methods of DI which effect desorption of molecular neutrals through rapid heating, and then ionize the sample by some auxillary means, such as an EI filament or a CI reagent gas. These methods are the subject of an excellent review article by Cotter (35). The main advantages of these methods are their simplicity and their ability to provide increased fragmentation relative to other DI methods such as FD. On the other hand, in-beam methods are generally considered to be more restricted to use with molecules of lower molecular weight and polarity than the other DI methods. They are included in this discussion both for historic reasons, and because of their impact on the current understanding of DI processes.

The most widely used in-beam method is desorption chemical ionization (DCI). Under DCI, a nonvolatile sample is coated onto the surface of a probe which is inserted into the plasma generated by a CI source, about 2-3mm from the EI beam. Upon heating, either resistively or through contact with the heated ion source, mass spectra may be obtained for several biomolecules including small molecular weight peptides and oligosaccharides (35,36). The first reported use of DCI was by Baldwin and McLafferty who obtained an $(M+H)^+$ ion and sequence information for an underivatized tetrapeptide from a glass surface (37). Later in 1975, Williams et al. used an analogous in-beam EI method to obtain both a molecular ion and fragmentation for the antibiotic Echinomycin (MW 1100) which only yielded a molecular ion by FD (38). Again, this approach operates by

positioning the probe a few millimeters from the EI beam except no CI reagent gas is present.

The first true understanding of the phenomena involved with in-beam methods was presented by Beuhler and Friedman in a pioneering paper using an "in-beam" CI method at Brookhaven National Laboratories (39). In this communication they made two suggestions for promoting the desorption of intact neutrals from nonvolatile compounds. First, since the energy input to break sample-surface attractions becomes distributed among the internal modes of the molecule, less pyrolysis occurs when samples are volatilized from low binding surfaces, such as Teflon. Consequently, several materials have been used, such as quartz, silicone gum, Vespel, and polyimide (40-42,36), to increase both the sensitivity and molecular weight range of DCI. Secondly, Beuhler and Friedman demonstrated that rapid heating of nonvolatile compounds favors desorption of intact neutrals as opposed to pyrolysis. The basis for this observation is kinetic, as can be confirmed by the data they obtained for thyrotropin releasing hormone (TRH) obtained by DCI from a copper surface and using a heating rate of 10°C/sec (Figure 1.2). Arrhenius plots for the relative abundances of the protonated molecule (m/z 363) and a decomposition product (m/z 235) indicate a competition between the rates of neutral desorption and decomposition; the former is favored at higher temperatures. The slopes of the lines support the assumption that the energy of activation for nonvolatile compounds is lower for decomposition than for evaporation. Further, if one assumes that the energy of decomposition is the rate limiting step for the desorption of a decomposed neutral, then rapid heating to an

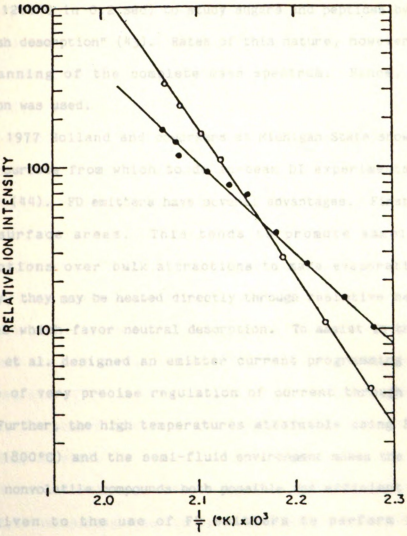

Figure 1.2 Relative intensity of the protonated molecule, m/z 363 (open circles) and a prominent decomposition product, m/z 235 (filled circles) for thyrotropin releasing hormone plotted as a function of 1/T. Data obtained by a proton transfer rapid heating technique. Reprinted from reference 39, with permission from the American Chemical Society.

elevated temperature becomes necessary to minimize this process. Taking full advantage of this data, Daves et al. used fast heating rates (1200°C in 0.2 sec) to study sugars and peptides by the method of "flash desorption" (43). Rates of this nature, however, prohibit the scanning of the complete mass spectrum. Hence, photoplate detection was used.

In 1977 Holland and coworkers at Michigan State showed that the optimum surface from which to do in-beam DI experiments was an FD emitter (44). FD emitters have several advantages. First, they have large surface areas. This tends to promote sample-surface interactions over bulk attractions to make evaporation easier. Secondly, they may be heated directly through resistive heating, and at rates which favor neutral desorption. To assist in this process, Holland et al. designed an emitter current programming (ECP) unit capable of very precise regulation of current through FD emitters (45). Further, the high temperatures attainable using FD emitters (up to 1800°C) and the semi-fluid environment makes the analysis of several nonvolatile compounds both possible and efficient (44). The name given to the use of FD emitters to perform in-beam EI experiments by Holland et al. was "electron impact desorption" (EI/D). This work led to an analogous method which incorporated FD emitters as surfaces for in-beam CI called CI/D (46).

F. Ion Formation from Solutions

The final section in this discussion of DI methods concerns two methods which sample ions that exist in solution: electrohydrodynamic

ionization (EHMS) and thermospray (TSP). The first method, EHMS works by extracting ions from a liquid meniscus at the end of a capillary tube using strong electric fields. The voltage used to create molecular ions is usually 7.6 kV and is strongly dependent on the solution from which desorption-ionization occurs; the greater the conductivity, the lower the droplet size produced and the larger the yields of molecular ions. EHMS essentially operates by extracting droplets from solution which desolvate to yield smaller clusters and ions from the analyte as a result of the influence by the electric field. The most widely used liquid support is NaI in glycerol which promotes formation of analyte ions typically under 1000 amu. Factors affecting this process have been addressed by Chan and Cook (47). Since the introduction of this method by Evans and coworkers in 1972 (48), EHMS has been applied to amino acids, sugars, nucleosides and peptides; all of relatively low molecular weight. Fragment ions are generally not observed which is one reason why the technique has not been widely adopted.

The second method, thermospray, also forms analyte ions from an electrolyte-containing solution by a desolvation mechanism, but uses heat instead of an applied field to promote the process. During thermospray, the analyte-containing liquid is forced through a heated metal nozzle ofdiameter 150μm to produce a supersonic jet vapor which effects desolvation. Originally, this approach was to be used as the method of solvent removal for an LC-MS interface which incorporated EI as the mode of ionization. However, Vestal soon reported thermospray as a method for desorption-ionization after it was noticed that superior results were obtained with the EI filament off

(49). Ensuing investigations showed that analyte ions could be formed by this process if the solution had a sufficient ionic strength. The current understanding of this method of ion formation from liquid droplets has been outlined by Vestal in a review article on DI methods (17). At present, thermospray is rapidly becoming the most widely employed inerface for LC-MS; particularly for reverse phase HPLC where analytes are frequently too nonvolatile for conventional methods. Also, as opposed to other approaches to LC-MS, thermospray can accomodate normal flow rates (2 ml/min) to obtain maximum sensitivity. Papers which address operational principles and the optimization of thermospray are also available (50,51).

III. Background Information About FAB

A. Analyte Ion Types

FAB, like all DI methods, is known for producing large abundances of molecular ions which may exist in a variety of forms. Similar to CI, the molecular ion most commonly takes the form of the protonated molecule $(M+H)^+$. In the negative ion mode, one typically observes $(M-H)^-$ as the molecular species. The ability to produce both positive and negative ions with nearly equal facility (52) is advantageous to both molecular weight confirmationand structural elucidation by FAB. The charge polarity of the ions produced depends largely on the acidity/basicity of the molecule, the matrix used, and the chemical environment within the matrix. For example, the addition of an acid to the matrix can increase the concentration of

protonated molecules both in solution and ultimately in the gas phase; provided that hydrolysis is not a problem. Conversely, if the molecule is an acid the best strategy is to add base to enhance negative ion formation. For example, the formation of a carboxylate anion is essentially equivalent in many cases to forming $(M-H)^-$. In either case, pre-ionization is favorable from a thermodynamic point of view because energy to ionize the molecule does not have to be provided from the atom beam.

Other frequently observed ion types arise from the process of cation attachment. Conversely, negative ions are formed from the attachment of anions present in solution. Conceivably, any singly-charged cation or anion may be used. In the positive ion mode the alkali, silver, and ammonium cations are frequently used examples. Biological samples, for instance, often generate $(M+Na)^+$ and $(M+K)^+$ ions due to the ubiquitous presence of sodium and potassium in nature. In analogous fashion, negative ion adducts reflect the singly-charged anions in solution where the most common example is $(M+Cl)^-$. A standard procedure in FAB is to promote the formation of molecular ions by judiciously adding the appropriate salt to the matrix. In the positive ion mode, both ammonium and alkali salts tend to form adducts which are more stable than the protonated molecule to effect greater sensitivity. An important example is oligosaccharides where protonation at a hydroxyl group can lead to a loss of water, whereas the addition of NaCl often leads to intense natriated adducts. In some cases this can lead to a decrease in desired fragmentation, however, because alkali adduct ions tend to be more stable than their protonated counterparts (53). Also, it may be advisable to remove

excessive sodium from biological samples because it can promote chemical interference (15).

Other types of alkali adducts exist. For example, $(M+2Na-H)^+$ ions frequently arise as do $(M-Na)^-$ ions. The former occurs generally when excess sodium is present and may also be viewed as the sodium adduct to the intact salt of the analyte. The latter corresponds to the anion formed from the loss of sodium from a salt, where M in this case would be the molecular weight of the salt. Often, the abundance of sodium-containing adducts increases as the matrix burns out which may be explained in terms of relative concentration and proximity of sodium in the sample. In contrast, ions depending on the matrix, such as $(M+H)^+$ or $(M+glycerol+H)^+$ fade as the more volatile matrix either evaporates or becomes sputtered away. A detailed study of the chemistry of cation attachment in FAB, published by Keough, is available to the concerned reader (54).

Although several ion types exist in FAB, there is one simplifying rule: the products observed are almost exclusively singly-charged. For instance, since quaternary ammonium compounds already contain a positive charge, the ion observed is the molecular cation (M^+) instead of $(M+H)^+$. This even electron species should not be confused with the odd electron molecular ion $M^{\ddagger}$ produced in electron impact and field desorption. Besides salts, the other place where M^+ ions exist is in the FAB analysis of transition metal complexes (55-59). Presumably M^+ ions are formed because of the low ionization potentials of the metals involved. Yet, it has been widely documented that even when higher valences are present in solution the resulting ions produced by FAB almost invariably have a

+1 charge. This is not clearly understood at present. The obscurity of multivalent ions in FAB is not just particular to organometallics. In fact, very few cases have been reported for even divalent species. For example, large peptides sometimes yield diprotonated ions $(M+2H)^{2+}$. However, because divalent ions are routinely observed in DI techniques where fields are present (EHMS, FD, TSP) it has been suggested that fields are necessary to overcome the attractive forces holding the cation to the condensed phase (60). Another explanation is that in some cases there may not be sufficient energy available to the molecule under the conditions of FAB to surpass the second ionization potential of organic molecules.

In addition to granting molecular weight confirmation, FAB spectra can afford considerable structural information. In certain cases, such as peptides, the modes of cleavage are well documented (61). Apart from the biopolymers, however, the rules of fragmentation by FAB are less established, especially when compared to electron impact. Generally, the best approach is to start with logical inductive and homolytic cleavages and to try to account for the observed fragment ions using general rules for ion stability (62). Somewhat surprisingly, however, the reproducibility of the fragmentation patterns observed by FAB were shown by an interlaboratory study to be as reproducible as those by EI (63).

While FAB exhibits more fragmentation than some DI techniques, such as FD, the extent of fragmentation is sparse compared to EI. In fact, the internal energies of most ions are only on the order of a few electronvolts. While this amount is sufficient for many smaller molecules, a problem arises when molecules exceed about 2000-3000u.

Here, the amount of available energy becomes partitioned between too many vibrational modes to provide adequate fragmentation (64,65). Hence, incomplete sequence information may result in these cases. One method for producing more fragmentation (regardless of molecule weight) is to use an excessive concentration of analyte. This effect may be the result of a limited capacity by the matrix to act as an energy buffer under high analyte concentrations. Nonetheless, since this is certainly not a desirable approach, research needs to be done in the areas of promoting and predicting fragmentation by FAB.

B. FAB Matrices

Because of the importance of matrices to the FAB process, a brief overview shall be given which introduces the major classes of compounds used and their applications. A more complete review was published by Gower, and should be read by anyone interested in performing FAB (66). The structures of the compounds discussed shall not be listed here as they are easily obtained in the references given.

As indicated in the initial discussion of FAB, the quality and, to some extent, the very existence of FAB spectra may be attributed to the use of a matrix. While glycerol is by far the most widely used viscous liquid, many other compounds have been tested since the scope of analysis by FAB is a direct function of available matrices. Glycerol may be used to illustrate several important properties of matrix compounds. First, it has the proper physical properties which may include such things as viscosity, surface tension, vapor

pressure, and fluidity. Many of these properties are critical to the longevity of a FAB analysis. For example, a matrix must not only be able to replenish the analyte sputtered during bombardment, but it also cannot be too volatile so that acceptable lifetimes may be obtained. Further, it is almost imperative that the matrix act as a solvent for the analyte to be studied. Part of the reason for the amazing sucess of glycerol is that it is a ready solvent for many classes of polar molecules. In cases where solubility in glycerol has been marginal, successful analyses have been reported when a co-solvent is added with the analyte to the matrix to increase solubility. Examples include: alcohols, DMSO, and DMF. In one example where chlorophyll-a was totally insoluble in glycerol, Triton X-100, an alkylphenylpolyethylene glycol, was used as a solubilizing agent to procure a successful analysis (12).

Probably the second most widely used matrix is thioglycerol (3-mercapto-1,2-propandiol). Although it is more volatile than glycerol, it has been extensively used in the analysis of peptides because it frequently gives results superior to glycerol. As an example, Lehmann et al. reported at least a 5-fold enhancement in sensitivity relative to glycerol in the analysis of angiotensin (67). Thioglycerol has also been used as the solvent of choice for a variety of applications including a series of cationic technetium and iron complexes (58). In another study, the glycerol analog aminoglycerol was found to be useful for certain glycopeptides that gave unsatisfactory results using glycerol (66).

Another important class of matrix compounds, the polyethylene glycols (PEG), have been used in selected applications; usually in

cases involving molecules which are more nonpolar. A mixture of 400 and 600 molecular weight fractions is typically used to achieve the proper viscosity. Rose et al. demonstrated the use of PEG as a matrix for both positive and negative ion spectra of small oligosaccharides (68). In another study Przybylski used PEG as the matrix to analyze a hexapeptide (69) as well as peptide antibiotics of lower polarity. For compounds too nonpolar to dissolve in glycerol, Rinehart suggests the use of the various PEGs such as tetragol and for extreme cases the methyl ether analog, tetraglyme (70).

The related compounds diethanolamine (DEA) and triethanolamine (TEA) have been used in numerous applications and are often suggested for use in negative ion FAB because of their inherent basicity. Both DEA and TEA have been used extensively in applications involving saccharides (71,72) and antibiotics (73). In another application, Meili and Seibl reported the use of either DEA or TEA to analyze for folic acid after glycerol had failed (74). Further applications of these matrices include: unsaturated fatty acids, surfactants, steroid glycosides, and glycosphingolipids.

A unique area of FAB application is to the area of organometallic complexes. Several new matrices have been tested for use in this area with varying degrees of success. A matrix of 90% 18-Crown-6 and 10% tetraglyme has found several applications since its introduction by Minard and Geoffrey (75). Several other matrices have been reported for use when glycerol and thioglycerol have failed. For example Davis et al. have used both diaminophenol (DAP) and even the GC stationary phase Carbowax 200 for certain transition metal

complexes (55). The matrix material tetramethylene sulfone (sulfolane) has been used by Unger (58) and later by Bojesen (59) in attempts to analyze a variety of transition metal complexes. In the more selected application to rhodium and osmium complexes thio-2,2'-bis (ethanol) has been reported as a viable matrix when glycerol fails (66), while the rhodium complex Wilkinson's catalyst was successfully analyzed by Davis et al. (55).

Finally, several miscellaneous materials have been reported as matrix compounds for FAB. Compounds in this category often address a problem area in FAB where compounds are too nonpolar to be analyzed in glycerol, but are too nonvolatile for conventional methods of ionization. In the early stages of FAB viscous liquids found in the laboratory such as Apiezon oil or diffusion pump oil (polyphenylether) were tested for this purpose but yielded marginal success. Perhaps the best matrix in this category is a 5:1 mixture of the solids dithiothreitol to dithioerythritol which, when combined, form a viscous liquid at room temperature. The success of this matrix has prompted the investigators who discovered it to name it the "magic bullet" (76). Meili and Seibl reported the use of several other compounds which gave varying results where glycerol had failed (74). Among these were triethylcitrate (TEC), dibutylsuccinate (DBS), linoleic acid (LA), oleic acid (OA), squalene (SQ), and o-nitrophenyloctylether (o-NPOE). Probably the most useful compounds in the category are TEC and o-NPOE. In a subsequent communication, these authors reported on the success achieved for nonpolar compounds when using 80% p-nitrobenzylalcohol/20% 1,2,4-trichlorobenzene as a matrix (77). This matrix was used by

Vetter and Meister to analyze the very thermally labile compound β-carotene (78).

C. Applications

The purpose of this section is to serve as a reference source for the several classes of nonvolatile compounds analyzed by FAB. Detailed information regarding these applications, such as fragmentation pathways, may be obtained from the references given. The applications discussed are divided into two categories. The first deals with the analysis of biopolymers and the second portion with other non-oligomeric application. It should be emphasized that the applications covered here are not intended to be a complete listing of work done to date.

Biopolymers

This section describes applications of FAB-MS to three types of oligomers: peptides, saccharides, and nucleotides.

Peptides

By far, the most widely studied group of compounds by FAB is peptides. Because of their tendency to carry a net charge, peptides are readily analyzed with good sensitivity. Molecular weight confirmations can routinely beobtained with 0.1-10nmol for most peptides (79). Furthermore, the tendency of peptides to cleave at the relatively labile amide linkages makes direct sequencing possible because either the N- or C-terminus is retained in each fragment ion.

In other words, fragmentation begins at either end of the molecule and proceeds in consecutive fashion. The ability to observe positive and negative ions with comparable facility grants added confirmation to proposed assignments. Complete sequences have been obtained, with as little as 1-10nmol, for peptides up to about 10 amino acids in length (79,80). As the size of the peptide increases, however, the amount of internal energy available is insufficient to result in complete fragmentation. This, coupled with the problem of matrix interference, often leads to incomplete sequence information by FAB. Hence, FAB must play a supporting role in the sequence analysis of larger peptides, especially when analyzing unknowns. For instance, FAB is routinely used to expedite peptide sequencing by granting sequence information on smaller peptides produced from enzymatic cleavage of a larger parent peptide or protein.

FAB has been a welcomed addition to the arsenal of methods for peptide sequencing because traditional methods are often more tedious and labor intensive. In the most common approach, known as Edman degradation, amino acids are cleaved in succession and analyzed by HPLC as their phenylthiohydantoin derivatives. Because this process may only be performed on relatively small peptides, larger peptides are first hydrolyzed into pieces amenable to this technique. If this process is repeated using different peptidase enzymes, each performing specific cleavages, the original peptide sequence may be deduced from the overlap in the individual sequences obtained.

Mass spectrometry provides a useful complement to the Edman technique, especially in cases where a blocked N-terminus prevents this wet chemical approach. Additionally, mass spectrometric

analysis may be carried out more quickly, since a complete sequence of up to 10 amino acids may be possible from one analysis. Prior to FAB, peptide analysis strategies were developed using GC-MS. This approach has the added advantage that mixtures of small peptides may be analyzed. The major drawback to this method is that ionization by EI or CI requires extensive chemical derivatization to enhance the volatility of the peptides studied. The two most frequently prepared derivatives are N-acetyl-N,O-permethyl analogs (81) or a reduction to trimethylsilyl polyaminoalcohols (82). Although these methods yield reliable sequence information, about 40 nmol is required for each peptide component to be analyzed. FAB, in contrast, enables direct equence determination to be made on peptides of similar length usually with less material.

The fragmentation patterns of peptides by FAB have been documented by numerous investigators. However, the schemes for naming the types of ions produced are almost as abundant as the number of investigators. Recently, a common nomenclature was proposed by Roepstorff which has become fairly well adopted (61). The general scheme is shown in Figure 1.3. As indicated, the three possible cleavage points about the peptide bond are called A, B, or C when the charge is retained at the N-terminal side of the fragment, and X, Y, or Z when the charge resides on a C-terminus containing fragment. Subscripts are used to specify the amino acid where cleavage occurred. Finally, since ion formation is frequently accompanied by the transfer of one or more hydrogens, the number of hydrogens transferred is indicated by the number of primes present as superscripts.

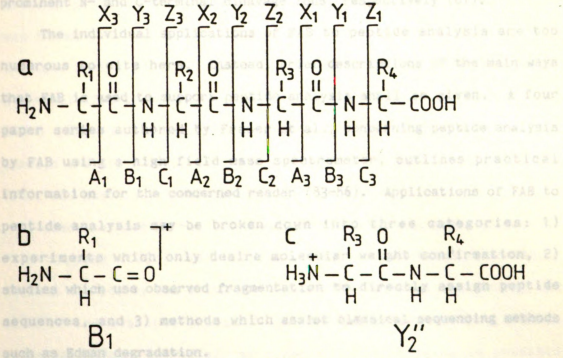

Figure 1.3 Nomenclature proposed by Roepstorff for peptide fragmentation. Reprinted from reference 61, with permission from Wiley Heyden.

In addition to sequence information, confirmation of the amino acids present in the peptide is possible from their presence as protonated iminium ions in the FAB mass spectrum. For example, the A_1 ion shown in Figure 1.3 corresponds to the protonated iminium ion for the N-terminal amino acid. Present in the lower part of Figure 1.3 are structures assigned as B_1 and Y_2, which are often the most prominent N- and C-terminal cleavage ions, respectively (61).

The individual applications of FAB to peptide analysis are too numerous to cite here. Instead, brief descriptions of the main ways that FAB is used to support peptide analysis shall be given. A four paper series authored by Fraser et al., concerning peptide analysis by FAB using a high field mass spectrometer, outlines practical information for the concerned reader (83-86). Applications of FAB to peptide analysis may be broken down into three categories: 1) experiments which only desire molecular weight confirmation, 2) studies which use observed fragmentation to directly assign peptide sequences, and 3) methods which assist classical sequencing methods such as Edman degradation.

As part of the first category, FAB has been used to observe molecular ions from peptides exceeding 5000 in molecular weight. Such confirmations have been made possible by advances in high field magnet technology. Recent developments have pushed the mass range of magnetic sector instruments past 10,000u. Analyses above mass 2000 are complicated by the contribution from isotopes, whose summed abundance becomes significant at this point. Hence, a molecular cluster of peaks is observed, where the most abundant peak is not at the monoisotopic mass of the $(M+H)^+$ ion. Generally, the most

abundant mass is shifted up by one mass unit above m/z 2000, two mass units above m/z 3200, and three mass units for ions greater than m/z 5000 (84). Thus, confirmation depends upon matching an observed cluster to theoretically calculated intensities. Figure 1.4 displays the molecular ion cluster for porcine insulin (MW 5773.63) obtained using repetitive scanning over the molecular ion region (87). Several peptides have been analyzed by this approach. The largest was human proinsulin (MW 9390) (88). Other insulins observed include: bovine (MW 5729), equine (MW 5743), and ovine (MW 5699) (87). A partial list of other peptides observed includes: monellin II (MW 5831) (89), bovine parathyroid hormone (MW 4106) (84), the β-chain of insulin (MW 3495) (90), glucagon (MW 3480) (91), mellitin (MW 2844) (91), and gastrin I (MW 2906) (92).

Also included in the first category is a general approach called "FAB mapping" (93). FAB mapping refers to the process of screening protein digests by FAB either to provide fast answers concerning the size of the peptides produced, or as a method for verifying peptide sequences deduced previously by other methods. Mapping is possible because small mixtures of peptides may be analyzed directly from enzymatic digests to give predominantly molecular ions, and little or no fragmentation. Further, FAB covers a sufficient range in mass to make this approach a viable method to study proteins of appreciable size. However, because FAB mapping relies on the assumption that FAB can be used to analyze small mixtures, caution should be exercized because results suggest this method is only semi-quantitative (93), and can be unreliable (94). The applications of FAB mapping are quite diverse. In one study, Self and Parente used FAB to follow the

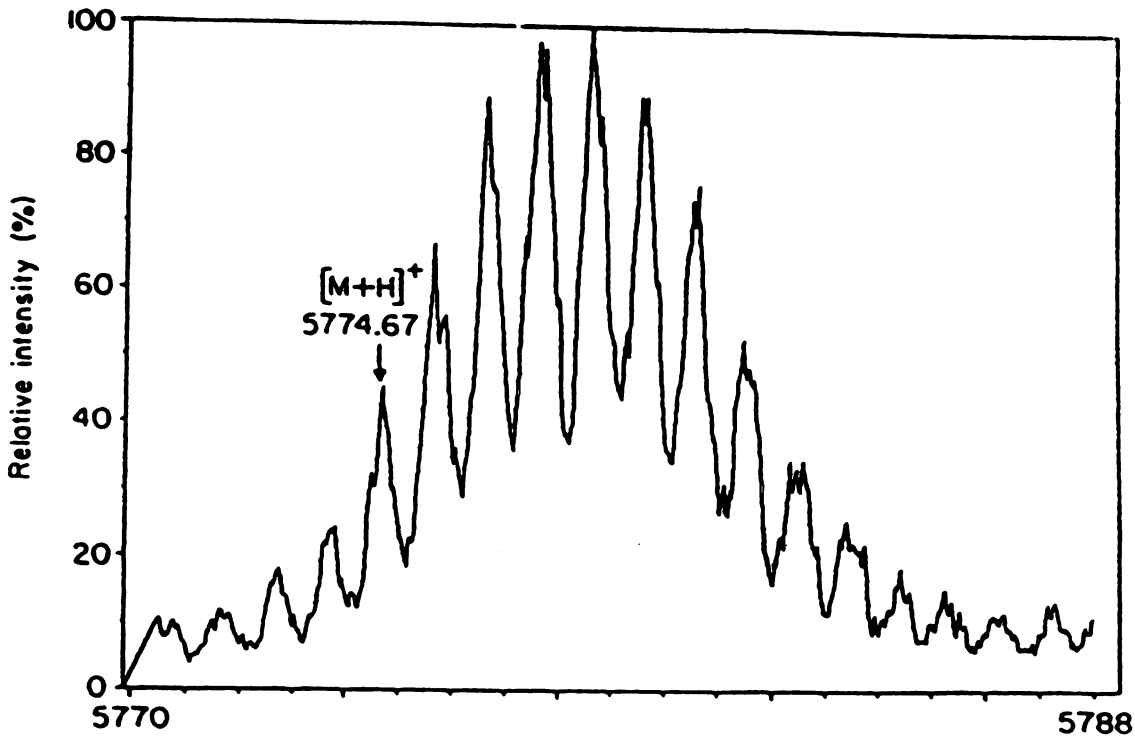

Figure 1.4 Molecular region of the positive ion FAB spectrum of porcine insulin, showing the isotope distribution for the protonated molecule. Reprinted from reference 87 with permission of Wiley Heyden.

time course of the exopeptidase digestion of a protein from the papaya mosaic virus by removing aliquots at intervals and recording changes in the FAB mass spectra produced (95). Since exopeptidases perform successive cleavages from a given terminus, peptide sequences may be determined in this manner. Caprioli and coworkers showed that enzymatic digestion may be viewed in real time by continually collecting FAB spectra as a digestion proceeds in glycerol on the probe tip (96).

Other applications of mapping involve the confirmation of proposed sequences for large proteins. For example, Shimonishi et al. demonstrated that over 90% of the sequences of two lysozymes (MW > 3000) could be confirmed by the direct FAB analysis of 5μg of a trypsin/CNBr digest (97). In other unrelated studies, the protein products from a recombinant DNA procedure (98), and structural variants of hemoglobin (99) were examined by FAB mapping. Perhaps the most impressive work has been done by Biemann who used mapping to check the primary sequence of several proteins predicted previously by DNA sequencing. Because nucleotide sequencing is more rapid than protein sequencing, this method is used to obtain protein sequences whenever the gene which codes for the protein may be identified. The problem is that nucleotides outnumber amino acids 3 to 1 giving a greater chance for error. While some errors will only change the assignment of one amino acid, error involving shifts in the reading frame may alter large sequences. FAB may therefore be used to quickly test reported sequences by digesting the protein and looking for predicted masses from the peptides produced. Using this approach, Biemann identified an error in the reported sequence of

glutamine-tRNA synthetase (550 amino acids long) (100). Finally, by a similar procedure, Beckner and Caprioli verified nine regions ranging from 13 to 42 residues in a bacteriophage P22 tail protein, 667 amino acids in length (101).

The second class of methods for peptide analysis relies on fragmentation produced during FAB to enable sequence determination. The basic approach here is to digest larger peptides down into pieces which may be fully sequenced by FAB. In this case, the mixture must be separated into individual components whose FAB spectra are obtained. While HPLC is usually used for this purpose, in some cases the mixture analysis capability of MS/MS can provide another alternative. The largest drawback to this general approach is that sequence information by FAB may be incomplete as a result of insufficient fragmentation or matrix interference. MS/MS is very helpful in this regard, since it can select for a desired parent ion (e.g., $(M+H)^+$), and record its daughter ion spectrum following a process known as collisionally activated dissociation (CAD). This process gives more reliable structural information. The details of this process are illustrated in Chapter 2 where the added selectivity of MS/MS is presented as a method for eliminating matrix interference.

Complete sequences for peptides up to 10 residues in length have been reported without the aid of MS/MS. Common examples include the angiotensins (102), the enkephalins (52), and the bradykinins (80). Sequencing in this fashion typically requires both positive and negative ion data, a pure sample, and at least 10 nmol of the peptide. In the examples listed, however, the sequence was known a priori. A

study of 16 small peptides by Roepstorff et al. concluded that when dealing with unknowns, the maximum length which may be accurately sequenced by FAB is 6 amino acids (103). In addition, the amino acid pairs leucine and isoleucine (MW 113) and glutamine and lysine (MW 128) can not be distinguished by FAB.

Because of the uncertainty of FAB for providing sequence data, FAB-MS/MS has become quite popular. Although controlled fragmentation grants more complete sequence information, the process is still limited to about 10 amino acids, and usually requires more extensive metastable mapping to verify a longer sequence. While the approach to MS/MS varies, the most frequently used strategy is to record the daughter ions of a selected parent by a linked scan approach on a double-focusing instrument. For example, Eckart used the B/E linked scan method to unambigously sequence the 5-residue peptide adipokinetic hormone I in less than 4 hours (104). Other reported examples include: angiotensin I and II (102), leu-enkephalin (105), met-enkephalin (106), neuropeptide substance P (107), antiamoebin I (106), cyclic peptides (108), a synthetic heptapeptide (109), and a series of other synthetic peptides (110). To aid such determinations, a computer program (PAAS 3) was introduced to generate probable sequences for peptides sequenced by FAB (111).

As a third role in peptide analysis, FAB may be used to assist classical, wet chemical approaches to peptide sequencing. Such approaches typically involve the cleavage and analysis of amino acids in succession from a particular terminus to sequence small peptides. FAB is then used to provide a rapid answer after each step. In one procedure, dansyl amino acids are prepared by reaction with the

N-terminus of a peptide, and subsequent cleavage. Beckner and Caprioli showed that dansyl amino acids may be quantitatively analyzed by FAB at the 0.1 nmol level (112).

The more common approach is Edman degradation. Again, a reaction occurs at the N-terminus, followed by cleavage to yield a derivative of the amino acid. Benninghoven demonstrated the use of SIMS to identify phenylthiohydantoin amino acids produced by this method (113). However, a more viable approach, developed by Bradley et al., uses a strategy called "subtractive" Edman degradation (114). In this procedure, an aliquot is removed from the reaction mixture, and analyzed by FAB to determine the weight of the amino acid lost. By analyzing for the peptide instead of the derivatized amino acid the procedure is simplified and hence more expedient. For peptides too long to be sequenced by the Edman technique, Bradley et al. suggest the combined use of carboxypeptidase digestion (to sequence C-terminal amino acids) with subtractive Edman degradation.

Saccharides

Similar to the analysis of peptides, oligosaccharide analysis by FAB provides a very fast and convenient method for obtaining molecular weight and structural information without the need for derivatization. Although oligosaccharide spectra have been reported on molecules exceeding 6000u, the sensitivity is normally lower than observed for peptides. This difference, which can be as large as an order of magnitude, probably reflects differences in pre-ionization. While $(M+H)^+$ and $(M-H)^-$ ions are observed, the best sensitivity occurs for adducts such as $(M+Na)^+$ and $(M+Cl)^-$. The influence of

matrix basicity and alkali cation selection on the adduct formation have been investigated by Puzo and Prome (71,115). They demonstrated that cationized saccharide molecular ions arise in part through gas phase desolvation.

Fragmentation pathways for oligosaccharides have been documented (116). The most important, and abundant, fragmentation involves cleavage of the glycosidic bond between the anomeric carbon and the interglycosidic oxygen of the glycosidic bond. This reaction occurs in both the positive and negative ion mode, and is accompanied by a hydrogen migration to the interglycosidic oxygen. Thus, the loss of a hexose corresponds to a decrease of 162 mass units. As a consequence, insufficient information is available to discriminate between stereoisomeric monosaccharides, such as glucose and galactose. Further, the position and configuration of the glycosidic linkages can not be defined. On the other hand, residues which differ in mass, such as hexose and pentose subunits, can be distinguished as can linear versus branched polysaccharides.

In addition to these problems, incomplete sequence data is a problem,especially for larger oligosaccharides. Hence, MS/MS is an attractive option. Carr and coworkers, in a paper which discussed structural determination of oligosaccharides by FAB MS/MS, displayed specific oligomeric sequence information not observed under normal FAB (65). Their work also suggested that carbohydrate composition can strongly influence fragmentation. For example, sequence-specific fragments are often absent or in low abundance in the FAB spectra of N-linked, high manose oligosaccharides. In contrast, partially methylated oligosaccharides from a mycobacterial glycolipid, analyzed

by Dell and coworkers, gave abundant sequence-related fragmentation (117). As a result of this observation, Dell et al. prepared permethylated derivatives for use in FAB and demonstrated their usefulness in directing fragmentation (118).

In addition to using MS/MS to obtain sequence data, Puzo et al. showed that MIKES spectra can be used to distinguish stereoisomeric hexoses (119). By their approach, the relative abundance of the products from unimolecular dissociation of (hexose-Na-matrix)$^+$ clusters was used for isomer identification. Unfortunately, it is unlikely that this approach can be extended to polysaccharides.

Several applications of FAB to oligosaccharide sequencing have been reported. However, because complete structural elucidation is not possible, FAB is again relegated to a supporting role. In many instances, the saccharides studied were the glyco portions of glycolipids and glycoproteins. Dell and coworkers obtained FAB spectra of deca-, dodeca-, and tetradecasaccharides isoalted from the urine of a patient with gangliosidosis (118). No sequence information was present without permethylation. Dell and Ballou also obtained FAB spectra for several lipopolysaccharides including a mycobacterial 6-O-methylglucose polysaccharide (MW 2852), which aided in a structural analysis that revised a previous structure proposed for this molecule (120). In other investigations, these workers analyzed blood group glycosphingolipids and some permethylated glucans exceeding m/z 6000 (118).

Kamerling et al. applied FAB to a series of underivatized oligosaccharides and glycopeptides derived from glycoproteins of the N-glycosidic type; sequence data was reported and discussed (116).

Finally, many of the oligosaccharides studies by Carr and coworkers were of glycopeptide origin. As an example, FAB spectra were presented for linear and branched hexasaccharides from a blood group A active glycoprotein (65).

Nucleotides

The third general class of oligomers routinely studied by FAB is oligonucleotides. Because of their size, polarity, and extreme thermal laibility, it is easy to understand why conventional forms of mass spectrometry are seldom used for nucleotide analysis. However, FAB enables molecular weight confirmation and complete sequence data to be obtained for nucleotides up to 10 residues in length, on as little as 10 nmol (121). Also, FAB is helpful whenever nucleotides contain either a naturally or synthetically blocked terminus which precludes sequencing by chemical methods.

Another area of intense investigation is the use of FAB to monitor the products of oligonucleotide synthesis. Ulrich and coworkers showed that FAB is useful in monitoring a condensation step in oligonucleotide synthesis (122). Their method enabled analysis of three synthetically protected dinucleotides involved in synthesis, and also enabled detection of unwanted side products. In other similar studies, the FAB spectra of several mono-, di-, and trinucleotides have been recorded to show the viability of FAB as an aid to oligonucleotide synthesis (123-125). In one of these studies, FAB-MS/MS allowed two unblocked isomeric deoxynucleic acid dimers to be differentiated (123).

Since many nucleotides are analyzed as salts, several cation adducts are possible, such as $(M+Na)^+$ and $(M+2Na-H)^+$. Other positive ions include $(M+H)^+$, $(M+G+H)^+$, and in some cases protonated or natriated dimers. Negative ions, on the other hand, may include $(M-H)^-$, $(M+G-H)^-$, and sometimes the doubly charged species, $[M-2H]^{2-}$. The general consensus is that negative ion spectra are more sensitive, structurally informative, and easier to interpret. Often times the $(M-H)^-$ ion is the base peak in a negative ion spectrum, which indicates that considerable pre-ionization occurs at the phosphodiester moiety (123). In addition, facile cleavage about the phosphodiester linkage creates very predictable sequence information.

Grotjahn and coworkers made extensive use of this fragmentation pattern to sequence several oligonucleotides in the negative ion mode (121,126). The bonds most likely cleaved in this process are the bonds between the carbon of a sugar moiety and the phosphate oxygen. Two possibilities exist depending upon which side of the phosphodiester linkage cleavage occurs. Hence, the major fragments produced have either a 3'- or a 5'-terminal phosphate. Grotjahn et al. observed that 3'-phosphate sequence ions are always more abundant than corresponding 5'-phosphate sequence ions having the same number of nucleotide units. This simple fragmentation behavior allows direct sequencing from either the 3'- or the 5'-end (bidirectional sequence analysis).

FAB sequencing in the negative ion mode is presently the fastest method for sequencing small oligonucleotides (e.g., $\leq$ 10 residues) (126). Because of several advances in DNA synthesis methodologies, it appears that sequence analysis is the rate limiting

step in the overall process. Therefore, the use of FAB for oligonucleotide analysis should steadily increase, particularly in the areas of high mass and/or MS/MS.

Other Applications

In addition to biopolymer sequencing, FAB has been used in numerous applications. The range of compounds studied is quite large as are the nature of the investigations. Some compound classes, for example, coordination compounds, were mentioned previously in the context of FAB matrix applications. For the sake of brevity, only the general classes of compounds shall be referenced here. A partial list includes: antibiotics (127-130), amino acids (131,132), bile salts (133), ceramides (134), dyes (135-137), glucosinolates (138), glucuronides (142-143), glycosides (144-147), glycosphingolipids (134,148), hydrocarbons (12), lead isotopes (149), leukotrienes (150), macrocycles (151,152), molten salts (153), mycotoxins (154,155), organometallic complexes (55-59) pharmaceuticals (15,156-158), phospholipids (159-162), porphyrins (163,164), retenoids (78,165), salts (166-169), surfactants (170-172), and vitamins (173,174).

D. Fast Atom Sources

Although several varieties of FAB sources exist, all have one thing in common. Fast atoms are produced from the neutralization of fast ions. Two primary mechanisms for neutralization are believed to

be operative; the extent to which each occurs is governed by the mode of operation of the particular atom gun. The first, known as resonant charge exchange, occurs whenever fast atoms become neutralized by "near-miss" collisions with neutral atoms having only thermal energies. The result of these encounters is the production of fast atoms which suffer little or no loss in forward momentum. While center-of-mass collisions occur, the chance of these events producing particles with both the proper energy and direction to bombard the sample is remote.

$$\underset{\text{fast}}{Xe^{+}} + \underset{\text{slow}}{Xe^{\circ}} \longrightarrow \underset{\text{fast}}{Xe^{\circ}} + \underset{\text{slow}}{Xe^{+}}$$

Resonant Charge Exchange

The earliest fast atom sources, such as that used by Devienne and Roustan for molecular beam solid analysis (MBSA), relied on resonant charge exchange. Their design contained separate chambers for ion production and neutralization (175). Fast ions were formed and accelerated in a "duoplasmatron" ion source which used a filament to effect ionization. The ions were then neutralized with 10-30% efficiency in a separate chamber containing 10^{-3} torr of the same gas used to create the fast ions. Afterwards, the transmitted ions were purged from the beam by electrostatic deflection.

The second mechanism for neutralization is that of resonant electron capture. Here fast ions become transformed into fast atoms

through encounters with slow moving thermal electrons. Little or no loss in forward momentum occurs because of the low mass and energy of thermal electrons. This interaction, depicted below, is believed to be the primary method for producing fast atoms in saddle field FAB sources.

$$Xe^{+}_{\text{fast}} + e^{-}_{\text{slow}} \longrightarrow Xe^{\circ}_{\text{fast}}$$

Resonant Electron Capture

The saddle field fast atom source, produced commercially by Ion Tech, Ltd., is presently the most widely employed design (176). This source is also referred to as a "cold cathode" FAB gun since the electrons are initially produced through a discharge by the reagent gas instead of a filament. The mechanism of operation is shown in Figure 1.5. Neutral gas atoms flow into the gun where they encounter a washer-shaped anode which may acquire a potential of up to +10 kV. A discharge occurs under these conditions (10^{-4} torr) to produce a plasma containing ions, atoms, and electrons. While theions formed become accelerated toward the cathode held at ground, the electrons produced oscillate through the saddle point of lowest potential, located at the center of the anode, and are held in place. This method of producing an oscillating cloud of electrons is not unique to this application, but had been developed previously for unrelated investigations (177). The source of electrons is believed to be sustained by either further discharge, or by secondary emission of

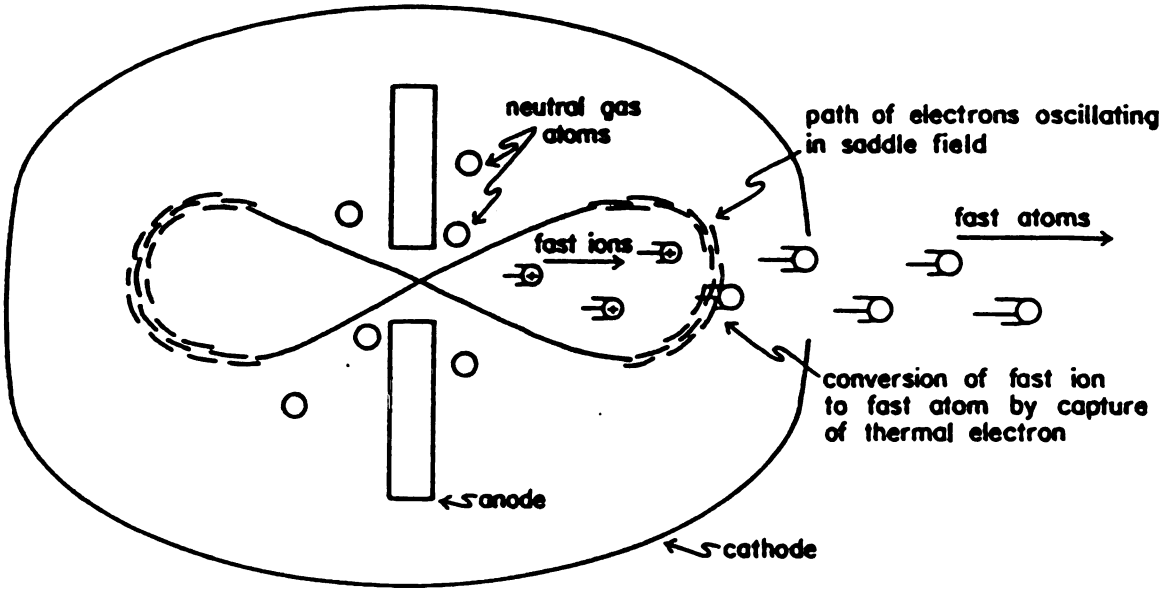

Figure 1.5 Schematic diagram of FAB gun using resonance capture of thermal electrons in a saddle field to convert fast ions to fast atoms. Reprinted from "Introduction to Mass Spectrometry" by J. T. Watson with permission from Raven Press.

electrons as fast particles collide with the walls of the chamber. Fast atoms are then produced by resonant electron capture near the aperture of the gun. The energy of the resultant fast atoms depends on how much acceleration the ion incurred prior to neutralization. The most probable point of capture is where the electrons reverse direction since their velocity at this point is zero. The fast atoms produced (with the proper trajectory) exit the gun enroute to the ion source of the mass spectrometer. The degree of transmitted ions is the subject of controversy. While Ion Tech claims almost complete conversion, Ligon demonstrated a substantial yield of ions are transmitted. Using xenon, Ligon detected ions of energies up to 30keV resulting from multiple charging, as well as ions of up to 3keV less than the applied voltage (178).

The saddle field source, which is about 10cm in length, must be mounted on an available port on the mass spectrometer. Also required is a line-of-sight entry for the atom beam into the ion source and a probe capable of inserting a sample in contact with the atom beam. Depending on the instrument, conversion to FAB can either be relatively simple or a dedicated and expensive project.

In response to the problems associated with installation of a saddle field FAB gun, Rudat introduced a source of simpler design known as the fast atom capillaritron source (FACS), or simply the capillaritron (179,180). The capillaritron, marketed by Phrasor Scientific, Inc., is a smaller source capable of fitting right inside the ion source of a mass spectrometer and is based upon a design introduced by Mahoney et al. (181,182). Originally the capillaritron was introduced as a simple sputtering device for SIMS, but was

applied to FAB analyses when it was discovered that a considerable amount of fast atoms were also produced (182). Although a larger pumping capacity is needed to remove excess gas, this gun is easier to implement since no extensive modification to the ion source housing is required.

A diagram of the capillaritron is shown in Figure 1.6. Gas is introduced through a capillary tube whose poential may range between 2 and 10kV. Ionization of the gas occurs as neutral atoms flow through the tappered nozzle of the gun which has an orifice diameter of only 25μm. The field, estimated to be 10^4V cm^{-1} at this point, helps generate and sustain a plasma in the region around the nozzle. The ions formed are immediately accelerated toward the counter electrode held at ground. Charge transfer occurs in the region just past the nozzle where a high concentration of ions and neutrals exist. Capillaritron sources are known to transmit a high content of fast ions unless they are removed by the deflectron plates.

Recently, Perel and Mahoney at Phrasor Scientific, Inc., developed a very convenient device for introducing the capillaritron on almost any instrument known as the direct insertion probe gun or DIP gun (183). In this case, the capillaritron is attached to the end of a probe which fits most standard probe inlet ports. Furthermore, since the beam bombards the sample placed in a holder attached to the probe in front of the nozzle, there is no need to tie up an available port on the mass spectrometer to perform FAB. This device has been installed by G. Dolnikowski on a triple quadrupole mass spectrometer at the Michigan State/NIH Regional Facility for Mass Spectrometry. Drawbacks to the capillaritron include: shorter

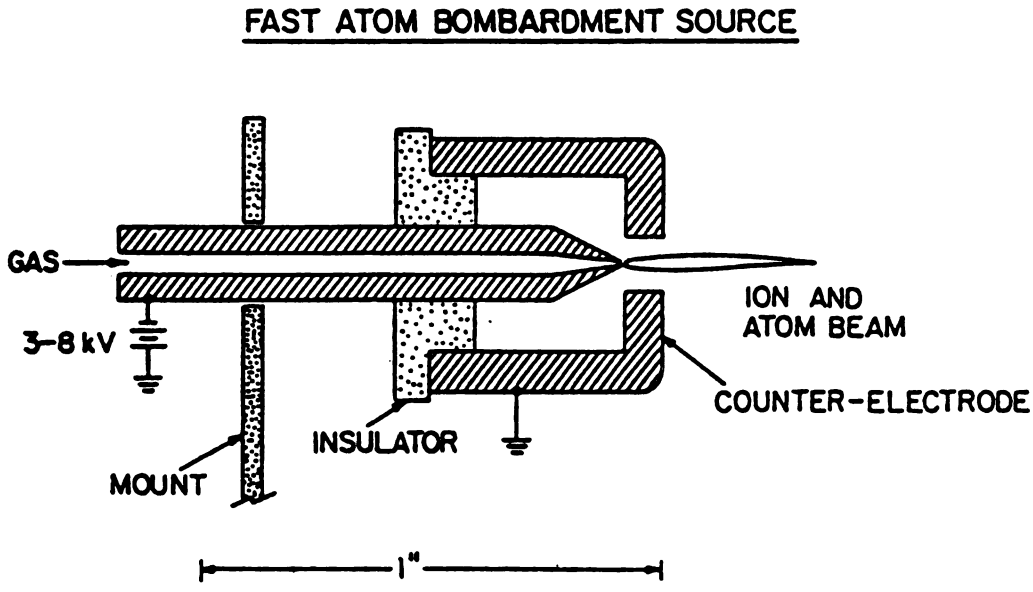

Figure 1.6 Schematic diagram of the fast atom capillaritron source (FACS). Reprinted from reference 179 with permission of the American Society for Mass Spectrometry.

sample lifetimes since the gun is normally a few cm from the sample, the cost and inconvenience of nozzle replacement, and usually a higher consumption of gas than experienced with saddle field sources.

Much attention is now being redirected towards the development of simplified SIMS sources following a comparison made between FAB and SIMS by Aberth and coworkers on the same mass spectrometer (14). While the FAB source was commercially obtained, the SIMS gun was homemade and mounted directly inside the ion source. Cesium ions were prepared by heating a filament coated with cesium alumina silicate. The filament was biased +6kV positive with respect to the ion source and the ion beam was focused with a simple extraction plate/Einzel lens system. The entire gun was only 3.4cm long. Although SIMS previously had a reputation for creating defocusing by charging the sample, this was found only to be true for insulating substances, and not true for samples dissolved in polar liquids such as glycerol (14). It was this paper where the term liquid-SIMS was introduced as a more appropriate name than the acronym FAB.

SIMS sources offer advantages to both time-of-flight (TOF) and Fourier transform (FT) ion detection schemes as both require low pressure sources which can be pulsed. Obviously, FAB would not suffice. Russell and Castro successfully installed a Cs^+ ion gun, modeled after the design of Aberth, to a Nicolet FTMS-1000 (184). While the Cs^+ ion gun operated well below the high vacuum conditions needed for FTMS ($<10^{-7}$ torr), liquid matrices could not be used because of their vapor pressure. Fortunately, the current generation of FTMS instruments have a dual cell arrangement to allow ionizaton

and mass analysis to occur in separate, differentially-pumped chambers. Hence, the use of viscous liquids should be feasible.

Shortly after Aberth et al. reported their findings, McEwen produced a similar source-mounted cesium ion gun except it was simplified by not having lenses to focus the incident ion beam (185). His design simply placed a filament, coated with CsCl inside a ceramic tube adjacent the ion source. The filament could be biased to provide a Cs^+ ion beam for either positive or negative ion detection, and gave results similar to FAB for the nonapeptide bradykinin. While this may be the design easiest to implement, Stoll et al. recently demonstrated that focusing an ion beam to a spot smaller than the FAB target can provide better sensitivity than either FAB or SIMS guns which do not focus the beam on to the liquid sample (186). Apparently, without focusing, several of the ions formed are not accepted by the point focus selection of ion optics. Also, because glycerol is still able to renew its surface following impact with a focused beam, lower detection limits and longer lifetimes may be realized by this approach (186).

Since both FAB and SIMS initiate desorption-ionization with a collisional cascade that depends on the momentum, investigators have shown the value of increasing the mass of the primary particle (187). For FAB, some investigators have gone to the extreme (and inconvenience) of using mercury (188) and trimethylpentaphenyltrisiloxane (189) in conventional FAB sources. The latest trend in source design is the liquid metal ion (LMI) primary source introduced by Barofsky et al. (190). Their design incorporates a special emitter prepared by coating a pointed tungsten anode with a molten liquid metal (Ga,

In, SiAu, or Bi). The ions formed at the anode are accelerated through a potential drop of 3-10kV before striking the sample. These authors reported a 10-50-fold enhancement over FAB using Ar, and a strong increasing dependence of molecular ion abundance on the atomic number of the bombarding element. Sputtering with negative particles has also been reported (191). Using an unfocused Cs^+ ion gun, McEwen and Hass bombarded a gold cone having a negative bias of 12kV. The sputtered Au ions were then accelerated into the ion source (+8kV) to strike the sample with 20keV.

As described, several approaches exist for preparing beams for keV particle impact. The choice depends on convenience, cost, reliability, and frequently on the design of the mass spectrometer to be modified.

E. Exact Mass Determination by FAB

Mass determinations performed by mass spectrometry can frequently be made to within a milli-mass unit by comparison to either an internal or external standard of known mass. Usually an error of <10ppm is needed to preclude other elemental compositions of the same nominal mass value. Most measurements are accomplished on high resolution magnetic sector instruments by a method known as peak matching. Using this method, the reference peak from an internal standard is first brought into focus and viewed on an oscilloscope. Next, without changing the current of the magnet, the peak from an unknown is brought into focus by altering the accelerating voltage by

means of a precise series of decade resistors. Since observed mass to charge ratio is inversely proportional to acceleration potential, two masses may be brought into focus alternatively by changing the acceleration potential at constant mass. When the two peaks are exactly superimposed in this manner, the mass of the unknown may be calculated directly from the resistance setting used to effect superposition.

Examples of exact mass measurements by FAB are too numerous to cite. However, the basic considerations shall be discussed. First, when peak matching by FAB it is important to have at least enough resolution to resolve any isobaric interference from the matrix. Next, since there is a trade-off between sensitivity and resolution with magnetic instruments, it is important to have ample signal from the compound of interest. When signal intensities are a problem integrative techniques such as photoplate detection (192) and multi-channel analysis (193) have been used; the former was used for FD.

Frequently samples are peak matched either to a known glycerol peak or to a peak from an internal standard added to the matrix. Unfortunately, it is not always possible to obtain adequate sensitivity for both the reference and unknown because of the competition for ionization which occurs during FAB. One alternative, proposed by Occolowitz et al. (194), is to use a split probe tip which places an external standard and an unknown on separate ends of the same FAB probe surface. Although this metod eliminates competition within the matrix, the focus cannot be optimized simultaneously for each peak. This complication creates errors on

the order of 10ppm. A better approach, devised by the same investigators, places the sample on opposite sides of a rotary probe tip so that rotation by 180° puts the unknown into focus at the same point in the ion source as the reference standard. This approach gave errors of only 1ppm by peak matching (194).

Ultimately, peak matching is a tedious task which has an inherent degree of subjectivity. Hence, computerized methods of data acquisition have been developed to obtain accurate masses below m/z 1000 while scanning a full mass spectrum. This approach eliminates the need to peak match when there are several peaks of interest. The precision of this method is directly linked to the reproducibility of the relationship of magnetic field to time, and is only possible when using a finely laminated magnet to reduce hysteresis. However, Occolowitz and coworkers have succeeded in developing two methods (e.g., internal and external standard) for obtaining accurate masses (<5ppm) while scanning below m/z 1000 using FAB (195).

F. Quantitative FAB

Quantification by mass spectrometry typically involves monitoring the ion current from an analyte (usually the molecular ion) and comparing the intensity obtained to that observed for a standard of known quantity. In all instances, a calibration curve should be prepared to ensure linearity and to measure precision. The standards used are of three varieties, 1) external standards 2) structurally homologous internal standards, and 3) stable isotopically-labeled internal standards. Although the initial

consensus was that matrix effects inherent to FAB would restrict the technique to being merely qualitative, examples have been reported using all three types of standards with varying degrees of success.

Using an external standard, a calibration curve is prepared from known quantities of the analyte in a series of determinations separate from the unknown. Calibration curves in FAB are generally restricted to less than two orders of linear dynamic range (196). The lower limit of detection is usually determined by background interference, while a leveling off of signal intensities at higher concentrations has been explained as a saturation of analyte at the surface (196). In one dramatic example Lehmann et al. demonstrated reasonable linearity for the $(M+H)^+$ ion of the peptide angiotensin over four orders of magnitude (1ng-10μg) (67). Although linear calibration curves may be generated using FAB, external standards are only reliable to at best ± 10% RSD, and are not recommended for use. Problems arise from having slightly different focus conditions for separate analyses, and from minor changes in the sample matrix between the analyte and standards.

Internal standards can be used to minimize differences associated with separate determinations, and are considered to be more reproducible. Internal standards are added prior to sample work-up, where the assumption made is that the standard has similar extraction and ionization efficiency as the analyte. This assumption is sometimes valid using structural homologs as internal standards. For example, Caprioli and Beckner demonstrated the feasibility of using dansyl-asparagine as an internal standard for dansyl-glutamine over the concentration range 0.5 to 250nmol μl^{-1} (197). However,

Riley et al. were unable to use a similar approach for the determination of a photostabilizer in paint because of matrix effects (198). Generally, homologous internal standards are not recommended for precise quantification by FAB because the desorption-ionization efficiency of similar compounds can be unpredictable especially when they are analyzed together.

The most reliable results for quantification by FAB are obtained when the internal standard is a stable isotopically-labeled analog of the analyte. Only in this case can the extraction and desorption-ionization efficiency be considered equal for both compounds. In fact, according to a workshop report for quantitative DI techniques, held at the 32nd Annual Conference of the American Society for Mass Spectrometry (1984), isotope-labeled internal standards are required in addition to purified samples for optimal results (199). By this method, a labeled internal standard is added to the sample matrix and carried thorugh all steps of the analysis. The mass spectrometer then records the intensity of the two molecular ions, which differ in mass according to the isotopes added, to establish an intensity ratio. The analyte concentration may be derived from this ratio by comparison to a standard curve prepared by analyzing a series of known solutions containing different concentrations of the analyte, but the same amount of the labeled standard as added previously to the unknown. Calibration plots made in this fashion frequently yield lines of slope one going through the origin. In one example, Caprioli et al. prepared a standard curve for the neurotransmitter 4-aminobutyric acid (GABA) using fifteen solutions ranging between 3 and 200 nmol μl^{-1} in concentration (197).

Each solution also contained 10nmol μl^{-1} of the deuterated analog, $^{2}H_{2}$-GABA. The observed ratios for the $(M+H)^{+}$ ions (unlabeled:labeled) were plotted against the prepared GABA/$^{2}H_{2}$-GABA ratios to yield a slope of 1.09 (correlation coefficient 0.9996).

Several reported examples have demonstrated the ability to obtain quantitative results by FAB when isotopically-labeled standards. Beginning with the determination of steroid sulfates by Gaskell et al. (200), the range of application includes acylcarnitines (201), blood platelet activating factor (202), phosphatidylcholines (203), surfactants (204), and paint additives (198). FAB has also been used for quantitative elemental analysis. Examples include a determination of total iron in foods (205) and a direct determination of calcium in biological fluids (206). As a final note, a very promising method for quantitative FAB is to use isotopically-labeled standards with MS/MS methods. MS/MS enables greater selectivity and can remove matrix interference. Using an ^{18}O-labeled internal standard and a method involving linked scanning, Desiderio et al. measured the levels of various brain peptides known as enkephalins (105). In another study, Straub and Levandoski developed a quantitative assay for a bioactive metabolite from a cardiovascular drug by employing the method of selected reaction monitoring (SRM) on a triple quadrupole mass spectrometer (207).

G. Theoretical Considerations

Desorption of intact nonvolatile molecules and ions by sputtering with keV particles is truly an amazing process. It is

also a process that is not fully understood at present. While several theories have been proposed, there is no general consensus among investigators. The formation of similar ion types, and sometimes even superimposible mass spectra, by different DI methods has led some investigators to speculate about a unified model for desorption-ionization (17,208). However, critical to any detailed understanding of FAB is to determine exactly how the matrix participates in the process which is the topic of much debate at present.

Since FAB is a keV particle impact technique, it is universally accepted that sputtering begins with a collisional cascade, where energy is initially dispersed by momentum transfer (17). This is in contrast to MeV particle impact, where energy is transfered primarily through electronic excitation (20). Further, it is known that bombardment at grazing angles to the surface increases the desorption yield of intact species, as does the use of heavier mass incident particles. Both of these observations are consistent with the collisional aspect of desorption-ionization by FAB. To hopefully shed some light on possible events which govern FAB, the following section shall present condensed versions of three reported models.

The first theory is known as the "precursor" model (209). This model, reported by Benninghoven, has its basis in static SIMS and draws heavily from classical sputtering mechanisms. Prior to bombardment, a precursor of the emitted secondary ion is believed to exist at the surface. As depicted in Figure 1.7, the fate of the precursor depends on its proximity to impact by the primary particle. This diagram is a qualitative distribution expressing the energy

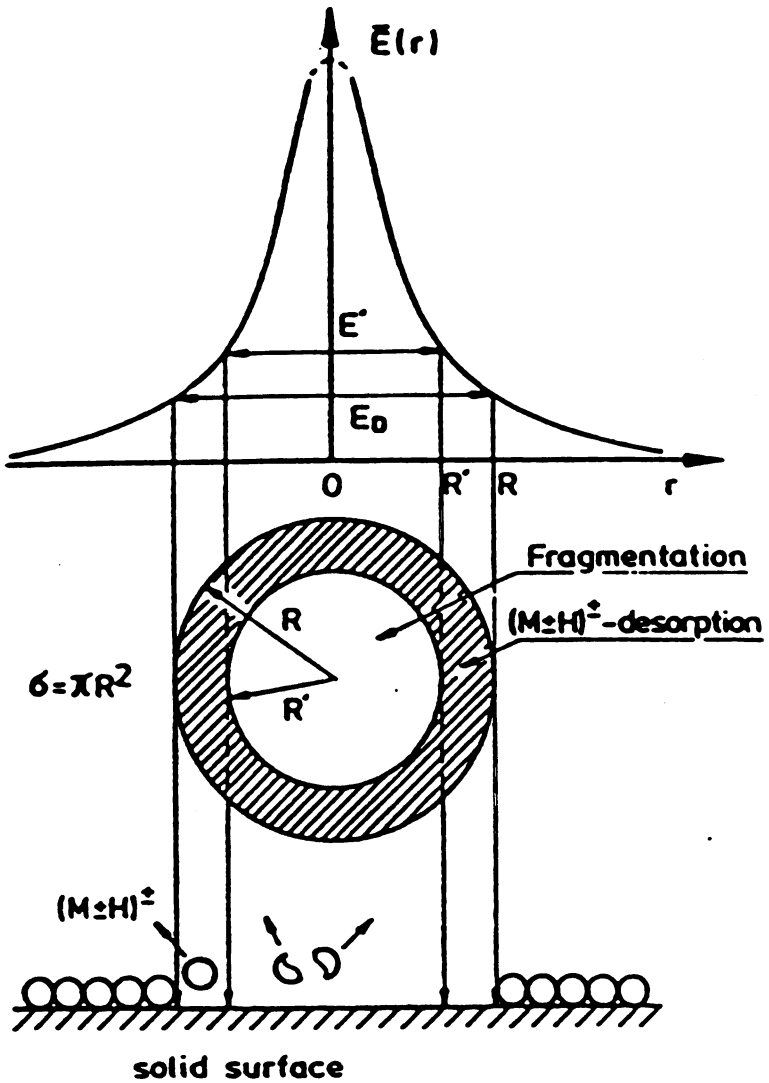

Figure 1.7 Qualitative shape of the function $\bar{E}(r)$, indicating the average energy $\bar{E}(r)$, transferred to a surface particle as a function of its distance r from the point or primary particle impact, as suggested by the precursor model of Benninghoven. Reprinted from reference 209 with permission from Elsevier Science Publishers.

transferred to surface species as a function of distance from the primary impact. The shaded area represents the region where desorption of the intact precursor occurs. This region is believed to be an area excited by the tail end of linear collision cascades which pass near the surface. While this area is typically about 30A away from the point of impact, the size of the region depends greatly on the particular solid or liquid surface from which sputtering occurs. Beyond a distance R, there is insufficient energy to desorb the precursor from the surface. At the other extreme (e.g., for distances less than R') fragmentation of the precursor occurs prior to desorption. The use of a liquid matrix, in essence, widens the shaded region to favor desorption of intact precursors. The use of glycerol also gives mobility to the analyte to result in a continuous regeneration of the target surface, as well as supplying a good environment for precursor formation.

According to this model, precursor desorption occurs from a rapid transfer of energy ($<10^{-12}$ s) from the collision cascade. Hence, the desorption of either intact or fragmented precursors is assumed to be a Frank-Condon process such that the integrity of the species remains intact. Finally, it is acknowledged that additional fragmentation may occur in the gas phase from unimolecular decomposition after the intact precursor is desorbed.

The next model, advanced by Cooks (208), was initially presented at a conference in Munster, Germany in 1980 (210). Although much of the initial data for the model was again collected using SIMS, the model was intended to apply to several DI methods including FAB. One of the chief tenets in thedesorption-ionization theory of Cooks, is

that chemical rather than physical factors are primarily responsible for the nature of DI spectra and ion yields. It is noteworthy that he credits J.F. Holland for first bringing such factors to the attention of the DI community in landmark investigations of FD (208).

A pictoral summary of the processes which occur during desorption-ionization according to Cooks is shown in Figure 1.8. This diagram plots energy deposition against the distance from impact, and also illustrates the various events which may occur in the gas phase above the condensed surface. The diagram also emphasizes another important point of the model, namely desorption and ionization are two separate processes. The first step of the process is labeled as energy isomerization, which implies that the amount of energy deposited, and not its type, determines the nature of desorption. In this way several methods which differ in their approach to DI may be unified. While the randomized energy may be viewed as thermal, no equilibrium is implied since the various mechanisms for energy transfer are too rapid. In contrast to Benninghoven, however, Cooks claims that energy is transferred to the vibrational modes of the analyte and matrix. The large desorption yields of intact molecules and ions therefore reflects the amount of energy available. In other words, low energy intermolecular interactions, such as hydrogen bonds, are dissociated in favor of the stronger covalent bonds within the molecule. This mechanism would account for the low energies of the ions observed by DI, and would explain why pre-ionization is so important from an energetic standpoint.

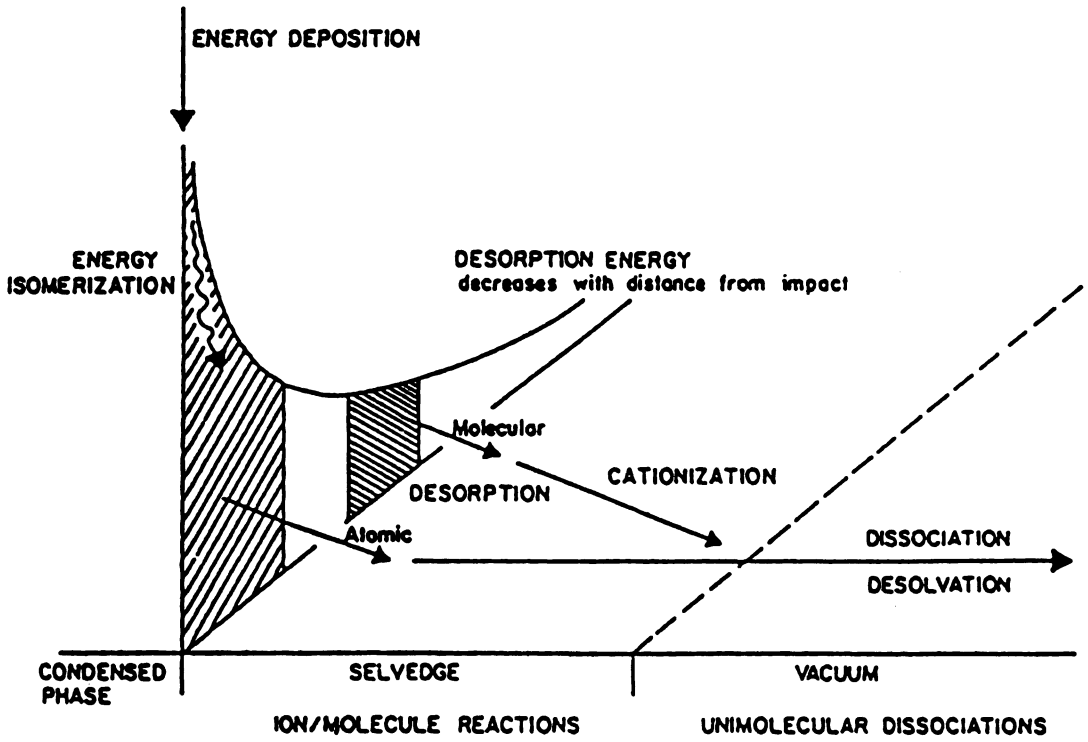

Figure 1.8 Schematic overview of desorption-ionization by FAB according to R. G. Cooks. Reprinted from reference 208 with permission from Elsevier Science Publishers.

According to Figure 1.8, following desorption, chemistry can occur in two distinct regions. The first is known as the "selvedge". The selvedge is a region of relatively high pressure immediately above the condensed state. Here, several processes may occur involving both ions and neutrals. For example, fast ion-molecule reactions could account for some of the adduct formation observed by FAB. Also, neutrals may be ionized by processes such as charge exchange. Beyond the selvedge is a region of low pressure where collisions no longer take place. The selvedge boundary has therefore been defined as the limit beyond which no ionization occurs.

In the vacuum region two types of dissociations may occur: unimolecular decomposition or desolvation. The former occurs whenever desorbed ions have sufficient internal energy to fragment. In fact, Cooks maintains that unimolecular decomposition in the gas phase is the only mechanism for fragmentation in FAB. He points to several examples where metastable decomposition processes observed by MS/MS mirror the fragmentation seen in DI mass spectra, and concludes there is little reason to invoke processes of direct beam-induced fragmentation or surface mediated events. Finally, gas phase desolvation in the vacuum region may be an important process when matrices are used in DI methods. In other words, solvated analyte clusters may be desorbed intact only to desolvate and give analyte ions or in some cases solvated analyte ions. Puzo and Prome gave evidence for this process by using MS/MS to show that ions of the type $(M+glycerol+H)^+$ desolvate in the gas phase to give $(M+H)^+$ ions as daughters (71). This observation helps to explain the efficiency

of forming intact molecular ions when a matrix is used; excess internal energy may be consumed by the dissociation of matrix-matrix or matrix-analyte interactions, either on the surface or in the gas phase, to give more stable gas phase ions. This also correlates with the observation that analyte fragmentation in FAB is favored as the concentration of analyte within the matrix is increased.

A third model for desorption-ionization, presented by Vestal (17), is an outgrowth of work done to formulate an understanding of ion formation from liquid droplets during thermospray. Again, the initial step of energy deposition leads to an intermediate state which is essentially independent of the initial event. The basic premise of the model is that the intermediate between energy deposition and pseudomolecular ion formation is a cluster or droplet which may be separated from the bulk by a rapid, nonequilibrium process. While some events may be explained by equilibrium models, it is evident that the overall DI process is irreversible. Further, the observation, in both laser desorption and particle impact studies, that an increase in energy deposition favors intact desorption over fragmentation suggests rapid, nonequilibrium energy transfer occurs.

Research into nonequilibrium methods of heat transfer in multiphase systems has led Vestal to postulate a "thick sauce" model to account for desorption in FAB as well as in other methods. In this model, under conditions of rapid heating, bubble formation occurs beneath the surface. Nucleation sites are provided by residual solvent or impurities. The bubbles then migrate to the surface and burst violently sending their gaseous contents, as well

as clusters and droplets of the surrounding liquid, into the vacuum. By this mechanism, desorption is believed to occur almost exclusively as large clusters that undergo desolvation in the gas phase to yield the ion types observed. Similar to the Cooks model, fragmentation occurs unimolecularly after desolvation, and ion-molecule reactions may occur.

Regardless of how FAB occurs, there is little uncertainty about where it occurs. FAB is essentially a surface phenomenon, as would be predicted by sputtering theory. At the incident angles used, the collisional cascade penetrates only a depth of a few monolayers, and selects for species at or near the surface (24). This conclusion is supported by several investigations by Ligon which clearly demonstrate the correlation between increased surface activity and sensitivity (13,211,212). Furthermore, the fact that calibration curves obtained by FAB fall off at high concentraitons has been interpreted as monolayer formation by solutes at the surface of glycerol (196).

This phenomenon was investigated by Barber and coworkers who recorded the spectrum of cetylammonium bromide at various concentrations in glycerol in order to study the effects of monolayer formation on FAB mass spectra. According to classical thermodynamics, monolayer formation in a dilute solution depends on the solute surface tension (γ) and bulk concentration (C_s). Monolayer formation implies a constant surface excess in solute concentration. This concentration is known specifically as the Gibbs adsorption isotherm Γ_s (12). Once monolayer formation occurs, may be expressed as:

$$\Gamma_s = - \frac{d\gamma}{d\,(\ln C_s)}$$

In other words, beyond this point which occurs at 5×10^{-4} M for cetylammonium bromide in glycerol (12), surface tension decreases linearly with the natural logarithm of bulk concentration. Barber et al. showed that the ion current ratio for cetylammonium bromide to glycerol dropped off dramatically at the onset of predicted monolayer formation, and remained constant in the region where γ decreased linearly (in accordance with theory) (12).

Interestingly enough, FAB has also been used to investigate equilibria occurring in the bulk (151). For example, Caprioli used FAB to verify pK_a values for weak acids (213), and to study enzyme kinetics (214). While such investigations may be possible, FAB should only be used to verify known equilibrium constants, since spurious results may occur when the bulk and surface concentrations differ. Additional complications may also arise if the species involved in the equilibria have different net charge or surface activity.

As a final note, one of the most intensely debated topics at present concerns the mechanism of analyte replenishment during FAB. Barber et al. maintain that replenishment occurs automatically by diffusion as the sample is sputtered from the surface (12). Hence, solubility of the analyte in the matrix is essential for diffusion, and to provide a reservoir of non-bombarded material. This claim is supported by a calculation by MaGee which predicts that diffusion

alone can account for surface replenishment before a critical dose 10^{13} particles/cm^{-2}) occurs (24).

A more extensive calculation was reported by Bursey et al. which considered two phenomena: 1) the rate of removal of material from the surface, and 2) the time between disruptions of the same surface (215). Assuming a diffusion model, and an incident flux of 6 x 10^{12} particles sec^{-1}, they concluded that sampling by the atom beam occurs faster than diffusion, from a surface whose ions are in equilibrium with the bulk of solution. In otherwords, the sputtering event is but a "snapshot" of a surface whose contents are replenished by diffusion in between consecutive disruptions of the same area on the surface.

Evidence contrary to a diffusion model was reported by Ligon as a result of analyzing glycerol-d_8 by FAB (216). In this study, prior to data collection, water vapor under normal conditions exchanged with the -OD groups to yield a fully hydroxylated surface (glycerol-d_5). According to Ligon, the signal from glycerol-d_5 persisted longer than would be predicted under a diffusion model. This study, in part, led Rollgen and coworkers to postulate a "surface self-cleaning" mechanism for FAB (217). Under this model, the surface damage caused by the collision cascade is almost completely removed, with formation of a clean surface after each sputtering event, and without need for renewal of the surface via diffusion. Unfortunately, the evidence for this model is rather tenuous. In addition, the reported results could not be repeated in our laboratory. Certainly this area will be the topic of continued research by several investigators.

IV. LIST OF REFERENCES

1. R.A. Yost and D.D. Fetterolf, Mass Spectrom. Rev. 2, 1 (1983).

2. C. Fenselau, Anal. Chem., 54, 105A (1982).

3. M.S.B. Munson and F.H. Field, J. Am. Chem. Soc., 88, 2621 (1966).

4. Pierce 1985-86 Handbook and General Catalog, p. 97, Pierce Chemical Co., Rockford, Illinois.

5. H.D. Beckey, Int. J. Mass Spectrom. Ion Phys., 2, 500 (1969).

6. D.F. Torgerson, R.P. Skowronski, and R.D. Macfarlane, Biochem. Biophys. Res. Comm., 60, 616 (1974).

7. K.L. Busch and R.G. Cooks, Science, 218, 247 (1982).

8. M. Barber, R.S. Bordoli, R.D. Sedgwick, and A.N. Tyler, J. Chem. Soc. Chem. Commun., 325 (1981).

9. J.A. McHugh in A. Czanderna, Ed., "Methods of Surface Analysis", Elsevier, New York, 1975.

10. A. Benninghoven, D. Jaspers, and W. Sichtermann, Appl. Phys., 11, 35 (1976).

11. F.M. Devienne and G. Grandclement, C.R. Acad. Sci., 262, 696 (1966).

12. M. Barber, R.S. Bordoli, R.D. Sedgwick, A.N. Tyler, and G.J. Elliott, Anal. Chem., 54, 645A (1982).

13. W.V. Ligon, Jr. and S.B. Dorn, Int. J. Mass Spectrom. Ion Proc., 61, 113 (1984).

14. W. Aberth, K.M. Straub, and A.L. Burlingame, Anal. Chem., 54, 2029 (1982).

15. B.L. Ackermann, J.T. Watson, J.F. Newton, Jr., J.B. Hook, and W.E. Braselton, Jr., Biomed. Mass Spectrom., 11, 502 (1984).

16. B.L. Ackermann, J.T. Watson, and J.F. Holland, Anal. Chem., 57, 2656 (1985).

17. M.L. Vestal, Mass Spectrom. Rev., 2, 447 (1983).

18. J.F. Holland, B. Soltmann, and C.C. Sweeley, Biomed. Mass Spectrom., 3, 340 (1976).

19. M. Barber, R.S. Bordoli, R.D. Sedgwick, and A.N. Tyler, Nature, 293, 270 (1981).

20. R.D. Macfarlane, Acc. Chem. Res., 15, 268 (1982).

21. P. Hakansson, I. Kamensky, B. Sundqvist, J. Fohlman, P. Peterson, C.J. McNeal, and R.D. Macfarlane, J. Am. Chem. Soc., 104, 2948 (1982).

22. P. Sigmund, J. Vac. Sci. Technol., 17, 396 (1980).

23. B. Sundqvist and R.D. Macfarlane, Mass Spectrom. Rev., 4, 421 (1985).

24. C.W. Magee, Int. J. Mass Spectrom. Ion Phys., 49, 211 (1983).

25. K.L. Busch, S.E. Unger, A. Vincze, R.G. Cooks, and T. Keough, J. Am. Chem. Soc., 104, 1057 (1982).

26. K.L. Busch, B.H. Hsu, Y.X. Xle, and R.G. Cooks, Anal. Chem., 55, 1157 (1983).

27. A. Benninghoven, Int. J. Mass Spectrom. Ion Phys., 46, 459 (1983).

28. F. Hillenkamp, "Laser Induced Ion Formation for Organic Solids." In: "Proceedings of 2nd International Workshop on

Ion Formation from Organic Solids"; A. Benninghoven, Ed.; "Springer Series in Chemical Physics"; Springer-Verlag, New York, 1983.

29. R. Kaufmann, F. Hillenkamp, W. Wechsung, H.J. Heinen, and M. Schurmann, Scanning Electron Microsc. II, 279, (1979). LAMMA is a registered trademark of Leybold-Heraeus.

30. E. Denoyer, R. vanGrieken, F. Adams, and D. Natusch, Anal. Chem., 54, 26A (1982).

31. D.M. Hercules, R.J. Day, K. Balasanmugam, T.A. Dang, and C.P. Li, Anal. Chem., 54, 280A (1982).

32. R.J. Cotter and J.-C. Tabet, Int. J. Mass Spectrom. Ion. Phys., 53, 151 (1983).

33. G.J.Q. Van Der Peyl, J. Haverkamp, and P.G. Kistemaker, Int. J. Mass Spectrom. Ion Phys., 42, 125 (1982).

34. F.P. Novak, K. Balasanmugam, K. Viswanadham, C.D. Parker, Z.A. Wilk, D. Mattern, and D.M. Hercules, Int. J. Mass Spectrom. Ion Phys., 53, 135 (1983).

35. R.J. Cotter, Anal. Chem., 52, 1589A (1980).

36. V.N. Reinhold and S.A. Carr, Anal. Chem., 54, 499 (1982).

37. M.A. Baldwin and F.W. McLafferty, Org. Mass Spectrom., 7, 1353 (1973).

38. A. Dell, D.H. Williams, H.R. Morris, G.A. Smith, J. Feeney, and G.C.K. Roberts, J. Am. Chem. Soc., 97, 2497 (1975).

39. R.J. Beuhler, E. Flanigan, L.J. Greene, and L. Friedman, J. Am. Chem. Soc., 96, 3990 (1974).

40. M. Ohashi, N. Nakayama, Org. Mass Spectrom., 13, 642 (1978).

41. J.G. Howlin, D.I. Carroll, I. Dzidic, M.G. Horning, R.H. Stillwater, and E.C. Horning, Anal. Lett., 12, 573 (1979).

42. R.J. Cotter and C.C. Fenselau, Biomed. Mass Spectrom., 6, 287 (1979).

43. W.R. Anderson, Jr., W. Fick, G.D. Daves, Jr., D.R. Barofsky, I. Yamaguchi, D. Chang, K. Folkers, and S. Rosell, Biochem. Biophys. Res. Commun., 78, 372, (1977).

44. B. Soltmann, C.C. Sweeley, and J.F. Holland, Anal. Chem., 49, 1164 (1977).

45. J.W. Maine, B. Soltmann, J.F. Holland, N.D. Young, J.N. Gerber, and C.C. Sweeley, Anal. Chem., 48, 427 (1976).

46. D.F. Hunt, J. Shabanowitz, F.K. Botz, and D.A. Brent, Anal. Chem., 49, 1160 (1977).

47. K.W.S. Chan and K.D. Cook, Anal. Chem., 55, 1306 (1983).

48. C.A. Evans, Jr., and C.B. Hendricks, Rev. Sci. Instrum., 43, 1527 (1972).

49. C.R. Blakley, J.J. Carmody, and M.L. Vestal, J. Am. Chem. Soc., 102, 5931 (1980).

50. C.R. Blakley and M.L. Vestal, Anal. Chem., 51, 750 (1983).

51. R.D. Voyksner and C.A. Haney, Anal. Chem., 57, 991 (1985).

52. M. Barber, R.S. Bordoli, G.V. Garner, D.B. Gordon, R.D. Sedgwick, L.W. Tetler, and A.N. Tyler, Biochem. J., 197, 401 (1981).

53. C.J. McNeal, Anal. Chem., 54, 43A (1982).

54. T. Keough, Anal. Chem., 57, 2027 (1985).

55. R. Davis, I.F. Groves, J.L.A. Durrant, P. Brooks, and I. Lewis, J. Organometal. Chem., 241, C27 (1983).

56. R.L. Cerny, B.P. Sullivan, M.M. Bursey, and T.J. Meyer, Anal. Chem., 55, 1954 (1983).

57. A.I. Cohen, K.A. Glavan, and J.F. Kronavge, Biomed. Mass Spectrom., 10, 287 (1983).

58. S.E. Unger, Anal. Chem., 56, 363 (1984).

59. G. Bojesen, Org. Mass Spectrom., 20, 413 (1985).

60. C. Fenselau, D.J. Liberato, J.A. Yergey, R.J. Cotter, and A.L. Yergey, Anal. Chem., 56, 2759 (1984).

61. P. Roepstorff and J. Fohlman, Biomed. Mass Spectrom., 11, 601 (1984).

62. F.W. McLafferty, "Interpretation of Mass Spectra", University Science Books: Mill Valley, California, 1980.

63. K.L. Clay, L. Wahlin, and R.C. Murphy, Biomed. Mass Spectrom., 10, 489 (1983).

64. K.B. Tomer, F.W. Crow, H.W. Knoche, and M.L. Gross, Anal. Chem., 55, 1033 (1983).

65. S.A. Carr, V.N. Reinhold, B.N. Green, and J.R. Hass, Biomed. Mass Spectrom., 12, 288 (1985).

66. J.L. Gower, Biomed. Mass Spectrom., 12, 191 (1985).

67. W.D. Lehmann, M. Kessler, and W. Konig, Biomed. Mass Spectrom., 11, 217 (1984).

68. L.J. Goad, M.C. Prescott, and M.E. Rose, Org. Mass Spectrom., 19, 104 (1984).

69. M. Przybylski, Fres. Z. Anal. Chem., 315, 402 (1983).

70. K.L. Rinehart, Science, 218, 254 (1982).

71. G. Puzo and J.C. Prome, Org. Mass Spectrom., 19, 448 (1984).

72. K.I. Harada, M. Suzuki, and H. Kambara, Org. Mass Spectrom., 17, 386 (1982).

73. B.N. Pramanik, A.K. Mallams, P.L. Bartner, R.R. Rossman, J.B. Morton, and J.H. McGlotten, J. Antibiot., 37, 818 (1984).

74. J. Meili and J. Seibl, Int. J. Mass Spectrom. Ion Phys., 46, 367 (1983).

75. R.D. Minard and G.L. Geoffrey, Presented at the 30th Annual Conference on Mass Spectrometry and Allied Topics, June 6-11, 1982, Honolulu, Hawaii.

76. J.L. Witten, M.H. Schaffer, M. O'Shea, J.C. Cook, M.E. Hemling, and K.R. Rinehart Jr., Biochem. Biophys. Res. Commun., 124, 350 (1984).

77. J. Meili and J. Seibl, Org. Mass Spectrom., 19, 581 (1984).

78. W. Vetter and W. Meister, Org. Mass Spectrom., 20, 266 (1985).

79. D.H. Williams, C.V. Bradley, S. Santikarn, and G. Bojesen, Biochem J., 201, 105 (1982).

80. M. Barber, R.S. Bordoli, R.D. Sedgwick, A.N. Tyler, and E.T. Whalley, Biomed. Mass Spectrom., 8, 337 (1981).

81. H.R. Morris, D.H. Williams, and R.P. Ambler, Biochem. J., 125, 189 (1971).

82. S.A. Carr, W.C. Herlihy, and K. Biemann, Biomed. Mass Spectrom., 8, 51 (1981).

83. A.M. Buke, L.R. Phillips, and B.A. Fraser, Biomed. Mass Spectrom., 10, 324 (1983).

84. A.M. Buko, L.R. Phillips, and B.A. Fraser, Biomed. Mass Spectrom., 10, 408 (1983).

85. A.M. Buko, L.R. Phillips, and B.A. Fraser, Biomed. Mass Spectrom., 10, 387 (1983).

86. A.M. Buko and B.A. Fraser, Biomed. Mass Spectrom., 12, 577 (1985).

87. M. Barber, R.S. Bordoli, G.J. Elliott, A.N. Tyler, J.C. Bill, and B.N. Green, Biomed. Mass Spectrom., 11, 182 (1984).

88. M. Barber, R.S. Bordoli, G.J. Elliott, N.J. Horoch, and B.N. Green, Biochem. Biophys. Res. Commun., 110, 753 (1983).

89. A. Dell and H.R. Morris, Biochem. Biophys. Res. Commun., 106, 1456 (1982).

90. M. Barber, R.S. Bordoli, G.J. Elliott, R.D. Sedgwick, and A.N. Tyler, Anal. Chem. Ser. A, 54, 645 (1982).

91. M. Barber, R.S. Bordoli, R.D. Sedgwick, A.N. Tyler, G.V. Garner, D.B. Gordon, L.W. Tetler, and R.C. Hider, Biomed. Mass Spectrom., 9, 265 (1982).

92. M. Barber, R.S. Bordoli, and R.D. Sedgiwck, in "Soft Ionization Biological Mass Spectrometry", ed. by H.R. Morris, p. 137 Heyden, London (1981).

93. M.R. Clench, G.V. Garner, D.B. Gordon, and M. Barber, Biomed. Mass Spectrom., 12, 355 (1985).

94. H.R. Morris, Int. J. Mass Spectrom. Ion Phys., 45, 45, 331 (1982).

95. R. Self and A. Parente, Biomed. Mass Spectrom., 10, 78 (1983).

96. R.M. Caprioli, L.A. Smith, and C.F. Beckner, Int. J. Mass Spectrom. Ion Phys., 46, 419 (1983).

97. T. Takao, M. Yoshida, Y.M. Hong, S. Aimoto, and Y. Shimonishi, Biomed. Mass Spectrom., 11, 549 (1984).

98. H.R. Morris, M. Panico, and G.W. Taylor, Biochem. Biophys. Res. Commun., 117, 299 (1983).

99. Y. Wada, A. Hayashi, T. Fujita, T. Matsuo, I. Katakuse, and H. Matsuda, Int. J. Mass Spectrom. Ion Phys., 48, 209 (1983).

100. K. Biemann, Int. J. Mass Spectrom. Ion Phys., 45, 183 (1985).

101. C.F. Beckner and R.M. Caprioli, Biomed. Mass Spectrom., 12, 393 (1985).

102. M. Barber, R.S. Bordoli, R.D. Sedgwick, and A.N. Tyler, Biomed. Mass Spectrom., 9, 208 (1982).

103. P. Roepstorff, P. Hojrup, and J. Moller, Biomed. Mass Spectrom., 12, 181 (1985).

104. K. Eckart, H. Schwarz, and R. Ziegler, Biomed. Mass Spectrom., 10, 623 (1985).

105. D.M. Desiderio, I. Katakuse, and M. Kai, Biomed. Mass Spectrom., 10, 426 (1983).

106. L.C.E. Taylor, D. Hazelby, and C.J. Wakefield, Int. J. Mass Spectrom. Ion Phys., 46, 407 (1983).

107. D.M. Desiderio and I. Katakuse, Anal. Biochem., 129, 425 (1983).

108. K.B Tomer, F.W. Crow, and M.L. Gross, Int. J. Mass Spectrom. Ion Phys., 46, 375 (1983).

109. W. Heerma, J.P. Kamerling, A.J. Slotboom, G.J.M. van Scharrenburg, B.N. Green, and I.A.S. Lewis, Biomed. Mass Spectrom., 10, 13 (1983).

110. D.L. Lippstreu-Fisher and M.L. Gross, Anal. Chem., 57, 1174 (1985).

111. T. Sakurai, T. Matsuo, H. Matsuda, and I. Katakuse, Biomed. Mass Spectrom., 11, 396 (1984).

112. C.F. Beckner and R.M. Caprioli, Anal. Biochem., 130, 328 (1983).

113. A. Benninghoven and V. Anders, Org. Mass Spectrom., 19, 345 (1984).

114. C.V. Bradley, D.H. Williams, and M.R. Hanley, Biochem. Biophys. Res. Commun., 104, 1223 (1982).

115. G. Puzo and J.C. Prome, Org. Mass Spectrom., 20, 288 (1985).

116. J.P. Kamerling, W. Heerma, J.F.G. Vliegenthart, B.N. Green, I.A.S. Lewis, G. Strecker, and G. Spik, Biomed. Mass Spectrom., 10, 420 (1983).

117. A. Dell and C.E. Ballou, Biomed. Mass Spectrom., 10, 50 (1983).

118. A. Dell, J.E. Oates, H.R. Morris, and H. Egge, Int. J. Mass Spectrom. Ion Phys., 46, 415 (1983).

119. G. Puzo, J.J. Fournie, and J.C. Prome, Anal. Chem., 57, 892 (1985).

120. L.C. Forsberg, A. Dell, D.J. Walton, and C.E. Ballou, J. Biol. Chem., 257, 3555 (1982).

121. L. Grotjahn, H. Blocker, and R. Frank, Biomed. Mass Spectrom., 12, 514 (1985).

122. J. Ulrich, A. Guy, D. Molko, and R. Teoule, Org. Mass Spectrom., 19, 585 (1984).

123. G. Sindona, N. Uccella, and K. Weclawek, J. Chem. Research (S), 184 (1982).

124. J. Eagles, C. Javanaud, and R. Self, Biomed. Mass Spectrom., 11, 41 (1984).

125. J.L. Aubagnac, F.M. Devienne, R. Combarieu, Org. Mass Spectrom., 17, 612 (1982).

126. L. Grotjahn, R. Frank, and H. Blocker, Int. J. Mass Spectrom. Ion Phys., 46, 439 (1983).

127. M. Barber, R.S. Bordoli, R.D. Sedgwick, A.N. Tyler, and B.W. Bycroft, Biochem. Biophys. Res. Commun., 101, 632 (1981).

128. K.L. Rinehart Jr., L.A. Gaudioso, M.L. Moore, R.C. Pandey, and J.C. Cook Jr., J. Am. Chem. Soc., 103, 6517 (1981).

129. M. Barber, R.S. Bordoli, R.D. Sedgwick, A.N. Tyler, B.N. Green, V.C. Parr, and J.L. Gower, Biomed. Mass Spectrom., 9, 11 (1982).

130. Y. Tondeur, M. Shorter, M.E. Gustafson, and R.C. Pandey, Biomed. Mass Spectrom., 11, 622 (1984).

131. D.J. Surman and J.C. Vickerman, J. Chem. Research (9) 170 (1981).

132. J. van der Greef, M.C. Ten Noever do Brauw, J.J. Zwinselman, and N.M.M. Nibbering, Org. Mass Spectrom., 17, 274 (1982).

133. J.G. Liehr, E.E. Kingston, and J.H. Beynon, Biomed. Mass Spectrom., 12, 95 (1985).

134. M. Iwamori, Y. Ohashi, T. Ogawa, and Y. Nagai, JEOL News, 21A, 10 (1985).

135. J.J. Monaghan, M. Barber, R.S. Bordoli, R.D. Sedgwick, and A.N. Tyler, Org. Mass Spectrom., 17, 569 (1982).

136. J.J. Monaghan, M. Barber, R.S. Bordoli, R.D. Sedgwick, and A.N. Tyler, Org. Mass Spectrom., 18, 75 (1983).

137. R.M. Brown, C.S. Creaser, and H.J. Wright, Org. Mass Spectrom., 19, 311 (1984).

138. G.R. Fenwick, J. Eagles, and R. Self, Org. Mass Spectrom., 17, 544 (1982).

139. C. Fenselau, L. Yelle, M. Stogniew, D. Liberato, J. Lehman, P. Feng, and M. Colvin Jr., Int. J. Mass Spectrom. Ion Phys., 46, 411 (1983).

140. J.P. Lehman and C. Fenselau, Drug Metabl. Dispos., 10, 446 (1982).

141. M. Stogniew and C. Fenselau, Drug Metabl. Dispos., 10, 692 (1982).

142. P.P. Wickramanayake, M.L. Deinzer, and A.L. Burlingame, Biomed. Mass Spectrom., 12, 127 (1985).

143. W.D. Lehmann, H.M. Schiebel, J. Bottcher, H. Bassmann, and R. Schuppel, Biomed. Mass Spectrom., 12, 215 (1985).

144. M. Adinolfi, L. Mangoni, G. Marino, M. Marrili, and R. Self, Biomed. Mass Spectrom., 11, 310 (1984).

145. F.A. Mellon and G.R. Fenwick, Biomed. Mass Spectrom., 11, 375 (1984).

146. C.G. deKoster, W. Hoerma, G. Dijkstra, and G.J. Niemann, Biomed. Mass Spectrom., 12, 596 (1985).

147. D. Fraisse, J.C. Tabet, M. Becchi, and J. Raynaud, Biomed. Environ. Mass Spectrom., 13, 1 (1986).

148. M.E. Hemling, R.K. Yu, R.D. Sedgwick, and K.L. Rinehart, Jr., Biochem., 23, 5706 (1984).

149. G.G. Dolnikowski, J.T. Watson, and J. Allison, Anal. Chem., 56, 197 (1984).

150. R.C. Murphy, W.R. Mathews, J. Rokach, and C. Fenselau, Prostaglandins, 23, 201 (1982).

151. R.A.W. Johnstone and M.E. Rose, J. Chem. Soc. Chem. Commun., 1268 (1983).

152. D. Parker, Org. Mass Spectrom., 20, 260 (1985).

153. B.L. Ackermann, A. Tsarbopoulos, and J. Allison, Anal. Chem., 57, 1766 (1985).

154. J.R.J. Pare, R. Greenhalgh, P. Lafontaine, and J.W. ApSimon, Anal. Chem., 57, 1472 (1985).

155. M.L. Gross, D. McCrery, F. Crow, K.B. Tomer, M.R. Pope, L.M. Cuiffetti, H.W. Knoche, J.M. Daly, and L.D. Dunkle, Tetrahedron Lett., 23, 5381 (1982).

156. D.V. Dung, J. Marien, E. DePauw, and J. Decuyper, Org. Mass Spectrom., 19, 276 (1984).

157. D.A. Kidwell, M.M. Ross, and R.J. Colton, Biomed. Mass Spectrom., 12, 254 (1985).

158. M.M. Siegel, P. Bitha, R.G. Child, J.J. Hlavka, Y.I. Lin, and T.T. Chang, Biomed. Environ. Mass Spectrom., 13, 25 (1986).

159. G.R. Fenwick, J. Eagles, and R. Self, Biomed. Mass Spectrom., 10, 382 (1983).

160. P. Varenne, B.C. Das, J. Polonsky, and M. Tence, Biomed. Mass Spectrom., 12, 6 (1985).

161. W.R Sherman, K.E. Ackermann, R.H. Bateman, B.N. Green, and I. Lewis, Biomed. Mass Spectrom., 12, 409 (1985).

162. F.H Chilton, III and R.C. Murphy, Biomed. Environ. Mass Spectrom., 13, 71 (1986).

163. L. Kurlansik, T.J. Williams, J.M. Strong, L.W. Anderson, and J.E. Campana, Biomed. Mass Spectrom., 11, 475 (1984).

164. H. Schwarz, K. Eckart, and L.C.E. Taylor, Org. Mass Spectrom., 17, 459 (1982).

165. A.J. Clifford, C.S. Silverman-Jones, K.E. Creek, L.M. DeLuca, and Y. Tondeur, Biomed. Mass Spectrom., 12, 221 (1985).

166. C. Javanaud and J. Eagles, Org. Mass Spectrom., 18, 93 (1983).

167. A.J. DeStefano and T. Keough, Anal. Chem., 56, 1846 (1984).

168. S.S.J. Ho, M.E. Coddens, and C.F. Poole, Org. Mass Spectrom., 20, 379 (1985).

169. D.A. McCrery, D.A. Peake, and M.L. Gross, Anal. Chem., 57, 1181 (1985).

170. P.A. Lyon, F.W. Crow, K.B. Tomer, and M.L. Gross, Anal. Chem., 56, 2278 (1984).

171. P.A. Lyon, W.L. Stebbings, F.W. Crow, K.B. Tomer, D.L. Lippstreu, and M.L. Gross, Anal. Chem., 56, 8 (1984).

172. R.J. Cutter, G. Hansen, and T.R. Jones, Anal. Chim. Acta, 136, 135 (1982).

173. I. Jardine, G.F. Scanlan, V.R. Mattox, and R. Kumar, Biomed. Mass Spectrom., 11, 4 (1984).

174. M. Barber, R.S. Bordoli, R.D. Sedgwick, and A.N. Tyler, Biomed. Mass Spectrom., 8, 492 (1981).

175. F.M. Devienne and J.C. Rostan, C.R. Acad. Sci. Paris, 283, 397 (1976).

176. J. Franks, Int. J. Mass Spectrom. Ion Phys., 46, 343 (1983).

177. A.M. Ghander and R.K. Fitch, Vacuum, 24, 483 (1971).

178. W.V. Ligon, Jr., Int. J. Mass Spectrom. Ion Phys., 41, 205 (1982).

179. M.A. Rudat, Presented at the 30th Annual Conference on Mass Spectrometry and Allied Topics, June 6-11, 1982, Honolulu, Hawaii.

180. M.A. Rudat, Anal. Chem., 54, 1917 (1982).

181. J.F. Mahoney, J. Perel, and A.T. Forrester, Appl. Phys. Lett., 38, 320 (1981).

182. J.F. Mahoney, D.M. Goebel, J. Perel, and A.T. Forrester, Biomed. Mass Spectrom., 10, 61 (1983).

183. J. Perel, K. Faull, J.F. Mahoney, A.N. Tyler, and J.D. Barchas, Am. Lab., 16, 94 (1984).

184. M.E. Castro and D.H. Russell, Anal. Chem., 56, 5 (1984).

185. C.N. McEwen, Anal. Chem., 55, 967 (1983).

186. R.G. Stoll, D.J. Harvan, and J.R. Hass, Int. J. Mass Spectrom. Ion Proc., 61, 71 (1984).

187. S.A. Martin, C.E. Costello, and K. Biemann, Anal. Chem., 54, 2362 (1982).

188. R. Stoll, V. Schade, F.W. Rollgen, V. Giessman, and D.F. Barofsky, Int. J. Mass Spectrom. Ion. Phys., 43, 227 (1982).

189. S.S Wong, R. Stoll, F.W. Rollgen, Z. Naturforsch, A., 37A, 718 (1982).

190. D.F. Barofsky, V. Giessmann, A.E. Bell, and L.W. Swanson, Anal. Chem., 55, 1318 (1983).

191. C.N. McEwen and J.R. Hass, Anal. Chem., 57, 890 (1985).

192. H.R. Schulten and H.D. Beckey, Org. Mass Spectrom., 7, 861 (1973).

193. K.L. Clay and R.C. Murphy, Int. J. Mass Spectrom. Ion Phys., 53, 327 (1983).

194. J.M. Gilliam, P.W. Landis, and J.L. Occolowitz, Anal. Chem., 55, 1531 (1983).

195. J.M. Gilliam, P.W. Landis, and J.L. Occolowitz, Anal. Chem., 56, 2285 (1984).

196. R.M. Caprioli, C.F. Beckner, and L.A. Smith, Biomed. Mass Spectrom., 10, 94 (1983).

197. C.F. Beckner and R.M. Caprioli, Biomed. Mass Spectrom., 11, 60 (1984).

198. T.L. Riley, T.J. Prater, J.L. Gerlock, J.E. deVries, and D. Schuetzle, Anal. Chem., 56, 2145 (1984).

199. D.R. Knapp, Biomed. Mass Spectrom., 12, 47 (1985).

200. S.J. Gaskell, B.G. Brownsey, P.W. Brooks, and B.N. Green, Int. J. Mass Spectrom. Ion Phys., 46, 435 (1983).

201. D.S. Millington, Presented at the 31st Annual Conference on Mass Spectrometry and Allied Topics, May 5-8, 1983, Boston, MA.

202. K.L. Clay, D.O. Stene, and R.C. Murphy, Biomed. Mass Spectrom., 11, 47 (1984).

203. B.C. Ho, C. Fenselau, G. Hansen, J. Larson, and A. Daniel, Clin Chem., 29, 1349 (1983).

204. A.J. DeStefano and T. Keough, Presented at the 31st Annual Conference on Mass Spectrometry and Allied Topics, May 5-8, 1983, Boston, MA.

205. A.A.R. Gharaibeh, J. Eagles, and R. Self, Biomed. Mass Spectrom., 12, 344 (1985).

206. D.L. Smith, Anal. Chem., 55, 2391 (1983).

207. K.M. Straub and P. Levandeski, Biomed. Mass Spectrom., 12, 338 (1985).

208. R.G. Cooks and K.L. Busch, Int. J. Mass Spectrom. Ion Phys., 53, 111 (1983).

209. A. Benninghoven, Int. J. Mass Spectrom. Ion Phys., 53, 85 (1983).

210. K.L. Busch, S.E. Unger, and R.G. Cooks, Presented at IFOSI, Symposium on Ion Formation from Organic Solids, University of Munster, October, 1980.

211. W.V. Ligon Jr., and S.B. Dorn, Int. J. Mass Spectrom. Ion Proc., 63, 315 (1985).

212. W.V. Ligon, Jr., Anal. Chem., 58, 485 (1986).

213. R.M. Caprioli, Anal. Chem., 55, 2387 (1983).

214. L.A. Smith and R.M. Caprioli, Biomed. Mass Spectrom., 11, 392 (1984).

215. M.M. Bursey, G.D. Marbury, and J.R. Hass, Biomed. Mass Spectrom., 11, 522 (1984).

216. W.V. Ligon, Jr., Int. J. Mass Spectrom. Ion Phys., 52, 183 (1983).

217. S.S. Wong, F.W. Rollgen, I. Manz, and M. Przybylski, Biomed. Mass Spectrom., 12, 43 (1985).

Chapter 2

CURRENT APPROACHES FOR CONTENDING WITH THE PROBLEM OF CHEMICAL INTERFERENCE IN FAB MASS SPECTRA

I. Introduction

Chapter 1 laid the foundation for a discussion of FAB and its relationship to other desorption-ionization methods. Hopefully, it also provided sufficient background information to recognize the potential of FAB as an analytical technique. Since FAB is a relatively new method, much is yet to be known about its mechanism and scope of application. However, as more is discovered about FAB, its shortcomings also become apparent and require attention. This dissertation is devoted to the refinement and optimization of FAB, and is primarily concerned with one of the fundamental limitations of the method, chemical interference.

When one acquires a FAB mass spectrum, it is seldom the spectrum of one component. Rather, it is usually a mixture of several components whose identity may or may not be known. Even in the case where a pure compound is run, there is still a contribution from glycerol ions to the FAB mass spectrum of the analyte. Peaks not originating from the analyte in a FAB mass spectrum are known collectively as "chemical interference" and are undesirable since they can mask the peaks representing the analyte ions.

It is instructive to divide chemical interference into two general categories according to the origin of the interference. The

first source is sample-related and includes impurities which survive the particular scheme of isolation or purification employed to obtain the analyte. The second source is related to the viscous liquid support used to hold the analyte during FAB. While the first class of chemical interferences may usually be removed upon further purification, matrix interference is omnipresent and requires different strategies for its removal.

The potential for excessive sample-related interference in FAB was first realized during an initial project undertaken for this dissertation. This study, which is the subject of Chapter 4, used FAB to identify urinary metabolites of the drug acetaminophen following isolation by reverse phase HPLC. Because of the possibility for chemical interference when dealing with such a complex matrix as urine, obtaining acceptable results by FAB was a significant challenge. Therefore, a large segment of this investigation was devoted to preparing a set of recommendations or guidelines for the efficient off-line use of FAB and HPLC with attention given to minimizing chemical interferences (1).

The remainder of this work concerns the development and application of a new method of matrix preparation for FAB called thermally-assisted FAB or TA-FAB (2,3). This approach incorporates resistive heating as a way to make immobile substances fluid enough for use as FAB matrices. In addition, the variable of temperature is shown to have some profound consequences on the data obtained, including a possible selection against background. The operating principles behind TA-FAB are outlined at the end of this chapter. Prior to this discussion an example of a FAB analysis is given to

acquaint the reader with the problems associated with matrix interference. This shall be followed by a review of current approaches to the problem of matrix interference in FAB before introducing TA-FAB as an alternative.

II. Problems Associated with Matrix-Related Interference

Although the introduction of liquid matrices is primarily responsible for the success of FAB, matrices also confront FAB with one of its most severe limitations, the imposition of chemical interference. While some are worse than others, all matrices generate background; especially at low mass where ions from the matrix typically dominate a FAB mass spectrum. The intensity of matrix peaks vary considerably. At one extreme, it is not uncommon to have the base peak in a FAB mass spectrum come from the matrix. The most prominent matrix peaks are often easily assigned to products resulting from clustering, adduct formation, and fragmentation. On the other hand, there are frequently several peaks of minor intensity whose origin cannot be readily deduced. Using glycerol, for instance, it is not uncommon to see some contribution at virtually every mass to about m/z 500. At present, no cogent explanation exists to account for the several extraneous peaks which dominate FAB mass spectra.

The level of matrix interference not only depends on the matrix employed, but on the concentration of the analyte as well. For example, cases of matrix suppression have been reported when enough analyte is present to completely cover the surface of glycerol (4).

Thus, one way to suppress matrix interference is to use more sample. Stated alternatively, matrix interference becomes the limiting factor to the detection of analyte peaks in FAB. As a consequence, it is not appropriate in FAB to describe sensitivity in terms of signal to noise (S/N), since noise is random and chemical interference is not. A more realistic concept is signal to background (S/B). This notion is developed in Chapter 4 and is used throughout this dissertation.

To illustrate the problem of matrix interference, a FAB spectrum of the tripeptide alanyl-leucyl-glycine is shown in Figure 2.1. To acquire this data, 1μg of the tripeptide was added to 1μl glycerol and bombarded with 7keV xenon atoms. The scan shown represents an average of ten mass spectra. Notice that the largest peaks in the mass spectrum come from glycerol and are labeled with the letter "B" to denaote background. Glycerol also contributes the several minor peaks which give the spectrum its "busy" appearance. Fortunately, peaks from the analyte are also evident; each is indicated by an asterisk in Figure 2.1. The most important peak is that for the protonated molecule at m/z 260, as this confirms the molecular weight (e.g., 259). The other analyte peaks are fragments indicative of the peptide structure. Certainly, the most important peptide fragments are those which grant sequence information. Using MS/MS, Barber and coworkers prepared a metastable map for the fragmentation of alanyl-leucyl-glycine which indicated that the peaks at m/z 185 and 189 enable the sequence of the tripeptide to be determined (5). However, m/z 185 also corresponds to the intense protonated glycerol dimer. Since this is such a dominant ion in the spectrum of glycerol, any contribution from the fragment would go unnoticed. As

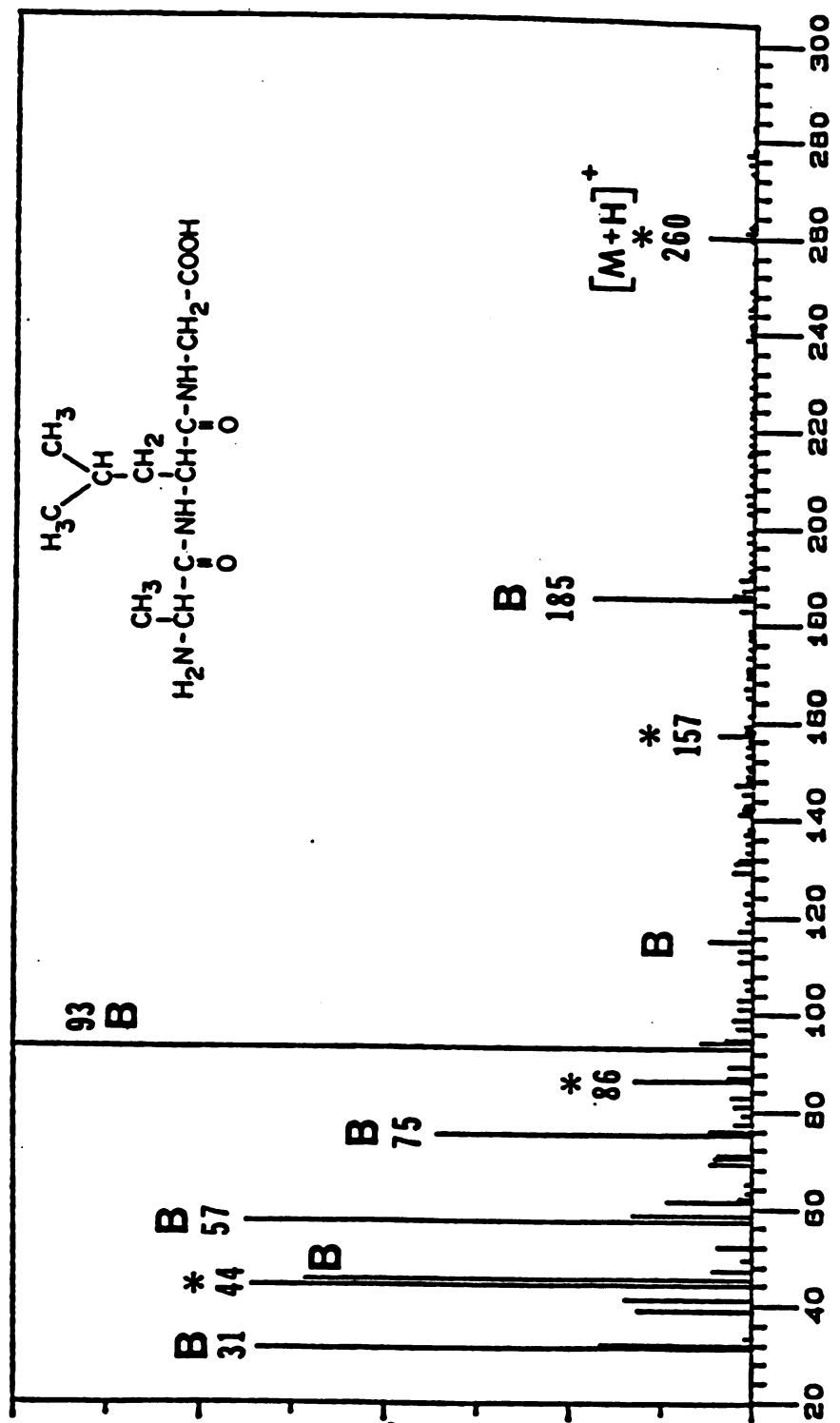

Figure 2.1 Averaged FAB mass spectrum of 1 µg alanyl-leucyl-glycine (MW 259) in 1 µl glycerol. The prominent background ions from glycerol are denoted with the letter "B"; each discernible analyte peak is designated by an asterisk.

a result, the peptide cannot be sequenced from the mass spectrum of Figure 2.1.

Hence, the problem with matrix interference is that it can, in essence, bury the information encoded by the analyte peaks of a FAB mass spectrum. In other words, for analyte peaks to be recognized, they must be large enough to stand above the level presented by background. This may not be possible either where matrix peaks are large (e.g., Figure 2.1) or conversely when analyte peaks are small. The latter scenario is frequently encountered when assigning fragmentation in FAB. Another place where the superposition of background becomes important is when isotope intensities are used to verify a proposed composition for an ion in a FAB spectrum. Isotopic abudances are only reliable in FAB if the analyte signal is strong and the matrix interference can be estimated.

III. Present Methods to Contend with Matrix Interference

Because of the impact that chemical interference has on FAB mass spectra, investigators have sought ways to minimize the problem. The methods used vary as to the approach taken and in their effectiveness. The current approaches may be described as one of three types: chemical, instrumental, or computer-aided background subtraction.

A common practice in FAB is to add a chemical reagent to the matrix to enhance the secondary ion yield from the analyte. Several practices have evolved which either increase sensitivity or make the information obtained by FAB more interpretable. Although these methods do not remove matrix interference, they can help to alleviate

some of the problems it causes. A brief survey of the reagents used shall be given to illustrate the methods available.

As discussed in Chapter 1, the ion types produced during FAB are frequently adducts to the analyte which yield an overall charge of ± 1. Furthermore, there is a great deal of evidence which suggests that many of the ions observed in FAB exist as pre-formed ions in solution prior to sputtering by the atom beam. A study reported by Caprioli which used the ions formed during FAB to quantitatively confirm dissociation constants for weak acids supports this claim (6). More recently a study in our laboratory showed direct evidence for pre-formed ions by making a direct correlation between known changes in visible spectroscopic data with corresponding changes in FAB mass spectra as a function of pH (7). Therefore, reagents are often added to a matrix with the intention of pushing an equilibrium in the direction of a charged state. Analytes can even be chemically derivatized prior to encountering the matrix in an attempt to improve their desorption/ionization characteristics by FAB. Such reactions are in direct contrast to the derivatization procedures carried out in GC-MS which enhance volatility. As a result, Cooks refers to the chemical transformations performed in DI methods as "reverse derivatization" (8).

Perhaps the simplist and most widely used method to promote ion formation is through acid-base chemistry. Several acids have been used successfully to enhance yields of $(M+H)^+$ ions by FAB. While acids such as hydrochloric or acetic work well, Cooks recommends p-toluene sulfonic acid because it is non-volatile (8). In one example the addition of 5% p-toluene sulfonic acid increased the

yield of the pentapeptide met-enkephalin 20-fold (9). However, one problem with this particular acid is, because it is non-volatile, it will produce background peaks in a FAB mass spectrum.

Just as acids promote $(M+H)^+$ ion formation in the positive ion mode, the addition of base will often increase the yield of negative ions when the analyte has an acidic moiety. Good examples are molecules containing a carboxylic acid group, since the corresponding anion is easily produced and quite stable. While acids and bases may be used to advantage in FAB, one should always be cautious to avoid hydrolysis if the analyte is susceptible under these conditions.

Singly charged cations and anions have been used extensively to promote adduct formation in FAB. The alkali metals and ammonium are the best known examples for cations, whereas chloride and thiocyanate are commonly used anions. Such adducts have been shown to enhance sensitivity because they are very stable and tend to resist fragmentation. In some cases, cation attachment offers the only way to observe the intact molecule when $(M+H)^+$ ions are unstable or when molecules can not become pre-charged. Although these adducts form readily to several analytes, presumably through ion-dipole interactions, they also bind to matrix species as well. However, selective attachment was reported in one example where Musselman spiked glycerol with silver salts and observed adducts almost exclusively to the analytes tested and not to the matrix (10). Silver also formed stable adduct ions which were easily recognized from the isotopic doublet occurring at 107 and 109 mass units above the molecular weight of the analyte.

Quaternary nitrogen species may be analyzed with high sensitivity by FAB due to their pre-charged behavior in solution and their high surface activity. Therefore, several investigators have performed chemical derivatizations to attach quaternary nitrogens onto analyte molecules to enhance their performance by FAB. This approach was first reported by Cooks et al. who reported two methods for quaternization (8). The first method used methyl iodide to exhaustively methylate amines, whereas the second used pyrrolidinium perchlorate to form iminium salts from aldehydes and ketones. Another method for making quanternary compounds from molecules with carbonyl groups is to react them with Girard's reagents (11). These compounds are either pyridinium or ammonium acylhydrazides that react with carbonyls to form hydrazones which contain a quaternary group. Kidwell and coworkers, using SIMS, applied this derivatization to several keto steroids and carbonyl containing pollutants with good sensitivity (11,12). A similar study using Girard's reagents to detect keto steroids by FAB was published by Busch (13). Kidwell et al., again using SIMS, described the use of other reagents for the prparation of quaternary compounds and demonstrated the ability to detect ppm levels of selected compounds in complex mixtures by this method (11). In this study, select drugs were detected in aqueous mixtures and in urine by using two derivatization methods. The first used 4-triethylammonium-1-chloro-2-butene to form quaternary species out of molecules with active hydrogens. In the second procedure, iodomethane was used to exhaustively methylate amine groups to form quaternary analogs. Finally, in a study performed in our laboratory, oligosaccharides were reacted with p-aminobenzoic ethyl ester at

their reducing end to prepare derivatives which could be observed using UV-detection with HPLC. Following reductive amination with sodium cyanoborohydride, these derivatives contained a quaternary nitrogen which aided in their detection by FAB (14).

In addition to enhancing sensitivity, the other major reason that reagents are added in FAB is to aid in the interpretation of the data. Biemann recommends the use of "shift" reagents in FAB to determine the presence of specific functionalities by following the change in mass after chemical modification (15). For example, the addition of acetic anhydride to a sample/glycerol mixture can lead to an increase in the $(M+H)^+$ ion by 42 mass units for every functional group present which can be acetylated. Similarly, addition of methanol/HCl indicates the presence of carboxyl groups through methylation (15). A more reliable approach, used to determine the number of aspartic and glutamic acid residues in peptides, involves glycinamidation (16). The corresponding mass increase in this case is 56 mass units.

As in the example of glycinamidation, many of the reaction schemes developed were to assist the sequencing of biopolymers by FAB. A common practice for peptide sequencing is to perform an N-acetylation of the N-terminus with a 1:1 mixture of acetic anhydride:$^2H_3$- acetic anhydride. This procedure, developed by Morris, enables the analyst to determine the N-terminal fragments by the occurrence of characteristic 1:1 doublets appearing at 42 and 45 mass units above the original peaks (17). Another problem in peptide sequencing is to determine the location of disulfide linkages. While several methods may be used, perhaps the simplist is to use a matrix

prepared from a 5:1 (w/w) mixture of dithiothreitol and dithioerythritol. This matrix reduces these linkages to sulfhydryl groups to give an increase of two mass units (18). Perhaps the most dramatic in situ reaction using peptides was reported by Caprioli et al. These workers succeeded in following the enzymatic digestions of various peptides on the probe tip in real time (19).

Derivatization procedures have also aided the FAB analysis of oligosaccharides. Rose and coworkers, for instance, showed that certain boronide acids can form boronate complexes with hydroxyl groups to yield both sensitive detection as negative ions, and information regarding confirmation (20). In another study, Dell et. al. showed that derivatives for GC-MS (e.g., acetyl, permethyl, methoxime) can be useful in the FAB analysis of carbohydrates by directing fragmentation and aiding in interpretation (21). Under these conditions, dosing of the matrix with various salts was necessary to promote molecular ion formation.

Another chemical approach to matrix interference involves the use of surfactants to modify analyte responses in FAB mass spectra. Because the FAB beam selects for molecules at or near the surface of the sample solution, anything that increases the surface activity of the analyte will result in greater sensitivity and perhaps a selection against background. A method introduced by Ligon uses surfactants of opposite charge to the analytes being detected. These compounds occupy the surface and attract oppositely charged analyte ions thereby increasing their surface concentration (22). Furthermore, since the surfactants are of opposite charge, they cause minimal interference to the mass spectra of the analyte. Ligon and

Dorn used the cationic surfactant tetradecyltrimethylammonium hydroxide to increase the response of several inorganic anions in glycerol (23). Ligon recently showed that analytes may be reacted to increase their surface activity and hence sensitivity. For this purpose, hydrocarbon chains were attached to the amino groups of small peptides through a Schiff base formation with dodecanol (24). The increase in signal intensity observed ranged from 2- to 8-fold. As mentioned previously, the chemical modifications discussed make the data more interpretable but do not remove the interference from the matrix. Therefore, investigators have developed more effective methods using an instrumental approach.

Two types of instrumental methods may be considered as ways to remove matrix interference. The first is to simply scan under high resolution. Several, more sophisticated mass spectrometers have the ability to discern mass values beyond nominal mass resolution. Therefore, it might be possible to scan a double-focussing instrument while using a resolution sufficient to literally resolve the matrix interference from the analyte peaks. This approach is not used however, because of the enormous loss that would result in sensitivity.

Instead a more viable route is to separate the analyte peaks from the matrix by the approach of mass spectrometry/mass spectrometry (MS/MS). The two major uses of MS/MS are for structural elucidation and mixture analysis. Through use of this latter mode, matrix ions as well as impurities may be removed; the problem of chemical interference in FAB is in reality one of mixture analysis. Many examples of FAB-MS/MS appear in the literature. However, no

attempt will be made to review them here. Instead, an illustration of how the method works is presented using data acquired on the triple quadrupole mass spectrometer at the MSU-NIH Mass Spectrometry Facility.

At the top of Figure 2.2 a FAB mass spectrum appears, again for the analysis of 1 μg alanyl-leucyl-glycine in glycerol. In this example, xenon atoms were produced by a capillaritron source housed within a removable DIP gun (25). The mass spectrum shown at the top of Figure 2.2 is intended only to show the ions formed and their relative abundances as they occur inside the ion source (e.g., prior to mass analysis). As before, the primary background peaks, which are the most intense peaks in this spectrum, are designated with the letter B. The analyte peaks in Figure 2.2 are labeled with stars, as indicated.

The process begins with the selection of the protonated peptide molecule at m/z 260 using the first quadrupole mass filter. Using the first mass analyzer in a static mode, all other ions occurring in the source are not transmitted and are thus removed from consideration. In this way a selection is made against all glycerol ions, except for any interference isobaric with the $(M+H)^+$ ion at m/z 260. Next, the $(M+H)^+$ ions are focussed into a second quadrupole filter which is operated in the rf-only mode to eliminate mass selection. This quadrupole contains an elevated pressure of argon to serve as a collisional target for the parent ions from the peptide. Here a process of collisionally-activated dissociaton (CAD) takes place to fragment the parent ion; a quadrupole is used as a collision cell to improve the transmission of the ions produced.

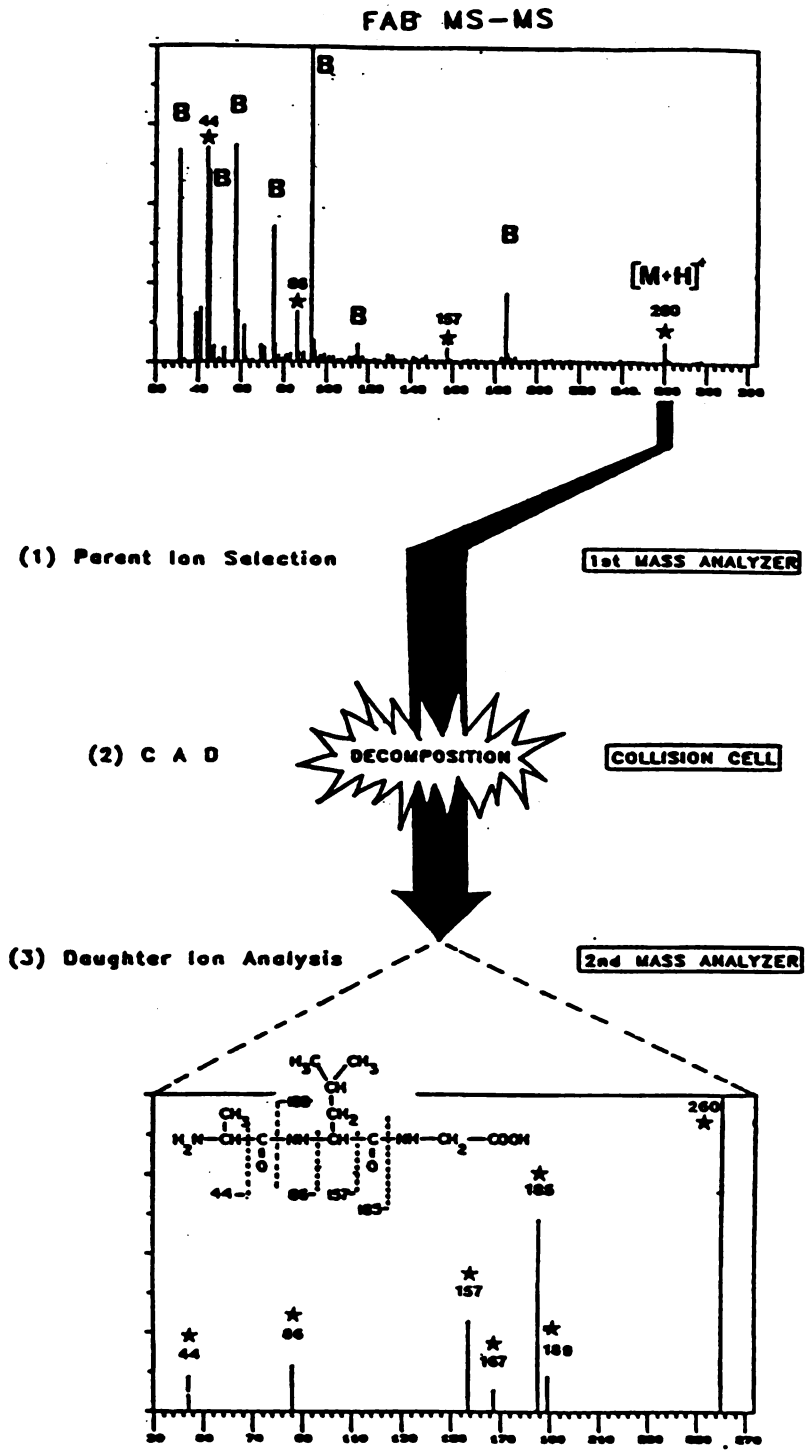

Figure 2.2 Pictoral representation of the use of MS/MS to remove matrix interference from glycerol in the FAB analysis of 1 µg alanyl-leucyl-glycine.

These ions are then mass analyzed by a third quadrupole operating in a scanning mode so that the analyte ions may be sequentially transmitted to the detector to give the mass spectrum at the bottom of Figure 2.2. As indicated, this process was very effective in removing the glycerol peaks and at providing substantial signal to noise for the analyte ions. Furthermore, it is recalled from the example in Figure 2.1 that under conventional FAB there was interference from glycerol at m/z 185 which masked a sequence-specific ion. The existence of this ion was confirmed by MS/MS.

While MS/MS can be very efficient at removing chemical interference, the cost of the instrumentation required is prohibitive to many users who have access to FAB. For example, FAB may be installed on an instrument for $10,000-30,000 depending on the modifications required on the particular mass spectrometer. By comparison, one can not acquire an instrument with MS/MS capabilities without investing at least $300,000. Another limitation to MS/MS should also be recognized. Sensitivity in FAB-MS/MS is frequently limited by the efficiency of the collision cell used. Many collision cells have transmission capabilities only on the order of 1-10% (26). Although greater yields are reported for triple quadrupoles (27), this certainly classifies as a bottleneck step.

A final approach to the problem of background, that of computer-aided background subtraction, is the most frequently used method for removal of matrix interference. During this process, a blank solution is used to obtain a background spectrum in a separate determination from the analysis which contained the analyte. This

spectrum is then subtracted from the analyte-containing mass spectrum using the computer to effect removal of background. Although this practice can provide insight, it is far from a quantitative process and can lead to spurious results.

The fundamental problem is that both background and analyte have similar temporal characteristics. In other words, there is no one scan in a FAB analysis which contains a representative view of background only on which to base a subtraction. As shown in the next section, this is a different situation from the familiar case of in GC-MS where computer-aided background subtraction is carried out routinely and often quantitatively because there is usually a scan off to the side of the peak which represents the background that co-elutes with the analyte. In FAB, however, the probe must be removed to perform a separate determination. Poor reproducibility in the total ion current (TIC) associated with probe position and ion-focussing conditions decreases the validity of this approach to background subtraction.

Another limiting factor is that the TIC varies according to sample composition. For example, when an analyte is present in glycerol, the glycerol peaks normally become suppressed relative to the blank determination where only glycerol is present. The obvious tendency here is to oversubtract. This can lead to serious errors when an analyte is present in low concentration, because minor analyte fragments might not survive over subtraction. Furthermore, intensities for individual peaks vary with respect to one another during the course of a FAB analysis. Hence, the likelihood that a particular background scan will properly represent intensities for

all peaks of interest is remote. Because of these problems and the general uncertainty involved, it is unlikely that a "subtraction factor" can be used to normalize differences in TIC which result from a separate determination to assess background.

Finally, another problem may arise when performing a separate analysis for background, namely the need to obtain an acceptable blank. Granted, in some cases the problem is trivial. For example, when neat solids are mixed with glycerol to form a mull, the appropriate blank would simply be glycerol. However, this is a very simplified case in comparison to situations where a small quantity of analyte is present in a complex sample matrix and wheneverthere is limited information regarding the structure or identity of the compound. In these cases having a reliable blank may be very critical because if interferences are not removed by subtraction, or at least attenuated, they will be falsely assigned as belonging to the analyte. Hence, computer-aided background subtraction can be a helpful option in FAB analyses, but the operator should be aware of the shortcomings involved and should exercise caution especially when viewing a weak analyte signal amidst formidable background.

IV. Fundamentals of Thermally-Assisted-FAB

As an introduction, this section will describe basic operating principles of TA-FAB and shall qualitatively discuss the format of the data obtained. A more complete discussion of this approach is found in Chapters 4 and 5.

Thermally-assisted FAB refers to the process of heating substances which are inherently too immobile to serve as FAB matrices inside the mass spectrometer to make them viable for use in FAB. While several materials have been considered, initial success has been achieved using saturated aqueous solutions of highly hydroxylated compounds (fructose, glucose, thioglucose, and tartaric acid). During TA-FAB, the probe tip is resistively heated in a controlled fashion to effect physical changes in the analyte/matrix solution while undergoing FAB. Saturated saccharide matrices, which exist as solutions under the low pressure conditions of the mass spectrometer, upon heating, simulate the desired properties of glycerol yet produce less background. As a further consequence, by controlling the temperature of the matrix solution, it is possible to optimize the conditions for analyte desorption-ionization as a function of temperature. On the other hand, since matrix desorption-ionization is relatively independent of the applied temperature, a linear temperature ramp produces a desorption profile for analyte ions which is readily distinguishable from that of the matrix ions. This behavior is in contrast to conventional FAB where the desorption profiles for analyte and matrix ions have similar temporal relationships.

Several important consequences result from the ability to alter the desorption profiles of the analyte ions relative to matrix ions during TA-FAB. These include: 1) the ability to optimize for the desorption of analyte as a function of temperature, 2) the capability of identifying analyte peaks by the nature of their

desorption profiles, and 3) the possibility of performing a valid background subtraction.

For the purpose of addressing these points, Figure 2.3 gives a conceptualized view of the temporal behavior for analyte and background observed by three methods: GC-MS, FAB, and TA-FAB. In each case the abscissa is scan number (or time) and the ordinant is signal intensity in arbitrary units and is not intended to be quantitative.

The first example in Figure 2.3 is that of GC-MS. Figure 2.3a shows the reconstructed total ion current obtained for a single chromatographic peak following ionization and analysis by mass spectrometry. Shown in Figure 2.3b is the profile for a continuous form of background, in this case column bleed, which often accompanies GC-MS analyses whenever packed columns or capillary columns having non-bonded stationary phases are used. Fortunately, in GC-MS there is a temporal distinction between the behavior of analyte and background. The subtraction process is essentially quantitative whenever two requirements are met. First, a region in the profile must exist which contains background only. Secondly, the background in this region must be representative of the background present as the analyte elutes.

The second example in Figure 2.3 displays the nature of the data obtained using conventional FAB. In contrast to GC-MS, FAB creates profiles for analyte and background ions which are virtually indistinguishable and which tend to remain fairly constant over time. A valid background subtraction cannot be performed because there is no one scan representing background only. Under these circumstances,

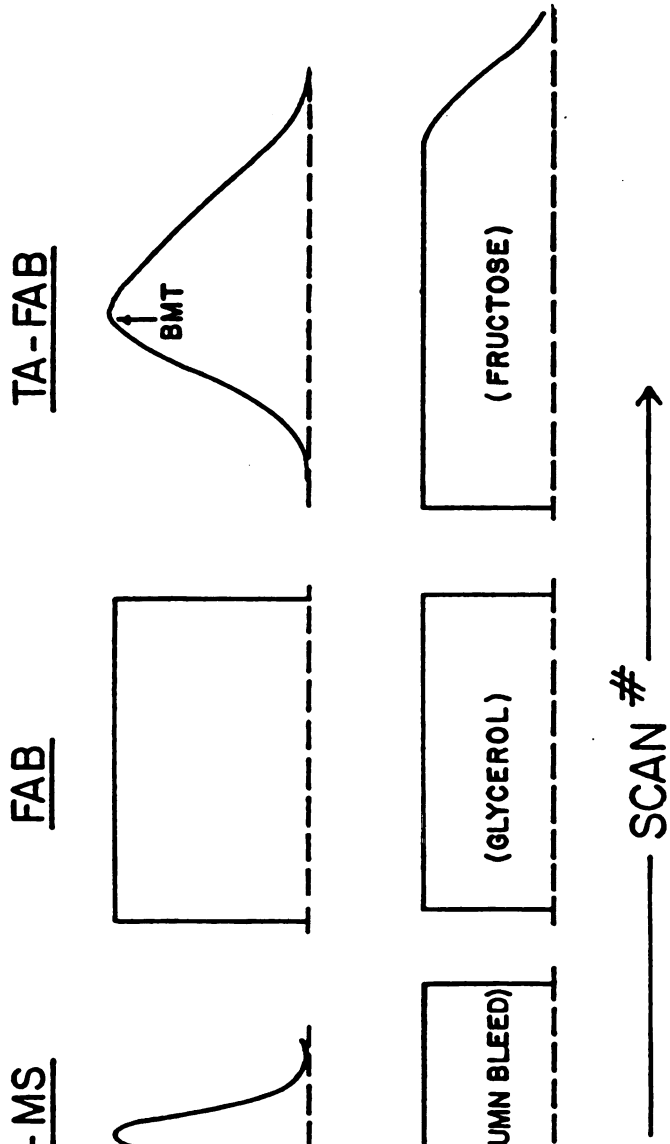

Figure 2.3 Conceptualized diagram comparing the temporal relationship of ion profiles observed by GC-MS, FAB, and TA-FAB: (a) analyte ion profiles; (b) background ion profiles.

a separate FAB analysis of an appropriate blank solution is used to provide data for background subtraction. The problems associated with this approach were defined in the previous section.

The final set of profiles in Figure 2.3 depicts typical results obtained in a TA-FAB experiment inorporating a saturated saccharide solution as the matrix. In this example, the abscissa corresponds to temperature, as well as scan number, since a slow linear ramp of current proceeds through the probe tip during the analysis. As shown, the desorption of analyte ions is clearly a function of temperature (upper trace) in contrast to the desorption of matrix ions which is fairly independent of temperature (lower trace).

At the beginning of a TA-FAB experiment data are normally collected without heating (FAB only). Often under these conditions desorption-ionization occurs exclusively from the matrix since unheated saturated aqueous solutions of saccharides are apparently too viscous to permit sufficient desorption-ionization of the analyte. However, upon heating, the saccharide solution becomes less viscous and hence more similar to glycerol. This corresponds to the point in the profile where analyte desorption begins to occur. The analyte signal continues to rise past this point as the probe tip experiences a slow, linear increase in temperature. Eventually an optimum point is reached where the desorption of analyte is at a maximum. By analogy to field desorption nomenclature, the temperature corresponding to maximum analyte desorption in TA-FAB is called the "best matrix temperature" or BMT. With continued heating beyond the BMT, the intensities of analyte and matrix ion current diminish. We attribute this effect primarily to the decreased mobility of the

analyte due to the loss of water from the matrix. In other words, as the matrix dries out, desorption of the analyte ceases and desorption by the matrix diminishes also.

Similar to the situation in GC-MS, the profiles shown in Figure 2.3 for TA-FAB contain a region at the beginning of the run where only background ions are present. Furthermore, since the background spectrum recorded prior to desorption of the analyte (no heat) is similar in both content and intensity to the background co-recorded later with the analyte, in favorable cases data may be collected for a valid subtraction of matrix-related background using TA-FAB. This process is illustrated using real examples in Chapter 5. However, before this is done, the instrumental modifications needed to perform TA-FAB are discussed in the chapter that follows.

V. LIST OF REFERENCES

1. B.L. Ackermann, J.T. Watson, J.F. Newton, Jr., J.B. Hook, and W.E Braselton, Jr. Biomed. Mass Spectrom. 11, 502 (1984).

2. B.L. Ackermann, J.T. Watson, and J.F. Holland, Anal. Chem., 57, 2656 (1985).

3. B.L. Ackermann, J.T. Watson, and J.F. Holland, paper submitted to Biomedical and Environmental Mass Spectrometry.

4. M. Barber, R.S. Bordoli, G.J. Elliot, R.D. Sedgwick, and A.N. Tyler, Anal. Chem., 54, 645A (1982).

5. M. Barber, R.S. Bordoli, R.D. Sedgwick, and L.W. Tetler, Org. Mass Spectrom., 16, 256 (1981).

6. R.M. Caprioli, Anal. Chem., 55, 2387 (1983).

7. B.D. Musselman, J.T. Watson, and C.K. Chang, Org. Mass Spectrom., 21, 215 (1986).

8. K.L. Busch, S.E. Unger, A. Vincze, R.G. Cooks, and T. Keough, J. Am. Chem. Soc., 104, 1507 (1982).

9. M. Barber, R.S. Bordoli, G.V. Garner, D.B. Gordon, R.D. Sedgwick, L.W. Tetler, and A.N. Tyler, Biochem. J., 197, 401 (1981).

10. B.D. Musselman, J. Allison, and J.T. Watson, Anal. Chem., 57, 2425 (1985).

11. D.A. Kidwell, M.M. Ross, and R.J. Colton, Biomed. Mass Spectrom., 12, 254 (1985).

12. M.M. Ross, D.A. Kidwell, and R.J. Colton, Int. J. Mass Spectrom. Ion Phys., 63, 141 (1985).

13. G.C DiDonato and K.L. Busch, Biomed. Mass Spectrom., 12, 364 (1985).

14. W.T. Wang, N.C. LeDonne, Jr., B.L. Ackermann, and C.C. Sweeley, Anal. Biochem., 141, 360 (1984).

15 S.A. Martin, C.E. Costello, and K. Biemann, Anal. Chem., 54, 2362 (1982).

16. Y. Wada, A. Hayashi, I. Katakuse, T. Matsuo, and H. Matsuda, Biomed. Mass Spectrom., 12, 122 (1985).

17. H.R. Morris, Int. J. Mass Spectrom. Ion Phys., 45, 331 (1982).

18. A.M. Buko and B.A. Fraser, Biomed. Mass Spectrom., 12, 577 (1985).

19. R.M. Caprioli, L.A. Smith, and C.F. Beckner, Int. J. Mass Spectrom. Ion Phys., 46, 419 (1983).

20. M.E. Rose, C. Longstaff, and P.D.G. Dean, Biomed. Mass Spectrom., 10, 512 (1983).

21. A. Dell, J.E. Oates, H.R. Morris, and H. Egge, Int. J. Mass Spectrom. Ion Phys., 46, 415 (1983).

22. W.V. Ligon, Jr. and S.B. Dorn, Int. J. Mass Spectrom. Ion Proc. 61, 113 (1984).

23. W.V. Ligon, Jr. and S.B. Dorn, Int. J. Mass Spectrom. Ion Proc. 63, 315 (1985).

24. W. Ligon, Jr., Anal. Chem., 58, 485 (1986).

25. J. Perel, K. Faull, J.F. Mahoney, A.N. Tyler, and J.D. Barchas, Am. Lab., 16, 94 (1984).

26. R.A. Yost and D.D. Fetterolf, Mass Spectrom. Rev., 2, 1 (1983).

27. R.A. Yost and C.G. Enke, J. Am. Chem. Soc., 100, 2274 (1978).

Chapter 3

INSTRUMENTATION

I. Introduction

All FAB experiments undertaken for this dissertation were performed on a double-focusing mass spectrometer at the MSU-NIH Regional Facility for Mass Spectrometry. The instrument was a Varian MAT CH5 of Nier-Johnson geometry. This chapter will not discuss the experimental procedures associated with the various projects, as they are contained in separate sections in subsequent chapters. Rather, the material covered here shall discuss the necessary modifications to convert the CH5 to perform FAB, and the equipment that was used for TA-FAB experimentation. In addition, the basic components and operating principles pertaining to the instrumental configuration will be outlined.

A diagram of the mass spectrometer appears in Figure 3.1. The instrument is referred to as double-focusing because two stages of mass selection occur. First, ions are dispersed according to momentum as they pass through the magnetic sector followed by an additional focusing and filtering according to kinetic energy by an electrostatic analyzer (ESA). The additional sector accounts for the high resolution capability of the CH5 by selecting ions within a narrow range of energies, whereby individual masses may be separated to within a millimass unit. The CH5 may be described as having a reverse geometry since the magnetic sector precedes the electrostatic sector. This order was selected primarily to facilitate MS/MS data

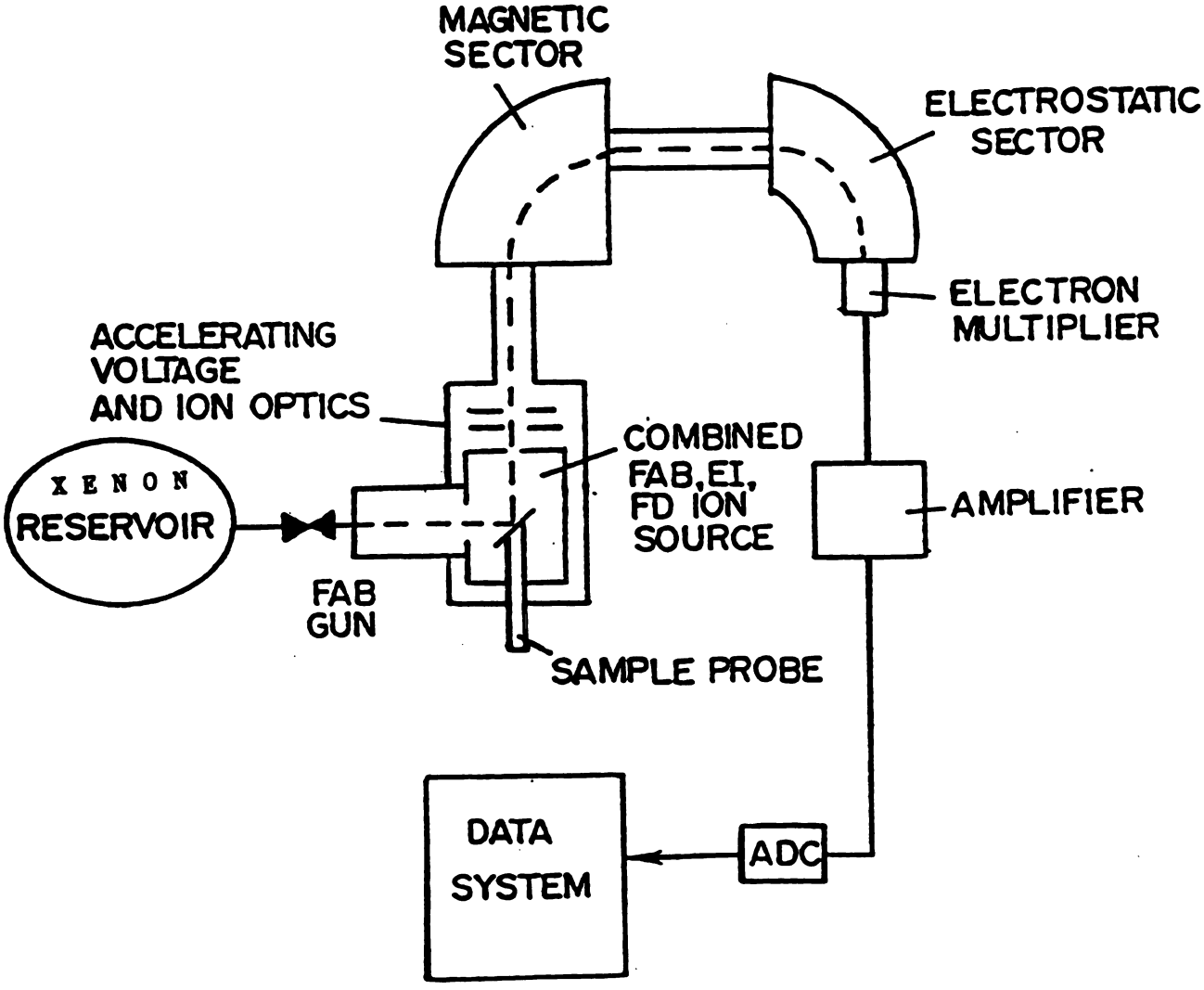

Figure 3.1 General diagram of the Varian MAT CH5-DF mass spectrometer.

acquisition. The approach here, known as MIKES, which stands for mass-analyzed ion kinetic energy spectra, was the earliest form of MS/MS. During MIKES, the products of the metastable decomposition of a parent ion, selected by the magnet, are sequentially passed by scanning the voltage on the plates of the electrostatic sector. This process is possible because the products of decomposition in the field-free region between the sectors have the same average velocity as the parent ion. Unfortunately, the efficiency of this process is limited on the CH5 because of the lack of a collision cell.

The fundamental relationship governing mass selection by a magnetic sector instrument may be expressed as:

$$m/z = \frac{B^2R^2}{2V} \qquad (1)$$

where m/z is the mass to charge ratio, B is the magnetic field strength, R is the radius of the magnet, and V is the acceleration potential. All the parameters on the right side of equation 1 are held constant, except for the magnetic field strength which may be varied to give a maximum field strength of 12 kGauss. The acceleration potential is +3000 volts and the radius of curvature for the flight tube through the 90° magnetic sector is 21.4 cm. Under these conditions, the particular mass to charge ratio transmitted through the magnetic sector depends only on the applied magnetic field. The mass range, at full accelerating potential, is 1200 u. However, as indicated by equation 1, this range can be extended to a

maximum of 3600 u by a lowering of the accelerating potential to 1kV. The problem with extending the mass range in this manner is that the ions move more slowly thereby impeding their transmission, and severely reducing the force with which they strike the electron multiplier detector. The loss in sensitivity is usually unacceptable.

II. Ion Source Configuration

Figure 3.2 is a simplified diagram of the ion source region of the CH5. The small box in the center of the diagram is the ion source itself. There are four ports shown. The lower opening accepts the FAB sample inserted on the probe used previously for FD through a vacuum lock. The FAB probe is colinear to the optical axis of the ion source and perpendicular to the atom beam. The FAB probe tips were fashioned from several materials including stainless steel, copper, and aluminum. Each was machined to have a 60° angle of incidence (i.e., the angle between the incident atom beam and a line normal to the probe surface), and had surface dimensions of (0.25 in. x 0.10 in.). Since the FAB probe tip is continuous to the ion source, it floats at 3000 ceramic (shaded). The FAB source was mounted to the ion source housing at the port which previously was used for a GC-MS interface. This was fortunate because there was already a hole in the ion source which could accept the FAB beam with a direct line-of-sight to the sample. This modification is addressed in more detail later. The ion source also has a port for a direct insertion probe (DIP), opposite to the FAB beam, which is used to

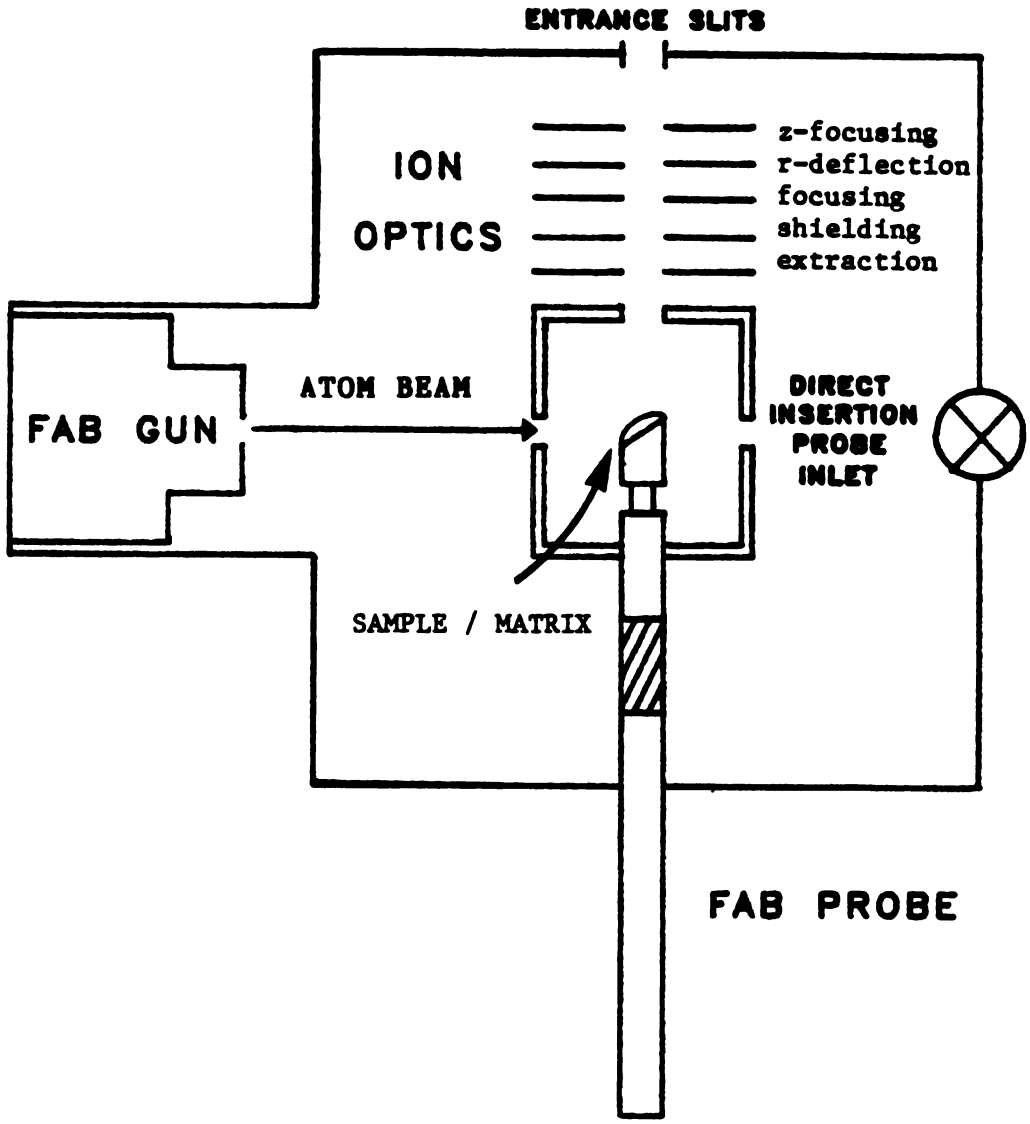

Figure 3.2 Diagram of the ion source region of the CH5 modified for FAB.

introduce solid samples for EI. The EI filament and trap are not shown, but are located directly above and below the FAB tip appearing in Figure 3.2. The secondary positive ions formed in the source are extracted by a lens known as the extraction lens which is biased slightly negative with respect to the ion source. The ion optics are a series of five lenses, each having an adjustable potential which becomes less positive as the ions move away from the source. Essentially, the lenses are connected to a large voltage divider which begins at the ion source.

After traversing the ion optics the ion beam is resolved by a set of entrance slits, held at ground potential, prior to mass analysis. Actually, there are two sets of slits at this point, one for low resolution and the other for high resolution. Each is adjustable. Located beyond the electrostatic sector, immediately preceding the electron multiplier, are two complementary sets of slits known as exit slits. The entrance and exit slits are adjusted in succession to give the resolution desired. During the acquisition of FAB mass spectra, a resolution of about 500 ($R = M/\Delta M$, 5% valley definition) was employed, set in the low resolution mode. Unfortunately, the maximum resolution obtained under high resolution during the course of this work was about 4000 (5% valley). The maximum resolution specified by the manufacturer is 10,000 (5% valley) (1). The poor resolving power of the instrument suggests the need to have the slits cleaned and repaired, a process which requires a skilled technician.

Focus in a double sector instrument is primarily done according to energy. This is because the electrostatic sector voltage (on the

order of 250 volts) is directly coupled to the accelerating potential to permit only ions having a preselected energy to be transmitted. Is is important to recognize two factors in a double-focusing instrument which alter the energy of the ions, and hence determine whether an ion will be transmitted and detected. The first is the position where the ion is formed, since this will determine the amount of energy the ion receives as it is accelerated out of the source towards ground potential. The second factor concerns the initial energy imparted to the ion during formation, as well as its initial direction. Hence, the ions observed under a particular focus represent a superposition of these two factors.

III. Vacuum System

High vacuum is essential to the mass spectrometer since the operating pressure within the instrument affects both resolution and transmission. The vacuum system of the CH5 consists of three oil diffusion pumps and three direct drive mechanical pumps. The diffusion pumps each contained 75-150 ml of a polyphenylether oil (Santovac 5, Monsanto, Inc). The instrument is partitioned into two sections, the source and analyzer regions, which are differentially pumped. Manual isolation of these two regions is possible by a valve, located after the entrance slits and before the magnet, which opens and closes the small orifice between the source and analyzer regions. Two diffusion pumps are used to evacuate the analyzer region whereas one larger diffusion pump which services the source. However, because of higher pressures experienced in the source, one

mechanical pump is assigned to provide fore vacuum to the source diffusion pump, whereas the analyzer region uses one mechanical pump to back both diffusion pumps. The third mechanical pump is used to provide rough vacuum throughout the instrument. By means of a branching manifold, this pump supplies rough vacuum ($\geq 10^{-2}$ torr) to the batch, direct probe, and FAB sample inlet ports, and also pumps the glass blown gas reservoir which supplies the FAB gun. All three diffusion pumps require manual isolation from the source and analyzer regions by separate "butterfly" valves.

The vacuum in the source and analyzer is detected by separate Penning gauges. During operation, the analyzer pressure is $< 1 \times 10^{-6}$ torr. In contrast, the source Penning gauge typically registers a pressure of 1×10^{-5} torr during FAB due to the pressure caused by xenon. A safety mechanism on the instrument prohibits operation whenever a pressure greater than 1×10^{-5} torr is registered by turning off power to the diffusion pumps. Therefore, to perform FAB this mechanism is overriden by a switch on the electronics cabinet of the CH5. In addition, a thermocouple vacuum gauge is located just above each mechanical fore pump to indicate when the capacity of each mechanical pump is exceeded. Beyond this pressure, which corresponds to a source pressure of 5×10^{-5} torr, the diffusion pumps are automatically turned off to limit back-streaming of oil vapor into either the source or analyzer.

Each diffusion pump is cooled with a coolant mixture of 50% (v/v) ethylene glycol in distilled water. The coolant passes in a series arrangement around each diffusion pump and the magnet. It is then cooled by recirculationthrough a reservoir/heat exchange unit

located in the penthouse of the Biochemistry building. A mechanical flow detector connected to a solenoid switch cuts power to the diffusion pumps in the event of a ceasation in coolant flow. Also, located above each diffusion pump is a baffle which contains 95% ethanol. The purpose of baffling is to condense oil vapors before they reach the ion source or the analyzer. The ethanol is kept cool by a flexible metal cold-finger containing freon. The circulating freon is refrigerated by a separate cryogenic cooling unit for each pump.

IV. FAB Instrumentation

The early stages of this project were devoted to converting the CH5 to accomodate a commercially-produced fast atom source. The gun purchased was a model B11NF saddle field fast atom source (Ion Tech Ltd., Teddington, U.K.). The method of fast atom production by this source was considered in detail in Chapter 1. This gun is commonly referred to as a "cold cathode" atom gun since the electrons which neutralize fast ions to produce fast atoms (via resonance electron capture) are not produced by a filament. Figure 3.3 shows a diagram of the construction of the gun. In addition, the cut-away section reveals the inner workings. Contained within the center of the gun is a washer-like, stainless steel anode which is isolated from ground by ceramic insulators. An adjustable voltage of +2 to 10kV may be placed on the anode through the high voltage connection shown. Because of poor fabrication by the manufacturer, this connection was fortified at the point where the flexible lead enters the gun. The

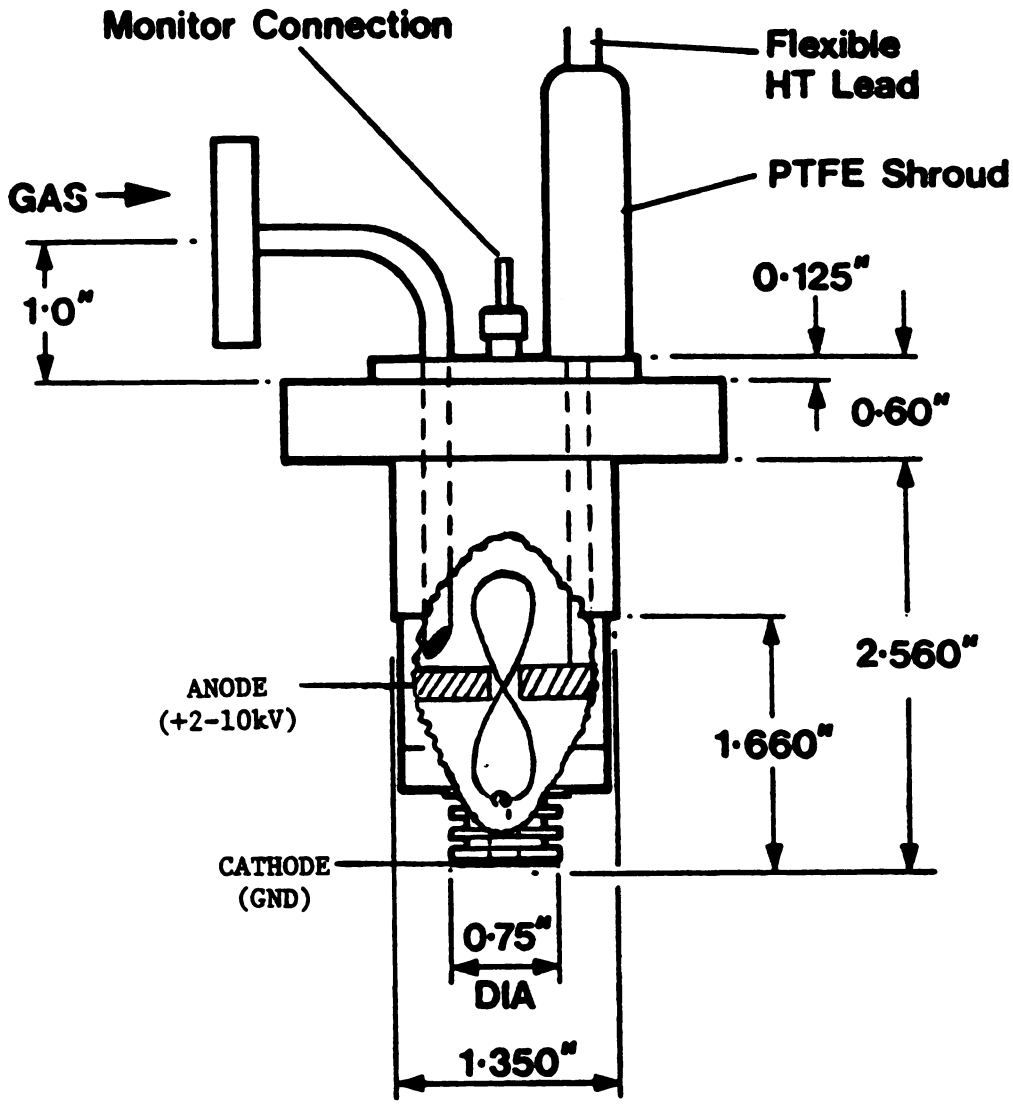

Figure 3.3 Diagram of the Ion Tech B11NF saddle field fast atom source.

voltage is supplied from an Ion Tech B50 current-regulated high impedence power supply capable of delivering a maximum output of 10 kV at 10 mA.

Xenon gas enters the gun through the curved 1/4 inch stainless tube shown in Figure 3.3. This tube is attached to a flange which has a finely-machined knife edge surface to accomodate a standard copper gasket (0.25 in. O.D., 0.125 in wide). The xenon gas enters through the conduit shown where it eventually flows in the vicinity of the anode. At a gas pressure of about 10^{-4} torr a discharge occurs and a plasma is sustained (2). Electrons, regardless of their initial direction, become continuously attracted to the saddle point which is located in the hole at the center of the anode. Thus, a constant flux of electrons is formed which oscillates through the anode as shown. Ionization of the xenon at the anode results in positive ions accelerated toward ground in all directions. Resonance capture of electrons to form fast atoms is believed to occur at the turn-around point in the trajectory of the electron (v=o). The aluminum cathode, held at ground, also has a hole to transmit fast atoms formed by this process. While other methods, such as charge exchange, can result in the formation of fast atoms, only the products of resonance electron capture statistically have the proper trajectory to traverse through the cathode as no loss in momentum occurs in these events. The aperture in the cathode is 1.5mm and an approximate 2° divergence angle is specified (3).

As discussed in Chapter 1, a considerable amount of fast ions are also produced by this gun. In fact, the fast ions produced are used to estimate the approximate flux of the atom beam since the two

are taken to be proportional. For this purpose, another aluminum cathode is located at the rear of the gun to measure the ion flux which occurs in this direction by virtue of the symmetry of the gun. The current produced may vary up to a maximum of 100 μA and is measured at the small monitor lead shown in Figure 3.3. Under typical operating conditions (anode 7 kV, power supply 1mA, source pressure 2 x 10^{-5} torr) the beam current measured was about 25 μA. Generally, an increase in gas flow will result in greater beam intensity. However the power supply must supply more current to maintain a constant anode voltage as more gas enters the gun.

Biemann suggested two modifications for reducing the gas consumption of the B11NF saddle field gun (4). The first was to block off the rear end of the gun with a piece of aluminum. This modification was incorporated and lowered the typical operating pressure from 2 x 10^{-5} torr to 1 x 10^{-5} torr inside the ion source. Biemann also suggested that the front cathode aperture be reduced to 0.5 mm (4). This refinement did not prove useful since a more stringent alignment of the anode was needed and because the aperature eventually becomes widened by sputtering.

V. Instrument Modification for FAB

It is recalled from the discussion of Figure 3.2 that the FAB gun was attached to a port on the CH5 which previously accomodated a GC-MS interface. Since the modification was essentially permanent, it was decided that the CH5 would be dedicated to desorption-ionization at the expense of GC-MS capabilities. This

port was ideally suited for FAB because the hole present in the ion source for the GC effluent gave a direct line-of-sight entrance for the FAB beam.

Modifications were needed prior to the installation of the FAB source. First, the port on the ion source housing was too close to the ion source itself which made direct installation of the gun physically impossible. Further, it was reported by Franks that the highest neutral/ion ratio was obtained when the saddle field gun was located a distance 11 cm away from the FAB probe target (2). Therefore, a cylindrical metal extension was attached to the ion source housing to approximate this distance and to house the FAB gun. This cylindrical steel FAB housing was purchased from Varian, and came equipped with ConFlat® flanges at both ends. ConFlat® flanges are circular stainless steel flanges with machined knife edge surfaces for use with copper gaskets under high vacuum conditions. The ConFlat® flange was chosen to mate with the 2.75 inch O.D. flange which came attached to the FAB gun as illustrated in Figure 3.3. A standard copper gasket (2 in. O.D., 1/4 in. wide) fits between the two flanges to hold high vacuum. Unfortunately, the ConFlat® flange at the opposite end of the extension did not mate directly to the flange on the ion source. To rectify this situation, the knife edge flange was removed and replaced by a standard CH5 flange which was welded to the end of the tube to make a vacuum tight seal. Instead of having a knife edge arrangement, these two flanges mated along a flat surface. A silver-tin gasket was made to hold high vacuum along this interface.

High purity xenon gas (99.995%) was purchased in 50-liter quantities from Matheson, Gloucester, MA., for all experiments. However, since the gas could not be admitted directly into the gun, a special inlet system was designed. The system is primarily composed of a glass blown reservoir (c.a. 11) and a Nupro® double-stemmed, precision metering valve. The valve has two functions: it adjusts the flow of xenon into the gun, and isolates the gun (high vacuum) from the glass-blown inlet (1 atm). The double-stemmed arrangement enables both coarse and fine adjustment. Gas flows from the valve to the gun through 1/4 inch copper tubing which mates to a 1.375 inch diameter flange opposite to the gas seal flange shown in Figure 3.3. All connections to the copper tubing were made with Swagelok® fittings capable of maintaining high vacuum.

The glass blown gas reservoir, on the high pressure side of the needle valve, was blown at the MSU glass-blowing shop in the Department of Chemistry. This device is simply a glass bulb (5" dia.) connected to a glass tube accessed by five ports. The glass bulb was wrapped with electrical tape as a safety measure against implosion or explosion. Gas enters through a port in the bottom of the glass bulb which is separated from the xenon tank and regulator by an o-ring valve. Below this valve there is a 1/4 inch diameter piece of Kovar metal which is annealed directly to the glass. This metal is then connected to a 1/4 inch diameter piece of copper tubing, leading to the xenon tank, by a Cajon® o-ring fitting. Two other ports to the bulb have similar o-ring valves, the connection to rough vacuum and a vent. These valves, which were blown directly into the system, are able to hold xenon in the bulb for days so that

the gas reservoir does not need to be evacuated and refilled daily. The remaining two ports to the system both have Kovar/glass connections. One connection is to a thermocouple vacuum gauge, and the other is the connection to the needle valve. To relieve stress on the glass blown system, the latter connection was made with a one inch piece of tygon tubing and band clamps. The entire inlet system was mounted directly on the instrument and protected by a plexiglass cover.

VI. Cleaning the FAB Gun

The gun may be easily removed for maintenance by loosening the flange to the gun, and the Swagelok® connection to the gas inlet. The electrical connections are also designed for easy removal. Because of the simple design of the gun, it may be disassembled, cleaned, and reassembled in a few hours time. The major parts are first scrubbed with either alumina or a non-abrasive soap powder. Following a thorough rinse in distilled water, the parts are successively boiled in the following solvents: distilled water, toluene, methanol, and acetone. The ceramics are cleaned separately by boiling in aqua regia on a hot plate.

During maintenance, aluminum parts, such as the front cathode and the plate which blocks the rear of the gun, must be checked for wear due to sputtering and replaced accordingly. Also, the build-up of sputtered aluminum must be removed from the anode as well as from the inside of the barrel of the gun. Frequently, the build-up is so excessive that it restricts use of an anode alignment tool which

inserts through the barrel and into the hole in the center of the anode. The aluminum is therefore slowly removed by sandpaper and/or a file until the anode may be properly aligned. After cleaning in the afore mentioned solvent scheme, the gun is reassembled and installed.

VII. Modifications for TA-FAB

Under the conditions of TA-FAB, an analyte/matrix mixture applied to a conducting emitter surface is resistively heated in a precise and controlled manner while undergoing FAB. The emitters are prepared by spot welding a piece of 97% W, 3% Re EI filament ribbon (0.235 in. x 0.018 in. x 0.001 in.) across the stainless steel posts of an emitter base identical to those used to prepare activated emitters for FD. The ends of the posts are first filed in such a manner to approximate the preferred 30° angle between the spot welded band and the incident atom beam (e.g., angle of incidence 60°). Upon insertion into the ion source, a small stainless tab on the FD probe makes contact with a metal plate inside the source which supplies the current. This connection enables a path for current to flow through the tungsten emitter to a reference return which in this case is held at the potential of the ion source (+3kV). The same arrangement has been used previously for FD experiments.

Current is supplied to the tungsten band probe tip by an emitter current programming unit (ECP) designed earlier by Holland et. al. in this laboratory to provide precise regulation of current through FD emitters (5). A block diagram of the components involved in current

regulation is shown in Figure 3.4. The heart of the system is the ECP itself. The exact design of the ECP shall not be detailed here, since it is sufficiently described in the above reference. Briefly, the critical electrical consideration involved is the need to transfer low voltage control signals to the regulating device (e.g., emitter), which lies at 3 kV above ground. This is accomplished by high resistance optical couplers, GEH-15A1, which transmit information yet ensure electrical insulation. Current regulation is controlled by an analog regulator circuit inserted in series with a current supply and the emitter itself. In addition, sensing and feedback circuits permit closed loop regulation using a DAC output voltage comparison and level control.

Because of the lower resistance of the tungsten band relative to an FD emitter, the current output of the ECP had to be fortified to achieve acceptable temperatures in the tungsten band. Hence, the ECP was modified to introduce a simple feedback circuit capable of regulating the higher currents sought. This circuit, which is labeled as a current amplification/regulation circuit in Figure 3.4, is drawn in schematic form in Figure 3.5. As shown in the circuit, a 12 volt lead storage battery is incorporated as the power source. Originally, a transformer was intended for this purpose, but this idea was abandoned because a custom-made transformer was needed to accomodate the specifications required by the circuit and the application. The leadstorage battery, however, is capable of providing currents in excess of 3A through the tungsten band emitter. Therefore, the total current gain from this modification was approximately 30-fold. In normal operation, however, the maximum

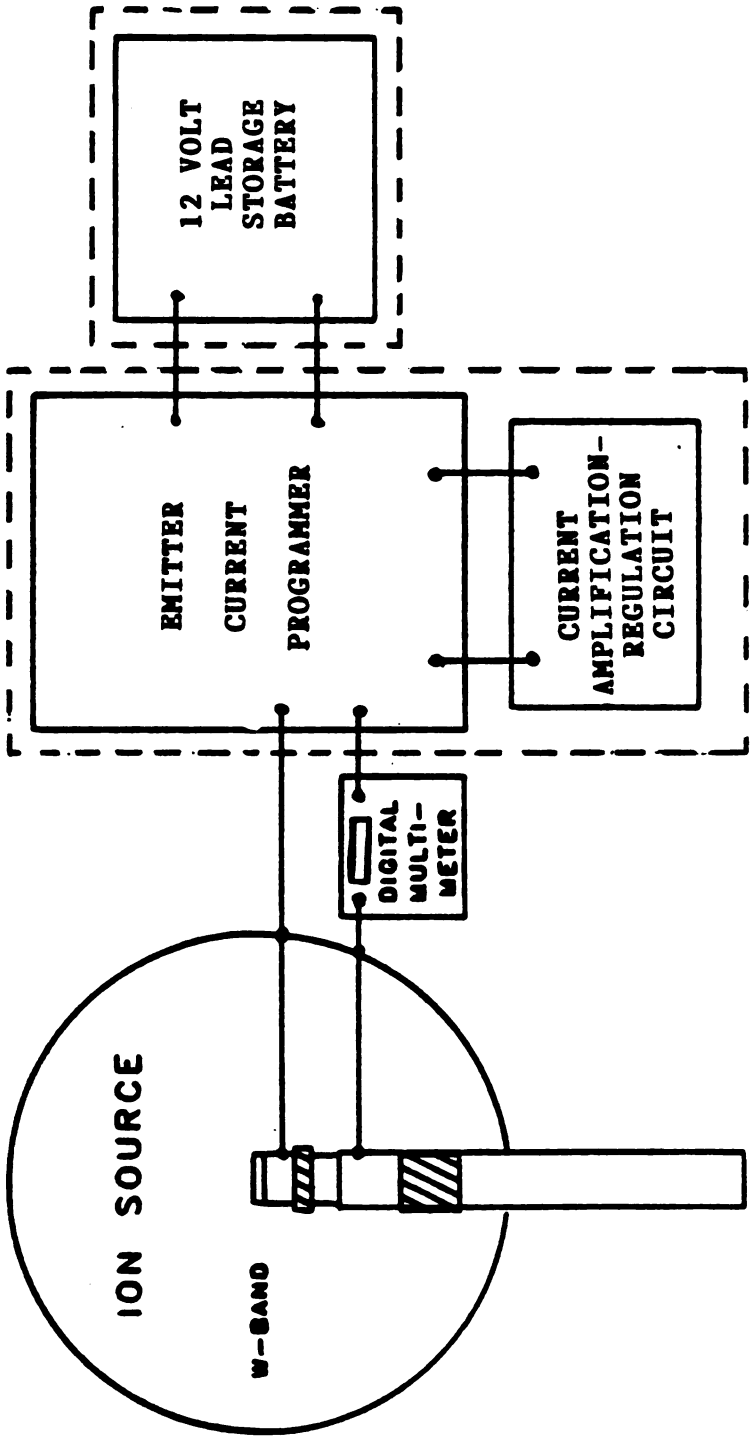

Figure 3.4 Block diagram showing the basic components involved in current regulation for TA-FAB.

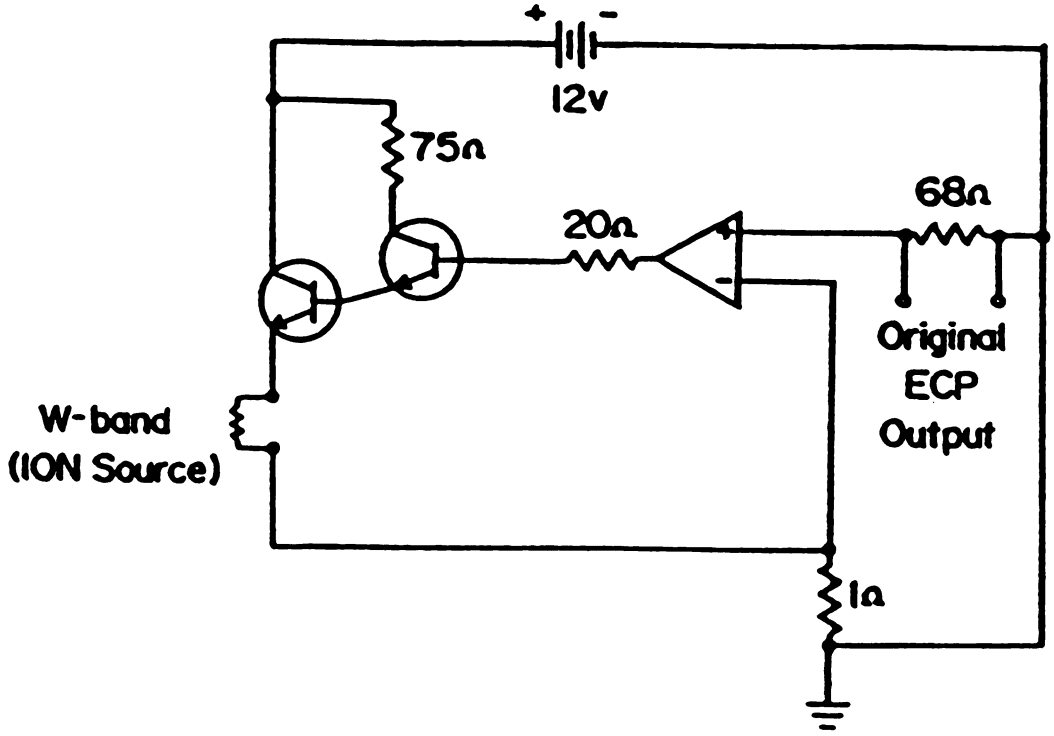

Figure 3.5 Schematic diagram of the current amplification/regulation circuit constructed to increase the output of the emitter current programming unit (ECP).

current employed is about 1.5A. The battery is able to supply operational currents for periods greater than two weeks between recharging. Because the battery floats at source potential, it must be isolated from ground. A polyethylene battery box (Rubber Queen Marine Products, Jackson, OH) is used for this purpose. The dotted lines around the various components in Figure 3.4 indicates the devices which are electrically insulated from ground. A Fluke Model 77 digital multimeter acts as an ammeter for the system. This meter is connected in series to the TA-FAB emitter as shown at the 10A (unfused) output of the meter.

VIII. Overview of Data System and Interface to CH5

A block diagram showing the data system and the basic components involved in the interface to the mass spectrometer is shown in Figure 3.6. The central components of the data system are two Digital Equipment Corporation (DEC) PDP-8/e, 12-bit minicomputers. Because each computer controls separate functions, they are referred to as the "host" and the "front-end". This dual arrangement allows for real time data acquisition because the two computers act as a foreground-background system. While the host computer operates several background tasks, such as communicating with various peripheral devices and executing programs, these operations are interrupted whenever the foreground task of data collection occurs. Thus, the front-end is dedicated to collecting data in the form of mass to charge and signal intensity. It is also responsible for

setting a signal to initiate a scan, checking the status of the magnet current supply, and setting a time delay between scans.

The host computer runs several programs which are managed by the DEC-OS8 operating system. In addition, several programs have been written in assembly language for rapid, flexible data collection and processing. The major programs include MSSIN, MSSOUT, MSSTST, MSSAVA, and MSSCAL. MSSIN collects data when the CH5 is in the low resolution scanning mode. MSSOUT displays the data as they are collected, or after a run has been closed. The data are typically displayed either as digitized mass spectral bargraphs, or as mass chromatograms. MSSOUT has several commands for data processing such as scan averaging, integration, and background subtraction. MSSTST is an interactive program which monitors the status of several parameters involved with data collection, and is therefore useful for troubleshooting. MSSAVA is used to collect data in the selected ion monitoring mode by the method of acceleration voltage alteration (e.g., AVA). Finally, the program MSSCAL is used to calibrate the mass axis prior to data collection.

Mass calibration requires a calibration compound, or mixture, which gives intense peaks of known mass value at regular intervals throughout the mass range of interest. A saturated CsI/glycerol solution was chosen for this purpose. This mixture forms several intense peaks from clusters involving CsI and/or glycerol. Also, CsI is an ideal compound because neither Cs or I have multiple isotopes to complicate the mass spectrum. This mixture enabled mass calibration to be obtained out to about mass 1000. During mass calibration, peaks of known mass from the calibration mixture are

assigned to specific voltages which are recorded from a Hall probe inserted between the poles of the magnet. Actually, these voltages are first squared so they will be proportional to mass by the relationship given in equation 1. Since the observed Hall voltages are directly related to magnetic field strength and hence mass, calibration may be achieved by relating observed voltages to known mass values. The software in MSSCAL enables one to effect linearization of the relationship between (Hall voltage)^2 and mass, thereby calibrating the mass axis. The calibration file constructed from known peaks of CsI/glycerol and their Hall values was given the name CSICAL.

As indicated in Figure 3.6, the host computer communicates and handles I/O from a Plessey model PM-DD/8C disk drive and a Tektronics 4010 graphics terminal. The disk drive contains both fixed and removal disks. Images on the CRT of the terminal may be recorded for documentation using a Tektronics model 4631 hard copy unit. The host PDP-8/e is also responsible for communication and data transfer to a larger time-shared DEC PDP-11/44, 16-bit minicomputer. The program MSSTRN enables the user to access the PDP-11/44 from the host. Once logged on the PDP-11/44, MSSTRN may be used to transfer data files up to the larger computer for storage and for more extensive data manipulation. The PDP-11/44 contains a more sophisticated version of MSSOUT, written in FORTRAN, that has more powerful data handling capabilities. Also, from this program, data may be output in manuscript quality on a Hewlett Packard model 7475A plotter. Data files stored on the PDP-11/44 may be archived on 9-track magnetic tape using the tape drive interfaced to the PDP-11/44.

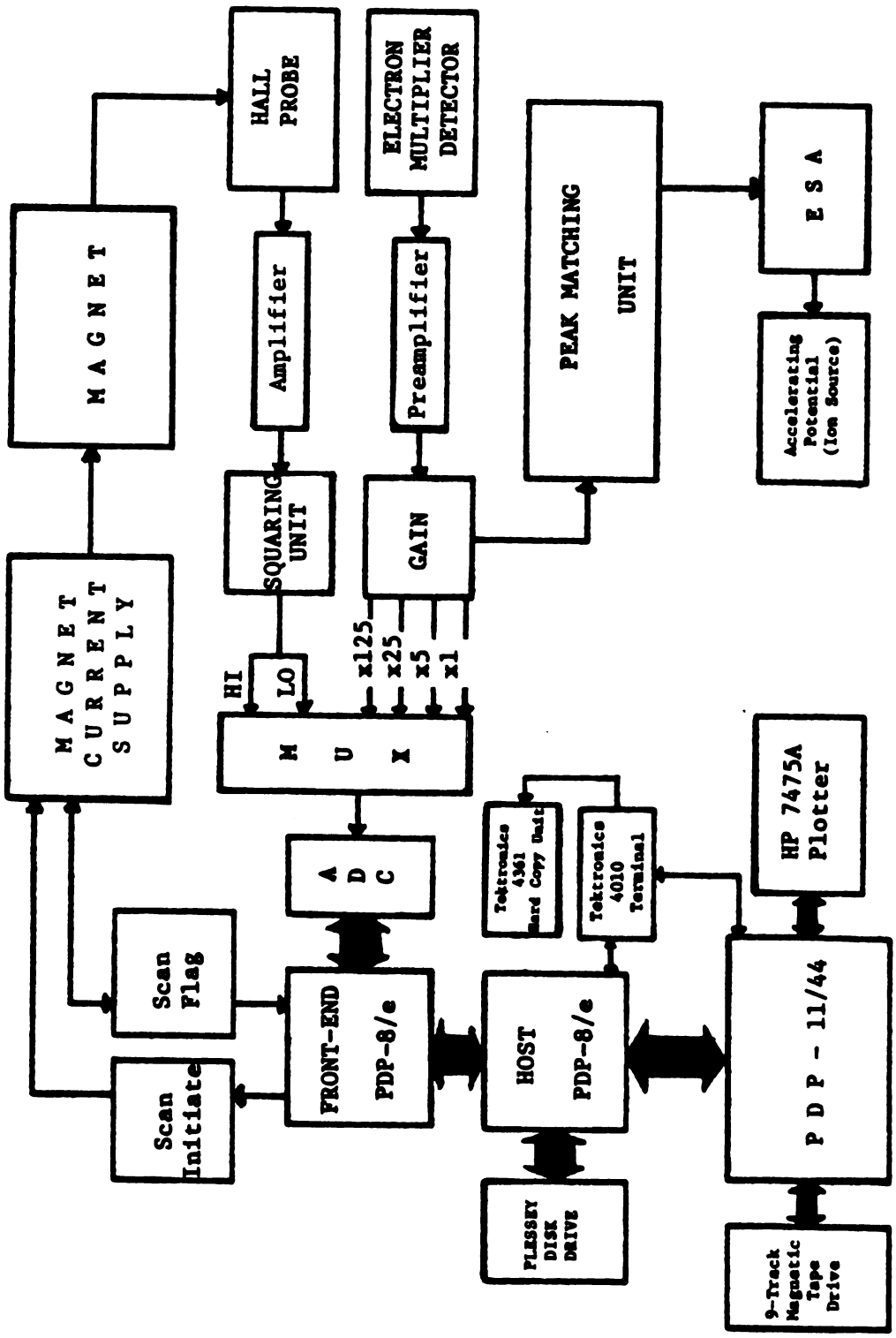

Figure 3.6 Block diagram showing the interaction between the major components in the computer interface to the CH5.

The upper part of Figure 3.6 illustrates the interface to the CH5. Data collection begins when a signal from the front-end triggers a scan initiate circuit. This in turn causes the magnet current supply to begin scanning the magnet of a rate selected by the scan control unit on the instrument. A potentiometer, also on this unit, selects the upper mass limit. When this value is reached, as detected by a comparator circuit set by the potentiometer, another circuit sends a scan flag back to the front-end to inform the computer of the status of the magnet. The time interval before the next scan is initiated, depends on a delay controlled by the front end which is set in MSSIN as the duty cycle for the whole process.

As mentioned previously, the magnetic field intensity is encoded with a Hall probe. The Hall probe is essentially an n-type semiconductor inserted between the poles of the magnet such that the current flow is perpendicular to the magnetic field. When a constant current flows through the probe, a voltage proportional to magnetic field develops across the semiconductor. Since the potential developed is only in the range of millivolts per killogauss, the Hall voltage is amplified to be compatible with the data system. The voltage is then squared so that it is directly proportional to mass. This is accomplished by an amplification circuit (Analog Devices 428J). The squared signal is then multiplexed before being sent to a 12-bit Analogic, successive approximation analog-to-digital converter. The Hall voltages are multiplexed as two channels (low and high mass) so that each mass range receives the full 12-bits of resolution. The two channels differ by an offset voltage that

defines a point known as the "Hall-crossover" which is adjusted to occur at about m/z 500.

The other signals entering the multiplexer originate from a 14-stage (discrete) electron multiplier detector. The detector presently installed is a Hamamatsu model 515 electron multiplier. The transmitted positive ions, having 3 keV of kinetic energy, strike an initial dynode held at a potential of minus 2.0-2.5kV. The secondary electrons produced experience amplification along the dynode chain, where the final stage is held at ground. The signal produced is sent through a preamplifier which produces a current to voltage conversion. Next, the signal is amplified to give selectable gains of x1, x5, x25, and x125 which are multiplexed separately. However, in the scanning mode only the most sensitive setting is monitored. The analog signal is digitized and sent to the front-end computer which registers one intensity for each m/z value. The intensities are expressed in arbitrary units.

IX. High Resolution Measurements by Peak Matching

The amplified signal from the detector is also sent to the peak matching unit of the instrument. The oscilloscope associated with this unit displays peaks when the system is not under computer control. In addition, this unit has the power supplies for the acceleration potential and the electrostatic analyzer. The ratio of these two voltages is selected by a potentiometer on the unit. The peak matching unit also contains the circuitry for MIKES. Under these conditions, the acceleration and ESA voltages are uncoupled so

that the acceleration potential no longer tracks the ESA. The ESA voltage may then be scanned toward lower potential to pass the daughter ions of metastable decomposition.

In addition to these functions, the peak matching unit enables exact mass measurements to be performed. By this method, a reference peak of known mass is first focussed on the oscilloscope under high resolution, at full acceleration potential. Next, the acceleration potential is lowered using a series of precision decade resistors until the profile of an unknown peak of higher mass is exactly superimposed upon the reference which is still observed at full acceleration. The two peaks are viewed simultaneously on the oscilloscope by acceleration voltage switching. The exact mass of the unknown may be calculated to six figures directly from the resistor settings used to superimpose the peaks. The accuracy of the measurement, however, depends upon the signal intensity of the two peaks, and the resolution under which the measurement is obtained.

X. LIST OF REFERENCES

1. Varian MAT CH5-DF owners manual, 1970.

2. J. Franks, Int. J. Mass Spectrom. Ion. Phys., 46, 343 (1983).

3. FAB B11NF Saddle Field Gas Gun, owner's manual, Ion Tech, LTD., 1981.

4. S.A. Martin, C.E. Costello, and K. Biemann, Anal. Chem., 54, 2362 (1982).

5. J.W. Maine, B. Soltmann, J.F. Holland, N.D. Young, J.N. Gerber, and C.C Sweeley, Anal. Chem., 48, 427 (1976).

Chapter 4

APPLICATION OF FAB-MS TO BIOLOGICAL SAMPLES: ANALYSIS OF URINARY METABOLITES OF ACETAMINOPHEN

I. Introduction

Soon after the introduction of FAB in 1981, applications of the technique began to flourish. Papers appeared in several journals, each demonstrating the usefulness of FAB for the analysis of a particular set of compounds. Typically, the major ion types observed were documented and explanations offered for their origin. While this was useful information, the fanfare which surrounded FAB tended to give potential users a distorted view regarding the strength of the technique because questions concerning practical details such as: limits of detection, mixture analysis, quantitation, structural analysis in unknown materials, and chemical interference in FAB mass spectra remained to be addressed. In fact, a majority of the early application studies used commercially-available compounds as opposed to those isolated from biological origin. In addition, unrealistic quantities (several micrograms) of these materials were used in order to obtain peaks with good signal to noise ratios for varous fragment ions. Finally, claims of structural elucidation were somewhat overstated because analyses were, more often than not, carried out with an a priori knowledge of the compound's structure.

More recently, investigations have sought to more appropriately define the analytical merit or boundaries of FAB, and have yielded

some consensus. For example, quantitation by FAB is now regarded as possible, but generally requires an isotopically-labeled internal standard for reliable results (1). Small mixtures may be analyzed by FAB, but yield only semi-quantitative results at reduced sensitivity (2). As for structural analysis of unknown materials, FAB is best used in support to other analytical techniques, even when analyzing such heavily investigated compounds as peptides (3). Hence, the trend is away from quick application papers and towards more realistic investigations. In fact, the policy of at least one journal is to not accept papers for publication of the variety described above (4).

One issue which requires more attention is the problem of chemical interference in FAB mass spectra. As noted in Chapter 2, chemical interference has two origins: specific contaminants which result from incomplete sample purification, and matrix-related background. Chemical interference, whether it comes from the matrix or otherwise, can impose the most severe limitation to FAB since it reduces the certainty of structural assignments as well as the overall sensitivity of a FAB analysis. Furthermore, the problem is considerably magnified when FAB analyses are performed on analytes isolated from complex mixtures such as urine or plasma, because specific interferences become dominant. In these cases, larger sample sizes and considerable purification may be necessary before acceptable data may be acquired.

The severe limitation imparted by sample-related chemical interference to FAB was recognized in the early stages of work done for this dissertation during a project, in conjunction with

researchers at the Michigan State University Department of Pharmacology, which sought to use FAB to identify the complete set of metabolites from the analgesic acetaminophen (APAP). To this end, samples were collected from urine following therapeutic dosages, and purified by reverse phase HPLC prior to FAB. The off-line combination of these two methods constitutes a very powerful and expedient route to metabolite identification providing that steps are taken to minimize the level of competing interferences that restrict analysis by FAB. The objectives of this initial investigation were three-fold. First, to use FAB to obtain spectra for all APAP metabolites without prior derivatization; particularly the polar conjugates of APAP which were previously not amenable to other methods of mass spectrometry. Second, a tentative set of recommendations for the efficient off-line use of HPLC and FAB was desired; with particular attention given toward minimizing interferences. Third, to demonstrate the merit of a proposed method for estimating signal to background (S/B) values for analyte peaks in FAB spectra, and to show the usefulness of this parameter in judging the quality of data obtained by FAB.

II. Acetaminophen Metabolism and Historical Perspective

Acetaminophen (acetyl p-aminophenol (APAP)), the active ingredient in Tylenol® has found widespread use as an aspirin substitute. However, reports of hepatic necrosis and renal failure following ingestion of large dosages of APAP have stimulated the

development of methodology to characterize the molecular species responsible for this toxicity.

The metabolic fate of APAP has been the topic of extensive research in recent years (5-9). APAP is primarily transformed by the liver into water-soluble sulfate and glucuronide conjugates which facilitate excretion (Figure 4.1). A small portion of APAP is metabolized via a cytochrome P-450 dependent mechanism into a reactive electrophilic intermediate, thought to be an imidoquinone, which reacts with endogenous nucleophiles such as glutathione (GSH) or protein. The reaction is directed towards the 3-position of the aromatic ring forming a thioether linkage as shown (Figure 4.1). Following enzymatic cleavage to yield the cysteine conjugate, acylation yields the mercapturic acid derivative which also may be readily excreted. However, when renal and hepatic GSH concentrations become depleted, cellular macromolecules containing sulfhydryl groups compete for binding to the electrophilic intermediate ultimately leading to cellular pathogenesis. Additionally, 3-methylthio and 3-methoxy metabolites are present in the urine in small amounts; however, their origin is less well documented.

Mass spectrometry has been useful in identifying APAP metabolites involved in hepatic and renal toxicity. Early attempts to characterize metabolites of APAP were generally thwarted by instability of the metabolites during purification and the lack of derivatives sufficiently stable for gas chromatography-mass spectrometry (GC-MS) under conditions of electron impact (10,11). Following the introduction of HPLC, Knox and Jurand (12) were able

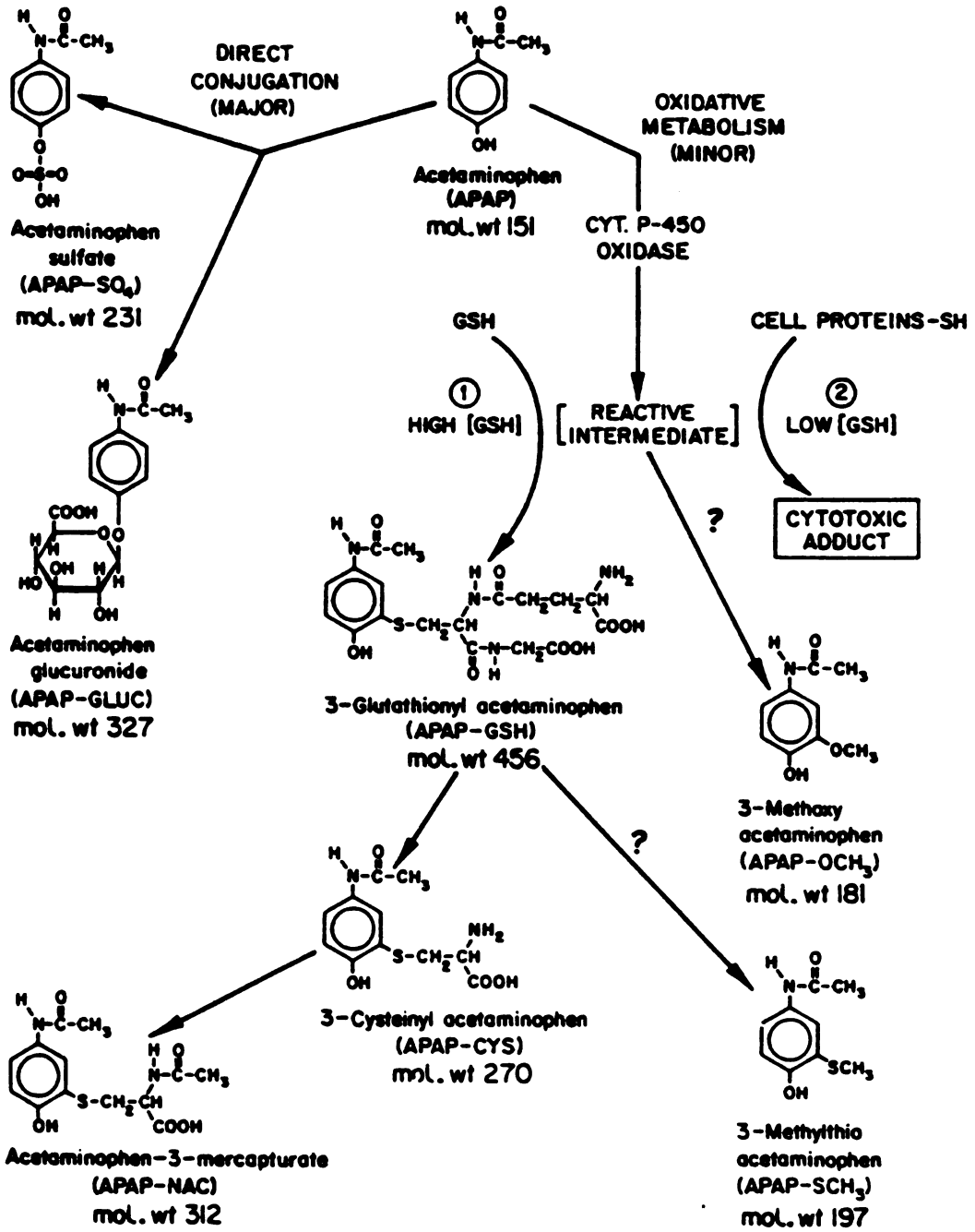

Figure 4.1 The metabolism of acetaminophen.

to purify and characterize several of the APAP metabolites using electron impact (EI) high resolution mass spectrometry. However, the polarity and thermal instability of the thioether conjugates precluded molecular identification by these techniques in most cases.

More recently Baillie, Nelson and co-workers (13) used EI, chemical ionization (CI), and field desorption (FD) to provide spectra for the major APAP metabolites from both synthetic and biological origin. Their report compared the fragment and molecular ion information attainable by each method of ionization using synthetic metabolites. EI and CI were suitable for analysis of the relatively nonpolar metabolites (e.g., 3-thiomethyl acetaminophen, N-acetyl- and cysteinyl-acetaminophen), but required large amounts of sample (e.g., 1-20 μg). In most cases, FD provided molecular ion species for metabolites that were intractable under EI and CI. An exception was the polar sulfate conjugate which eluded analysis over a wide range of experimental conditions. Furthermore, experimental difficulties associated with FD, such as the transient nature of the spectrum and the requirement for extensive purification, made the analysis cumbersome for the other metabolites.

Recent work in our laboratory has shown that fast atom bombardment (FAB) may be used to obtain molecular information on all major metabolites of APAP from both synthetic and biological sources (isolation from urine using HPLC). In particular, FAB readily produced a spectrum of the sulfate conjugate which was refractory to other ionization techniques including FD. Efforts were made to obtain spectra from realistic concentrations of the metabolites

rather than from high concentrations associated with overdose cases. To achieve this goal, a procedure was developed which enabled fractions taken from reverse phase HPLC to be analyzed by FAB mass spectrometry.

III. Experimental

A. Materials

The synthetic metabolites of APAP used for both HPLC and FAB analyses were obtained from Gemborys and Mudge (14). NADP and p-toluenesulfonic acid were purchased from Sigma Chemical Co. (St. Louis, Missouri). Glycerol, potassium chloride and glacial acetic acid were obtained from Mallinckrodt, Inc. (Paris, Kentucky). Tetrabutylammonium phosphate (PIC-A) was received as a pre-concentrated solution from Waters Associates (Milford, Massachusetts). All solvents used for either HPLC or FAB were of spectroscopic quality and obtained from either MCB, Inc., Fisher Scientific Co., or Burdick and Jackson, Inc. The hepatic microsomes used for the *in vitro* preparation of the thioether metabolites were obtained from male CB1 mice purchased from Harlan, Inc. (Indianapolis, Indiana).

B. Chromatography

All chromatography was performed on an HPLC system consisting of a M6000-A solvent delivery system, a U6K loop injector, a model

441 ultraviolet detector set at 254 nm, a model 721 system controller and data module (Waters Associates, Inc., Milford, Massachusetts). Preparative chromatography was carried out on reverse phase μ-Bondapak C18 column (30 x 0.78 cm) employing a methanol/water/glacial acetic acid mobile phase whose composition was varied according to the particular assay (vide infra). Isolated metabolites were quantified prior to FAB analysis by extrapolation from peak area calibration curves of synthetic standards. All quantification was performed using a Dupont Zorbax C18 column (25 x 0.46 cm) and a mobile phase of 10% acetonitrile, 1% glacial acetic acid in water; flow rate 1.5 ml min^{-1}. Solvents were passed through a 0.2 μm filter prior to being used.

Metabolites were isolated from the urine of a volunteer subject following a 2.1g oral dose of APAP. The morning fasting urine was collected, centrifuged through a 0.2 μm filter, and diluted 1:4 with mobile phase prior to injection. Injection volumes ranged from 50 to 125 μl depending upon the relative concentration of each metabolite. Several runs were required to obtain sufficient quantities of each metabolite for analysis by FAB.

The thioether conjugates (APAP-CYS and APAP-GSH) were obtained through incubation of APAP with mouse liver microsomes using an NADPH generating system as described previously by Mitchell et. al. (15). APAP-GSH is quickly metabolized and therefore not present in urine. While APAP-CYS may be found in urine, the concentration following therapeutic dosages of APAP is extremely small. Metabolites resulting from microsomal preparations were first

centrifuged through 0.2 μm filters and diluted 1:4 with mobile phase before injection onto the column.

The original assay designed for the separation of urinary APAP metabolites involved a gradient elution starting with 12.5% methanol and following an exponential climb to 25.0% methanol. The gradient was initiated 7.50 min into the run. The concentration of acetic acid (1.0%) remained constant. Under these conditions, the retention times in minutes for the metabolites were: APAP-GLUC (5.52), APAP-CYS (7.05), APAP-SO_4 (7.58), APAP-OCH_3 (12.19), APAP-NAC (15.20), and APAP-SCH_3 (17.54).

Later the concentration of acetic acid was attenuated after noting the adverse effect it had on FAB spectra; the amount of background present correlated directly to the level of acetic acid used in the mobile phase. Therefore, the minimum amount of acetic acid capable of providing an acceptable separation was used in each case. Henceforth, three different assays were developed to accommodate each group of metabolites: (a) The fast eluting polar metabolites (APAP-GLUC, APAP-SO_4), (b) the thioether products of incubation (APAP-CYS, APAP-GSH), and (c) the slow eluting less polar conjugates (APAP-OCH_3), APAP-NAC, APAP-SCH_3. Each assay was run under isocratic conditions with a flow rate of 3.5 ml min^{-1}. The polar glucuronide and sulfate conjugates were separated using 12.5% methanol and 0.05% acetic acid in water. Their respective retention times were 4.80 and 8.81 min. APAP-CYS and APAP-GSH were chromatographed using 25.0% methanol, 0.05% acetic acid in water to give retention times of 6.01 and 9.38 min, respectively. The less polar APAP-OCH_3, APAP-NAC, and APAP-SCH_3 were chromatographed with

25.0% methanol, 0.42% acetic acid in water and eluted with retention times of 5.75, 7.11, and 8.70 min, respectively. Samples were collected manually into vials with the objective of collecting only the portion between the inflection points of the eluting peaks.

C. Processing of HPLC samples

Following collection, the samples were lyophilized to remove the mobile phase. The samples were reconstituted with 5 ml methanol and vortexed. Each solution was transferred successively into a 1.0 ml conical REACTI-VIAL® (Pierce, Rockford, Illinois) where the methanol was continuously evaporated under nitrogen. The dried samples were redissolved in 500 µl of 1:1 methanol/water and vortexed. A 10 µl aliquot was taken for HPLC quantification as described earlier. After quantification, the volume was adjusted to give the desired concentration. To allow for convenient application to the FAB probe tip, analyte concentrations exceeding 1 nmol μl^{-1} were sought.

D. Application of FAB samples

One µl of vacuum distilled glycerol was applied to the probe tip for all experiments. This yielded a thin, non bead-like film on the probe surface. Next, samples were applied as solutions using a solvent system readily miscible with glycerol (e.g., methanol/water). Aliquots of about 1 µl were applied in succession from a 10 µl Hamilton syringe; the tip was then heated with a heat gun to remove

the excess solvent. A practical cumulative limit of about 5 µl could be added in this fashion. Between samples the tip was wiped clean with Kimwipes® and rinsed thoroughly with glass-distilled acetone (99.6% MCB, Inc.). Background subtraction was accomplished in the following manner. During a run, the probe was removed and cleaned. Next, the same matrix containing the control sample was applied. The probe was then re-inserted and adjusted to give maximum total ion curent. Selected scans could then be chosen for subtraction using the computer.

Unless stated otherwise, the gun was operated to give 8.6 keV xenon atoms; the accompanying pressure inside the ion source housing was 2×10^{-5} torr.The electron multiplier was operated at minus 2.37 kV and a scan speed of 25 sec decade^{-1} was used throughout the experiments.

IV. Results and Discussion

The off-line combination of FAB and reverse phase HPLC has many advantages for the identification of drug metabolites in biological fluids. First, the methods are compatible since they both are amenable for use with polar compounds. Further, reverse phase solvent systems are readily miscible with most FAB matrices such as glycerol or thioglycerol. Finally, since neither technique requires derivatization to enhance analyte volatility, fractions taken from HPLC may be analyzed with minimal work-up. Thus, the consecutive use of these two techniques offers a very rapid and sensitive

approach provided steps are taken to minimize competing interferences.

The thermospray method for LC-MS has also received much attention for use in this area (16) and offers the advantage of being an on-line method. Although this is a viable approach, there are some constraints to this method: (1) the operational parameters of the interface require optimization for each analyte tested, (2) a pumping system capable of removing the mobile phase is required, and (3) compared to FAB, each analyte is only present for a brief period to undergo mass analysis.

A. FAB Mass Spectrum of APAP-SO_4

Many drug metabolites exist as highly polar conjugates to facilitate excretion in urine. For acetaminophen the metabolites in the highest abundance (APAP-GLUC, APAP-SO_4) are also the most polar and consequently the most difficult to analyze by mass spectrometry. However, in contrast to the difficulty experienced with other methods, including FD, these conjugates readily yielded mass spectra by FAB. In addition to granting the first mass spectrum of the polar sulfate conjugate, FAB displayed a wider range of analysis than reported for other methods of ionization because for the first time molecular weight confirmations were obtained for all metabolites of APAP by one method of ionization.

Obtaining useful FAB spectra of compounds present in complex biological matrices such as urine presents a formidable and realistic challenge due to problems associated with background. For

example, while good FAB spectra may be obtained from 5 nmol of all synthetic metabolites (shown in Figure 4.1), similar results for their urinary counterparts may only be obtained after extensive purification to minimize the chemical background which competes for ionization. Figure 4.2(a) is a FAB mass spectrum of APAP-SO_4 isolated from urine by HPLC. Figure 4.2(b) is the net spectrum resulting from subtraction of the FAB spectrum of a control urine sample from the spectrum shown in Figure 4.2(a). The control urine was used to represent the non-drug-related background constituents in the subject's urine. This control urine was obtained from the same subject (who provided the urine for Figure 4.2(a)) under drug-free conditions; the control urine was processed under the same protocol. The HPLC chromatogram shows the portion of the peak (shaded) isolated for analysis by FAB.

B. Signal to Background Determination

As illustrated in the analysis of APAP-SO_4 (Figure 4.2(a)), data recognition in FAB analyses is not always straightforward; especially when searching for small quantities of a metabolite present in a complex sample matrix such as urine. Although the picture becomes clearer after subtraction (Figure 4.2(b)), background subtraction is not always a reliable process for several reasons, as discussed in Chapter 2. Therefore, caution should be exercised when viewing the results of computer-aided background subtraction as performed in the manner described in the experimental section. Regardless, analyte recognition in FAB mass spectra is

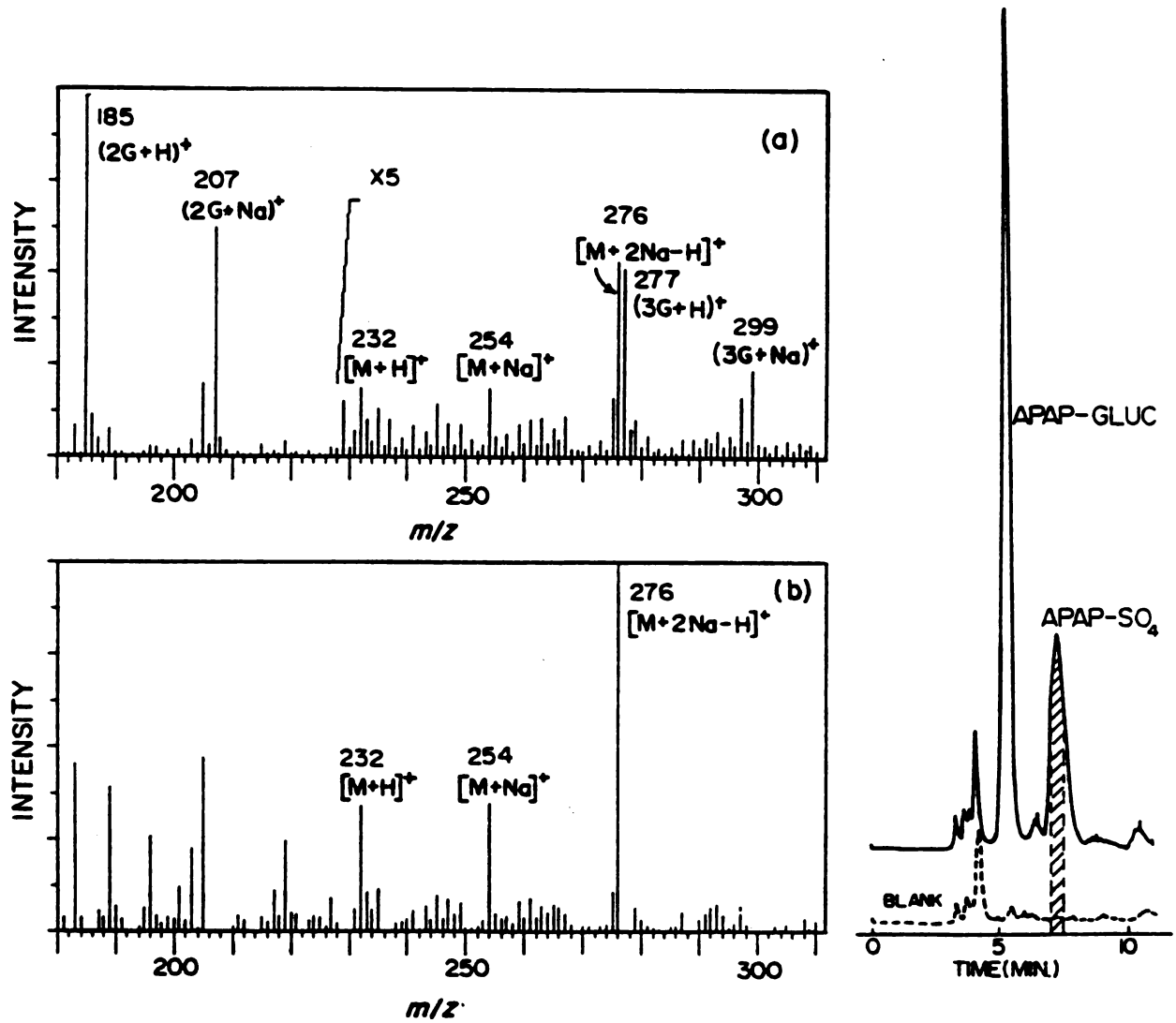

Figure 4.2 (a) FAB mass spectrum of APAP-SO_4 (35 nmol) isolated from urine by HPLC. Predominant peaks labeled where (G=glycerol= 92 u). (b) The same spectrum following subtraction of a control spectrum derived from the urine of the same subject under drug-free conditions. Both samples were processed under identical conditions; the same retention interval was sampled over several HPLC runs in both cases (eluent collected during shaded area of HPLC chromatogram).

generally limited by background interference, unless operating at high mass. Traditionally, analytical chemists have described the detection of an analyte in terms of the observed signal-to-noise ratio, where the noise is the standard deviation observed in a series of determinations of a blank (17). While noise may arise from several sources, it is usually a random phenomena and treated accordingly. In contrast, the factor which limits detection in FAB is the chemical interference or background. While background may also come from several sources, it is certainly not random and requires a separate treatment to assess the detection of analyte ions.

Recognition of an ion derived from the analyte is a function of how far the corresponding peak extends above the neighboring peaks which constitute the background. Thus a more reasonable way to assess sensitivity in FAB spectra is through an estimation of signal to background (S/B) rather than signal to noise (S/N). Further applications of S/B might include its serving as an objective index by which to judge the success of a particular purification step, or the effectiveness of subtracting the spectrum of a control sample from that of a given analyte sample. Therefore, the concept of signal to background is not limited to this study. Rather, it pertains to any application of FAB where chemical interference is a limiting factor. Pursuing this concept, we have adopted the following general rules for estimation of S/B: (a) the background is estimated by averaging the peak intensities 3-14u above and 1-14u below the candidate peak; (b) this average background is then subtracted from the candidate peak of interest to obtain the analyte

signal; and (c) finally, the analyte signal is divided by the average background to obtain S/B.

S/B may be expressed mathematically as:

$$S/B = \frac{(RI)_A - \left[\sum_{i=A+3}^{A+14} (RI)_i + \sum_{i=A-1}^{A-14} (RI)_i\right] \Big/ 26}{\left[\sum_{i=A+3}^{A+14} (RI)_i + \sum_{i=A-1}^{A-14} (RI)_i\right] \Big/ 26}$$

where $(RI)_A$ = S' = total relative intensity (%) present for the m/z value of the analyte, B = average background relative intensity (%).

As defined, signal to background really describes the degree to which the analyte signal stands above or exceeds the average background. Since S' is simply the relative intensity of the candidate peak, the distinguishing factor in calculating S/B is in the assessment of average background B. The primary consideration as expressed by the above formula was to obtain a set of background peaks in the vicinity of the candidate which in no way contain a contribution from the analyte. The boundary given to the background set is 14 mass units above and below the candidate peak. This was done primarily because peaks 3-14u below the candidate represent an unlikely neutral loss. A range of 14u was considered above the candidate to preserve symmetry. Although peaks 3-14u are traditionally cited as unlikely losses (18), the average background also contains the peaks one and two masses below the candidate since these losses are rare in FAB. Consideration of peaks 3 to 14 mass

units above the candidate peak avoids contribution from isotope peaks of the analyte. Of course, when the analyte has known isotopic contributions at m/z values greater than two units above the candidate, these peaks should be removed from consideration and the denominator reduced accordingly. The computation also avoids contribution by a potassium adduct $[M+K]^+$ when the candidate is $[M+Na]^+$ and vice versa, because these two cations differ by 16 mass units.

As in the case for additional isotopic contributions, several other valid exceptions should be tended to accordingly. For example, when samples are spiked with lithium, the $[M+Li]^+$ peaks 6 and 7u above the $[M+H]^+$ candidate should be omitted from consideration. Other exceptions can occur when analyzing small mixtures of known molecular weight. A common occurrence with materials such as ceramides which possess long alkyl side chains is to obtain mixtures of homologues differing by 14u. In this case, a boundary for background of 13 mass units is acceptable. Certainly, other jusifiable exceptions can be envisioned and should be specified when reporting corrected S/B values.

Sometimes it may be desirable to correct the average background for known major ions from the matrix. Often when a predominant glycerol ion is included in an S/B calculation, its magnitude may be so large that it makes the average background larger than the relative intensity of the analyte peak. Thus to avoid negative values for S/B, it may be necessary to omit a predominant glycerol peak that is frequently present when calculating the average background.

Another complication exists when too few background ions are recorded. When this occurs the analyte S/B may be misleadingly high since the peak intensity of background ions (particularly those associated with glycerol) diminishes with increasing m/z values. Eventually peak heights fall below the threshold set by the data system. This may result in the acquisition of only a few relative intensity values for m/z values in the region representing the background. Thus, the average background (B) is artificially reduced making S/B values for even small analyte signals noticeably large.

Random noise on the detector affects all intensity values in a mass spectrum. Hence, the value calculated for the average background (B) is composed of two parts: (a) chemical background and (b) random noise. Therefore, when too few background peaks are present to calculate a realistic S/B value, the noise threshold should be lowered to permit acquisition of a greater proportion of the intensity values thereby including the second component of the background. We suggest that at least two-thirds of the peaks (e.g., 18) in the specified mass range be present to make a reasonable statistical estimate of signal to background. When too few peaks are present to permit an accurate estimation of background, one might consider the legitimacy of a signal to noise calculation.

C. Ions observed for APAP metabolites

At the concentrations used for this study, good molecular weight confirmations were made for each of the APAP metabolites.

However, the amount of fragmentation observed was sparse by comparison to data reported using electron impact and assignments were often tenuous due to competition from background. The paucity of fragments observed reflects three factors. First, fragmentation in FAB is concentration dependent. Fragments were more discernible when larger amounts of the synthetic metabolites were used. Second, simple mixtures analyzed by FAB tend to give only molecular weight information. Hence, the interferences present in the urinary samples would diminish fragmentation of the analyte. Finally, the endogenous levels of sodium and potassium in urine led to the formation of stable molecular adducts. Hence, when analyzing low levels of materials in biological samples, FAB is primarily a tool for molecular weight confirmation rather than structural elucidation.

The FAB mass spectra of the major APAP metabolites are summarized in Tables 4.1 and 4.2. Table 4.1 displays the predominant molecular ion-containing species present in the FAB spectra of the synthetically obtained metabolites. Values for the maximum signal to background $(S/B)_{max}$ are listed for each ion. Occasionally, it is necessary to omit major glycerol ions from the background to yield a reasonable S/B value. Only S/B values greater than 1 are recorded in Table 4.1. Table 4.2 is the corresponding data base obtained for urinary APAP metabolites. There was no substantial increase in sensitivity when analyzing synthetic as compared to urinary metabolites. However, this was dependent upon the purification scheme used. Background appearing in the spectra of urinary metabolites was more extensive in comparison to

TABLE 4.1. SIGNAL TO BACKGROUND (S/B) MAXIMA FOR PREDOMINANT IONS IN SPECTRA OF SYNTHETIC METABOLITES

Metabolite	Mol. wt	Amount (nmol)	$(S/B)_{max}$[a]			
			$[M+H]^+$	$[M+Na]^+$	$[M+K]^+$[c]	$[M+2K-H]^+$[d]
APAP-OCH_3	181	11	4.1[e,f]		2.0[g,h]	
APAP-SCH_3	197	6	9.8[f]			
APAP-SO_4[b]	231	10	2.6[h]		2.5[i]	20
APAP-CYS[b]	270	10	20[i]	2.7	1.4	
APAP-NAC[b]	312	3	7.4[j]	5.5	5.5	
APAP-GLUC	327	5	2.7[k]		11[m]	16[n]
APAP-GSH[b]	456	10	6.5[p]	1.9	4.3	

[a] Methodology for $(S/B)_{max}$ determination discussed previously in text; only values greater than one are presented.
[b] Compound present as potassium salt.
[c] Ion may also be rationalized as a proton addition to the intact potassium salt.
[d] Ion may also be rationalized as a potasium addition to the intact potassium salt.
[e-p] The following major glycerol ions were omitted when estimating the average background (G=glycerol, Mol. wt 92).

	m/z	Ion		m/z	Ion
e	169	$(G+2K-H)^+$	j	299	$(3G+Na)^+$
f	185	$(2G+H)^+$	k	315	$(3G+K)^+$
g	207	$(2G+Na)^+$	m	369	$(4G+H)^+$
h	223	$(2G+K)^+$	n	407	$(4G+K)^+$
i	277	$(3G+H)^+$	p	461	$(5G+H)^+$

TABLE 4.2. SIGNAL TO BACKGROUND (S/B) MAXIMA FOR PREDOMINANT IONS IN SPECTRA OF URINARY METABOLITES

Metabolite	Mol. wt	Amount (nmol)	$(S/B)_{max}$[a] $[M+H]^+$	$[M+Na]^+$	$[M+2Na-H]^+$
APAP-OCH_3	181	6	11[b]	1.1[c]	
APAP-SCH_3	197	5	2.6		
APAP-SO_4	231	12	2.5		2.4
APAP-CYS	270	6	12[d]	4.1[e]	2.1
APAP-NAC	312	6	5.2[e]	3.2	
APAP-GLUC	327	8	6.4	5.9	1.7[f]
APAP-GSH	456	8	3.2[g]	4.9	4.4

[a] Methodology for $(S/B)_{max}$ determination discussed previously in text; only values greater than one are presented.

[b-g] The following major glycerol ions were omitted when estimating the average background (G=glycerol, Mol. wt 92).

	m/z	Ion
b	185	$(2G+H)^+$
c	207	$(2G+Na)^+$
d	277	$(3G+H)^+$
e	299	$(3G+Na)^+$
f	369	$(4G+H)^+$
g	461	$(5G+H)^+$

background peaks found in spectra for the synthetic counterparts, which were attributed to ions derived from glycerol. As a result, spectra from the synthetic compounds are more frequently and easily corrected for the predominant known glycerol (G) ions.

A general trend was observed in the spectra of both synthetic and urinary metabolites: the protonated molecular ion $[M+H]^+$ exhibited an intense signal early in the run which faded as the glycerol was "sputtered" away or evaporated during bombardment. Later in the run dominance by cation adducts was observed. Exceptions were in obtaining the spectra of the thiomethyl and methoxy metabolites in which there was a conspicuous absence of cation adducts. Apparently, it was the lack of an acidic moiety such as COOH or SO_3H which retarded such adduct formation.

Differences in the multiplicity of the molecular ion adduct species were dependent on cations in the salt. Whenever the synthetic analog exists as the potassium salt (APAP-SO_4, APAP-CYS, APAP-NAC, and APAP-GSH), proton addition was observed not only to the free acid (M_A), but to the potassium salt (M_S) as well. Thus, $M_S = M_A + 38$. For example, the spectrum of synthetic APAP-SO_4 produced a peak corresponding to proton addition to the free acid (e.g., $[M_A + H])^+$) at m/z 232. The peak at m/z 270 can be rationalized as either a potassium addition to the free acid (e.g., $[M_A + K]^+$) or the addition of a proton to the intact salt (e.g., $[M_S + H]^+$. Similarly, the peak at m/z 308 can be viewed as the addition of two potassium ions to the anion of the free acid (e.g., $[M_A + 2K - H]^+$) or a potassium adduct to the potassium salt (e.g., $[M_S + K]^+$). In any event, the preparation of the synthetic APAP metabolites as

potassium salts accounts for the abundance of potassium adducts observed in the FAB spectra presented here. In contrast, the high concentration of sodium in urine generated the predominance of natriated species found in the spectra of urinary metabolites. Assuming that the sulfate conjugate existed primarily as the free acid (mobile phase pH less than 3), the ions at m/z 232, 254, and 276 corresponded to $[M_A + H]^+$, $[M_A + Na]^+$, and $[M+2Na-H]^+$, respectively. Again, the ions at m/z 254 and 276 could correspond to $[M_S + H]^+$ and $[M_S + Na]^+$ resulting from analyte molecules existing as the sodium salts M_S (mol. wt = 253) where $M_S = M_A + 22$.

Studies were undertaken to determine the inter-run reproducibility of $(S/B)_{max}$. Data were collected over several runs using three synthetic metabolites: APAP-NAC (6 nmol), APAP-SO_4 (10 nmol), and APAP-CYS (11 nmol). The results of several runs (minimum of four) were used to calculate the relative standard deviation (% RSD) in all cases. Close attention was given to preserve the set of experimental conditions used to study each particular compound. Hence, the deviations observed for $(S/B)_{max}$ were primarily a reflection of instrumental variance as well as uncertainty in the ionization process itself. The lowest uncertainties in $(S/B)_{max}$ were observed for $[M + H]^+$ species, while the values for the major cation adducts monitored were somewhat elevated. For example, the total average relative standard deviation in $[M + H]^+$, found by pooling the values of all studies, was 8.6% RSD. The least variation was obtained for APAP-CYS (3.6% RSD) and the highest for APAP-SO_4 (15% RSD). Values calculated for mono- and di-cation species all fell within a range of 9-25% RSD with the precision of

di-cation species being slightly higher in most cases. The better precision of S/B maxima for $[M + H]^+$ ions could be explained by the presence of excess glycerol on the sample probe early in the run when the maxima occur. In contrast, cation adducts normally exhibit maximum S/B later in the run when the glycerol becomes depleted and hence may be subject to fluctuations in available sodium or potassium ion concentrations.

D. Application of (S/B)

Assessing the effectiveness of matrix "spiking"

Acids, bases, or alkali salts are frequently added to the glycerol matrix to enhance the yield of molecular ion adducts in both positive and negative ion FAB spectra. By increasing the preformed concentration of analyte ions in the matrix this method can raise the intensity of the corresponding analyte peaks relative to their neighbors making them more discernible. Alternatively, spiking can generate new ion types which, due to their complementary nature, aid in the confirmation of molecular weight assignments. S/B computations can be useful in providing objective assessments of matrix spiking. Figures 4.3(a) and (b) depict the influence on the FAB spectra when synthetic APAP-NAC (6 nmol) is spiked with p-toluenesulfonic acid (100 nmol). Shown are the regions of the mass spectra surrounding the $[M + H]^+$ ion at m/z 313 before and after spiking in Figures 4.3(a) and 4.3(b), respectively. The calculated $(S/B)_{max}$ ratios are given. A net enhancement factor of

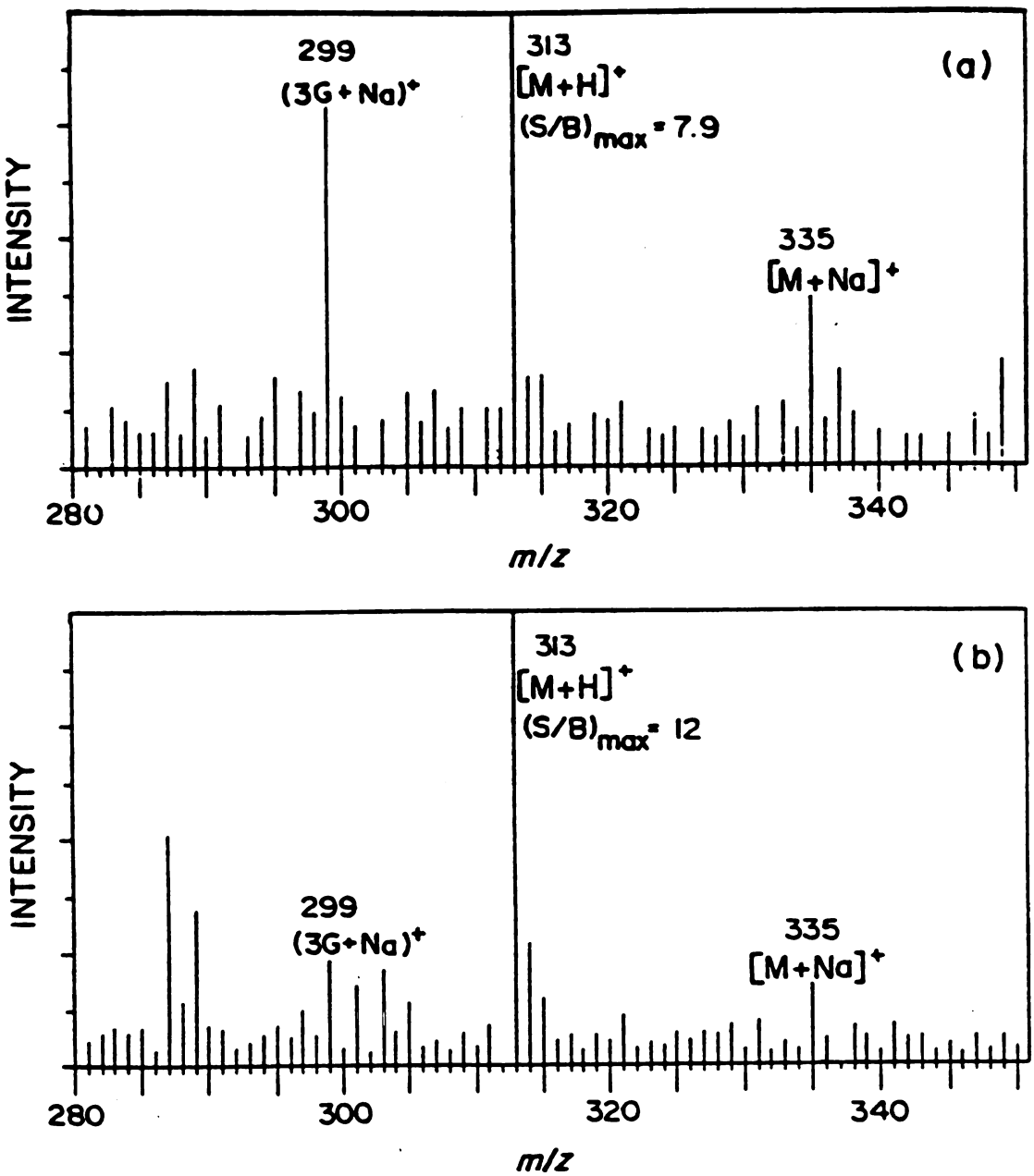

Figure 4.3 (a) Region of FAB spectrum containing peak for the protonated molecular ion of APAP-NAC. An $(S/B)_{max}$ of 7.9 at m/z 313 was obtained when 6 nmol APAP-NAC (synthetic) was subjected to bombardment by 8.6 keV xenon atoms in µl glycerol. (b) Spectrum obtained when 6 nmol APAP-NAC (synthetic) was present in a matrix containing p-toluenesulfonic acid in glycerol (100 nmol μl^{-1}). Under these conditions, the observed $(S/B)_{max}$ was 12 at m/z 313.

1.5 was achieved for the $[M + H]^+$ ion by spiking the glycerol matrix with the acid.

Assessing the effectiveness of sample repurification

The purity of an analyte solution following separation is a critical factor controlling the success of analysis by FAB mass spectrometry. Additional purification may be necessary in some cases to minimize unwanted background which competes for ionization. Signal to background is a useful criterion for judging the success of an additional purification. To illustrate this, a sample containing 8.5 nmol μl^{-1} of APAP-GLUC, isolated from urine in the manner described previously, was repurified as follows. After evaporating the 100 µl solution under nitrogen, it was reconstituted in 400 µl of mobile phase (e.g., 12.5% methanol, 0.05% acetic acid, in water). The whole volume was injected onto a prep C18 column and recollected. The eluent was processed as before bringing the final volume to 100 µl with 1:1 methanol/water. One µl of this solution was analyzed by FAB and compared to the result where 1 µl (8.5 nmol) of the original solution was tested under identical instrumental conditions. The results of this repurification procedure are tabulated in Table 4.3 in the form of maximum S/B ratios for predominant analyte species. The predominant glycerol ion at m/z 369 was not used in the computation of (S/B) for the $[M + 2Na - H]^+$ ion in Table 4.3. While the $[M + H]^+$ intensity is attenuated following repurification, the natriated adducts are significantly enhanced allowing greater recognition of the metabolite.

TABLE 4.3. RESULTS OF AN ADDITIONAL PURIFICATION OF URINARY APAP-GLUC

m/z	Assignment	$(S/B)_{max}$ Before	After	Enhancement factor
328	$[M+H]^+$	6.4	4.4	0.69
350	$[M+Na]^+$	5.9	14	2.4
372	$[M+2Na-H]^+$	1.6	5.0	3.1

E. Commentary on problems encountered in FAB-MS of reversed phase HPLC fractions.

Achieving proper concentration of analyte

A practical problem encountered when isolating metabolites for analysis by FAB mass spectrometry is that of obtaining the analyte in sufficient concentration. Because only a few microliters can be placed on conventional probe tips, it is desirable to use concentrations exceeding 1 nmol μl^{-1} depending upon the analyte and the separation procedure. Hence, repetitive collections of the same peak were made during several runs on a preparative column and the mobile phase was removed by lyophilization to obtain sufficient amounts for analysis. Whenever possible, control samples should be processed under identical conditions to serve as blanks for background subtraction.

Paired-Ion Chromatography (PIC)

Paired-ion reagents such as tetrabutylammonium phosphate and heptane sulfonic acid are commonly employed in reversed phase assays to retard organic molecules with ionic functionalities and to improve peak shape. In fact, the original assay developed for the separation of APAP metabolites required 5 mM tetrabutylammonium phosphate in the mobile phase to promote ion pairing (9). PIC reagents were shown to create problems for subsequent analyses by

FAB because they generated strong signals in the observed mass spectra. Martin et.al. (19) encountered a similar phenomenon in which the spectrum of the oligopeptide bradykinin was suppressed in the presence of the ionic denaturing agent guanidine hydrochloride. Unfortunately, a simple compromise could not be struck because rather large concentrations of the PIC reagents are needed for effectve ion pairing. The situation became further complicated when the eluent from several runs was consolidated to obtain sufficient analyte for analysis by FAB. During fraction consolidation the PIC reagent, even when present in reduced concentrations, accumulated and was not removed with the aqueous portion of the mobile phase during lyophilization.

To illustrate this point, 6 nmol of synthetic APAP-SCH_3 was analyzed by FAB with and without PIC reagent present. Both samples were prepared in water, one having 5 mM tetrabutylammonium phosphate. A net amount of 15 nmol tetrabutylammonium phosphate was present on the probe tip. Each sample was subjected to 8.6 keV xenon atoms; portions of each mass spectrum appear in Figure 4.4. In calculating values for S/B in both cases, the contribution from glycerol at m/z 185 again was not included. The spectrum without PIC reagent had a $(S/B)_{max}$ value of 8.5 whereas the highest calculated S/B ratio for the sample containing the PIC reagent was only 0.0087. The resulting enhancement approaches three orders of magnitude. If the predominant ion at m/z 184 (originating from the PIC reagent as established by exact mass measurement) is omitted, the $(S/B)_{max}$ for m/z 198 becomes 2.5.

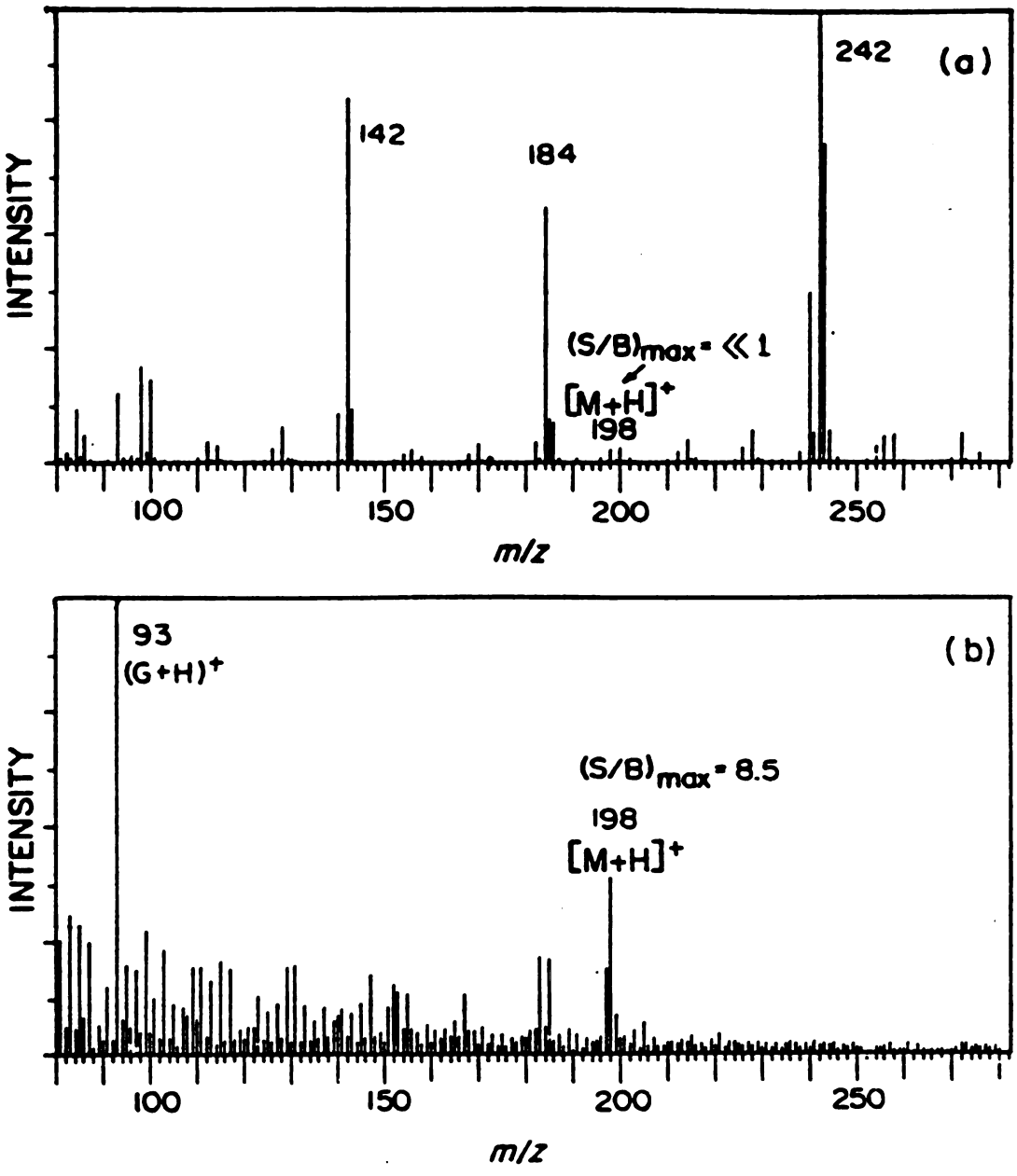

Figure 4.4 Spectra obtained from 6 nmol synthetic APAP-SCH_3 with and without a paired-ion reagent present. When 1.5×10^{-2} M tetrabutylammonium phosphate was present the maximum S/B value recorded for the $[M+H]^+$ ion at m/z 198 was only 0.0087 (a). However, when the PIC reagent was absent (b) the maximum S/B rose to 8.5, an increase of nearly 1000. The intense background peak at m/z 184 was shown by exact mass measurement to be $C_{12}H_{26}N^+$ (a fragment ion of the PIC reagent).

PIC reagents dominate FAB mass spectra due to their high surface activity and charge. This behavior has been extensively studied by Ligon et.al. (20).One way to counter the effect of a PIC reagent would be to acquire mass spectra by detecting the ions of opposite polarity to the PIC reagent used.For example, since the tetrabutylammonium phosphate used here should produce positive ions almost exclusively, negative ion detection would eliminate the interference from the PIC reagent. Unfortunately, because the CH5 was not equipped for negative ion detection, this hypothesis could not be tested using the original assay developed for separation of the APAP metabolites where 5 mM tetrabutylammonium phosphate was used (9).

Half-width peak collection

Efforts to maximize the amount of analyte relative to the chemical background present in the sample will result in greater effective sensitivity. Therefore, if one collects the volume indicated between the inflection points (half-width) of a peak rather than by the peak in its entirety (baseline), the resulting eluent should be more concentrated in the solute of interest, and less contaminated by other materials. For a Gaussian peak shape, it is theoretically possible to collect 68% of the eluting solute corresponding to the peak area between the inflection points. To test the above hypothesis, APAP-GLUC was collected from urine (diluted 1:4) using both half-height and full-peak collection and prepared for analysis by FAB. In both cases a 50 µl aliquot was

placed onto the C18 prep column with a mobile phase consisting of 12.5% methanol and 0.05% acetic acid in water. Both samples were subsequently quantified against a standard of synthetic metabolite to reveal that the half-height collection contained 0.87 nmol μl^{-1} whereas the full-peak collection had 0.57 nmol μl^{-1}. The samples were then concentrated 10-fold by evaporating them under nitrogen and reconstituting the solution with 1:1 methanol/water. The volumes placed on the probe tip were adjusted so that equal amounts of APAP-GLUC (i.e., 26 nmol) were present with 1 µl of glycerol during each analysis. The results of this study are summarized in Table 4.4. The average enhancement factor for the three major analyte ions observed is 1.33; each enhancement factor exceeds the limit of inter-run variance in $(S/B)_{max}$.

The effect of mobile phase acidity

Relatively strong acids such as glacial acetic and phosphoric acid are frequently added to the mobile phase to buffer a reversed phase system at low pH. However, the presence of a strong acid at levels commonly associated with reverse phase assays (e.g., 1.0%) can prove deleterious to subsequent analysis by FAB. Figure 4.5 shows the effect of acetic acid concentration in the mobile phase on the ensuing FAB spectra of APAP-CYS.

When an HPLC fraction (eluted with 1% acetic acid) from a microsomal incubation was analyzed by FAB, the $(S/B)_{max}$ recorded for the $[M + H]^+$ ion was only 1.8. The representative spectrum in Figure 4.5(a) contains intense background at virtually every mass.

TABLE 4.4. COMPARISON OF FULL-WIDTH vs. HALF-WIDTH PEAK COLLECTION FOR URINARY APAP-GLUC

	Amount APAP-GLUC	Collection interval (min)	$(S/B)^{max}$ $[M+H]^+$	$[M+Na]^+$	$[M+2Na-H]^+$
Full-width	26 nmol	5.03-6.12	2.7	12	9.4
Half-width	26 nmol	5.15-5.57	3.7	16	12
Enhancement factor			1.4	1.3	1.3

Figure 4.5 (a) FAB spectrum of 30 nmol APAP-CYS, isolated from a microsomal incubation, yields an $(S/B)_{max}$ of only 1.8 at m/z 271 when 1.0% acetic acid is present in the HPLC mobile phase; matrix:KCl in glycerol (100 nmol μl^{-1}). (b) FAB spectrum of 5.7 nmol APAP-CYS, again isolated from a microsomal incubation but with 0.05% acetic acid in the mobile phase. The $(S/B)_{max}$ of 8.4 corresponds to a relative enhancement of 4.7 with five times less sample present; matrix:KCl in glycerol (100 nmol μl^{-1}). (c) FAB spectrum of 5.4 nmol synthetic APAP-CYS in KCl/glycerol (100 nmol μl^{-1}). The $(S/B)_{max}$ of 8.0 for $[M+H]^+$ illustrates that spectra from biological samples can compare favorably to those of synthetic origin; the prominent glycerol ion at m/z 277 was omitted in each case.

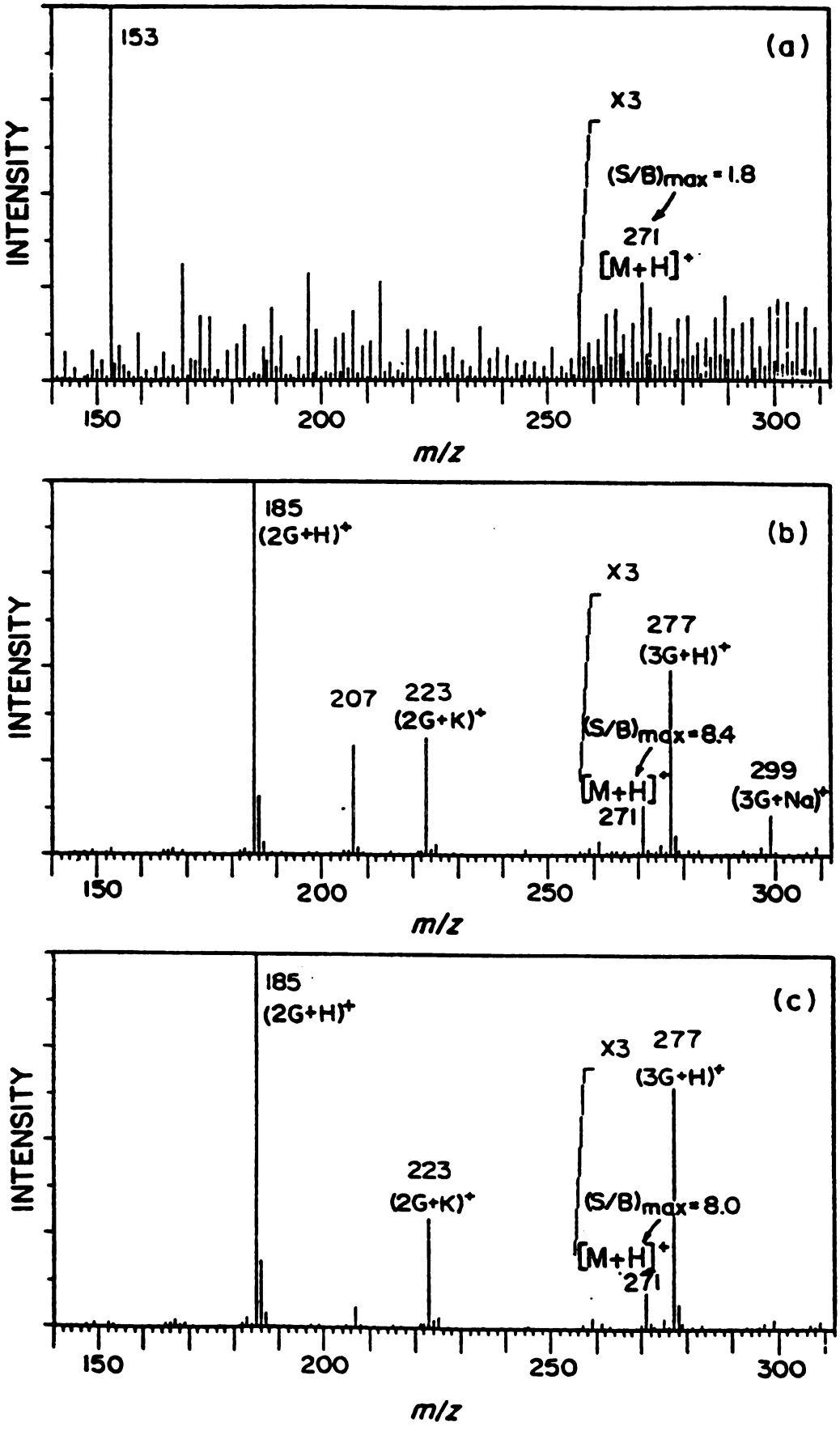
153
(a)
X3
(S/B)max = 1.8
271
[M+H]+
INTENSITY
150
200
250
300
m/z
185
(2G+H)+
(b)
X3
277
(3G+H)+
207
223
(2G+K)+
(S/B)max = 8.4
[M+H]+
271
299
(3G+Na)+
INTENSITY
150
200
250
300
m/z
185
(2G+H)+
(c)
X3
277
(3G+H)+
223
(2G+K)+
(S/B)max = 8.0
[M+H]+
271
INTENSITY
150
200
250
300
m/z

Another sample was isolated similarly, however, only 0.05% acetic acid was used in the mobile phase; this was the lowest amount of acetic acid capable of providing an acceptable separation by reverse phase HPLC. The result in Figure 4.5(b) shows a dramatic decrease in background allowing for an $(S/B)_{max}$ of 8.4 to be obtained for five times less sample (i.e., 5.7 nmol) when the lesser amount of acetic acid was used. Evidently, acetic acid combines with the sodium present in biological samples to form sodium acetate. While acetic acid may be removed during lyophilization, sodium acetate and other salts persist. In fact, a white solid material was noticed in the conical vials used to concentrate samples following lyophilization of the HPLC eluent collected over several runs. In all cases, the amount of solid material correlated to the percentage of acetic acid used in the HPLC assay. Finally, Figure 4.5(c) displays the result when 5.4 nmol of synthetic APAP-CYS was analyzed by FAB mass spectrometry. The calculated $(S/B)_{max}$ of 8.0 indicates that results for samples obtained from biological sources can compare favorably to their synthetically obtained counterparts when proper attention is given to the preparation of HPLC samples for analysis by FAB mass spectrometry.

V. Conclusion

The capability of using FAB to characterize and identify a complete set of metabolites of a pharmaceutically important drug, acetaminophen, has been demonstrated. Of particular interest is the spectrum obtained for the polar acetaminophen sulfate which was

previously unattainable by other mass spectral techniques, including field desorption. In addition, a methodology has been established enabling FAB to be used in the analysis of urinary fractions for metabolites at therapeutic levels in urine following purification by reverse phase HPLC. While great analytical potential may be realized through the interaction of these two techniques, this study indicates that an approach must be taken which minimizes the sources of specific chemical interference that compete for ionization during fast atom bombardment.

Further, this study illustrates the important problem of chemical interference in FAB mass spectra. Unfortunately, even when steps are taken to minimize specific interferences present in biological samples, there is still the problem of interfering ions from the viscous liquid matrix used to perform FAB. This portion of the problem shall be addressed in the next chapter where thermally-assisted FAB is formally introduced. The concept of signal to background developed for use in the analysis of the urinary metabolites of acetaminophen can be a useful parameter to judge the ability to discern analyte peaks above background in other applications as well and shall be used throughout the remainder of this dissertation.

VI. List of References

1. D.R. Knapp, Workshop report for the committee for Quantitative Organic Analysis at the 32nd Annual Conference of the American Society for Mass Spectrometry, San Antonio, Texas, May 1984, Biomed. Mass Spectrom., 12, 47 (1985).
2. M.R. Clench, G.V. Garner, D.B. Gordon, and M. Barber, Biomed. Mass Spectrom., 10, 357 (1985).
3. P. Roepstorff, P. Jojrup, and J. Moller, Biomed. Mass Spectrom., 12, 181 (1985).
4. C. Fenselau and D. Games, editors-in-chief, BMS Forum, Biomed. Mass Spectrom., 11, 495 (1984).
5. T.D. Boyer and S.L. Rouff, J. Am. Med. Assoc., 218, 440 (1971).
6. D.J. Jollow, J.R. Mitchell, W.Z. Potter, D.C. Davis, J.R. Gillette, and B.B. Brodie, J. Pharmacol. Exp. Ther., 187, 195 (1973).
7. R.J. McMurtry, W.R. Snodgrass, and J.R. Mitchell, Toxicol. Appl. Pharmacol., 46, 87 (1978).
8. J.G. Kleinman, R.V. Breitenfield, and D.A. Roth, Clin. Nephrol., 14, 201 (1980).
9. J.F. Newton, W.E. Braselton, C.H. Kuo, W.M. Kluwe, M.W. Gemborys, G.H. Mudge, and J.B. Hook, J. Pharmacol. Exp. Ther., 221(1), 761 (1982).
10. D.J. Jollow, S.S. Thorgeirsson, W.Z. Potter, M. Hashimoto, and J.R. Mitchell, Pharmacology, 12, 251 (1974).
11. J.E. Mrochek, S. Katz, W.H. Christie, and S.R. Dinsmore, Clin. Chem., 20, 1086 (1974).

12. J.H. Knox and J. Jurand, J. Chromatogr., 1442, 651 (1977).

13. S.D. Nelson, Y. Baishnav, H. Kambara, and T.A. Baillie, Biomed. Mass Spectrom., 8, 244 (1981).

14. M.W. Gemborys and G.H. Mudge, Drug Metab. Dispos., 9, 340 (1981).

15. A.R. Buckpitt, D.E. Rollins, S.D. Nelson, R.B. Franklin, and J.R. Mitchell, Anal. Biochem., 83, 168 (1977).

16. C.R. Blakely and M.L. Vestal, Anal. Chem., 51, 750 (1983).

17. H.V. Malmstadt, C.G. Enke, and S.R. Crouch, "Electronics and Instrumentation for Scientists", p. 409, Benjamin/Cummings: Menlo Park, California, 1981.

18. F.W. McLafferty, "Interpretation of Mass Spectra", third edition, p. 34, University Science Books:Mill Valley, California, 1980.

19. S.A. Martin, C.E. Costell, and K. Biemann, Anal. Chem., 54, 2362 (1982).

20. W.V. Ligon, Jr. and S.B. Dorn, Int. J. Mass Spectrom. Ion Proc., 61, 113 (1984).

Chapter 5

THE DEVELOPMENT AND APPLICATION OF THERMALLY-ASSISTED FAB

I. Introduction

In this chapter, TA-FAB is formally introduced as a method for optimizing analyses by FAB. As indicated in the descriptive overview given at the conclusion of Chapter 2, TA-FAB is essentially a method for producing new matrices for FAB out of materials which until heated are too immobile to act as substrates for FAB. This idea is a direct extension of the observation that all successful FAB matrices have a certain degree of fluidity, which enables them to accomodate the chemical and physical events responsible for ion desorption by FAB. This approach to matrix production was developed in response to two existing problems with FAB matrices at present. First, while several materials have been reported for use (1), the number of viscous liquids which can be used is limited, which in turn limits the scope of potential applications in FAB. Second is the problem of matrix interference in FAB. The intent therefore was to develop viable matrix candidates with the hope that some would exhibit less background than presently observed with materials such as glycerol.

Several materials have been proposed for use in TA-FAB. For instance, viscous polymers, such as GC stationary phases, might serve as matrices when heated. Originally solids were chosen because of their ability to undergo a phase change upon heating to

a liquid state, and because there were examples in the literature where solids had been used successfully as matrices for desorption-ionization. Friedman and Beuhler reported increased yields for the desorption of small peptides while performing rapid heating in the presence of either urea or oxalic acid (2). More recently, Cooks and coworkers found that the desorption efficiency of molecular ions was increased for the SIMS spectra of organic salts when ammonium chloride was used as a matrix (3). They also observed a decrease in analyte fragmentation and less spectral background by this method. Analogous results were reported by Vestal et al. who used inositol and tartaric acid to enhance the respective desorption of erythromycin and histidine from a moving belt LCMS interface using laser desorption (4).

Initial success was achieved using saturated aqueous solutions of small saccharides such as glucose. Saccharides were among the first solids investigated because of their obvious structural similarity to glycerol. Aqueous solutions were used to facilitate application of the solid matrix onto a TA-FAB probe tip fashioned from a piece of EI filament ribbon. However, saccharides displayed a unique characteristic not observed for the other solids tested: the ability to retain water under the low pressure conditions of the mass spectrometer (ca. 1×10^{-5} torr). This observation, along with studies done to determine the temperature of the probe, indicated that the success realized using saturated aqueous solutions of saccharides as TA-FAB matrices was not a consequence of melting. Rather, it is believed that the capacity of saccharides to retain water under the reduced pressure of the mass

spectrometer permits efficient mass transport during desorption-ionization. The processes involved with the release of water under the conditions of TA-FAB are both dynamic and temperature-dependent. It is proposed that these factors are largely responsible for the observed differentiation between the profiles for analyte and matrix ions in TA-FAB, as illustrated in Chapter 2. A proposed mechanism for TA-FAB is discussed in Chapter 6.

Throughout this research, three objectives were cited as goals to document the types of results attainable by TA-FAB: first, to show that saturated matrices, when heated, often yield less background than the viscous liquids used in conventional FAB; second, to demonstrate that the desorption profiles of matrix and analyte under the controlled heating of TA-FAB are, in certain cases, distinguishable, thereby creating a viable situation for background subtraction; third, to show how the TA-FAB process may be optimized by selecting a matrix which is physiochemically suited to the particular analyte under study.

Results consistent with these objectives are given in the discussion that follows. The remainder of this chapter is devoted to an actual application of TA-FAB to the analysis of a series of cyclic tetrapeptide mycotoxins isolated from the fungus helminthosporium carbonum.

II. Experimental

A. Materials

In the preliminary work that follows, all reagents used either as substrates or analytes were obtained through one of several commercial sources. Each was of reagent purity requiring no purification prior to use. The analyte solutions were prepared with either distilled water or aqueous methanol (HPLC grade, MCB, Inc.) solution depending upon the solubility of a particular solute. For the application to the helminthosporium carbonum mycotoxins (HC-toxins), the samples were received as a gift from R.P. Scheffer, Department of Plant Pathology, Michigan State University, and were isolated using the procedure outlined below. The saturated matrix solutions used in the initial TA-FAB studies were 50% methanol in distilled water, primarily to facilitate rapid evaporation of excess solvent prior to introduction of the sample into the mass spectrometer. The work with the mycotoxins was performed using matrix solutions prepared using water as the only solvent. While no qualitative differences have been documented regarding the effect of solvent composition on TA-FAB, this will be the topic of a subsequent investigation. For comparisons of TA-FAB to conventional FAB, 0.5µl of vacuum distilled glycerol was applied to the same probe tip used for TA-FAB experiments from a 5µl graduated glass micropipet (Fisher Scientific Products).

B. Isolation and Purification of the Helminthosporium Carbonum Mycotoxins

The HC-toxins were received as dried samples whose weights had been determined previously. Each was reconstituted with 1.0ml of HPLC grade methanol giving concentrations of 1.5, 3.0, and 1.5µg/ul, for toxins HC-I, II, and III, respectively. Each vial was purged with nitrogen prior to storage (-20°C) to prevent oxidation.

The detailed procedure (5) for isolation and purification of the HC-toxins involved culturing the fungus for 21 days on a modified Fries medium prior to filtration concentration, and deproteinization. The aqueous filtrate was extracted with methylene chloride and chromatographed on Sephadex LH-20 with methanol. The active fractions then underwent two stages of flash chromatography on silica. The first stage (1:1:1 hexane, methylene chloride, acetone) was used to isolate the primary toxin, HC-I. A second pass with 1:1 methylene chloride/acetone was necessary to further purify the minor toxins (HC-II, III) which still co-eluted under these conditions. Finally, the toxins underwent two stages of HPLC, first by reverse phase and then by normal phase, prior to analysis by mass spectrometry.

The reverse phase analysis was accomplished using a µ-Bondapak C18 column (30 x .78cm) having a 10µm particle diameter (Waters Associates, Inc., Milford, Mass.). The samples underwent a linear gradient elution from 7 to 20% (ethanol in water) over 30 min. at 2ml/min on a Varian 5000 HPLC unit. These conditions were

sufficient for the purification of HC-I, but did not resolve the more quickly eluting minor toxins. Normal phase separation of HC-II and III was subsequently accomplished on a Whatman Partisil-10 silica column (25 x .46cm) under isocratic conditions using a mobile phase of 95% hexane/5% ethanol.

C. Mass Spectrometry

The Varian MAT CH5 mass spectrometer described previously was used for all TA-FAB and FAB experiments. Fast xenon atoms between 6.8-7.0keV were used in all analyses; source pressure: 1×10^{-5} torr. The electron multiplier was operated at -2.25kV to detect the positive ions produced. This value was later increased to 2.5kV during the HC-toxin work due to the age of the multiplier. Initial studies used a magnet scan rate of approximately 25 s/decade, but was increased to 13 s/decade during the HC-toxin analyses to acquire more mass spectra across the TA-FAB ion desorption profiles. Samples were introduced into the mass spectrometer through a vacuum lock using a probe colinear to the optical axis which also accommodates field desorption samples. Once introduced, the probe containing the sample was inserted until it intercepted the atom beam at 90°. At this point, the probe position, lens potentials, and acceleration potential were adjusted to achieve a set of optimum focus conditions. Mass calibration was routinely obtained by performing FAB on saturated CsI/glycerol on the TA-FAB probe tip without heating.

In the TA-FAB application to the HC-toxins, a comparison was made to electron impact. All EI data were recorded on a Hewlett-Packard 5985 quadrupole mass spectrometer. Each toxin (ca. 1.5μg, except 3.9μg of HC-II) was analyzed in succession using a direct insertion probe. The probe was heated from 40°C to 280°C at 30°C/min for each sample. During this interval EI mass spectra were repetitively recorded with the electron multiplier at -1.8kV.

D. Sample Preparation and Analysis by TA-FAB

Samples were applied to the tungsten band in the following manner. First, a 0.5μl droplet of the saturated matrix solution was applied from a 10μl Hamilton syringe (Reno, NV) and the solvent removed with a heat gun. For the fructose solution, 1μl was found to contain 60±5μg of fructose. When the saccharide matrices were used, the desolvation process appeared to be incomplete, leaving a syruplike coating on the band rather than a well-defined solid. One microliter of analyte solution was then administered onto the matrix after which the mixture was gently blown with a heat gun to remove excess solvent, and to promote mixing. A study using alanyl-leucyl-glycine at the 5μg level revealed that changing the order of analyte and matrix application made no significant difference to the results obtained. Following sample application, the probe was then introduced into the mass spectrometer and inserted until contact was made with the ECP. The FAB gun was turned on and the instrument focused on a background peak while applying little or no heat to the band so that early desorption of

the analyte could be avoided or minimized. During the initial three scans in all the TA-FAB runs, data were collected similar to that by conventional FAB (no heat). During the fourth scan, the current was manually increased (slowly) to a value of 0.90A. Beginning with the fifth scan, a heating rate of approximately 100mA/min was initiated using the ECP. The current was allowed to increase beyond the point of maximum analyte desorption before returning to 0.00A.

E. Comparison between FAB and TA-FAB for the Analysis of the HC-toxins

Several comparisons were made between FAB and TA-FAB for each of the HC-toxins at the 1.5µg level. In each case, 0.5µl of the appropriate matrix was used (e.g., glycerol for FAB, saturated aqueous solution of fructose for TA-FAB). TA-FAB matrices are commonly referred to as saturated, the reason being that regardless of the water content present during sample application, after experiencing high vacuum the sample solutions were observed to have a consistency very similar to saturated fructose. This assumption shall be investigated by viscosity measurements. Conventional FAB analyses were conducted with both the tungsten band emitter (0.235" x 0.018" x 0.001") and a regular stainless steel probe tip that had a considerably larger surface (0.250" x 0.125"). For conventional FAB, 0.5µl of vacuum distilled glycerol was applied to the band or tip from a 5µl graduated glass micropipet. Next, one-half microliter of the appropriate toxin in methanol was applied from a

10µl syringe; prior to this step, toxins HC-I and II were concentrated to 3µg/µl so that a 0.5µl aliquot of each of the three toxins would result in 1.5µg of applied sample. Finally, the contents on the tip were gently warmed with a heat gun to remove excess solvent and to promote mixing prior to analysis.

For analyses by TA-FAB, 0.5µl of a saturated aqueous fructose solution was applied to the tungsten band followed by a 0.5µl aliquot of the appropriate toxin in methanol. The resulting liquid bead was then gently warmed by the heat gun to remove solvent and to promote mixing. The resulting sample introduced into the mass spectrometer was a thin film having a syruplike consistency which remained even under the conditions of high vacuum. Once the sample was inside the mass spectrometer, focus was achieved on a fructose background peak under FAB-only conditions (no heat). During a typical TA-FAB run, the initial heating current was 0.80A. Beginning at this current, a heating rate of approximately 100mA/min was initiated simultaneously with repetitive scanning of the magnet and data collection. The heating current was programmed to 1.40A which exceeded the BMT in all cases. A total of about 10 minutes elapsed during each TA-FAB analysis.

III. RESULTS AND DISCUSSION

A. Matrix Comparison:glycerol versus saturated fructose

As mentioned, saccharides were selected for use in TA-FAB because of their structural similarity to glycerol. However, prior

to heating, saturated saccharide solutions exposed to high vacuum exist as syruplike liquids more viscous than glycerol, which do not promote efficient analyte desorption-ionization. Upon heating, however, these same solutions acquire the physical traits necessary for analyte desorption-ionization to occur. Although heated fructose or glucose solutions behave similar to glycerol in their ability to provide FAB spectra, they also have some important differences. Foremost is that saccharide solutions generate less background interference in FAB.

Figure 5.1 displays a matrix comparison for glycerol and saturated fructose. The upper mass spectrum is an average of several spectra obtained from the bombardment of 0.5µl glycerol under standard FAB conditions. The lower spectrum (Figure 5.1b) is an average spectrum acquired from 0.5µl saturated fructose under the same conditions except that the sample was slowly heated manually from 0.00 to 1.50A during data collection; the ions observed from fructose and their relative ratios did not change significantly over this temperature interval.

Several differences are apparent from this comparison. First, the ions in the glycerol spectrum are much more intense. The base peak for glycerol, the protonated monomer at m/z 93, has an intensity exceeding 207,000 counts which is about five times greater than the base peak for fructose, m/z 85. The larger intensity for glycerol does not just apply to the most intense peaks, but to the smaller ones as well. This tendency is apparent from the regions above mass 400 where a magnification factor of 15 has been included in each mass spectrum. Here it is easy to

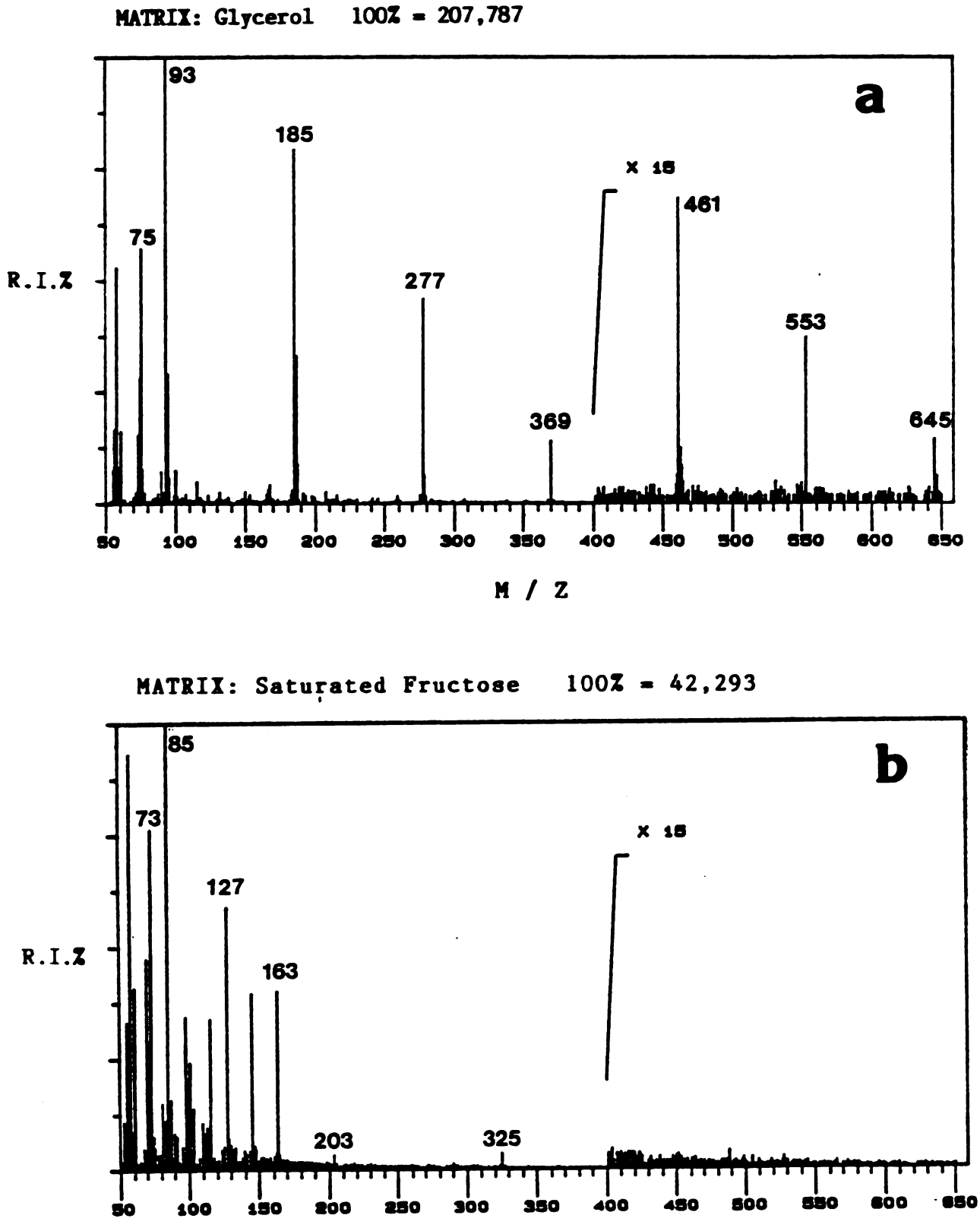

Figure 5.1 Matrix comparison: (a) averaged FAB spectrum of glycerol, (b) TA-FAB mass spectrum of saturated fructose.

observe the extent to which glycerol presents interference at almost every mass. One reason for the difference in background is that saccharides, in contrast to glycerol, resist cluster formation. The glycerol spectrum of Figure 5.1a is dominated by a series of protonated clusters which associate through hydrogen bonding and form the basis for many background ions observed at high mass. Saccharides, on the other hand, form ions primarily through fragmentation to form a reproducible series of ions below mass 200. Clustering by fructose does occur to some extent. A small degree of dimerization is witnessed by the peaks at m/z 365 and 325 which correspond to (2 fructose + Na - H_2O)$^+$ and (2 fructose + H - 2 H_2O)$^+$, respectively. However, the highest mass peak observed for glucose or fructose in many analyses is commonly the natriated parent (M + Na)$^+$ which occurs at m/z 203. No (M+H)$^+$ ions are observed for glucose, as protonation at a hydroxyl group results in the facile loss of water to give a peak at m/z 163. Further fragmentation gives rise to the observed fragment ions series at m/z 145, 127, 115, 97. 85, 73, 57, and 43. Even though these peaks can sometimes be large in magnitude, they fortunately appear at low mass, a region of little interest during most analyses by FAB-MS.

B. Comparison of FAB and TA-FAB for Thiamine Hydrochloride

To illustrate the reduction in matrix interference by TA-FAB a comparison between FAB and TA-FAB was peformed for thiamine hydrochloride (vitamin B_1). Figure 5.2 is a conventional (averaged) FAB spectrum of 3μg of thiamine hydrochloride dispersed

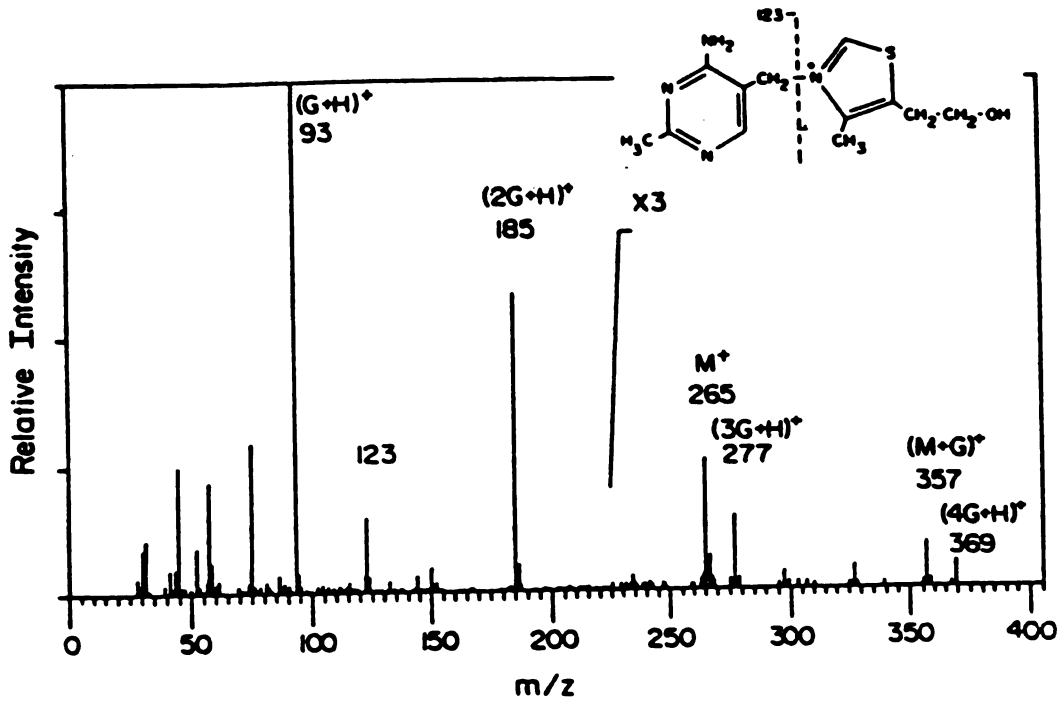

Figure 5.2 Conventional averaged FAB mass spectrum of 3 µg of thiamine hydrochloride in 0.5 µl of glycerol.

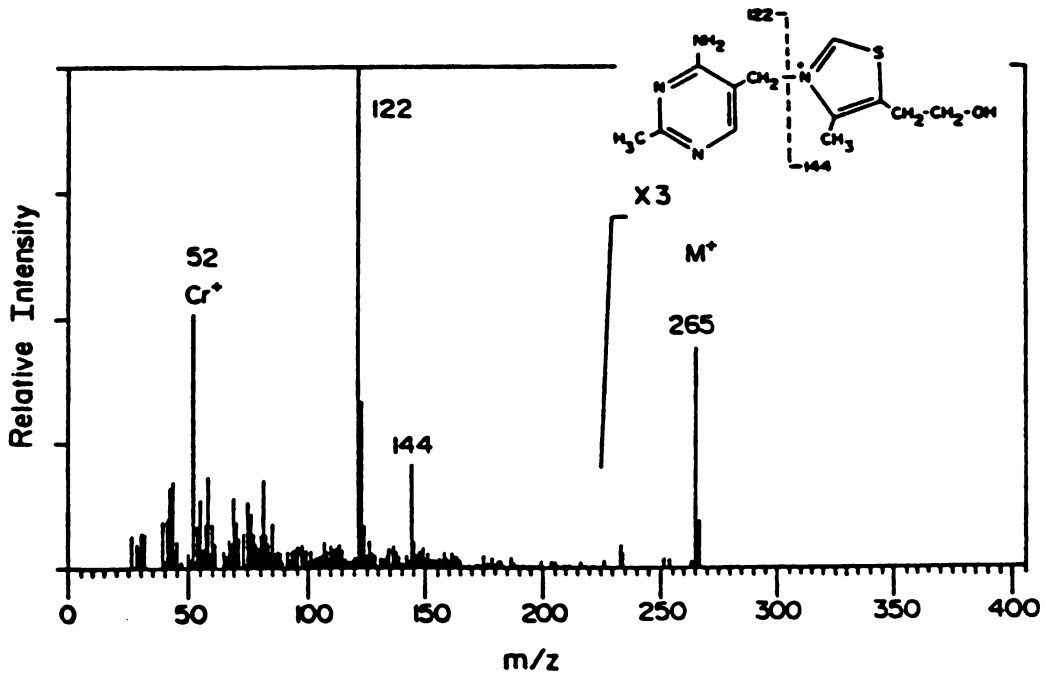

Figure 5.3 TA-FAB spectrum of 3 µg of thiamine hydrochloride in 0.5 µl of glucose averaged over the region of analyte desorption.

in 0.5µl of glycerol and bombarded with 6.8keV xenon atoms. The dominance by glycerol in this spectrum is apparent at m/z 93 and 185. These peaks which correspond to the protonated glycerol monomer and dimer, respectively. Because of the contribution by glycerol in this spectrum, only three peaks may be recognized as originating from the analyte. First, the ion of mass 265 is the intact cation of the thiamine hydrochloride salt. Secondly, the ion of mass 357 corresponds to the addition of glycerol to the intact thaimine cation. Finally, the peak at m/z 123 results from cleavage between the two heterocyclic rings of thiamine. The origin of this ion was revealed by Cooks et al. who used SIMS in connection with MS/MS to study the fragmentation of vitamin B_1 in glycerol (6). Their work demonstrated that the peak at m/z 123 results from collisionally activated dissociation of m/z 357 (e.g., $(M+G)^+$) and is not a daughter of M^+. Although Cooks also showed that two resonance-stabilized daughters (m/z 122, 144) result from fragmentation between the two rings when the thiamine cation (M^+) is the parent, neither is of sufficient intensity to make a reliale assignment in the FAB spectrum of Figure 5.2. The structure for the peak at m/z 123 is less easily rationalized. The most plausible explanation involves a proton transfer to the amino group of the 6-membered ring followed by cleavage between the rings. Ostensibly, the proton is transferred from the associated glycerol molecule.

As a comparison to conventional FAB, the experiment was repeated by TA-FAB using 0.5µl of saturated glucose instead of glycerol. The two runs were performed consecutively, under

identical experimental conditions. Between runs, the tungsten band was thoroughly cleaned with acetone, dilute HCl, and distilled water and then checked for the presence of memory effects by TA-FAB. Figure 5.3 displays the mass spectrum obtained by averaging the scans during which desorption of thiamine occurred. In this spectrum, clear evidence is given for the molecular cation at m/z 265 and also for the fragment ion peaks occurring at m/z 122 and 144. Again, these same peaks were observed by Cooks following collisionally activated dissociation of the molecular cation. The peak at m/z 52 is Cr^+ which originates from the stainless steel present in the probe tip. Even without subtraction, the selection against background is superior for TA-FAB as compared to the conventional FAB spectrum in Figure 5.2 where glycerol contributes the most intense peaks in the mass spectrum. Not only is the influence of glycerol (conventional FAB) more intense than that of glucose in TA-FAB, but the multiplicity of its appearance is greater due to clustering. For example, in Figure 5.2 clustering accounts for the peak 12 mass units above the thiamine molecular ion (e.g., $(3G+H)^+$, m/z 277). In contrast, in Figure 5.3, the lack of clustering by glucose confines most background peaks in the TA-FAB spectrum to the region below mass 200; none of the series of glucose ions (previously listed) may be readily discerned in this case. It should be noted that selection against glucose is not always as complete prior to subtraction as the data in Figure 5.3 indicate. Selection is dependent upon many factors which include analyte concentration, choice of substrate, and experimental conditions. However, while matrix peaks are commonly observed in

TA-FAB spectra, their overall contribution is generally less imposing than the background generated by glycerol.

The chronology of the TA-FAB experiment for thiamine may best be visualized by following the course of the two reconstructed mass chromatograms appearing in Figure 5.4. For the duration of the heating process, these are essentially ion desorption profiles. The upper mass chromatogram corresponds to the molecular cation of thiamine (m/z 265), while the lower trace is the mass chromatogram of the predominant glucose ion at m/z 73 ($C_3H_5O_2^+$). The plots in Figure 5.4 indicate the temporal nature of the desorption profiles attained by this method. The first four scans represent data collected by FAB only (no heat). These scans contained mostly glucose peaks. However, since the same glucose peaks were observed before and during heating, this region is indicative of the background which codesorbs later with the analyte. Next, the current was increased manually to 0.90A at scan 4, after which a controlled ramp of the curent was initiated at scan 5. The current increased linearly past the point of optimum analyte desorption, indicated by the point of maximum intensity in the mass chromatogram of m/z 265 (Figure 5.4). A current maximum of 1.54A was reached at scan 18 after which the ECP was turned to 0.00A.

Examination of the mass chromatogram at m/z 265 in Figure 5.4 shows that the temperature providing maximum desorption occurred at scan 13. We choose to refer to this point as the "best matrix tempeature" or BMT. This name was given by analogy to field desorption where the term "best anode tempeature" or BAT refers to the optimum desorption temperature for a particular FD analysis.

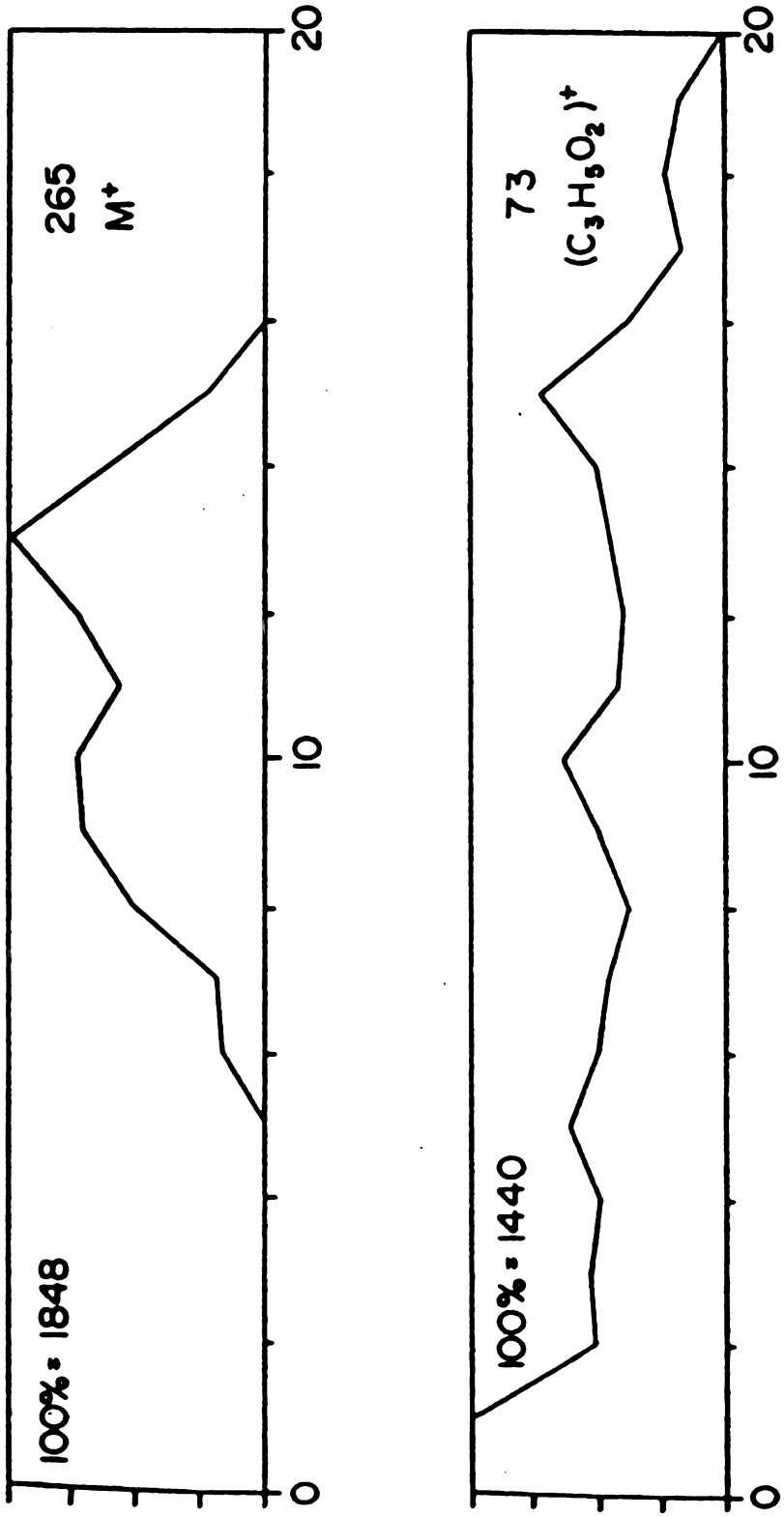

Figure 5.4 Reconstructed mass chromatograms for analyte (m/z 265) and background (m/z 73) ions for the TA-FAB analysis of 3 µg of thiamine hydrochloride in 0.5 µl of glucose.

The value for the BMT observed for thiamine in Figure 5.4 corresponds to a current of approximately 1.29 ± 0.05A. Differences in the observed BMT currents for repeated analyses can be attributed to chemical and instrumental variations experienced with sequential determinations. It is believed that the temperature at the BMT actually varies much less than this.

C. Potential for Background Subtraction Utilizing Differential Desorption Profiles

Consistent with the second objective, controlled heating of saturated saccharide matrices during FAB allows for a feature not available in conventional FAB, i.e., the possibility of differential desorption between analyte and background ions. Since m/z 73 is a reliable indicator of matrix desorption for glucose, it is clear from the data in Figure 5.4 that differential desorption between analyte (m/z 265) and background (m/z 73) was achieved during the TA-FAB analysis of thiamine hydrochloride in glucose. For this example, background subtraction was acceptable since the instrumental conditions and sample composition were not disturbed by removal of the probe to create a background-only situation by means of a second analysis.

To make background subtraction a reliable and quantitative procedure requires that the scan chosen for subtraction be a true representation of the background present during the region of analyte desorption. The best way to approach this ideal is to track several major background ions and find a scan (or an average

scan) containing only background that most accurately represents the intensity of these ions during the region of optimum analyte desorption. As illustrated in Figure 2.3, this situation closely resembles the approach taken to background subtraction in GC-MS.

Using the data in Figure 5.4, and assuming (for simplicity) that m/z 73 was representative of all background present, scan 2 would be a viable candidate as the spectrum for the background because the intensity for m/z 73 in this scan is approximately equal to the intensity found for this ion during the region of analyte desorption. However, the actual scan used was an averaged background spectrum formulated by averaging several spectra on both sides of the analyte desorption profile (m/z 265) to provide a more accurate representation of all background ions present. When this averaged background spectrum was subtracted from the thiamine-containing averaged spectrum of Figure 5.3, the result is the subtracted spectrum shown in Figure 5.5. The net result is a spectrum (Figure 5.5) virtually free from interfering background.

D. Structural Confirmation of Ala-Leu-Gly Obtained by TA-FAB

As in the case for the tripeptide alanyl-leucyl-glycine (Figure 2.1), matrix interference frequently imposes a greater restriction on structural information than molecular weight assignments in FAB mass spectra. This analyte was used to compare the structural information available by FAB and TA-FAB at the microgram level. A conventional (averaged) FAB spectrum of 1µg alanyl-leucyl-glycine dissolved in 0.5µl glycerol is shown in

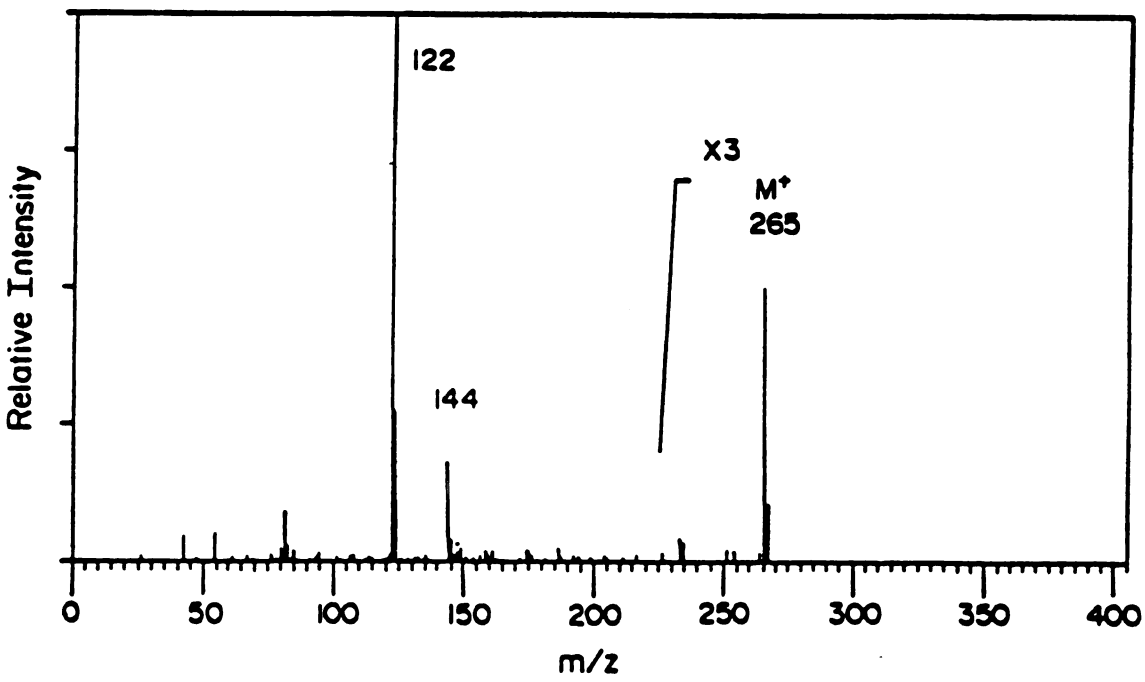

Figure 5.5 TA-FAB mass spectrum of 3 µg of thiamine hydrochloride in 0.5 µl of glucose following subtraction of an averaged background spectrum.

Figure 5.6. Molecular weight confirmation is possible from the intense peak for the protonated molecule at m/z 260, while the peaks at m/z 185 and 189 can be assigned to fragments of the tripeptide (as indicated in Figure 5.6). However, the undesired contribution from glycerol is apparent, especially at m/z 185 where the protonated glycerol dimer is isobaric with the proposed fragment $(M+H-Gly)^+$. Hence, the sequence of the tripeptide may not be obtained from this mass spectrum.

Barber et al. used linked-scanning to show that the $(M+H)^+$ ion of mass 260 does, in fact, give rise to a daughter of mass 185 for this molecule (7). However, an investigator without access to MS/MS or high-resolution MS would be forced to seek an alternate FAB matrix to alleviate the intense interference at m/z 185. While this may be a viable approach to the problem, it is a cosmetic solution which merely substitutes one form of background for another.

Figure 5.7a displays a spectrum, averaged over the region of the BMT, for 1 µg of alanyl-leucyl-glycine using fructose as the TA-FAB matrix. The instrumental conditions were the same as those used to obtain the conventional FAB spectrum of Figure 5.6. Complete sequence information is available from the assigned fragments, labeled on the mass spectrum, as very little competition from background is observed. Five major peaks in the mass spectrum (m/z 189, 185, 157, 86, 44) arise from fragmentation of the tripeptide. These peaks are consistent with the complete metastable analysis reported by Barber et al. for this compound

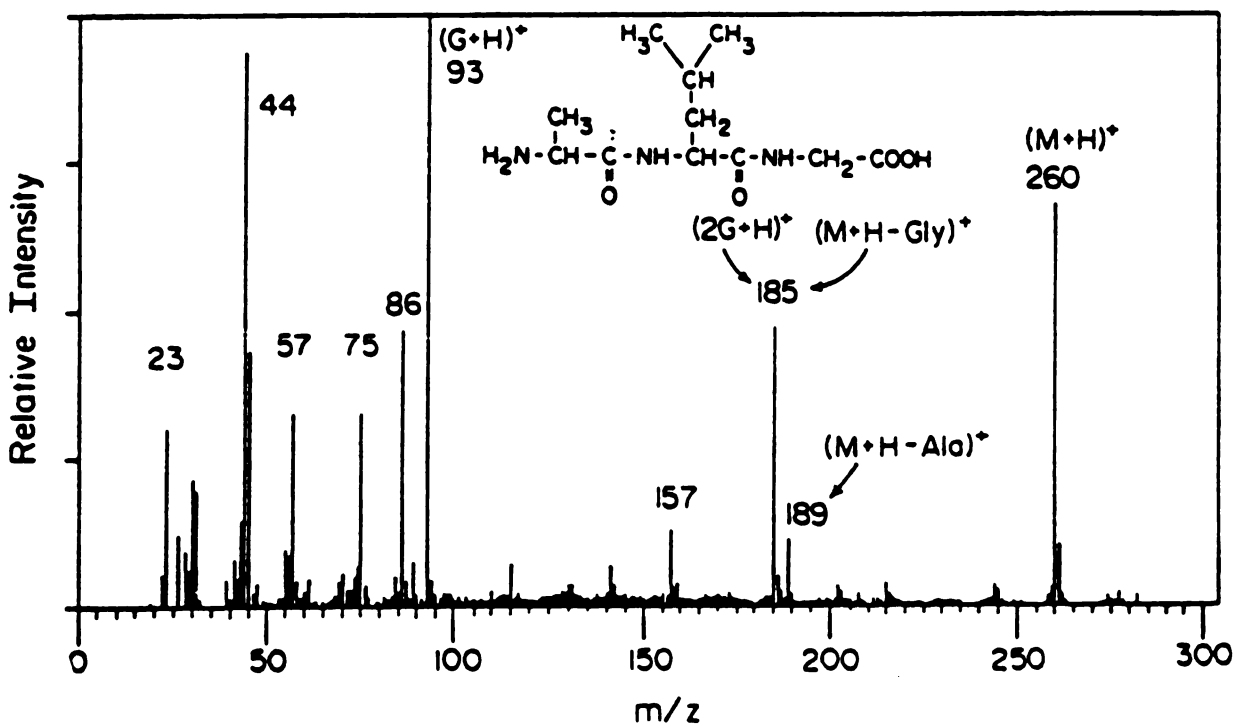

Figure 5.6 Conventional averaged FAB mass spectrum of 1 µg of alanyl-leucyl-glycine in 0.5 µl of glycerol.

with the observation that the peak at m/z 44 arise as a daughter of the fragment ion at m/z 157 (7).

Figure 5.7b represents the result obtained following the subtraction of an averaged background scan from the averaged spectrum of Figure 5.7a. Again, the result yields a clear picture showing the major fragments of the tripeptide as nearly all of the competition from background has been removed. Furthermore, not only does this result verify the loss of glycine at m/z 185, it also suggests that the competing loss of alanine occurs with about equal probability. This ratio seems rasonable since there is no compelling structural reason to favor one fragment over the other. However, since large deviations were sometimes apparent in the ratios of fragment ion intensities, it should not be concluded that the 185/189 ratio shown here is correct. Reexamination of the spectrm obtained using glycerol (Figure 5.6) shows a 185/189 ratio of about 5:1 which obviously does not reflect the fragmentation pattern of the analyte.

E. Desorption Profiles Indicate Origin of Ion Species

As previously demonstrated, differences in the desorption profiles of matrix and analyte ions made possible by TA-FAB can lead to a favorable situation for background subtraction. Another consequence of this behavior is that it is often possible to distinguish analyte peaks from background simply from their respective mass chromatograms. This is because analyte fragment ions have desorption profiles very similar to those of the

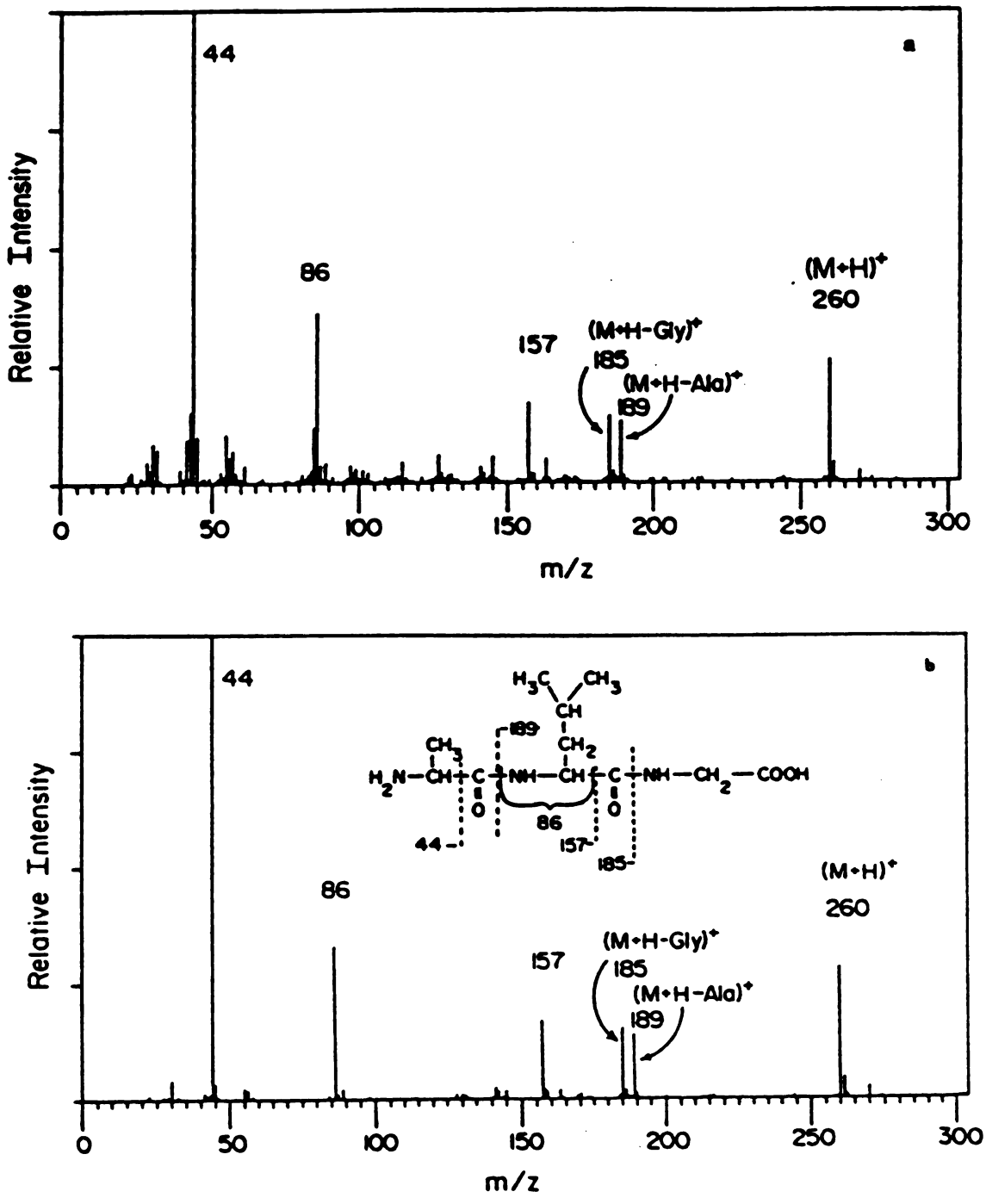

Figure 5.7 (a) TA-FAB mass spectrum of 1 µg of alanyl-leucyl-glycine in 0.5 µl of fructose averaged over the BMT. (b) TA-FAB mass spectrum of 1 µg of alanyl-leucyl-glycine in 0.5 µl of fructose following subtraction of an averaged background spectrum.

molecular ion and different from those of the background ions. This effect is illustrated in Figure 5.8 where the reconstructed mass chromatograms of the fragment ions at m/z 185 and 189 closely resemble that of the protonated molecule at m/z 260. Each analyte peak gave maximum intensity during scan 6 indicating the BMT occurred at a current of about 1.0A.

Also present is the profile of the fructose fragment $C_4H_5O_2^+$ (m/z 85) whose desorption is clearly different from those of the analyte peaks of the tripeptide. Unfortunately, the behavior of background ions in the region of the BMT is not always predictable, which can hinder the search for a background spectrum representative of the background at the BMT. Hence, it is possible to have good selection against background but not have the proper conditions for a quantitative subtraction whenever anomalous behavior is observed for the background ions in the region of the BMT. The cause of this behavior requires further investigation.

F. Optimization in TA-FAB by Proper Selection of Analyte/Matrix Combinations

The use of saturated solutions as matrices for FAB offers new possibilities for optimization of analysis by FAB. Simply because the number of potential candidates for TA-FAB matrices is large, it should be possible to find matrices having chemical and physical properties well suited to the particular analytes under study. Experimental confirmaton of analyte/matrix interaction may be evidenced by two distinct types of observations. The first is the

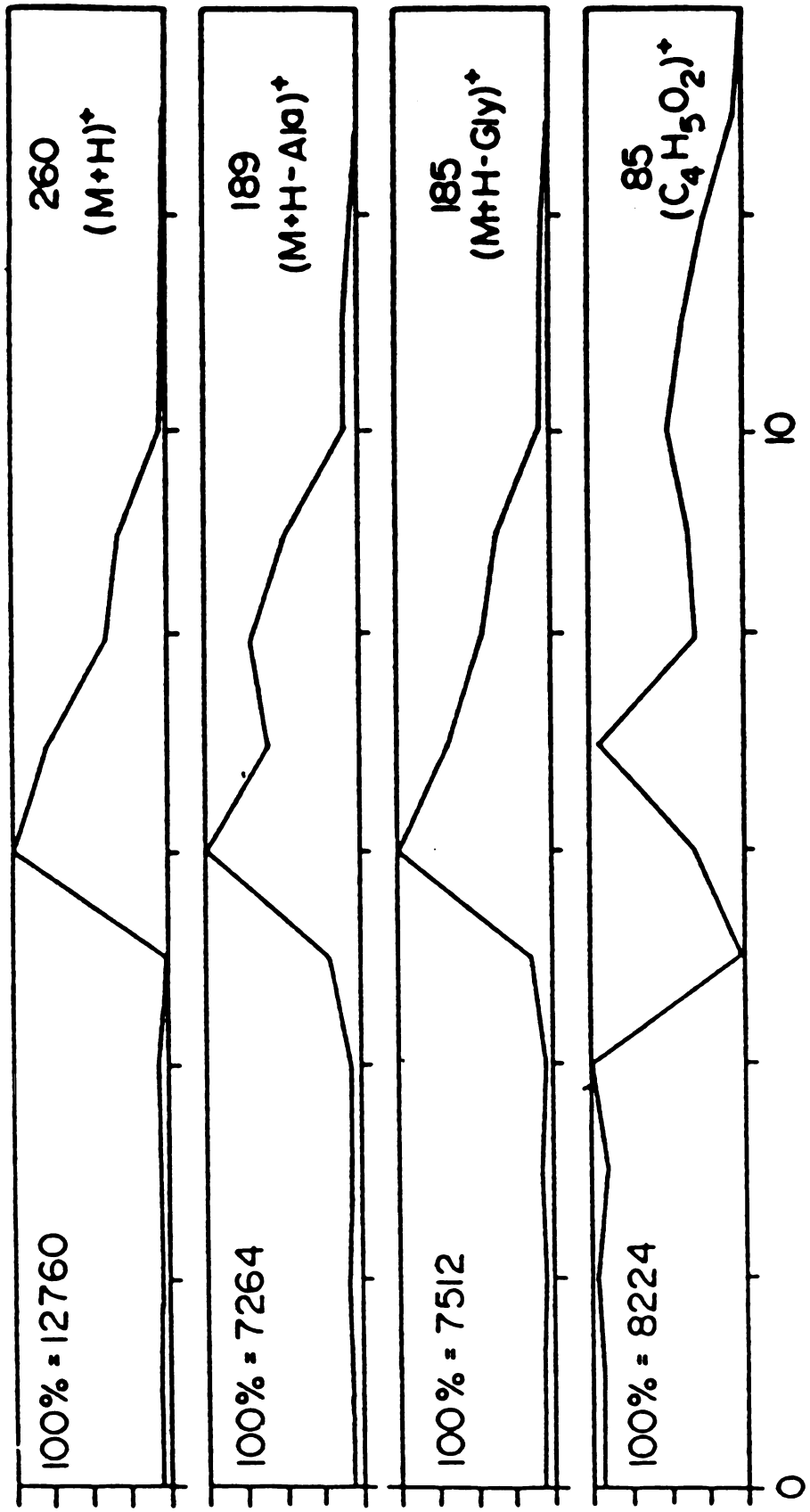

Figure 5.8 Reconstructed mass chromatograms for analyte (m/z 260, 189, 185) and background (m/z 85) for the TA-FAB analysis of 1 µg of alanyl-leucyl-glycine in 0.5 µl of fructose.

enhancement of analyte peaks over background. This effect may be empirically evaluated by S/B ratios. The second type of observation indicative of analyte/substrate interaction would manifest itself by changes in the analyte fragmentation pattern from one substrate to another.

Arginine was chosen to illustrate how important matrix selection is to the results obtained by TA-FAB. One microgram of arginine was analyzed by TA-FAB alternatively in tartaric acid and glucose keeping the conditions of analysis constant. One-half microliter of a saturated solution of each respective matrix was applied to the emitter in each case. The BMT observed for arginine in glucose was 1.02A, whereas the BMT in tartaric acid was somewhat higher (1.22A). Unlike most amino acids which form zwitterions, arginine contains an additional site of positive charge at the guanidinium group. Hence, it exists as an ion of charge +1 between pH 2.17 and pH 9.04. This ion has an m/z value of 175 and appears in the TA-FAB mass spectra of arginine using either glucose or tartaric acid.

A comparison of the data is presented in Figure 5.9. Figure 5.9a is the mass spectrum obtained at the BMT for 1μg of arginine in glucose, while Figure 5.9b is the corresponding spectrum using tartaric acid. Arginine may be distinguished from background in each case; however, the absolute intensity of the protonated molecule at m/z 175 was 3.86 times greater when analyzed in tartaric acid than when analyzed in glucose. The difference in sensitivity reflects the greater ability of tartaric acid to act as

a proton donor creating a larger concentration of $(M+H)^+$ ions for arginine.

Unfortunately, the comparison of absolute intensities does not give a true indication of sensitivity, since this measure does not include a factor to estimate the extent of background interference for each matrix. Therefore, signal to background calculations were performed on the data in Figure 5.9. As indicated in the unsubtracted mass spectra (Figures 5.9a, 5.9b), a 3-fold enhancement in signal to background was achieved for tartaric acid relative to glucose, in the observation of the $(M+H)^+$ ion for arginine at the 1μg level.

Figure 5.9c and Figure 5.9d display the results achieved after the background subtraction of glucose and tartaric, respectively, from the mass spectra in Figure 5.9a and Figure 5.9b; averaged background spectra were used in each case. Both subtractions yield more favorable data as the $(M+H)^+$ ion at m/z 175 becomes the base peak in each of the mass spectra shown. Yet, the presence of several background peaks of lesser intensity indicates that background subtraction was not 100% effective in either case. A visual inspection of Figure 5.9c,d reveals that less overall competition from background occurred for the tartaric acid exmaple. Again, this conclusion was verified from S/B calculations which show that there was more than a 3-fold advantage in the observed S/B ratio when using tartaric acid instead of glucose.

A dependency of fragment ion relative intensities or fragment ion type on the matrix employed would also indicate the presence of specific anayte/matrix interactions. Even though subtle

Figure 5.9 (a) TA-FAB mass spectrum recorded at the BMT for 1 μg of arginine in 0.5 μl of glucose. (b) TA-FAB mass spectrum recorded at the BMT for 1 μg of arginine in 0.5 μl of tartaric acid. (c) TA-FAB mass spectrum of 1 μg of arginine in 0.5 μl of glucose following subtraction of an averaged background spectrum. (d) TA-FAB mass spectrum of 1 μg of arginine in 0.5 μl of tartaric acid following subtraction of an averaged background spectrum.

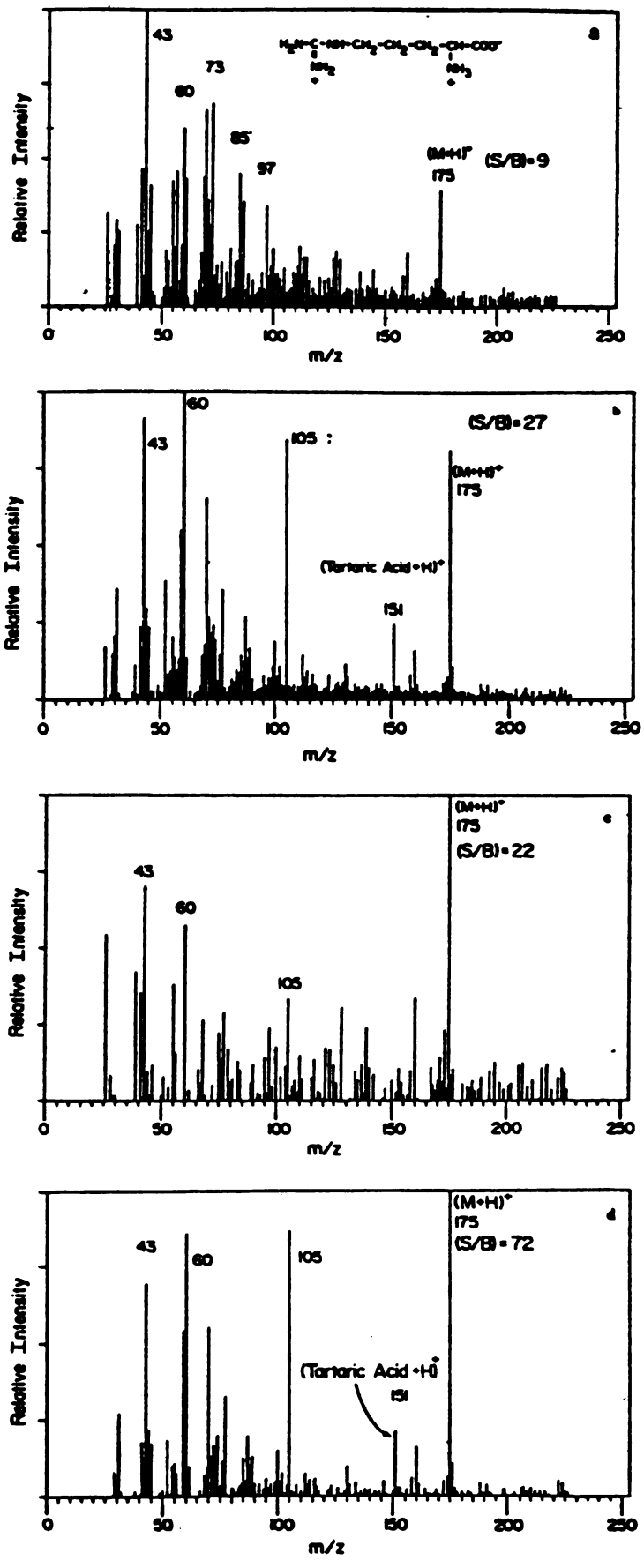
a
43
73
60
85
97
(M+H)+
175
(S/B)=9
Relative Intensity
m/z
b
60
43
105
(S/B)=27
(M+H)+
175
(Tartaric Acid+H)+
151
Relative Intensity
m/z
c
(M+H)+
175
(S/B)=22
43
60
105
Relative Intensity
m/z
d
(M+H)+
175
(S/B)=72
43
60
105
(Tartaric Acid+H)+
151
Relative Intensity
m/z

differences are apparent in the arginine spectra presented, there is presently not enough evidence to suggest that analyte/matrix interaction is responsible. To make such a determination, one would need to know the origin of each major fragment as well as the inter-run variance in fragment ion intensities.

At present, controlled experiments have been performed to assess the inter-run variation associated with the analysis of 1μg of alanyl-leucyl-glycine by TA-FAB using two matraices: fructose and tartaric acid. For each analysis, the intensities integrated over the BMT for the six most intense analyte ions were summed and ratioed to the total ion current integrated over the same interval. The calculated ratio appeared to be independent of the matrix used (e.g., fructose (22.0%), tartaric acid (21.2%)). In addition, the level of imprecision found in each case was encouraging considering the number of possible sources of error: fructose (average relative deviation 10%, n = 5) and tartaric acid (average relative deviation 8%, n = 7). It should be mentioned that it was necessary to consider the contribution from several major analyte ions in order to achieve the precision indicated above. Also, it was imperative that replicate anlyses be performed consecutively and under identical experimental conditions.

G. Present Applications of TA-FAB to the Analysis of Nonvolatile Biomolecules

To date, TA-FAB has been applied to a wide variety of nonvolatile molecules of biological interest yielding encouraging

results. Two examples are shown here to give an indication of the results obtained. Unfortunately, the limited mass range of the CH5 has restricted present applications in the mass range below m/z 1000. As the first example, 1μg of the antibiotic amipicillin was analyzed in fructose by TA-FAB. A background subtracted spectrum appears in Figure 5.10. In addition to the protonated molecule at m/z 350, five distinct fragment ions are present; each exhibited a desorption profile similar to that for m/z 350. The origin of the fragments at m/z 106, 160, and 192 is shown in Figure 5.10 and may be readily assigned to stable even-electron species. On the other hand, several possibilities could be proposed to account for the peaks at m/z 118 and 174. The latter might be the loss of water from the ion of mass 192.

As a final example, Figure 5.11 displays an unsubtracted averaged scan obtained over the region of the BMT for the TA-FAB anlaysis of 5μg of taurodeoxycholic acid in fructose. The base peak at m/z 544 corresponds to the addition of sodium to the intact sodium salt of this molecule. The most intense contribution from fructose is the $(M+Na)^+$ ion at m/z 203. The large degree of fragmentation seen below mass 200 originates not only from fructose but from successive decomposition of the steroid ring structure. The peaks at m/z 224 and 252 can be explained by fragmentation between the C and D rings of taurodeoxycholic acid.

A current list of applications for TA-FAB is contained in Table 5.1. Listed are both the matrices used and the compound classes studied; no correlation is intended between the two. The first three matrices, fructose, glucose, and sucrose are all

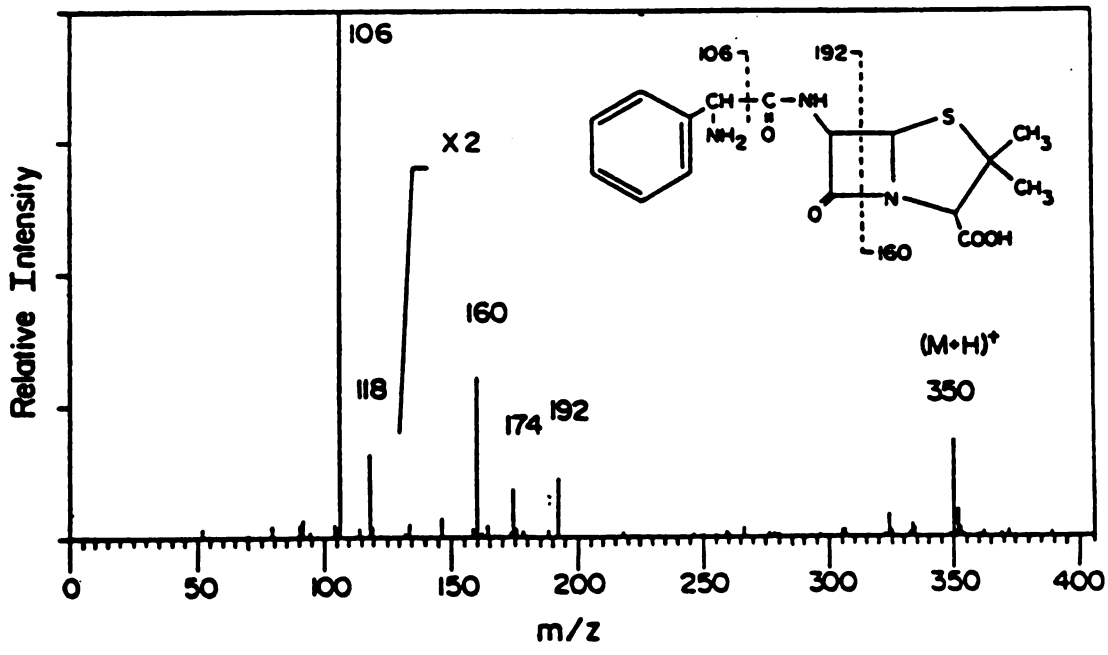

Figure 5.10 TA-FAB mass spectrum (averaged) of 1 µg of ampicillin in 0.5 µl of fructose following subtraction of an averaged background spectrum.

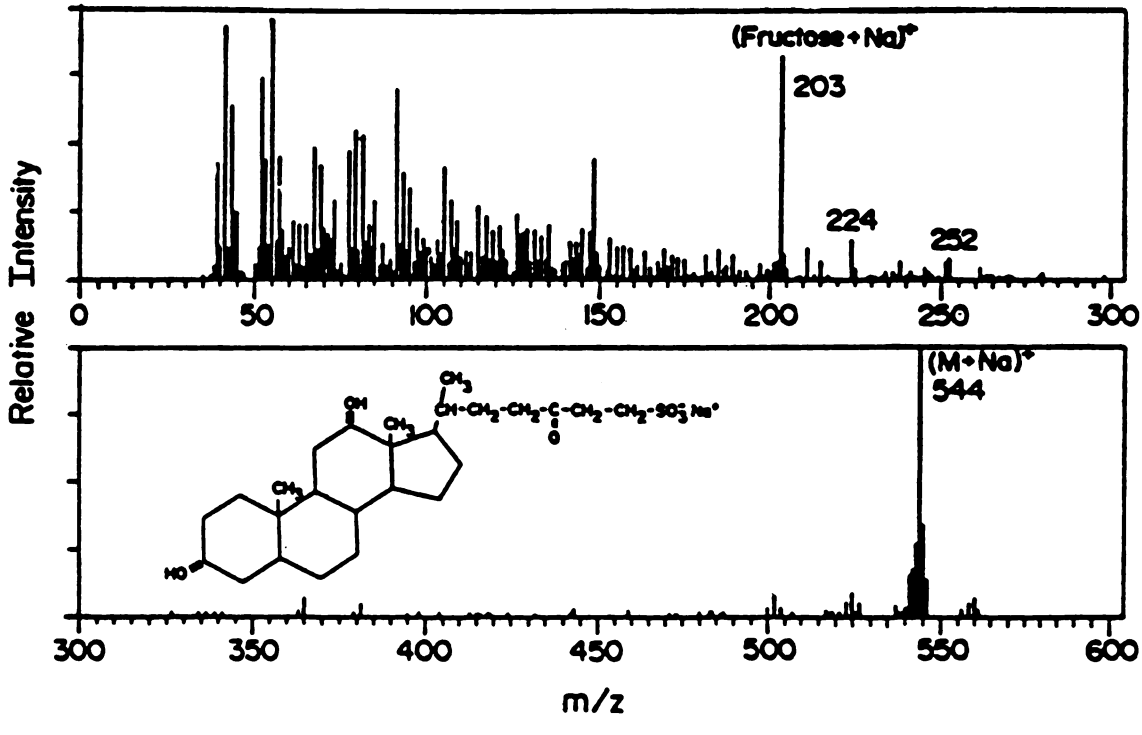

Figure 5.11 Unsubtracted TA-FAB mass spectrum of 5 µg of taurodeoxycholic acid (Na^+ salt) in 0.5 µl of fructose averaged over the region of analyte desorption.

chemically similar and give similar results as matrices. However, since they are all structurally similar to glycerol, their range of application appears to be almost congruent to glycerol for the compounds studied thus far. The major difference is that saccharide solutions are prepared with either water or methanol/water which are more polar than glycerol. This can lead to slightly greater problems of imiscibility with nonpolar analytes. As demonstrated, tartaric acid may be used to increase the yield of $(M+H)^+$ ions, which is important because only limited amounts of acid can be added to saccharides before degredation occurs. Finally, thioglucose has been used successfully as a TA-FAB matrix. The similarity here is to thioglycerol, which is the second most widely used matrix in FAB.

The list of compound classes studied by TA-FAB spans a wide range of analytes of biochemical interest. Results obtained for selected ceramides and glycosphingolipids were particularly satisfying since these compounds were water insoluble. These compounds, which were dissolved in 1:1 methanol/chloroform, formed natriated adducts with sodium ions in solution. Direct comparisons were made between TA-FAB and FAB at the 1-5μg level for several compounds listed in Table 5.1. These comparisons to FAB in glycerol were generally quite favorable suggesting that at least comparable sensitivity may be attained for most compounds by TA-FAB. Furthermore, the large S/B values observed for many of the analytes tested indicates that detection in the submicrogram range should be possible for several classes of compounds by TA-FAB.

TABLE 5.1

CURRENT LIST OF TA-FAB
MATRICES AND APPLICATIONS

MATRICES	ANALYTES
FRUCTOSE	ANTIBIOTICS
GLUCOSE	BILE SALTS
SUCROSE	CERAMIDES
TARTARIC ACID	GLYCOSPHINGOLIPIDS
THIOGLUCOSE	PEPTIDES
	PORPHYRINS
	SACCHARIDES
	VITAMINS

IV. Comparison of TA-FAB to Conventional FAB and EI Mass Spectrometry for the Analysis of the Helminthosporium Carbonum Mycotoxins

The second part of this chapter is devoted to a particular application of TA-FAB to the structural analysis of a series of biologically relevant mycotoxins isolated from the fungus Helminthosporium carbonum. The reasons for this study were 2-fold. First, to apply TA-FAB to a realistic application involving samples isolated from a biological matrix; until now all examples, except for a few glycosphingolipids, were purchased as synthetic reagents. Secondly, TA-FAB was investigated as a possible alternative to the other mass spectrometric techniques, used previously with varying degrees of success, to aid the structural analysis of the HC-toxins.

A. Historical Background

The fungus Helminthosporium carbonum has long attracted the attention of plant biologists due to its known pathogenicity toward certain varieties of corn. However, only recently have the structures of both the primary toxin (HC-I) and two minor toxins (HC-II and HC-III) undergone complete structural elucidation (8-13). While each is a tetrapeptide, the cyclic nature of these toxins prohibits sequencing by Edman degradatioan due to the lack of an N-terminus. As early as 1967, Pringle and Scheffer postulated that the host-specific toxin (HC-I) was a cyclic peptide containing

proline, alanine, and an unknown amino acid (8). These results have since been confirmed by a series of investigations leading to the exact structural identity of HC-I (9,10,11). Subsequent work has resulted in the isolation and structural characterization of the minor toxins HC-II (12) and HC-III (13). The currently accepted structure for each HC-toxin appears in Table 5.2. The structures indicate that the toxins differ merely by the exchange of one amino acid. Moreover, each contains the unusual amino acid 2-amino-8-oxo-9,10-epoxydecanoic acid (AOE), which is primarily responsible for the observed toxicity (14).

Mass spectrometry has played a vital role in the structural analysis of the HC-toxins by granting both molecular weight and structural information. Both electron impact (EI) and chemical ionization (CI) have been used to obtain exact mass measurements for HC-I (9,10,11). However, CI, being a softer method of ionization, is of lesser overall utility for structure elucidation because of the lack of analyte fragmentation achieved by this technique. In contrast, EI creates abundant fragmentation for the HC-toxins, but because the fragmentation pathways frequently involve rearrangemets (14), interpretation can result in equivocal sequence information. In fact, this problem led to a revision in the original sequence for HC-I proposed by Liesch et al. (9); the currently accepted structure (Table 5.2) was established independently by Gross et al. (10) and Walton and coworkers (11).

In more recent investigations, fast atom bombardment (FAB) has been used as the method of ionization. FAB provides both intense and long-lived signals from protonated molecules, an advantage

TABLE 5.2. STRUCTURES OF THE HC-TOXINS

Toxin	Mol. Wt.	Sequence	Structure	Reference
HC-I	436	PRO-ALA-ALA-AOE	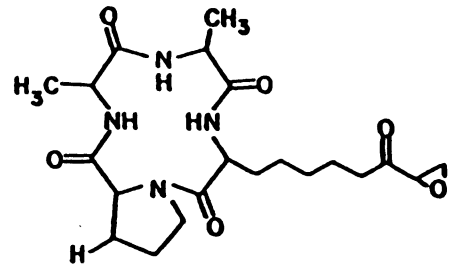	10,11
HC-II	422	PRO-ALA-GLY-AOE	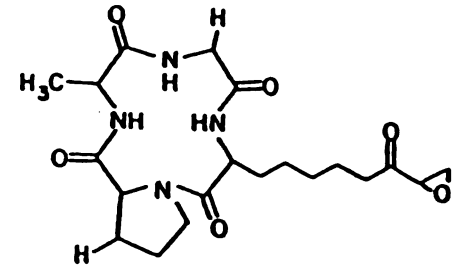	12
HC-III	452	HYP-ALA-ALA-AOE	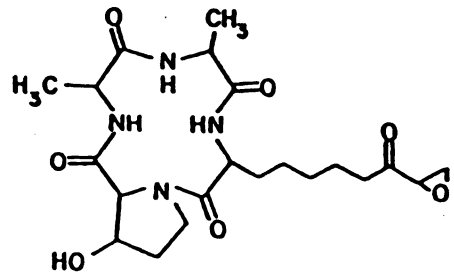	13

which has permitted facile exact mass determinations to be made on toxins HC-I, II, and III by high resolution peak matching (11,12,13). In addition, FAB sometimes produces structurally-informative ions relating both to the amino acid composition and the peptide sequence. Unfortunately, the large quantities of matrix-related ions produced during FAB can interfere with recognition of minor, but important, peaks in the mass spectra of the HC-toxins to restrict structural interpretation (especially when the toxins are analyzed at realistic levels).

As discussed in Chapter 2, MS/MS provides a viable solution to the problem of matrix interference in FAB mass spectra (15). FAB-MS/MS assisted in the structural elucidation of toxins HC-I and HC-II (10,12). The amino acid sequence of each cyclic tetrapeptide was deduced by the presence of daughter ions that would be predicted to arise from the structures shown in Table 5.2 as well as the absence of peaks relating to the other sequence possibilities. Unfortunately, the sensitivity of MS/MS is often limited by the efficiency of the CAD process. Furthermore, MS/MS is an expensive solution not available to many investigators who perform FAB.

This section reports on the success obtained for the TA-FAB analysis of HC-toxins I, II, and III in saturated fructose following isolation by HPLC. The investigation which follows compares EI, FAB, and TA-FAB for the analysis of the HC-toxins. The results demonstrate the superior capacity of TA-FAB to reduce the matrix interference observed using conventional FAB. In

addition, the available structural data for the HC-toxins was more readily discerned by TA-FAB than the other methods investigated.

B. Results

Comparison of TA-FAB and FAB for the Analysis of HC-II and HC-III

Initial work with the HC-toxins in this laboratory involved the use of conventional FAB to aid in the structural elucidation of HC-toxins II and III. Relatively large amounts of analyte (10μg) were required to obtain discernible peaks for fragment ions arising from the toxins. Analyses by FAB from the larger (e.g., stainless steel) probe tip typically yielded larger total ion currents but with no improvement in signal to background ratio. Hence, under these circumstances a comparable sensitivity for conventional FAB and TA-FAB was concluded.

Figure 5.12a displays the conventional FAB mass spectrum of 1.5μg HC-II (MW 422) dissolved in 0.5μg glycerol. This spectrum represents an average of 15 scans obtained using the smaller (tungsten) probe tip. At this concentration, only one peak (e.g., $(M+H)^+$, m/z 423) may be readily assigned to the analyte. The major background peaks designated by the letter "B" arise primarily from protonated polymeric clusters of glycerol (MW 92).

Figure 5.12b displays the corresponding TA-FAB mass spectrum obtained from analysis of 1.5μg HC-II in 0.5μl saturated aqueous solution of fructose. Here, an averaged spectrum was obtained over

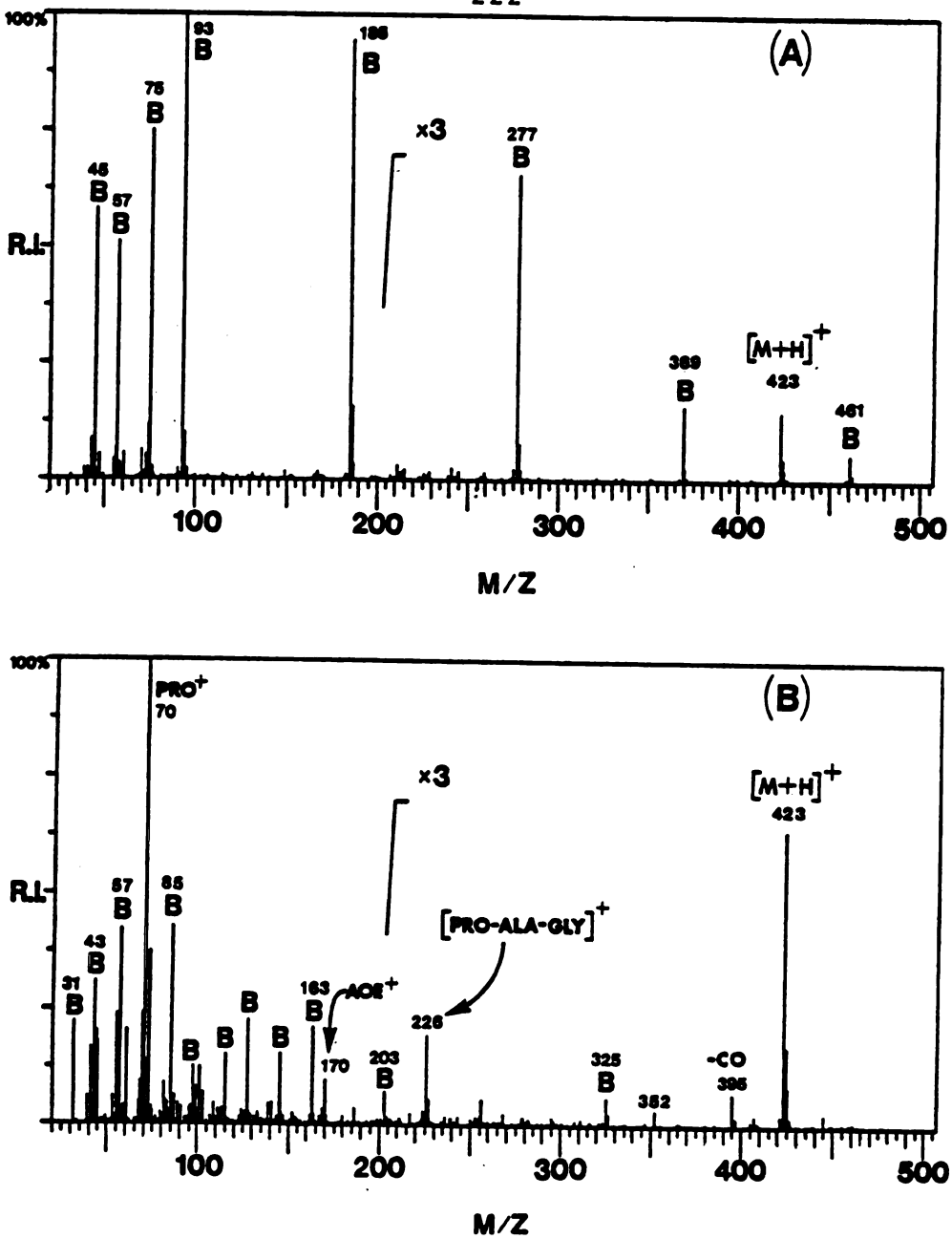

Figure 5.12 Comparison of FAB and TA-FAB for the analysis of 1.5 µg HC-II. (a) Averaged FAB mass spectrum of 1.5 µg HC-II in 0.5 µl glycerol; (b) averaged TA-FAB mass spectrum of 1.5 µg HC-II in 0.5 µl fructose.

the region in the TA-FAB profile where optimum analyte desorption occurred. In this case, several fragment peaks were visible as assigned in Figure 5.12b. Of particular interest are the peaks at m/z 70 and 170 which represent the amino acids proline and AOE, respectively, and the peak at m/z 226 which corresponds to the important sequence ion H-Pro-Ala-Gly$^+$ as assigned by Knoche et al. (12). Also apparent in the TA-FAB spectrum of figure 5.13b is a series of background peaks (B) which arise primarily from the fragmentation of fructose (m/z 73, 85, 97, 115, 127, 145, and 163). A majority of the background peaks are below m/z 200, except for the sodium adduct to fructose at m/z 203 and a product of dimerization at m/z 325 (2fructose + H - $2H_2O$)$^+$.

A similar comparison made with spectra obtained from 1.5µg HC-III (MW 452) is shown in Figure 5.13. The upper spectrum (Figure 5.13a) displays the result from the analysis by conventional FAB in 0.5µl glycerol on the stainless steel tip. Again, the letter B is used to denote the major matrix-related peaks. While good molecular weight confirmation is apparent at m/z 453, virtually no peaks representing analyte fragmentation are visible above the intense glycerol background at this concentration. A striking contrast was found after performing an analysis using the same analyte concentration, but in 0.5µl of the aqueous fructose solution by TA-FAB. The result appears in Figure 5.13b. Using TA-FAB, peaks relating to fragmentation of the toxin are now easily recognized. For example, the peaks at m/z 44, 86, and 170 give clear evidence for the amino acids present in HC-III: alanine,

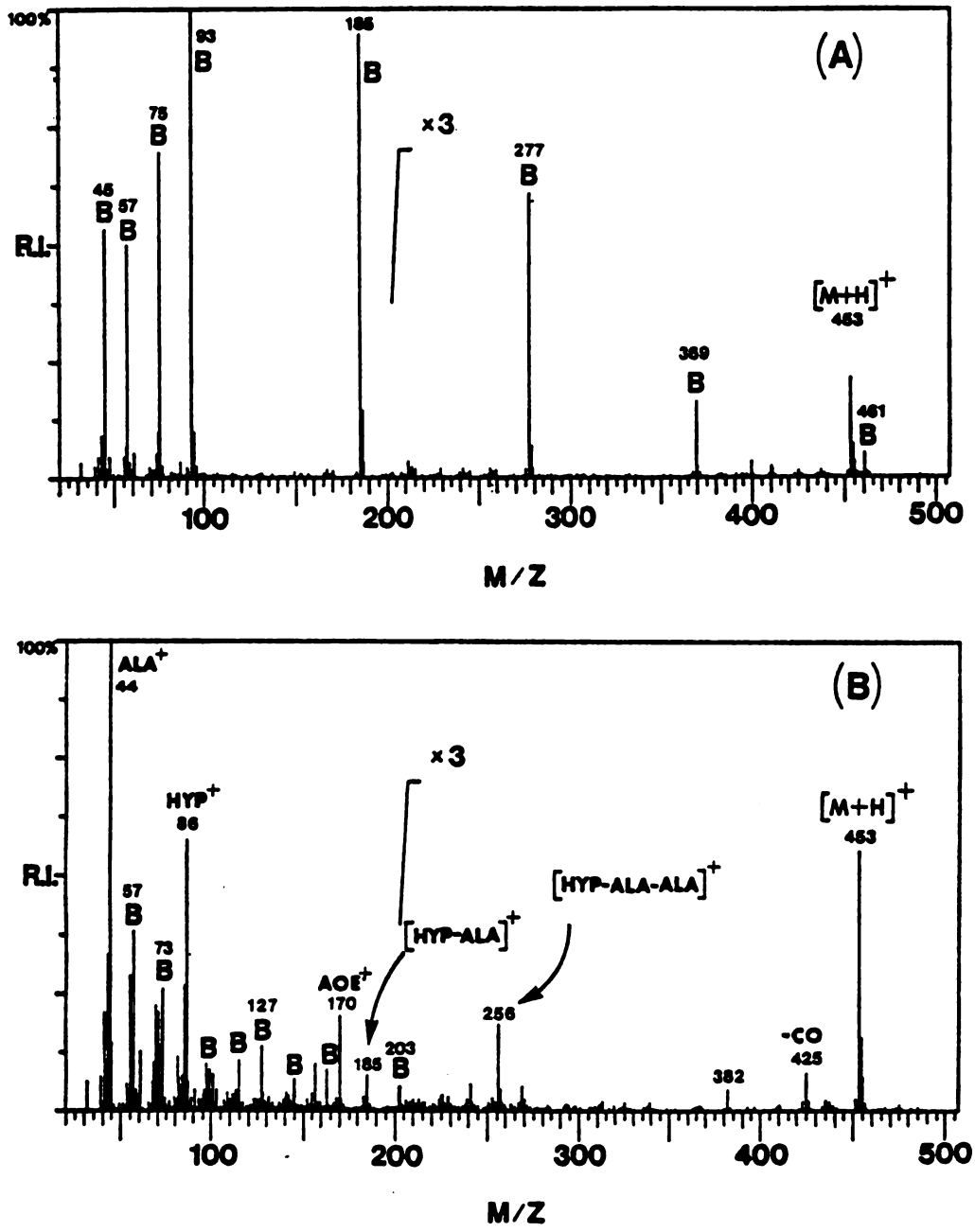

Figure 5.13 Comparison of FAB and TA-FAB for the analysis of 1.5 µg HC-III. (a) Averaged FAB mass spectrum of 1.5 µg HC-III in 0.5 µl glycerol; (b) averaged TA-FAB mass spectrum of 1.5 µg HC-III in 0.5 µl fructose.

hydroxyproline, and AOE, respectively. In addition, sequence information may be obtained from the peaks at m/z 185 and 256.

Desorption Profiles for the Analysis of 1.5μg HC-II by TA-FAB

The temporal behavior of the desorption process for the analyte and matrix during TA-FAB is illustrated in Figure 5.14 which consists of a set of profiles reconstructed from a series of consecutively-recorded mass spectra obtained while analyzing 1.5μg HC-II in 0.5μl saturated fructose. The upper two profiles represent production of analyte ions, the first being the protonated molecule of mass 423 and the second being a fragment resulting from the loss of the AOE residue to give a peak at m/z 226. For comparison, the bottom profile depicts background and displays the behavior of the prominent fructose fragment $(C_4H_5O_2)^+$ at m/z 85, a good representative of the other fructose ions present. For this particular experiment, the initial scan began with an emitter current of 0.80A and was increased linearly at a rate of about 100mA/min to a maximum value of 1.40A at scan 34.

Inspection of Figure 5.14 indicates that the analyte and matrix have distinctly different desorption profiles as a function of temperature. Furthermore, the ion at mass 226 may clearly be recognized as originating from the analyte because its profile resembles the profile for the $(M+H)^+$ ion at m/z 423 and is dissimilar from the matrix profile (m/z 85). During the initial stages of the analysis (scans 1-10) the majority of desorption-ionization comes from the matrix. However, as the

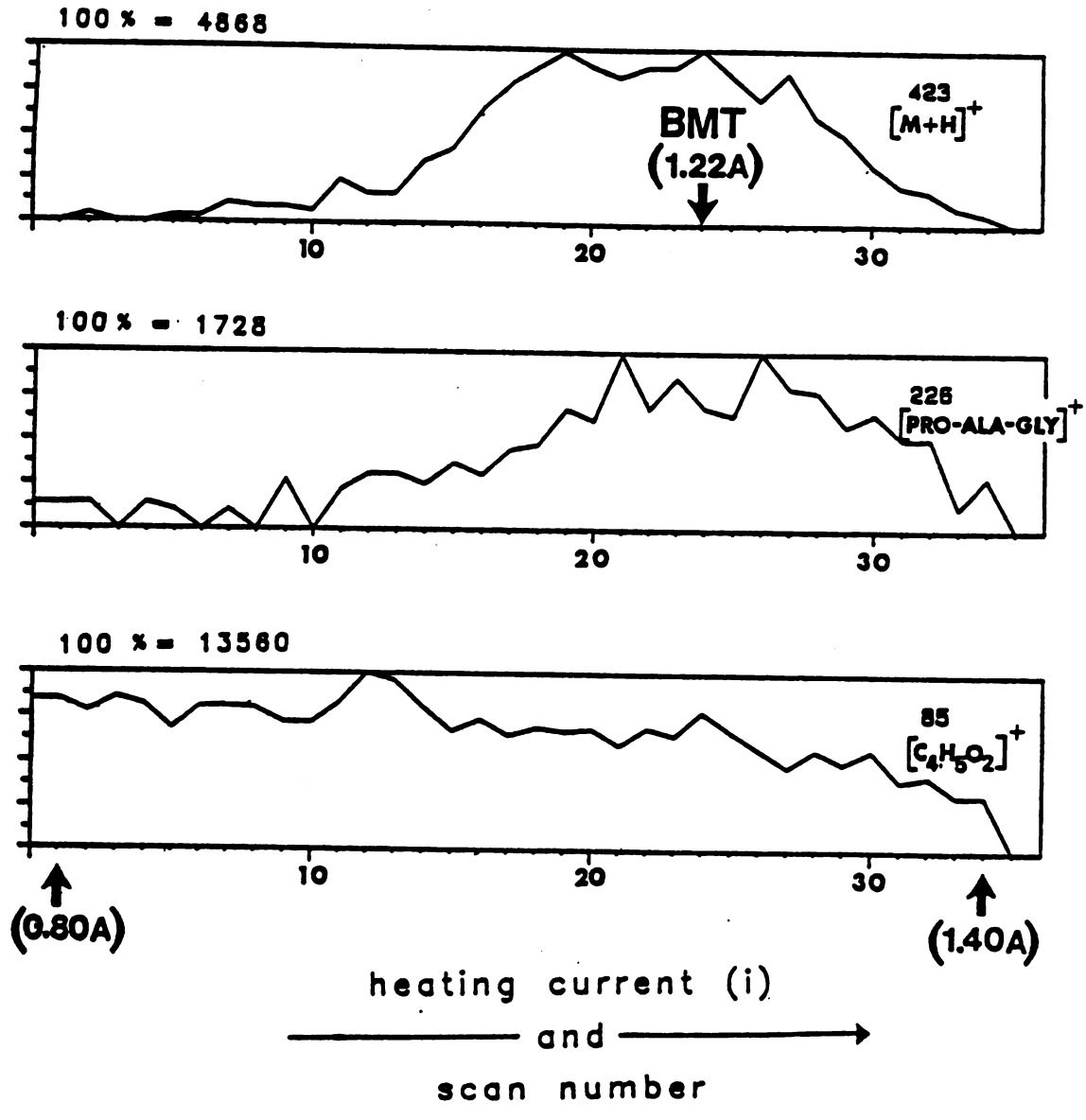

Figure 5.14 Desorption profiles for the TA-FAB analysis of 1.5 µg HC-II in 0.5 µl fructose.

temperature of the matrix increases, there is a corresponding increase in analyte desorption-ionization relative to background. Since the matrix does not respond to this rise in temperature, a selection against background occurs. Eventually at scan 24 (1.22A) the best matrix temperature (BMT) is reached as indicated by the maximum in the profile for the $(M+H)^+$ ion of HC-II. The gradual decline in intensity for all ions past this point is most likely due to a loss in mobility in the sample as it dries out.

Based on the data in Figure 5.14, the conditions for a valid background subtraction are reasonably well satisfied in the TA-FAB analysis of HC-II. For instance, prior to scan 10 there is a region depicting background only since most of the observed ionization comes from background (m/z 85) and very little from analyte (m/z 423, 226) early in the analysis. Secondly, the general appearance of the fructose background did not change to any significant degree as a function of applied temperature during the experiment. To obtain a computer-aided subtraction of background for HC-II a statistically representative background spectrum was prepared from an average of the first 10 scans. Next, this averaged spectrum was subtracted from an averaged spectrum obtained over the BMT (Figure 5.12b). The net result is the background-subtracted spectrum for 1.5μg HC-II shown in Figure 5.15. Nearly all background in this spectrum was removed to yield a clear view of the fragmentation pattern for the toxin. Two exceptions where subtraction was incomplete (m/z 163, 325) are labeled with the letter B. The data of Figure 5.15 were useful to the structural elucidation of HC-II by providing confirmation for the

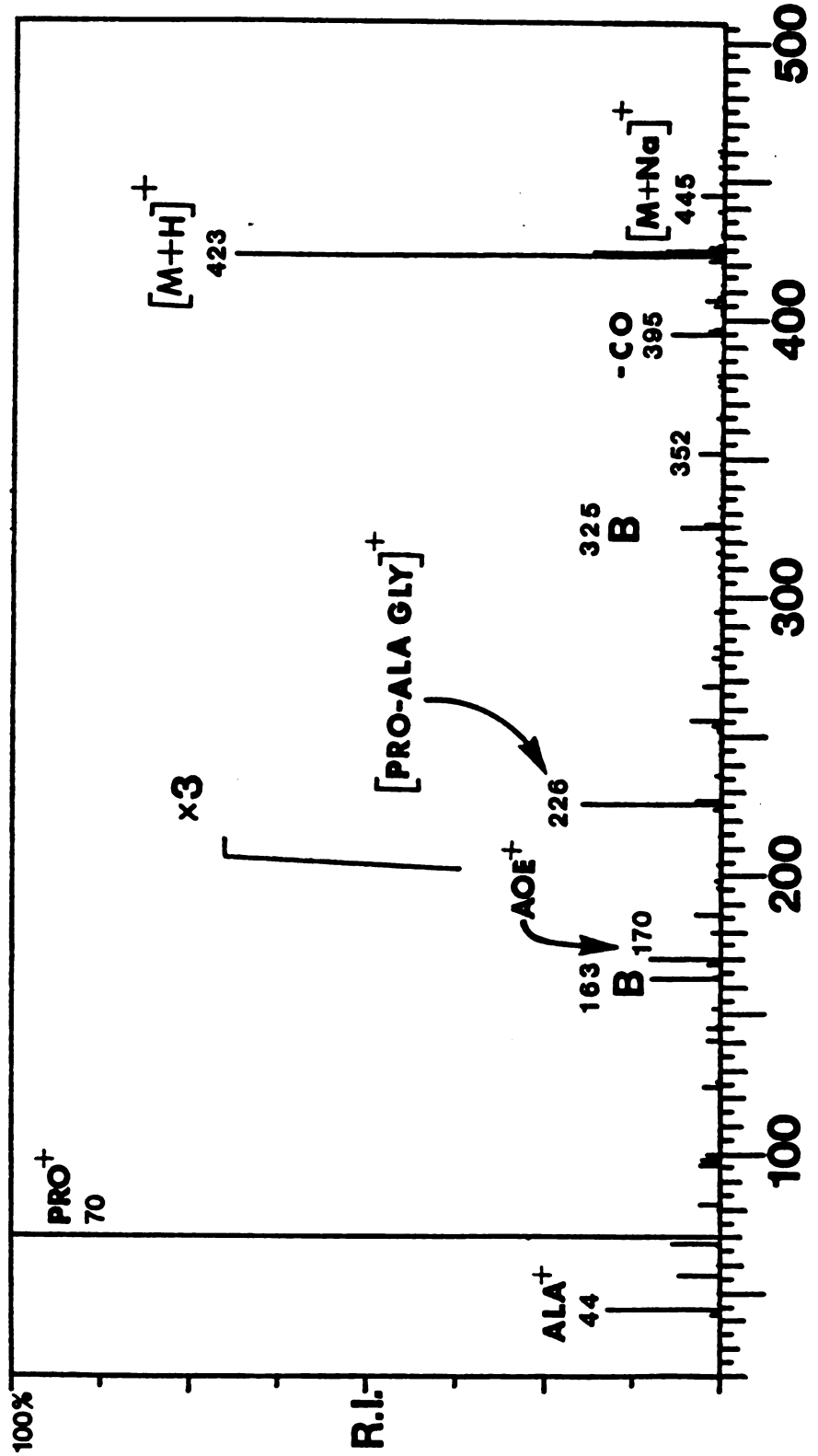

Figure 5.15 TA-FAB mass spectrum of 1.5 µg HC-II following background subtraction.

molecular weight, the amino acid composition, and the amino acid sequence. It should be mentioned, however, that complete structural elucidation of the HC-toxins can not be made exclusively by mass spectrometry.

High Resolution Data for the HC-toxins by Peak Matching

Prior to any structural analysis, the elemental constitution of the analyte is a very critical piece of information. Therefore, during the initial stages of this work exact mass measurements were performed on the HC-toxins using the method of peak matching. Conventional FAB in glycerol was employed for this purpose due to the paucity of suitable reference ions occurring from fructose under the conditions of TA-FAB. Initially, the protonated glycerol pentimer at m/z 461 was chosen as the reference ion. However, to obtain an acceptable resolving power (e.g., greater than 3000, 5% valley definition) with the aging CH5 mass spectrometer, excessive amounts of analyte were needed (greater than 10μg) which greatly reduced the relative signal from the glycerol reference peak. An alternative approach was then selected which used the protonated molecule of HC-I ($C_{21}H_{33}O_6N_4$, 437.2400) as the internal exact mass standard since the exact mass of this ion had been determined previously (10). Using this method, at a resolution of 3700, the exact masses of HC-II and III were determined to be 423.2216 (calculated, 423.2244) and 453.2360 (calculated, 453.2349), respectively. These data, which appear in Table 5.3a, support the proposed elemental compositions for toxins HC-II and HC-III.

TABLE 5.3A PEAK MATCHING DATA FOR HC-TOXINS

Toxin	Elemental Composition $(M+H)^+$	Molecular Wt. $(M+H)^+$	Rel. Error ppm	Resolution (5% Valley)
HC-I	$C_{21}H_{33}O_6N_4$	437.2400	*	*
HC-II	$C_{20}H_{31}O_6N_4$	432.2244	-6.4	3700
HC-III	$C_{21}H_{31}O_6N_4$	453.2349	+2.4	3700

* HC-I used as an internal exact mass standard for peak matching

TABLE 5.3B. PEAK MATCHING OF AMINO ACID FRAGMENT IONS

Toxin	Fragment	Theoretical Exact Mass	Rel. Error (ppm)	Resolution (5% Valley)
HC-I	$C_9H_{16}NO^+$(AOE)	170.1181	-6.0	3330
HC-II	$C_4H_8N^+$(PRO)	70.0659	+2.7	4000
HC-III	$C_4H_8NO^+$(HYP)	86.0602	-4.6	4000

Additional peak matching was performed on selected fragment ions of the toxins corresponding to specific amino acids. For instance, the protonated iminium ion from the AOE residue of HC-I (m/z 170) was peak matched to the protonated glycerol dimer at m/z 185. Similarly, evidence for the proline residue in HC-II (m/z 70) and the hydroxyproline moiety in HC-III (m/z 86) was obtained by peak matching to the prominent glycerol peaks at m/z 75 and 93, respectively. These results are summarized in Table 5.3b.

EI-Mass Spectrometry of the HC-toxins

For the sake of comparison to data obtained by TA-FAB, electron impact spectra were obtained for each of the three HC-toxins. Again, the samples were analyzed at the 1.5μg level with the exception of HC-II for which a larger amount (3.9μg) was used due to a poor response at the lower level. Despite their relatively nonvolatile nature, molecular ions were observed for each of the HC-toxins. However, because of extensive fragmentation, their intensities were much smaller than the corresponding values for the $(M+H)^+$ ion observed during TA-FAB. For example, the average percentage of TIC resulting from the molecular ions for the three HC-toxins under electron impact was only 0.44 ± 0.2%. In contrast, the average percentage of the TIC created by the analogous protonated molecules during TA-FAB was 2.1 ± 0.3%. This difference is quite significant considering that there is a contribution to the TIC from the fructose background ions in the case of TA-FAB. Following background subtraction, the

protonated molecules formed during TA-FAB constitute an average of 6.7 ± 2% of the total ion current.

Electron impact data were first presented by Liesch et al. who gave assignments to the 18 most significant ions for HC-I using data obtained under high resolution (9). The fragmentation pattern was then analyzed and the sequence AOE-ALA-ALA-PRO proposed. As mentioned previously, this sequence was subsequently revised from data obtained in two independent investigations to yield the currently accepted sequence PRO-ALA-ALA-AOE (10,11). Rearrangments occurring during fragmentation under EI resulted in the postulation of the incorrect sequence.

The results for the EI mass spectra of the HC-toxins are listed in Table 5.4. Proposed assignments for the major ions are given, in terms of their elemental formulas, as predicted from direct fragmentation of the structures shown in Table 5.2. These assignments should be viewed only as tentative; they are not intended to serve as sole evidence for the structures given above. Clearly, the qualitatiave information gained by EI are not of the caliber obtained by TA-FAB. Although TA-FAB generates fewer fragment ions than EI, the fragments produced are more structurally significant and, in this case, can be used in a straightforward manner for data interpretation. The EI mass spctra of the HC-toxins, on the other hand, contain several fragments, which are not unique to any one particular amino acid sequence. Hence, the added fragmentation by EI does more to complicate the picture than to illuminate it.

Table 5.4 EI-MS of HC-toxins

HC-I			HC-II			HC-III		
m/z	Formula	(RI%)	m/z	Formula	(RI%)	m/z	Formula	(RI%)
436	$C_{21}H_{32}N_4O_6$	1.9	422	$C_{20}H_{30}N_4O_6$	2.4	452	$C_{21}H_{32}N_4O_7$	1.6
408	$C_{20}H_{32}N_4O_5$	0.20	394	$C_{19}H_{30}N_4O_5$	0.40	409	$C_{19}H_{29}N_4O_6$	1.7
393	$C_{19}H_{29}N_4O_5$	0.52	379	$C_{18}H_{27}N_4O_5$	1.2	338	$C_{16}H_{27}N_2O_6$	0.98
367	$C_{17}H_{23}N_3O_6$	1.3	353	$C_{16}H_{23}N_3O_6$	0.76	324	$C_{16}H_{24}N_2O_5$	0.99
350	$C_{18}H_{26}N_2O_5$	0.74	310	$C_{15}H_{22}N_2O_5$	3.9	284	$C_{12}H_{18}N_3O_5$	3.7
324	$C_{16}H_{24}N_2O_5$	7.3	282	$C_{12}H_{16}N_3O_5$	0.33	255	$C_{11}H_{17}N_3O_4$	1.5
267	$C_{12}H_{17}N_3O_4$	1.9	254	$C_{11}H_{16}N_3O_4$	0.86	253	$C_{13}H_{19}NO_4$	1.9
253	$C_{13}H_{19}NO_4$	2.1	253	$C_{11}H_{15}N_3O_4$	1.0	213	$C_9H_{13}N_2O_4$	2.3
197	$C_9H_{13}N_2O_3$	1.3	196	$C_9H_{12}N_2O_3$	1.6	185	$C_7H_{11}N_3O_3$	1.9
196	$C_9H_{12}N_2O_3$	1.4	170	$C_9H_{16}NO_2$	19	184	$C_8H_{12}N_2O_3$	1.4
170	$C_9H_{16}NO_2$	16	169	$C_9H_{15}NO_2$	1.1	183	$C_8H_{11}N_2O_3$	1.6
169	$C_9H_{15}NO_2$	1.1	168	$C_8H_{12}N_2O_2$	1.3	170	$C_9H_{16}NO_2$	30
168	$C_8H_{12}N_2O_2$	1.0	167	$C_8H_{11}N_2O_2$	1.4	169	$C_9H_{15}NO_2$	2.1
167	$C_8H_{11}N_2O_2$	1.0	152	$C_8H_{10}NO_2$	2.1	168	$C_8H_{10}NO_3$	2.4
154	$C_9H_{14}O_2$	1.30	141	$C_8H_{13}O_2$	1.3	157	$C_6H_9N_2O_3$	3.0
152	$C_8H_{10}NO_2$	2.1	139	$C_7H_{11}N_2O$	1.6	155	$C_7H_{11}N_2O_2$	2.0
141	$C_8H_{13}O_2$	1.3	126	$C_6H_8NO_2$	1.4	152	$C_8H_{10}NO_2$	2.6
139	$C_7H_{11}N_2O$	1.3	124	$C_7H_{10}NO$	0.98	142	$C_6H_{10}N_2O_2$	3.1
126	$C_6H_8NO_2$	1.1	113	$C_5H_7NO_2$	1.5	141	$C_8H_{13}O_2$	2.5
124	$C_7H_{10}NO$	1.3	70	C_4H_8N	100	140	$C_7H_{10}NO_2$	2.8
70	C_4H_8N	100	55	C_2HNO	18	126	$C_6H_8NO_2$	2.3
55	C_2HNO	17	44	C_2H_6N	36	124	$C_7H_{10}NO$	1.4
44	C_2H_6N	54				113	$C_5H_7NO_2$	2.4
						99	C_5H_9NO	4.7
						86	C_4H_8NO	56
						70	C_4H_8N	23
						55	C_2HNO	31
						44	C_2H_6N	100

To illustrate this, the high resolution EI data for HC-I, obtained by Liesch et al., were applied to the revised structure shown in Table 5.2. The results indicated that 16 of the 18 ions listed for HC-I could be directly assigned to the new structure without changing their proposed elemental compositions. Interestingly, the remaining two ions (m/z 124, 152) were not easily assigned to the original structure either. The authors had postulated that a cleavage of a hydrogen from a methyl group on an alanine residue occurred in the formation of each of these fragment ions; such a process ishighly unfavorable. Nevertheless, it is evident that EI data are often not adequate for determining the sequence of cyclic peptide structures such as the HC-toxins.

Structural Data for the HC-toxins Obtained by TA-FAB

The fragmentation patterns observed by TA-FAB for the analyses of HC-toxins I, II, and III are listed in Table 5.5. In contrast to EI, the fragmentation patterns obtained by TA-FAB were much simpler and easier to interpret. At the same time, they provided sufficient information to confirm the reported amino acid compositions and their sequences. The assignments given to the observed peaks are not unique to this study, but are identical to those supplied from previous investigations based on FAB (10-13) and are used here for illustrative comparison. The fragments observed by TA-FAB for HC-I and II are also in direct agreement with the FAB-MS/MS data reported for these two compounds (10,12). While MS/MS has not been performed on the recently isolated HC-III,

Table 5.5 TA-FAB data for HC-toxins

HC-I			HC-II			HC-III		
m/z	(RI%),	Assignment	m/z	(RI%),	Assignment	m/z	(RI%),	Assignment
437	(18),	$(M+H)^+$	423	(21),	$(M+H)^+$	453	(18),	$(M+H)^+$
409	(1.6),	- CO	395	(2.3),	- CO	425	(2.8),	- CO
366	(1.1),	- 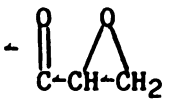	352	(1.1),	- 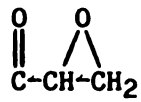	382	(1.5),	- 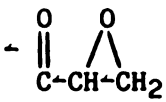
240	(4.3),	PRO-ALA-ALA^+	226	(6.6),	PRO-ALA-GLY^+	256	(6.2),	HYP-ALA-ALA^+
170	(12),	AOE^+	170	(9.9),	AOE^+	185	(7.5),	HYP-ALA^+
169	(6.3),	PRO-ALA^+	169	(3.5),	PRO-ALA^+	170	(20),	AOE^+
141	(6.68),	169-CO	70	(100),	PRO^+	157	(10),	185-CO
70	(100),	PRO^+	44	(20),	ALA^+	86	(58),	HYP^+
44	(60),	ALA^+				70	(21),	PRO^+
						44	(100),	ALA^+

the fragmentation by TA-FAB for this compound occurred in a fashion directly analogous to those of the other toxins.

The most important fragments in Table 5.5 are those which grant sequence information. Specifically, the peaks at m/z 240, 226, and 256 in the spectra of toxins I, II, and III, respectively, in conjunction with their respective daughter fragments, give evidence for the amino acid sequences listed for these ions. This approach to sequencing was first used by Gross et al. for the analysis of HC-I (10). They performed CAD on the PRO-ALA-ALA$^+$ fragment of mass 240 and observed m/z 169 (PRO-ALA$^+$) and m/z 70 (PRO$^+$) as daughters. Since the different daughter ions corresponding to the other sequence possibilities were not observed under CAD, the authors concluded the PRO-ALA-ALA$^+$ was the correct sequence. This method was soon repeated for the analysis of HC-II (12). By direct analogy to the FAB MS/MS data given for HC-I and II, the TA-FAB spectrum of HC-III contains peaks at m/z 256, 185, and 86 which may be assigned to the fragmentation sequence HYP-ALA-ALA$^+$ $\longrightarrow$ HPY-ALA$^+$ $\rightarrow$HYP$^+$. This result adds confirmation to the structure recently proposed by Tanis et al. for HC-III (13).

C. Discussion

Increased Structural Data Available by TA-FAB

Throughout the course of this work, TA-FAB showed a consistently higher level of structural information than conventional FAB. This tendency may be explained by a combination of two phenomena. First, thermal optimization which occurs during the TA-FAB experiment creates a selection against background to make the analyte peaks more visible. The second possibility is that TA-FAB promotes a discernible increase in the extent of analyte fragmentation.

The first of these two factors is considered in Table 5.6 which lists the fraction of the total ion current originating from the analyte in each analysis. For each toxin, the net contribution from the major analyte peaks (see Table 5.5) was summed and expressed as a fraction of the respective total ion current (Table 5.6). An exception was made for the analysis of HC-III by conventional FAB where the minor fragment ion of mass 185 was omitted because it was isobaric with the abundant protonated dimer of glycerol. Included for comparison are the results of analysis by conventional FAB using both probe tips (e.g., tungsten band and stainless steel). Even though the larger stainless steel probe tip tended to yield greater analyte ion currents, the difference is not significant as the fragment ions were not readily discernible using either probe tip for conventional FAB at this concentration. More importantly, a 4-fold increase in the fraction of analyte-related

TABLE 5.6. ANALYTE CONTRIBUTION TO TIC

Toxin	FAB (Tungsten Band)	FAB (Stainless Steel)	TA-FAB
HC-I	13%	8.1%	23%
HC-II	1.9%	3.0%	19%
HC-III	2.7%	4.0%	25%

ion current was observed for the TA-FAB analyses of the HC-toxins when compared to similar analyses performed by conventional FAB. This reflects the selection against background found using TA-FAB.

In pursuing the question as to whether the increased visibility of the analyte fragment peaks can be ascribed in part to more extensive fragmentation during TA-FAB, the summed intensity of the major analyte fragments in each case was expressed as a fraction of the intensity of the protonated molecule. If it can be assumed that fragmentation occurs at the expense of the protonated molecule, this ratio provides an index of the degree of fragmentation for each method of analysis. The calculated ratios, in Table 5.7 are useful for this purpose since they are independent of background. For conventional FAB in glycerol, the summed fragment ion intensity was approximately three times greater than the $(M+H)^+$ intensity and was independent of the probe tip used. By comparison, in TA-FAB the summed fragmentation was approximately 10 times the intensity for the protonated parent molecule. Since both FAB and TA-FAB produced $(M+H)^+$ ions for the HC-toxins with comparable facility (see Table 5.8), these results point to an increase in the level of fragmentation using TA-FAB.

It was initially thought that the added thermal energy which accompanies TA-FAB contributed to the observed increase in fragmentation. However, preliminary data obtained using a copper/constantan thermocouple to measure the temperature of the tungsten band indicate that typical operational temperatures during TA-FAB are below 100°C. This would correspond to a net increase in thermal energy of only 0.03eV; probably insufficient to completely

TABLE 5.7. DEGREE OF FRAGMENTATION

$$\frac{\Sigma\, I_{\text{fragments}}}{I_{(M+H)^+}}$$

Toxin	FAB (Tungsten Band)	FAB Stainless Steel	TA-FAB
HC-I	2.8	3.3	11
HC-II	2.9	2.8	6.8
HC-III	3.8	6.1	12

account for the observed increase in fragmentation. Therefore, the cause of the increase must be somehow related to the mechanism(s) by which the saturated saccharide matrix mediates the energy transfer from the atom beam during desorption-ionization.

One hypothesis that can be proposed is based on the gas phase desolvation model for ion formation in FAB. In other words, during FAB the atom beam removes large clusters containing analyte ions solvated by several matrix molecules so that ion formation during FAB may result in part from desolvation occurring in the gas phase. Puzo and Prome showed this process to be operative by observing the metastable decay of $(M+glycerol+H)^+$ to $(M+H)^+$ for the sugar trehalose (16). Also, the energy released by the dissociation of solvated matrix molecules lowers the energy of the analyte ions and explains the limited fragmentation observed in FAB. Unlike glycerol, however, fructose does not readily form cluster ions. In addition, since ions of the form $(M+fructose+H)^+$ have not been observed by TA-FAB, these observations point to a weaker association between fructose and analyte ions in the gas phase. Therefore, desolvation of analyte ions by fructose would liberate less energy leaving more internal energy to the analyte for fragmentation.

Fortunately, any added fragmentation imparted by TA-FAB has not significantly reduced the ability to observe $(M+H)^+$ ions for the compounds studied thus far. In general, TA-FAB and FAB produce peaks representing the intact analyte with comparable facility. To illustrate this point for the HC-toxins, Table 5.8 compares data from conventional FAB and TA-FAB after calculating the signal to

background (S/B) ratios for the respective $(M+H)^+$ ion of each analysis. Each value of S/B in Table 5.8 was obtained from an averaged mass spectrum which in the case of TA-FAB was recorded over the region of the BMT. Again, results for the two types of probe tips used in conventional FAB are included for comparison. The data show that TA-FAB was consistently superior to conventional FAB for providing molecular weight information for the HC-toxins at the 1.5μg level. The enhanced detectability reflects the lower degree of matrix interference from fructose during TA-FAB than from glycerol during conventional FAB in this region of the mass spectrum.

V. Conclusions

In this chapter, the ability of TA-FAB to reduce the problem of matrix interference was demonstrated. The initial work presented focused primarily on the analytical scope of the method with emphasis given to the three objectives cited: reduction of matrix interference, differential desorption of anayte and matrix ions, and matrix optimization. The second half of the chapter dealt with the application of TA-FAB to the analysis of a series of biochemically relevant cyclic tetrapeptide mycotoxins isolated from the fungus Helminthosporium carbonum by HPLC. In a series of comparisons, TA-FAB proved superior to both conventional FAB and electron impact by displaying the capacity to procure structurally significant fragmentation without a concomitant diminution in peaks representing the intact molecule. These qualitites make TA-FAB a

TABLE 5.8. SIGNAL TO BACKGROUND (S/B) RATIOS FOR PROTONATED MOLECULES PRODUCED BY FAB AND TA-FAB.

Toxin	FAB (Tungsten Band)	FAB (Stainless Steel)	TA-FAB
HC-I	71	58	85
HC-II	39	69	88
HC-III	21	32	72

simple, yet effective tool for the structural elucidation of biomolecules. For example, concern has been expressed that the thermal energy availale by conventional FAB is often insufficient to obtain complete sequence information for biopolymers such as oligopeptides and oligosaccharides at masses exceeding 2000 daltons (17,18). TA-FAB might be of use in this regard.

Although the bulk of analyses by TA-FAB have been devoted to development and application, investigations intent on understanding how the method works are underway. While more data are needed to establish the exact mechanism of TA-FAB, a hypothesis has been formulated which is the topic for the following chapter.

VI. List of References

1. J.L. Gower, Biomed. Mass Spectrom., 12, 191 (1985).
2. L. Friedman and R.J. Beuhler, 26th Annual Conference on Mass Spectrometry and Allied Topics, St. Louis, 1978, Workshop on Field Desorption.
3. K.L. Busch, B.H. Hus, Y. Xle, and R.G. Cooks, Anal. Chem., 55, 1157 (1983).
4. E.D. Hardin, T.P. Fan, and M.L. Vestal, Proceedings of the 32nd Annual Conference on Mass Spectrometry and Allied Topics, San Antonio, TX, 1984, 246.
5. J.B. Rasmussen, R.P. Scheffer, B.A. Horenstein, and S.P. Tanis, paper submitted for publication in Physiological Plant Pathology.
6. G.L. Glish, P.J. Todd, K.L. Busch, and R.G. Cooks, Int. J. Mass Spectrom. Ion Proc., 56, 177 (1984).
7. M. Barber, R.S. Bordoli, R.D. Sedgwick, and L.W. Tetler, Org. Mass Spectrom., 16, 256, 91981).
8. R.B. Pringle and R.P. Scheffer, Phytopathology, 57, 1169 (1967).

9. J.M. Liesch, C.C. Sweeley, G.D. Stahfeld, M.S. Anderson, D.J. Weber, and R.P. Scheffer, Tetrahedron, 38, 45 (1982).

10. M.L. Gross, D. McCrery, F. Crow, and K.B, Tomer, Tet. Lett., 23, 5381, (1982).

11. J.D. Walton, E.D. Earle, and B.W. Gibson, Biochem. Biophys. Res. Comm. 107, 785, (1982).

12. S.D. Kim and H.W. Knoche, Tet. Lett., 26, 969, (1985).

13. S.P. Tanis, B.A. Horenstein, R.P. Scheffer, and J.B. Rasmussen, paper submitted for publication in Tetrahedron Letters.

14. L.M. Ciufetti, M.R. Pope, L.D. Dunkle, J.M. Daly, and H.W. Knoche, Biochemistry, 22, 3507, (1983).

15. F.W. Crow, K.B. Tomer, and M.L. Gross, Mass Spectrom. Rev., 2, 47, (1983).

16. G. Puzo and J.C. Prome, Org. Mass Spectrom., 19, 448 (1984).

17. D.L. Lippstreu-Fisher and M.L. Gross, Anal. Chem., 57, 1174 (1985).

18. C.V. Bradley, D.H. Williams, and M.R. Hanley, Biochem. Biophys. Res. Comm., 104, 1221, (1982).

Chapter 6

HYPOTHESIS OF A MECHANISM TO ACCOUNT FOR THE TA-FAB PHENOMENON

I. Introduction

To date, TA-FAB experimentation has been primarily devoted to development and application. Recent investigations, however, have sought to uncover the mechanism behind TA-FAB. Such studies ultimately have additional benefit in that as more is known about the TA-FAB mechanism, more can be done to exploit the full potential of the technique. In this chapter, preliminary data are presented which allow some tentative conclusions to be drawn about the mechanism. These data were acquired with the assistance of C.E. Heine, who shall pursue these studies in more detail as part of a dissertation project. The results given here, therefore, represent only a beginning and are primarily qualitative.

In this chapter a plausible explanation or model is submitted to account for the behavior observed during TA-FAB. The intent is to formulate an understanding of how saccharide solutions under thermal perturbation alter the nature of the data obtained by FAB. No attempt shall be made to resolve the much debated issue of how FAB occurs. Instead, specific answers are sought for 1) the behavior of analyte ion desorption as a function of temperature during TA-FAB, 2) the behavior of matrix ion desorption under the same conditions, and 3) the ion types observed by TA-FAB when saccharide solutions are used as matrices.

The first observation, critical to an understanding of TA-FAB is that in TA-FAB a ternary system exists composed of analyte, substrate, and solvent. Thus, the matrix consists of two components, substrate (fructose) and solvent (water). The substrates which have yielded success thus far (previously listed in Table 5.1) are highly hydroxylated compounds. Although the solvent most frequently used is water, various aqueous methanol combinations have been used. The most important criterion for a successful matrix is the ability for the substrate to retain solvent under the high vacuum conditions of the mass spectrometer in order to preserve the ternary system.

Another point which bears repeating is that the saccharide solutions used for TA-FAB were not actually saturated before entering the mass spectrometer. The solutions used were approximately 1:1 (w/w). In reality, fructose does not become fully saturated until a ratio of 3:1 (or greater) fructose:water (w/w) is reached. However, when the saccharide solutions used for TA-FAB encounter high vacuum (10^{-5} torr) they lose water to become closer to saturation. A qualitative inspection between fructose solutions after exposure to high vacuum and actual saturated fructose indicated this to be the case. Preliminary viscosity measurements have been performed to confirm this assumption.

II. Three Regions of Desorption Behavior

For the purpose of explaining the trends in the ion current profiles observed during TA-FAB, it is instructive to break the ion current profiles down into three regions which differ as a function

of the matrix temperature, and hence fluidity. The term fluidity, as used here, is intended to be an indicator of the ease of mass transport within the matrix, and is therefore dependent on the viscosity of the ternary system. Figure 6.1 shows the desorption profiles for the TA-FAB analysis of 3μg thiamine hydrochloride in glucose that were used previously in Chapter 5 to illustrate the differential desorption which occurs for analyte and matrix ions in TA-FAB. In this case, however, the profiles are labeled with three separate regions along the abscissa, which is of course related to temperature. Again, the conditions were as follows. No heat was applied during scans 1-4 (FAB only). Beginning with the fifth scan, a current of 0.90A was applied and allowed to increase linearly to a value of 1.54A (scan 18) and then returned to 0.00A for the last two scans. The BMT for the molecular cation at m/z 265 occurred at scan 13 (1.29A). In chronological order, the regions may be referred to as 1) the non-heated region, 2) the region of analyte desorption, otherwise known as the interval of the BMT, and 3) the post-BMT interval where analyte and matrix ion desorption diminishes.

In the first region of Figure 6.1, a situation exists where little or no analyte signal is observed. Prior to heating the matrix remains in a highly viscous state. Although further viscosity measurements need to be performed, it can be conclusively stated that saccharide solutions which experience high vacuum are considerably more viscous than glycerol. Therefore, the situation which prevails in the initial stages of TA-FAB is more akin to SIMS than FAB. In static SIMS, where a liquid matrix is not employed, the lifetime of the experiment depends on the flux of the incident beam since there

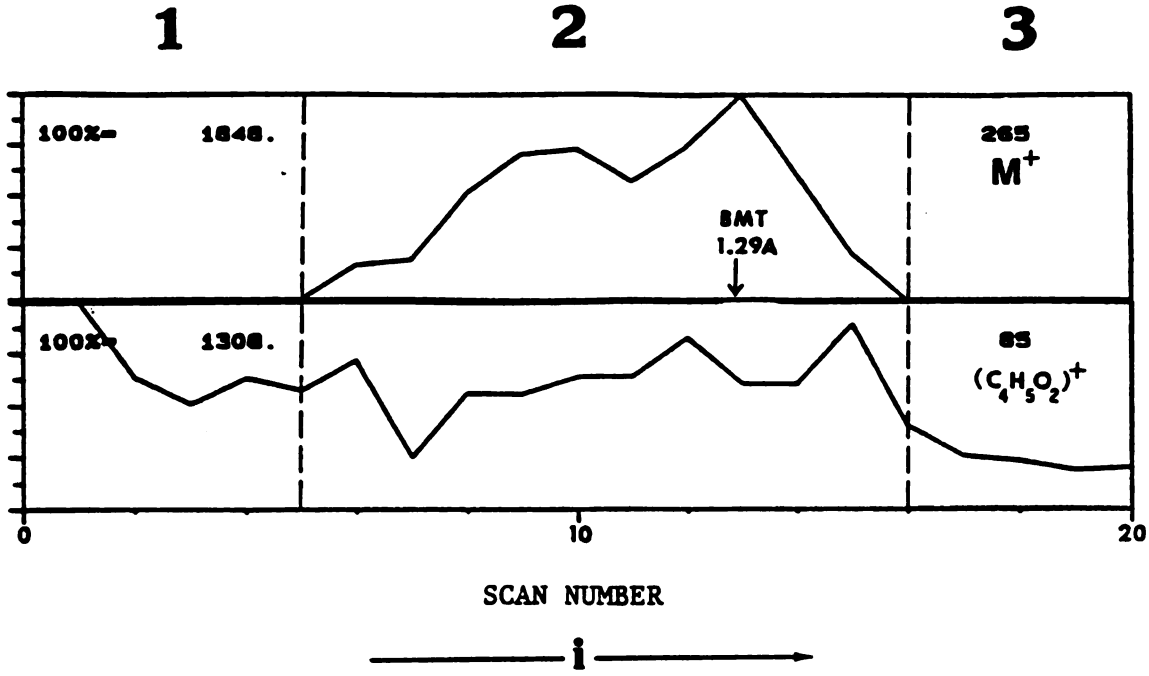

Stage	Heat	Desorption of Analyte	Matrix Behavior
1	No	Little or None	Unlike Glycerol
2	Yes	Strong	Like Glycerol
3	Yes	None	Unlike Glycerol

Figure 6.1 Desorption profiles for 3 µg thiamine hydrochloride showing the three regions of desorption behavior for analyte (m/z 265) and matrix (m/z 73) which are differentiated according to anticipated matrix fluidity.

is insufficient mass transport to make an analyte replenishment mechanism operative. Under SIMS, analyte ions are produced until a saturating bombardment flux is reached known as the "critical dose". Beyond this point, surface damage is too extensive to sustain analyte desorption-ionization. Values for this parameter have been estimated to be on the order of 10^{13} particles cm^{-2} (1). Therefore, to increase sample lifetimes the bombarding flux is attenuated to typically 10^{-9} A cm^{-2} to yield a process known as static SIMS (2).

In FAB, or liquid SIMS, this problem is not experienced because the liquid matrices employed permit adequate mass transfer to keep the surface relatively immune to the damage observed with solids. Hence, primary beams for FAB can have greater flux and experience better sensitivity without the concomitant loss in longevity found in static SIMS. For example, the flux produced by the B11NF Ion Tech saddle field FAB source is on the order of 1.5×10^{-4} A cm^{-2} (3). This value was calculated from an operating current of 25μA and a probe tip surface area of 0.16 cm^2. Thus, it is entirely possible that analyte ions desorbed without applying heat to the saccharide matrix are not observed on the time scale of the TA-FAB experiment.

Another reason for the paucity of analyte ions in the first region might be that the ions formed (most likely fragments) come off the probe surface with a different energy than the matrix ions and are therefore not observed with a double focusing instrument. However, attempts to focus for analyte ions in this region were in general unsuccessful. When analyte ions were observed in this region, they were predominantly products of fragmentation instead of representing the intact molecule. In addition, any analyte ion

current observed in the first region was of much lower intensity than when the sample was heated. This indicates that the conditions for analyte ion desorption are not favorable when the matrix is in a non-heated (immobile) state.

The second region of the TA-FAB experiment in Figure 6.1 shows that analyte ion desorption occurs simultaneously with the application of heat. Experiments, described later in this chapter, were performed to determine the temperature range of the BMT interval. It appears that optimum analyte ion desorption for ternary systems is between 80 and 100°C. While the net energy input to the system is not of great magnitude, the increased temperature can have considerable impact on analyte mass transport, analyte solubility, and matrix viscosity. A visual inspection of the sample, removed for inspection at the BMT region, revealed that the sample had flowed somewhat in response to the heat because the sample had relaxed to a thin film which was flatter than that observed before heating. Prior to heating, the sample had a slightly curved surface indicative of a higher water content.

In region 2 the matrix acquires the proper physical characteristics which favor analyte desorption. To draw a loose analogy, the saccharide matrices behave more like glycerol in this regard during region 2. On the other hand, since many of the factors involved are temperature dependent, an optimization of the analyte signal occurs during TA-FAB as the probe current is scanned. This does not occur for glycerol. The fact is that glycerol already has the desired characteristics to promote analyte ion desorption at

ambient temperature. Heating only detracts from these properties and makes for a shorter interval between source cleaning.

Another observation about region 2 is that the signals observed from the analyte are both stable and reasonably long-lived. This indicates that some mechanism for analyte replenishment is operative. Moreover, the mechanism is directly related to temperature and, in all likelihood, mass transport. This process shall be considered in more detail later.

Shortly after the BMT is reached, continued heating leads to a third part of the experimental profile where the analyte ion current diminishes to a level indistinguishable from background. Eventually, this is followed by a gradual diminution of all ion current. This effect is not due to a depletion of analyte. Rather it is linked directly to the removal of water, and hence fluidity, from the matrix. As a result, the matrix is no longer capable of supporting analyte desorption-ionization. This conclusion has been drawn from several experiments which shall be described later in more detail.

Thus, to a first approximation, the behavior of the analyte during TA-FAB correlates to the fluidity of the system. In essence, the high viscosity on either side of the BMT interval impedes analyte desorption-ionization. A more difficult task is to explain the behavior of matrix ions, both in the profiles obtained and the types of ions formed. The first of these questions is addressed next.

Unlike analyte ions, the behavior of the matrix ions during TA-FAB is less well defined. For example, in Figure 6.1 the glucose ion at m/z 73 remains fairly constant over the BMT region where the conditions for desorption-ionization would appear to be optimum.

While the behavior of the matrix is not always predictable, the change between the first and second regions of the profile is much less dramatic than that for the analyte. In some instances, matrix desorption has even decreased when heating occurs. These observations would tend to suggest a selection against matrix background over the interval of the BMT.

To investigate this idea, the TA-FAB profile for fructose was run several times without analyte to try to document the behavior of matrix ions as a function of temperature. It was concluded that matrix ions do in fact respond to changes in temperature, but the effect is less pronounced than that for analyte ions. Figure 6.2 shows ion current profiles from an experiment where 0.5µl aqueous fructose underwent TA-FAB under standard conditions. The first 5 scans were acquired without heat, then starting at scan 6 a current ramp was initiated going from 0.70A to a final value of 1.60A. Two ion current profiles are shown, m/z 163 (fructose + H - H_2O)$^+$ and m/z 85 ($C_4H_5O_2$)$^+$. Both of these ions exhibit distinct increases in intensity when heat is first applied. The rise appears more dramatic for the heavier ion (m/z 163) because less of this fragment was present initially. In other words, more extensive decomposition occurs when no heat is applied and the matrix is less fluid. Another possible explanation is that more fructose monomers are present in the BMT region due to the disruption of fructose-fructose interactions upon heating. Regardless, the converse to this situation is observed at the end of the run where the ion current at m/z 163 falls off more rapidly as water is lost from the matrix. It is apparent from Figure 6.2 that desorption of fructose is greater in

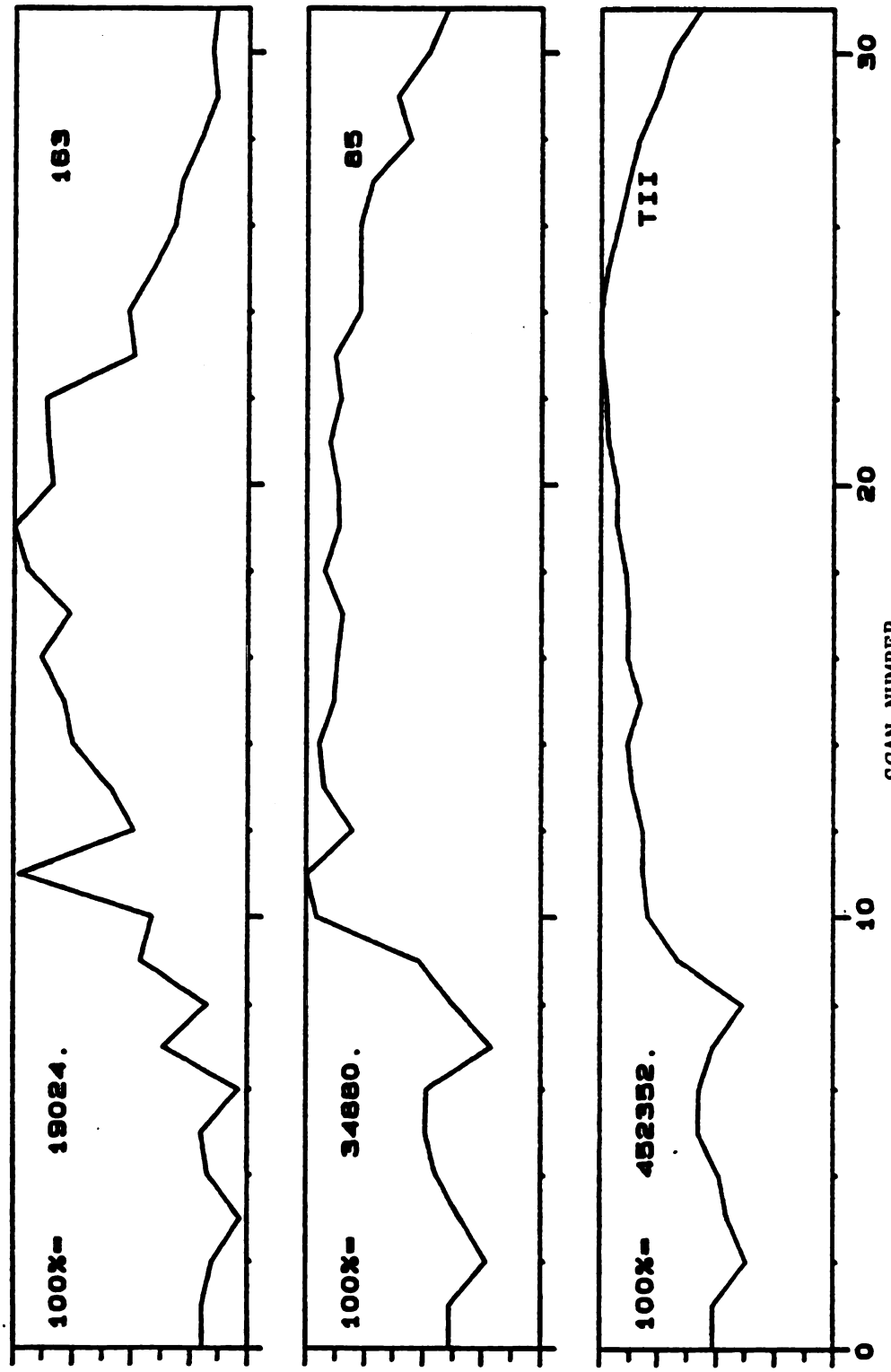

Figure 6.2 Desorption profiles for two representative matrix ions obtained when 0.5 µl aqueous fructose was analyzed under standard TA-FAB conditions.

the temperature region which corresponds to the BMT interval leading to the conclusion that a suppression of fructose ions occurs in this region during the TA-FAB analysis of ternary systems.

Suppression of background is not totally unexpected since the presence of an analyte instates a competition for desorption-ionization. However, the potential factors that govern this process need to be investigated. Generally, three factors contribute to the relative intensity of an analyte signal in FAB: concentration, extent of pre-ionization, and surface activity. The first of these factors apparently does not influence the observed selection against background. In fact, considering that the molar ratio between fructose and analyte is typically between 100 and 1000 to 1, it is remarkable that any selection is observed at all. The second factor probably explains some of this observation since the samples analyzed by TA-FAB tend to be more readily ionized than fructose in solution. However, it is unreasonable to assume that pre-ionization is the overriding factor because similar differences occur in conventional FAB between analytes and glycerol, yet a smaller selection against background is observed. Also, it is unlikely that heating creates any further analyte pre-ionization considering the low temperatures involved.

A third factor which determines sensitivity is the relative surface activity of the analyte. As discussed in Chapter 1, the FAB beam tends to sample those species which are at or near the surface. This factor would certainly favor the analyte over fructose since many of the molecules studied by TA-FAB contain both polar and hydrophobic constituents. Again, however, the same factors are

involved in glycerol, but the selection against background is far less dramatic. Because it is unlikely that the factors discussed fully account for the observed behavior, further explanation is necessary.

III. The Ternary Perculation Model for TA-FAB

A model known as ternary perculation (TP) has been postulated to account for the observed ion current profiles in TA-FAB, particularly in the region of the BMT where analyte ion desorption is optimal and a selection against matrix background is observed. This model is based on the same mass transport properties, conferred to the matrix by water, that are known to be responsible for sustaining analyte ion signals in TA-FAB. By this model, a preferential extraction of analyte coupled to the migration of water is proposed which selectively partitions analyte at the surface to be selected for by the atom beam. In other words, as the water escapes from the matrix, it continually transports the analyte to the surface. Further, the analyte is retained at the surface because of its low volatility and because the direction of flow is towards the surface.

The water content of the fructose matrix at any temperature during TA-FAB reflects a compromise between two opposing factors: the colligative effect by the fructose solute on the vapor pressure of the solvent, versus the boiling point reduction of water at reduced pressure. However, as the temperature is increased the tendency is to release water from the matrix. As the tungsten band is heated, it is plausible that bubble formation occurs near the band. The reduced

viscosity of the solution at elevated temperature enables the bubbles to migrate. While escaping bubbles may participate in analyte transport, a mechanism similar to Vestal's "thick sauce" model (4) is not implied because the phenomenon is an equilibrium process. In fact, due to the slow ramp in temperature (10°C/min), migration of water through the matrix most likely occurs in a series of successive equilibria between condensed and gaseous states responding to the thermal gradient produced (hence the term perculation). While this process is believed to be responsible for analyte transport, other factors such as convection should not be discounted.

An important question remaining to be addressed about the TP mechanism is why the analyte is transported preferentially over fructose in TA-FAB? This occurrence is not unreasonable if one considers the physical state of the ternary system as it exists in the mass spectrometer. A 1:1 (w/w) aqueous solution has exactly 10 water molecules per fructose molecule. For a saturated solution, however, this ratio is only about 3 to 1. The ratio of molecules in the matrix inside the mass spectrometer is probably at or below this second estimate. The point is that so much fructose dissolves in water that the fructose molecules are never completely solvated. In other words, the most abundant interactions in solution are the intermolecular interactions (i.e., hydrogen bonds) that occur between the fructose molecules. Therefore, saccharide matrices can be envisioned as gels which retain water, as opposed to aqueous solutions. In contrast, the analyte, which is initially introduced from a dilute solution, would tend to be more fully solvated by water, and hence more easily transported.

The thermodynamic viability of the TP hypothesis is dependent on the relative strength and number of the various intermolecular interactions within the ternary system. Six interactions are possible: fructose-fructose (FF), fructose-water (FW), fructose-analyte (FA), water-analyte (WA), water-water (WW), and analyte-analyte (AA). All of these interactions may be described through hydrogen bonding. Since hydrogen bond strengths only vary from about 4 to 7 kcal/mol (5), it is unlikely that the relative strengths for any of the interactions differ by more than a factor of two. Hence, the energy supplied by heating is sufficient to break each type of interaction. A far more important facator from a "bonds broken minus bonds formed" standpoint is the relative number of each type of interaction.

Basically, for the TP model to be operative the following statement must be true:

$$\sum (FF) + \sum (WA) > \sum (FW) + \sum (FA)$$

Stated simply, the net sum of the interactions which favor ternary perculation must outweigh the total interactions which stand in resistance to the TP mechanism. Obviously, both fructose-fructose and water-analyte interactions favor ternary perculation, whereas fructose interactions which retain either the analyte and water do not. Analyte-analyte interactions are not considered because they are few in number. Water-water interactions, on the other hand, are omitted because they are not as directly involved in the competition

which governs ternary perculation. While several arguments can be made concerning the various interactions above, the overwhelming force which drives the TP mechanism is the large number of fructose-fructose interactions which instate a considerable amount of order to the ternary system. Not only are these bonds the most prevalent, there is the possibility for several interactions on the per mole basis. Interestingly enough, the melting point for fructose is only 103-105°C. This suggests that individual FF interactions are about as strong as WW interactions. The fact that water escapes preferentially over fructose must therefore be explained by a larger number of FF interactions. Further support of the above inequality is derived from the fact that water is removed from fructose during TA-FAB (e.g., FW dissociation) and from the absence of fructose-analyte cluster ions in the mass spectra.

To substantiate the claim regarding the dominance of fructose-fructose interactions, X-ray diffraction data acquired by Mathlouthi (6) for aqueous fructose solutions are shown in Figure 6.3. Although X-ray diffraction has frequently been used to study crystalline carbohydrates, it had never previously been used to study solutions presumably because of an assumed lack of order and the inability to permit localization of hydrogen atoms. However, X-ray diffraction is possible, as the data in Figure 6.3 indicate, for a comparative study of aqueous saccharide solutions as a function of concentration.

Figure 6.3 contains several diffractograms ranging in fructose content from pure water (lower trace) to solid fructose (upper trace). Actually, two forms of the solid are present: lyopholized (L) and

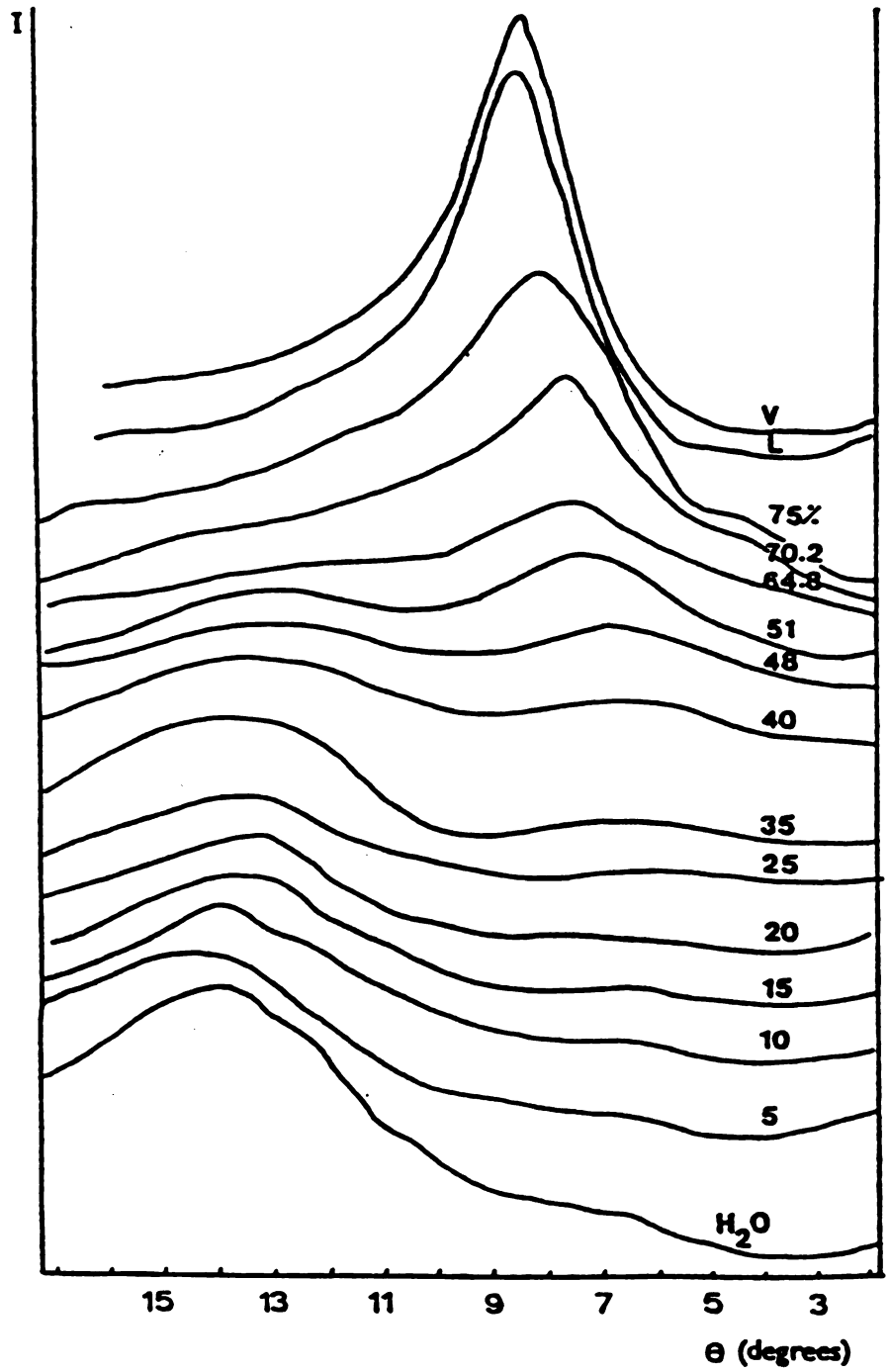

Figure 6.3 X-ray diffractograms obtained by Mathlouthi for aqueous solutions of D-fructose at different concentrations (% w/w), as well as solid fructose:lyophilized (L) and vitreous (V). Reprinted from reference 6 courtesey of Elsevier Scientific Publishing Co., Amsterdam.

vitreous (V). The latter, which is more free of residual water, was formed by rapid cooling of molten fructose. Each diffractogram plots the diffracted intensity observed versus Bragg angle for a particular fructose concentration. The author breaks a discussion of the data down into three regions according to fructose percentage. The region of importance here is the most concentrated region (e.g., > 51%) where the most predominant interaction in each case (ca. θ = 8°) resembles the ordering observed for solid fructose. Notice that as the solutions become more concentrated in this region, the maxima coincide more closely with that for solid fructose (θ = 8° 42'). In addition, the reduction of the smaller peaks on each side of this maxima can be interpreted as the exclusion of water as fructose-fructose interactions are maximized. Also the increase in intensity associated with this trend corresponds to a greater level of ordering at higher fructose concentrations.

From these data Mathlouthi concludes that, "The intensity maxima observed in this concentration range could be assigned to the regular repetition of planes containing carbohydrate molecules. The fact that the intensity maxima are localized at the same Bragg angle for concentrated solutions and freeze-dried samples suggests that the same, short-range order of sugar molecules exists in both cases".

Prior to acquiring X-ray data on saccharide solutions, Mathlouthi et al. published a laser Raman study for the same systems (7). Comparative data obtained at different saccharide concentrations agree with the conclusions drawn from the X-ray data, and offer additional support for the TP model as well. The Raman data confirm a trend known to occur for saccharides. At about 30-40%

(w/w) the process of prenucleation begins where solvated saccharide molecules associate to form aggregates which at larger concentrations form a compact network approaching crystalline organization. Hence sugar-sugar associations form at the expense of sugar-water interactions as the concentration of fructose increases (7).

In view of the X-ray data for fructose, it is easy to understand why transport via ternary perculation (water transport) would occur almost exclusively for analyte and not for fructose: while it may be possible to solvate the relatively few analyte species, the chance for full solvation of a fructose molecule is remote. Hence, a likely arrangement for the ternary system, prior to heating, can be envisioned as a fairly ordered fructose network which is disrupted by the random intercalation of analyte molecules or ions. Water then occupies the interstitial spaces, and is presumed to be capable of analyte solvation. An artist's conception of this initial situation is shown in Figure 6.4a, where the darkened circles represent analyte, and the small squares of almost equal size represent individual fructose molecules. As shown, the fructose molecules aggregate into larger clusters to maximize their interactions. Water then occupies the void volume.

Upon heating (Figure 6.4b) several interactions are broken which not only enable the release of water, but also the exclusion of the intercalated analyte. A well defined fructose lattice is not the suggested result of this action as certainly several fructose-fructose interactions are severed also. However, the opportunity to re-establish order within the fructose gel could be a driving force for the overall process. Further, in several

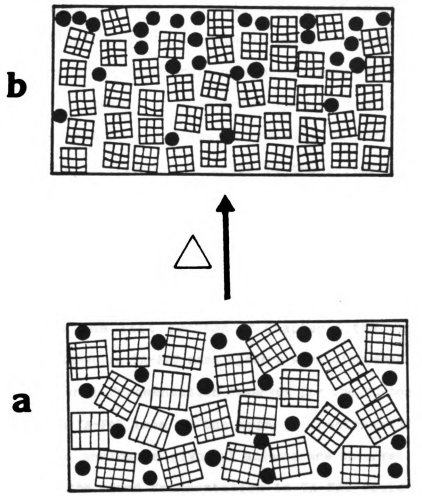

Figure 6.4 An artist's conception of the ternary perculation model depicting the system (a) before and (b) after heating. The darkened circles represent analyte molecules while fructose aggregates are shown as cross-hatched boxes; water then occupies the interstital spaces.

experiments it appeared that the initial heating current surge, prior to initiating the slow ramp, aided in the selection against background. Therefore, heating during TA-FAB turns the thermodynamically favorable process of analyte exclusion into a kinetically viable process as well. Precedence for this hypothesis occurs in the metallurgic process of "zone refinement". For example, zone refinement is frequently used in the semiconductor industry where heating and freezing are used to exclude impurities from silicon and germanium prior to the preparation of semiconductor devices for electronic circuits (8).

IV. Ion Types Observed by TA-FAB

In the last section of Chapter 5 the types of analyte ions encountered in TA-FAB mass spectra were discussed with regard to the additional fragmentation observed for the HC-toxins. It is recalled that in TA-FAB ions of the type $(M+fructose+H)^+$ are not observed, whereas analogous glycerol adducts are observed by conventional FAB. Hence, the added fragmentation in TA-FAB could be the result of a reduced tendency to experience gas phase desolvation, which is believed to reduce the available internal energy for fragmentation (4,9). Because of the aggregation of fructose within the ternary system, it can now be understood why solvation of the analyte by individual fructose molecules, or small clusters, is not an abundant occurrence.

A final observation that needs to be addressed is the tendency for saccharide solutions to favor formation of matrix fragments over

clustering, which is the case for viscous liquids. To answer this question one must consider the association of fructose within the ternary system relative to the association of glycerol as a viscous liquid. In other words, concentrated fructose solutions have a higher level of ordering than does glycerol, presumably because of more intermolecular interactions. In fact, as the concentration of fructose increases the equilibrium between the 5-membered (furanose) isomer and the 6-membered (pyranose) isomer becomes shifted towards the latter to promote a closer packing arrangement (10). Although glycerol can hydrogen bond effectively, facile free rotation prohibits any high level ordering.

The extensive matrix fragmentation observed by TA-FAB can be related to the high level of intermolecular interaction observed in concentrated saccharide solutions. Because fructose solutions are less resilient than glycerol, more energy is transferred to internal modes of the fructose molecules. Essentially, the kinetic energy of the atom beam is transferred to the sample either as translational energy or internal energy. Because of the fast rate of energy transfer, the majority is believed to be translational (i.e., momentum transfer). The point to be made here, however, is that concentrated fructose solutions represent a more rigid system than glycerol, even when the former are heated. Therefore, translational energy is transferred less efficiently to fructose because of the extensive intermolecular interactions. As a result, more energy must be taken up into the internal modes of fructose to promote fragmentation. It is well known that solids, whose molecules are restricted from moving translationally, fragment during particle

impact. In fact, only ionic bonding substances like CsI favor cluster formation. In contrast, liquids, because of their lack of order, may transfer translational energy more readily and as a result ions from the intact molecule are observed. In TA-FAB, although the matrix exists in a fluid state, the order of the saccharide substrate is substantial. Therefore, matrix fragmentation is not surprising. At present, it is impossible to tell whether this fragmentation occurs in the condensed or gaseous state (or both). However, even if molecular fructose ions are desorbed intact, the additional internal energy causes them to fragment in the gas phase to give the observed results.

V. Preliminary Data

Several experiments are being performed concurrently to probe the mechanism of TA-FAB. Unfortunately, since many studies are in progress it is premature to report on them here; these studies shall be the topic of a future publication. The results of three investigations, however, shall be considered. The common thread among the studies is that each can be used to document the importance of water to enable mass transport during ternary perculation.

A. Temperature Determination

To determine the temperature of the emitter during TA-FAB, a copper/constantan thermocouple was attached to the tungsten band using a thermally conductive, electrically insulating, epoxy adhesive

(OMEGABOND® 200, Omega Engineering, Inc., Stamford, Conn.). This epoxy had a reported volume resistivity of 10^{15} ohm cm, a thermal conductivity of 0.003 cal cm^{-1} sec^{-1}, and a maximum operating temperature of 260°C. The measurements were made inside the ion source (1 x 10^{-5} torr xenon) using the emitter current programmer to heat the band. The output from the thermocouple was connected to a digital multimeter and a strip chart recorder. Strip chart recordings verified the linear relationship between probe temperature and heating current using an ECP scan rate of 100mA/min. An ECP current vs. temperature calibration was prepared over the current range of 0.60 to 1.50A in intervals of 0.05A. The results appear in Figure 6.5. Unfortunately, because of the low pressure of the mass spectrometer and the size of the epoxy bead, thermal equilibrium occurred slowly. However, strip chart recordings taken at various currents showed that the temperature increase began to drop off after about 35 seconds. Therefore, all data were acquired after a 35-second equilibration period. While the shape of the curve in Figure 6.5 is fairly linear, slight deviations at the temperature extremes are probably artifacts of this method of temperature measurement. The temperature data were estimated to be accurate to within ±10°C. The temperature axis was calibrated by placing the TA-FAB probe tip (with attached thermocouple) inside a GC oven, and recording the thermocouple output voltage at various temperatures read from a thermometer. Under these conditions, thermal equilibrium took only a matter of minutes to occur.

To confirm the temperature data, melting point observations were carried out for six solids having melting points in the temperature

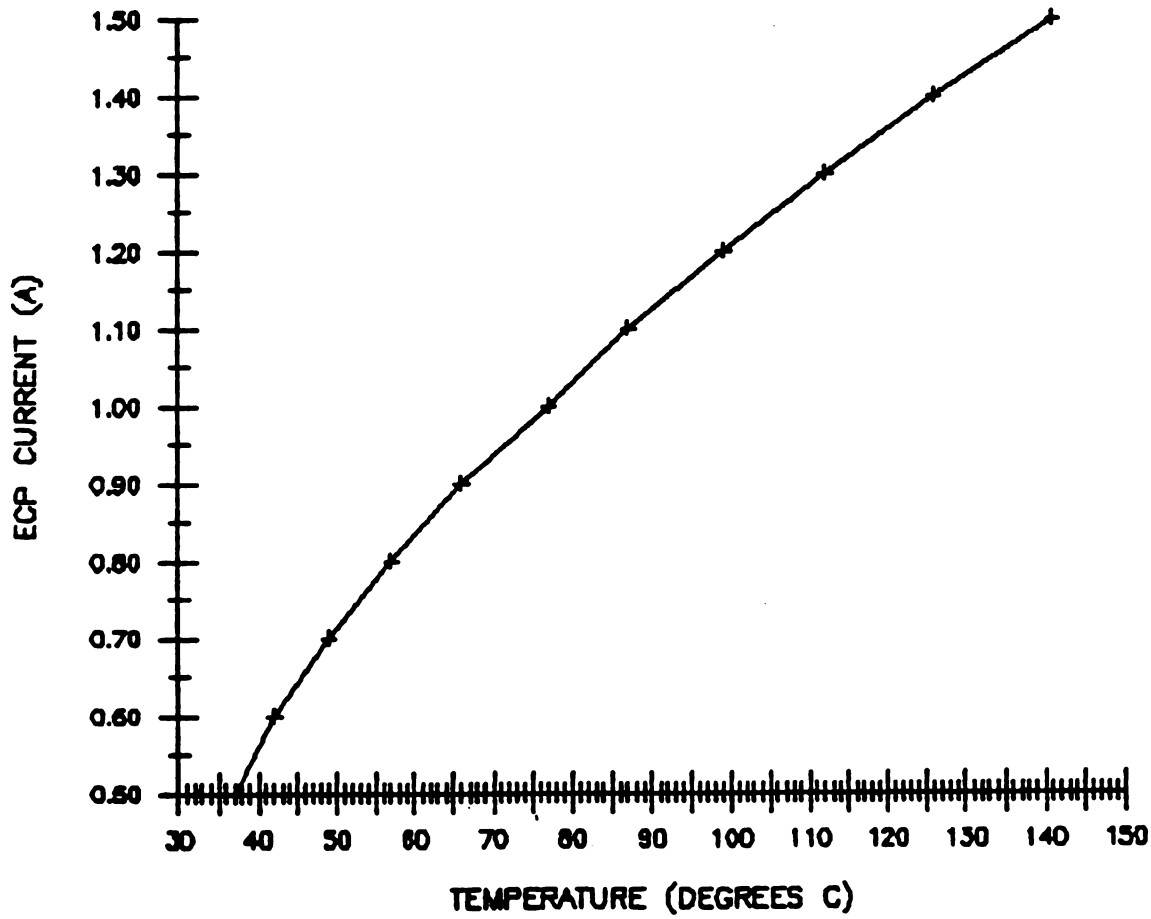

Figure 6.5 Temperature calibration obtained for the emitter current programmer (ECP).

range of 39°C to 113°C. The solids employed for this study were: myristyl alcohol, stearyl alcohol, stearic acid, arachidic acid, benzil, and α-ketoglutaric acid. While the melting point data corroborate the temperature calibration of Figure 6.5, these determinations were less precise. For example, two consecutive measurements for α-ketoglutaric acid varied by 0.15A. Such inconsistency in the current-temperature relationship could help explain changes in BMT location observed over periods of time. Nevertheless, the temperature data indicate that the range over which the BMT interval (region 2) occurs is approximately 60 to 105°C. This supports the claim of the TP model which suggests that mass transport is brought about by the migration and release of water under the conditions of TA-FAB.

B. Thermal Studies of Fructose Solutions

Thermogravimetric analysis (TGA) was selected as a method for monitoring the escape of water cited above. To this end, data were collected with the assistance of M.D. Uptmore (technical representative, E.I. duPont de Nemours and Co.) on a DuPont model 951 thermogravimetric analyzer. The TGA data for 25.21mg of aqueous fructose appear in Figure 6.6 where the percentage loss in sample weight is plotted against temperature. A heating current ramp of 10°C/min was used analogous to the rate of heating during TA-FAB. Unfortunately, the experiment could not be conducted under reduced pressure to simulate the conditions of the mass spectrometer. Despite this limitation, the curve indicates a smooth and continuous

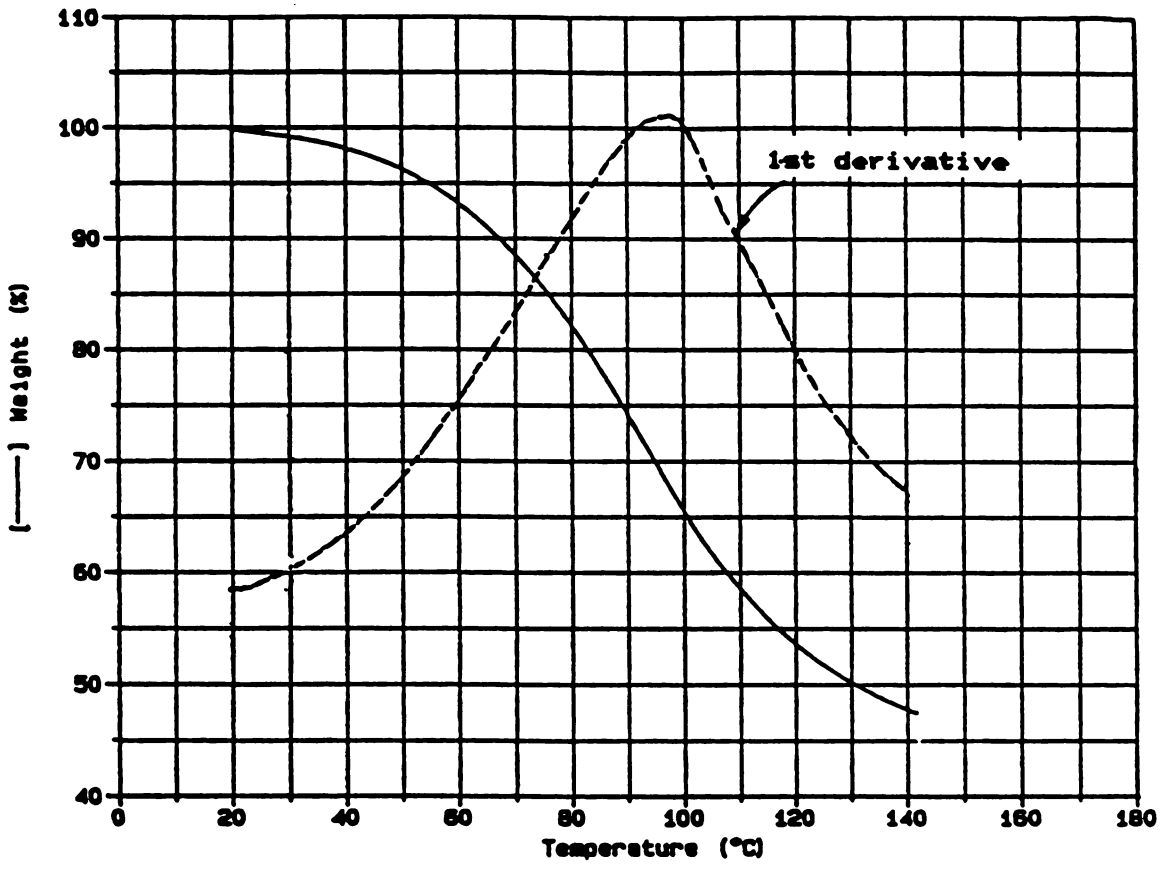

Figure 6.6 Thermogravimetric analysis of 25.21 mg aqueous fructose. Sample heated at 10°C/min, 1 atm.

loss in weight which had a maximum rate at ~ 97°C as determined by the first derivative plot (dashed line) included in Figure 6.6. Within experimental error, these data correlate well with the observed rate of boiling for similar fructose solutions recorded visually under analogous conditions. Hence, the weight loss may be attributed to the loss of water; a claim further supported by a large endothermic transition observed using differential scanning calorimetry (DSC) under the same set of conditions. A DuPont model 912 Differential Scanning Calorimeter was used for this measurement. Furthermore, the rate of water release, depicted by the first derivative curve in Figure 6.6, to a first approximation depicts the general profile for analyte ion desorption under TA-FAB. This suggests that analyte ion desorption profiles are related to the mass transport of water in the ternary system. Unfortunately, the fact that thermal experiments were conducted at ambient pressure means that the observed release of water occurs at a higher temperature than would be found during TA-FAB. However, since the BMT is believed to occur at temperatures below 100°C, it is likely that the release of water during TA-FAB can be directly correlated to the temperature interval for optimum analyte ion desorption under TA-FAB.

C. The Rejuvenation Effect

Perhaps the most convincing evidence for the importance of water to analyte ion desorption under TA-FAB comes from the fact that once the analyte ion current has diminished to a level comparable to that from the chemical background, it can be rejuvenated merely by the

addition of water. Furthermore, if the presence of the solvent is critical to maintaining analyte desorption, the analysis should be extended by holding the heating current steady at the BMT, instead of continuing towards higher temperatures. Both of these features have been verified as illustrated by the data shown in Figure 6.7 for the TA-FAB analysis of 2μg alanyl-leucyl-glycine in 1.0μl fructose. The ion profile displayed is that for the protonated molecule (m/z 260). A previous analysis of 1μg of this tripeptide, shown in Figure 5.8, gave a BMT of 1.00A; the analyte ion current lasted no longer than 5 minutes when a continuous heating current ramp was employed. In the present example, (Figure 6.7) the heating current for the sample was ramped to a value near the BMT (1A) and held there while the analyte ion current was monitored. The first 10 scans were acquired with no heat. Scans 11-18 were then collected while ramping the probe current from 0.80 to 1.00A. The probe was held at this heating current until scan 51, an interval of approximately 11 minutes. During this time the analyte ion current decreased steadily, but much more slowly than in the previous example (Figure 5.8). The total analysis time of roughly 14 minutes corresponds to about a 3-fold increase in analyte signal longevity as a result of using this new strategy for current programming. Unfortunately, a direct comparison of the integrated analyte ion currents for the two analyses can not be made because the amount of alanyl-leucyl-glycine used for the experiments was different, as were the experimental conditions. However, the results are encouraging and warrant further investigation under more controlled conditions.

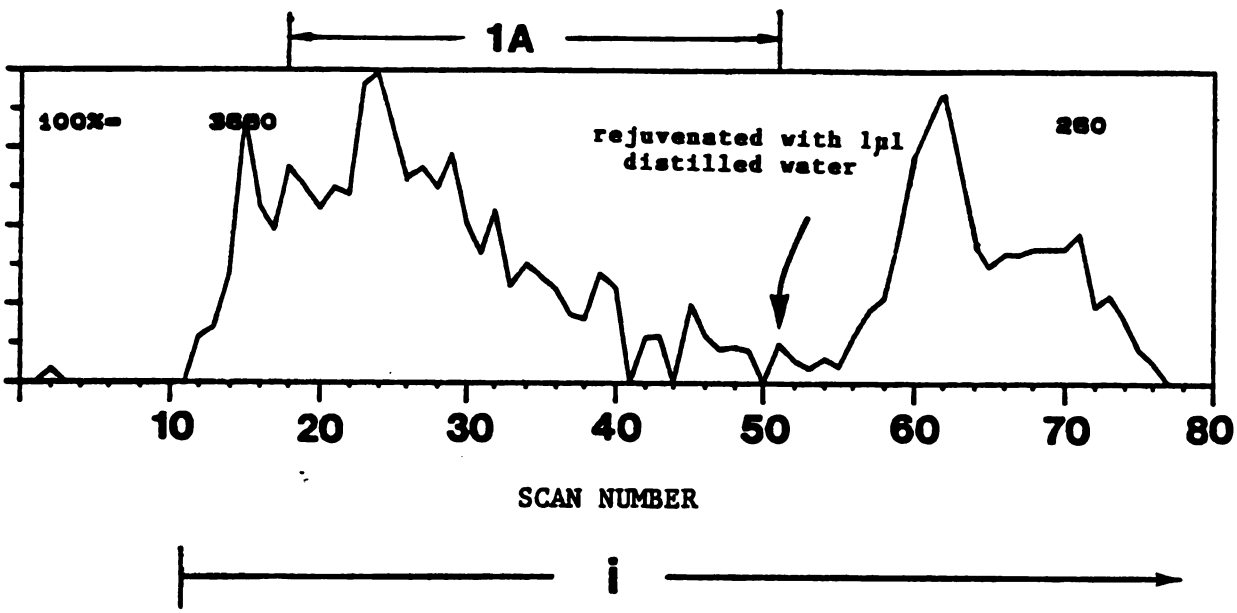

Figure 6.7 Desorption profile for the $[M+H]^+$ ion of alanyl-leucyl-glycine illustrating the ability to rejuvenate ion current profiles in TA-FAB by the addition of water.

The latter peak in the profile of Figure 6.7 displays the result of rejuvenation. Between scans 51 and 52 the probe was removed to add 1µl distilled water. The sample was blown down in the usual manner to remove excess water and to promote mixing, and then reinserted. Scans 52-56 were acquired with no heat. Beginning with scan 57 a ramp was initiated at 0.80A and allowed to proceed to a final value of 1.44A at the last scan of the run. These results point conclusively to the requirement of both heat and solvent for generating sustained analyte signals from the ternary systems used for TA-FAB.

Although the TP model is only speculation at this point, it does adequately account for the data obtained under TA-FAB. Certainly future experiments need to be conducted to test the validity of this model.

VI. List of References

1. C.W. Magee, Int. J. of Mass Spectrom. and Ion Phys., 49, 211 (1983).
2. A. Benninghoven, D. Jaspers, and W. Sichtermann, Appl. Phys., 11, 35 (1976).
3. FAB B11NF Saddle Field Gas Gun, Owners Manual, Ion Tech LTD., 1981.
4. M.L. Vestal, Mass Spectrom. Rev., 2, 447 (1983).
5. F.A. Cotton and G. Wilkinson, "Basic Inorganic Chemistry", p. 212, Wiley: New York, 1976.
6. M. Mathlouthi, Carbohydr. Res., 91, 113 (1981).
7. M. Mathlouthi, C. Luu, A.M. Meffroy-Biget, and D.V. Luu, Carbohydr. Res., 81, 213 (1980).
8. F.A. Cotton and G. Wilkinson, "Basic Inorganic Chemistry", p. 268, Wiley: New York, 1976.
9. R.G. Cooks and K.L. Busch, Int. J. Mass Spectrom. Ion Phys., 53, 111 (1983).
10. L. Hyvonen, P. Varo, and P. Koivistoinen, J. Food Sci., 42, 657 (1977).

Chapter 7

FUTURE DIRECTION

I. Summary

At present, TA-FAB has been applied to the analysis of several classes of biomolecules, and has often demonstrated results superior to FAB. However, the technique is still in the nascent stages of development, where several questions remain to be answered. Therefore, it is difficult to objectively assess the analytical utility of the method at this point in time. It is still worthwhile, however, to review the present strengths and weaknesses of TA-FAB since these factors will help determine its overall acceptance.

Many of the advantages of TA-FAB over conventional FAB have been previously described. First, saccharide solutions generate less background than conventional viscous liquid matrices. Second and foremost, when thermal assistance is applied to saccharide matrices, one observes a selection against background and the potential for valid background subtraction. Third, there is a tendency to observe more structural information by TA-FAB, either due to the selection against matrix interference or through an increase in fragmentation. Finally, these improvements to FAB do not come at the expense of analyte sensitivity or longevity.

In regard to the limitations of the method, one disadvantage is that TA-FAB requires more intervention or operator expertise as compared to conventional FAB which is relatively simple to perform.

As shall be addressed later in this chapter, there are many variables involved with the method of TA-FAB beyond those which exist in conventional FAB. Hence, there is an urgent need at present to find the optimum approach for performing TA-FAB. The results of such an investigation would not only improve the performance of TA-FAB, but would also answer many questions from potential users of the method.

A second drawback is that added instrumentation is required to perform TA-FAB. This limitation may, however, be minor because of the relatively low temperatures involved with the method. Depending on the design used for the TA-FAB probe tip, the means for applying heat to the sample may be already present with the direct insertion probe of the mass spectrometer. In other words, TA-FAB may be possible on most instruments with only a few minor modifications. A third drawback is that the practice of TA-FAB degrades the focus of the ion source more quickly than conventional FAB. While this leads to more frequent ion source cleaning, the problem is less severe than envisioned, particularly if the source is baked out after use. In this manner, experiments could easily be carried out for periods greater than 1 week before cleaning under the current experimental design.

Finally, the scope of application of TA-FAB at present is not as large as reported for conventional FAB. Specifically, because of the large water content of the ternary systems used for TA-FAB, more difficulty is encountered in the analysis of nonpolar nonvolatile samples due to insolubility. In addition, there are simply fewer TA-FAB matrices at present to choose from. However,

it should be noted that the drawbacks cited here reflect the current status of the technique, and therefore are not a statement of the ultimate potential of TA-FAB.

As the final section of this dissertation, recommendations for future work shall be suggested. The recommended experiments may be divided into three classifications, which in many ways are inter-related. The general headings are method optimization, mechanistic studies, and extending the scope of application of TA-FAB.

II. Optimization of Method

Several parameters of the TA-FAB experiment need to be optimized. Many of these are related to how the sample is heated: heating rate, interval before heating, and the current at which heating begins. Other factors requiring optimization are related to matrix composition, such as the percentage of fructose in the aqueous matrix solution. The effect of solvent composition should also be studied using various water/methanol ratios to dissolve fructose. The remaining parameters involve the method of sample application and includes the size and type of probe tip used for TA-FAB.

The results of optimization studies should be judged both on the sensitivity and precision of the analyte signals obtained. The reproducibility of the BMT, and the selection against background should also be considered. Once optimization has been realized, the approach used for TA-FAB should be tested for optimization

using different analytes, different matrices, and different analyte concentrations. These studies shall provide important criteria for judging the analytical utility of TA-FAB. Finally, after the approach to optimization has been documented, several figures of analytical merit, such as sensitivity, linear dynamic range, and detection limits need to be ascertained using representative analyte/matrix combinations to ensure against the possibility that the conditions for optimization are system-dependent. The application of TA-FAB to the newly-acquired JEOL-HX-110 should prove very helpful to this endeavor.

III. Mechanistic Studies

The second set of proposed studies concerns the ongoing investigation into the mechanism of TA-FAB. Some of the experiments suggested here are already in progress and shall be described in greater detail subsequently in the dissertation of C.E. Heine. The first general set of experiments involves making physical measurements of the ternary system used for TA-FAB to see if the results are consistent with the TP model. For example, X-ray diffraction studies, similar to the data presented by Mathlouthi in the last chapter, should be performed with analyte present. Further, data obtained at elevated temperatures might verify the exclusion of analyte and transport to the surface under TA-FAB. Raman spectroscopy could also be investigated as a means of probing the relative strength and number of intermolecular interactions present in the ternary mixture. Such data would also

test the viability of the ternary perculation hypothesis. A third set of measurements, which would be more easily obtained, is to determine the viscosity of the saccharide matrices both as a function of concentration and temperature. Comparisons could then be made to glycerol at ambient temperature to assess the ability for mass transport during the various stages of TA-FAB.

Several other experiments have been proposed to help elucidate the mechanism behind TA-FAB. For example, ternary systems have been prepared using ^{18}O-labeled water to document the evolution of the solvent during TA-FAB. However, since no ions were observed from the isotopically labeled water under TA-FAB, water is probably released as neutrals. An experiment where the EI filament is turned on at regular intervals along the TA-FAB experimental profile might make it possible to answer this question.

Other experiments have been proposed to define the role of the solvent during TA-FAB. For instance, if a system could be found where surfactant addition is required to enable the detection of a nonpolar nonvolatile analyte under TA-FAB, such data would support the claim that water is needed for analyte solvation and transport in TA-FAB. Another way to probe the interaction of the solvent is to study a binary system (e.g., analyte and matrix) as a control. For example, if results could be obtained using a viscous polymer as a matrix for TA-FAB, the profile for the matrix background would indicate whether or not the solvent participates in the observed selection against background in ternary systems. Data were obtained for the binary system of solid fructose and alanyl-leucyl-glycine, but the results were inconclusive. Finally,

the role of water in the ternary systems might be deduced from the following experiment. First, two analytes are chosen which are soluble in water, but to varying degrees. A comparison of the signal intensities obtained in glycerol (binary) relative to aqueous fructose (ternary) might reflect the role of water as a vehicle for transport in this latter system.

IV. Applications

Lastly, attention should always be given to experiments intent on broadening the scope of application of TA-FAB. For instance, while nonpolar nonvolatiles are typically problem compounds for FAB, they are particularly troublesome to TA-FAB for reasons mentioned previously. At least two options exist to obviate this limitation. First, surfactant-modified ternary systems should be investigated. A second option would be to search for binary systems where the matrix could solvate nonpolar nonvolatile analytes upon heating. Again, candidates would be viscous polymers, or solids which become fluid as a result of a phase change. Another area for investigation would be to see if the additional fragmentation observed for the HC-toxins can be extended to high mass biopolymers to achieve more abundant sequence information.

As a final note, it is hoped that this dissertation has helped to confront the problem of chemical interference in FAB mass spectra. It is further desired that TA-FAB will find increased

application as a viable alternative to analyses performed by FAB mass spectrometry.